

NINA ROL

RESTORING THE BALANCE
— OF —
**THE PULMONARY
ENDOTHELIUM**

THE SILVER LINING IN PAH?

VRIJE UNIVERSITEIT

RESTORING THE BALANCE OF THE PULMONARY ENDOTHELIUM

the silver lining in PAH?

ACADEMISCH PROEFSCHRIFT

ter verkrijging van de graad Doctor aan
de Vrije Universiteit Amsterdam,
op gezag van de rector magnificus
prof.dr. V. Subramaniam,
in het openbaar te verdedigen
ten overstaan van de promotiecommissie
van de Faculteit der Geneeskunde
op woensdag 30 september 2020 om 11.45 uur
in de aula van de universiteit,
De Boelelaan 1105

Restoring the balance of the pulmonary endothelium: the silver lining in PAH?
Nina Rol

ISBN/EAN: 978-94-6416-032-1

Financial support for printing this thesis was kindly provided by the Vrije Universiteit

Cover design by Chris M. Happé
Layout and design by Daniëlle Balk | persoonlijkproefschrift.nl
Printed by: Ridderprint | www.ridderprint.nl

Copyright © 2020 Nina Rol
All rights reserved. No part of this thesis may be reproduced, stored or transmitted
in any way or by any means without the prior permission of the author, or when
applicable, of the publishers of the scientific papers.

door

Nina Rol

geboren te Haarlem

promotoren:

prof.dr. H.J. Bogaard
prof.dr. M.J.T.H. Goumans

Voor Juliet & Hugo

Overige leden promotiecommissie:

Prof. dr. P.L. Hordijk

Prof. dr. P. ten Dijke

Prof. dr. P.A. Da Costa Martins

Dr. B.G. Boerrigter

Dr. P. Dorfmueller

The research described in this thesis was supported by grants from the Dutch Lung Foundation (Longfonds, grant number 3.3.12.036), the Netherlands CardioVascular Research Initiative: the Dutch Heart Foundation, Dutch Federation of University Medical Centers, the Netherlands Organization for Health Research and Development, and the Royal Netherlands Academy of Sciences grant number 2012-08 awarded to the Phaedra consortium (www.phaedraresearch.nl).

Research described in chapter 9 was supported by Boehringer Ingelheim.

Financial support for printing this thesis was gratefully acknowledged by the Dutch Heart Foundation and the Dutch Lung Foundation.

Contents

| | | |
|-------------------|--|-----|
| Chapter 1 | General introduction and thesis outline | 9 |
| Chapter 2 | Pathophysiology and treatment of Pulmonary Arterial Hypertension | 19 |
| Chapter 3 | Pneumonectomy combined with SU5416 induces severe pulmonary hypertension in rats | 45 |
| Chapter 4 | Vascular remodeling in the pulmonary circulation after major lung resection | 65 |
| Chapter 5 | Vascular narrowing in pulmonary arterial hypertension is heterogeneous: Rethinking resistance | 71 |
| Chapter 6 | Endothelial dysfunction in pulmonary arterial hypertension: loss of cilia length regulation upon cytokine stimulation | 87 |
| Chapter 7 | TGF-beta and BMPR2 signaling in PAH: two black sheep in one family | 107 |
| Chapter 8 | BMP9 pushes lung vasculature endothelial cells of pulmonary arterial hypertension patients into a mesenchymal phenotype | 129 |
| Chapter 9 | Nintedanib improves cardiac fibrosis but leaves pulmonary vascular remodeling unaltered in experimental pulmonary hypertension | 151 |
| Chapter 10 | Summary and future perspectives | 169 |
| Chapter 11 | Nederlandse samenvatting | 180 |
| | List of publications | 185 |
| | Curriculum Vitae | 187 |
| | Dankwoord | 188 |

1

Chapter 1

General introduction and thesis outline

The Discovery of the Pulmonary Circulation

In history, different views on the cardiovascular system have passed (figure 1).(1, 2) Around 300 years before Christ at the Alexandrian School of Medicine, Praxagoras, Herophilus and Erasistratus tried to get a better understanding of the heart and vessels. The diagnostic value of the pulse was discovered by Praxagoras. Herophilus described the anatomical difference between arteries and veins and even noticed the exception to this rule in the lung vasculature. Praxagoras, Herophilus and Erasistratus reasoned that the arteries carried air from the heart, while veins contain blood.(2-4)

Aelius Galenus, a philosopher and physician born around 129 AD, believed the source of all veins was the liver, producing blood. Blood was exchanged between the right and left ventricle of the heart via pores in the septum. He, on the contrary, believed that arteries are filled with blood mixed with air from the lungs.(2, 3) This theory lasted until the Renaissance, when Leonardo Da Vinci (1452-1512) was one of the first to oppose the anatomical theories of Galen. He described the heart as a muscle, but still depicted intraventricular pores as proposed by Galen.(1)

Galen's theories were seriously questioned when systematically performed human corpse dissections were done by Andreas Vesalius (1514-1564). He rectified the statement that veins originate from the liver and questioned the existence of the pores in the septum. In addition Michael Servetus (1511-1553) proposed that blood is brought from the right ventricle to the lungs to the left ventricle, but without experiments supporting this idea. Realdo Colombo (1516-1559), an Italian anatomist, could not prove the pores in the septum proposed by Galen and also theorized the passing of blood from the right ventricle through the lungs to the left ventricle based on anatomical studies. Earlier, Ibn Al-Nafis (1213-1288), an Arab physician from Damascus, had already described the pulmonary circulation in the mid-13th century. This work was translated to Latin a couple of years before Servetus and Colombo published their work, but no reference to Al-Nafis was made.(5)

It took until 1628 before William Harvey (1578-1657) published a book in which he describes the blood circulation closest to how we know it today. By using a tourniquet he proved the flow of blood into the arm through the arteries and returning through the veins, proposing a closed circulatory system (figure 1). He hypothesized that the heart, instead of the liver, is driving the circulation, and that blood flows from the right ventricle into the pulmonary circulation before entering the left ventricle. (1, 2)

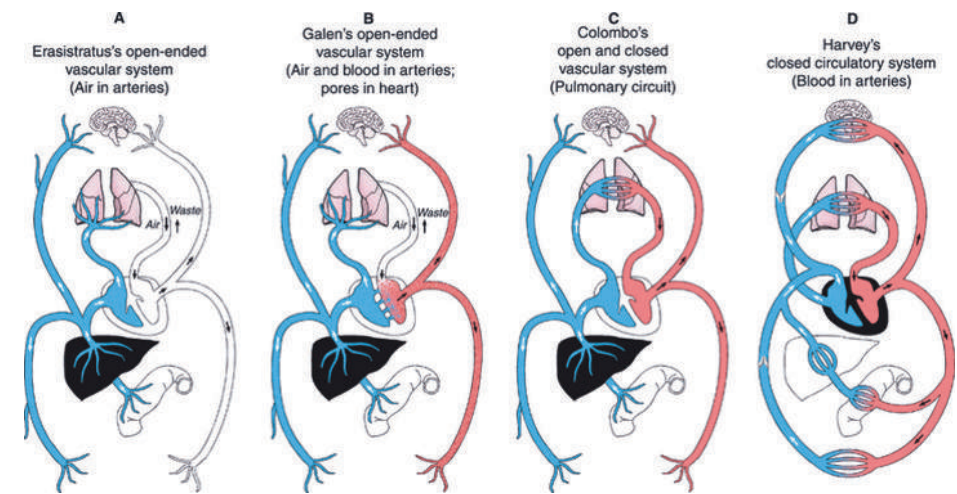


Figure 1 – Schematic overview of the discovery of the cardiovascular system over time(1)

The Pulmonary Circulation and Pulmonary Arterial Hypertension

It took hundreds of years of research to come to the extensive knowledge of the pulmonary (right) and systemic (left) circulation. As we know today, in the pulmonary circulation blood is pumped from the right ventricle into the main pulmonary artery. Blood is then distributed over the lung by the many vessels branching out further and further into arterioles and capillaries. After oxygenation, the blood flows back via the veins into the left side of the heart to be systemically distributed (figure 1).

There are marked differences between the vascular beds of the left and right circulation, including their reactivity to stress, hormones, and drugs.(6) The right circulation has a very thin air-blood barrier enabling sufficient gas exchange, serving the main purpose of the lungs: providing oxygen and eliminating carbon dioxide. In contrast to the high pressures (120mmHg) in the systemic circulation, the thin air-blood barrier in the lungs limits the circulation to low pulmonary pressures (12-16mmHg).(7) The pulmonary circulation is very sensitive to a small rise in pressure, a pathological condition called pulmonary hypertension (PH). The first clinical description of pulmonary hypertension was made in the 20th century by Abel Ayerza (1861-1918). He had no modern diagnostic tools like ECG or catheters at his disposal, but accurately described the condition in patients with varying etiology, including its concomitant chronic cyanosis, dyspnea, and the underlying sclerosis of the pulmonary artery with thickening and dilatation of the right ventricular wall.

We currently view PH, defined by a mean pulmonary artery pressure above 25 mmHg, as a heterogeneous group of disorders. It is classified in five groups based on differences in clinical, hemodynamic and histopathologic features: Pulmonary Arterial Hypertension (PAH), pulmonary hypertension due to left heart diseases, pulmonary hypertension due to chronic lung diseases and/or hypoxia, chronic thromboembolic pulmonary hypertension, and pulmonary hypertension due to unclear multifactorial mechanisms (WHO classification: table 1, chapter 2).(8, 9) In this thesis I will focus on PAH, characterized by precapillary pulmonary hypertension, defined by a pulmonary capillary wedge pressure below 15 mmHg. The etiology varies from idiopathic pulmonary hypertension, to heritable pulmonary hypertension, drug- and toxin induced pulmonary hypertension and pulmonary hypertension associated with other diseases. Besides the typical vascular remodeling (figure 2), persistent vasoconstriction, and increased circulating growth factors and inflammatory cytokines are contributing factors to PAH. A detailed description of the pathophysiology of PAH and currently available drug therapies targeting the pulmonary vasculature and the heart are discussed in **Chapter 2**.

Vascular remodeling in Pulmonary Arterial Hypertension

One of the hallmarks of PAH is the typical form of vascular remodeling in the lungs, which includes pulmonary arterial intimal fibrosis, medial hyperplasia, and the pathognomonic plexiform lesions.(10) Shear stress, as occurs in high flow states such as congenital systemic-to-pulmonary shunts, is considered a likely contributor to vascular remodelling, and hence, development of PAH.(10, 11) Shear stress can be explained as the frictional force of the blood on the vessel luminal surface parallel to the flow. Substantial loss of the available vascular bed due to major lung resections gives elevated systolic pressures in the pulmonary artery and approximately one third of pneumonectomized patients develop mild to moderate pulmonary hypertension one year postoperatively.(12, 13) It is yet unknown to what extent altered pulmonary blood flow alone contributes to vascular remodelling in PAH.(14, 15) We studied the effect of pneumonectomy in a rat model (**Chapter 3**) and retrospectively in the lungs of patients who underwent a major lung resection (**Chapter 4**). With lung resection, the same cardiac output is put through fewer pulmonary vessels, allowing the investigation of flow-induced structural changes. Performing a literature study we noticed that most studies on vascular remodeling were limited to a quantification of average increases in wall thickness. Importantly, information on number of vessels affected and diameter decreases for vessels of different sizes was limited or lacking entirely. We decided to quantify the structural changes in the lung vasculature and use these data to calculate the contribution of vascular remodeling, next to the contribution of vasoconstriction, possible loss of vessels, to the increase in pulmonary vascular resistance (**Chapter 5**).

Zooming in on the endothelium

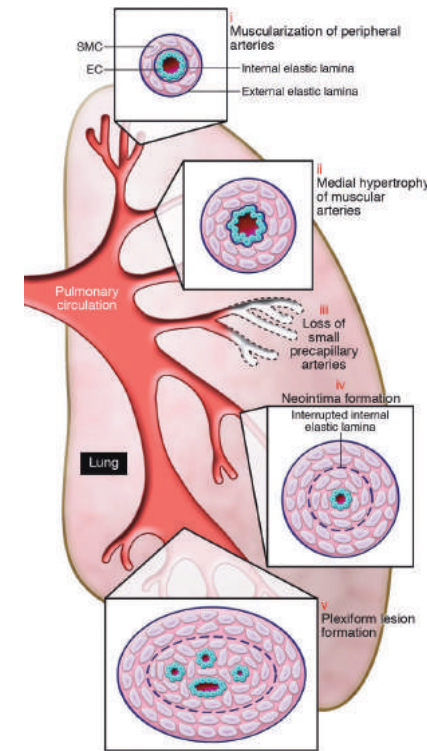


Figure 2 – Remodeling in PAH(16)

All approved PAH therapies target endothelial dysfunction, via three well characterized pathways: the endothelin-1, nitric oxide and prostacyclin pathways. However, the function of the endothelium is more diverse and complex. The endothelium functions as a barrier, takes part in many diverse complex signalling cascades and is continuously exposed to mechanical forces of the blood. The endothelium is the predominant sensor of shear stress, as it forms the inner layer of the vessels.(17) Endothelial cells seem to turn over more rapidly and have a higher DNA synthesis rate in a situation of disturbed flow than under static conditions.(18) Primary cilia located on the endothelium, are sensory antenna for fluid shear stress and pro- and anti-inflammatory responses, factors known to be important in the pathogenesis of PAH. (19, 20) In **Chapter 6** our objective was to study the cilia length in endothelial cells of PAH patients and their response to shear stress and inflammatory cytokines.

Not only shear stress, but also mutations, hypoxia, cytokines, vasoactive peptides, chemokines and growth factors contribute to endothelial dysfunction.(21) In the second part of this thesis, we looked at different aspects influencing the endothelium. Imbalance between the Transforming Growth Factor beta (TGF-beta) and Bone Morphogenetic Protein (BMP) pathways influences the pathogenesis of PAH. Since the discovery of the BMPR2 mutation, present in the majority of familial PAH patients, a lot of PAH research has been done on the TGF-beta/BMP pathway.(22-26) The signalling pathway, its effects on vascular remodeling and PAH related published studies (mostly focussing on the TGF-beta) are in detail described in **Chapter 7**. The strong association between PAH and BMPR2 creates an opportunity to develop and test therapeutic interventions. BMP9, a receptor ligand of the TGF-beta superfamily, was shown to reinstate BMPR2 levels in animals models and clinical trials are planned.(27, 28) On the other hand, a recent publication showed a protective effect against experimental pulmonary hypertension by BMP-9 inhibition.(29) In **Chapter 8** we looked into the responses of human derived endothelial cells of PAH patients to BMP9 supplementation to study its therapeutic potential to correct the TGF-beta/BMP imbalance.

Other compounds with treatment potential for PAH are tyrosine kinase inhibitors (TKI), specifically ones targeting growth factors that have increased expression in the lung of PAH patients, like TGF-beta, Vascular Endothelial Growth Factor (VEGF), Platelet Derived Growth Factor (PDGF), Fibroblast Growth Factor (FGF). (21, 30-35) Nintedanib, a TKI targeting above mentioned growth factors, has already been clinically approved for idiopathic pulmonary fibrosis. (34-36) In **Chapter 9** our aim was to study the effects of nintedanib on pulmonary endothelial cells *in vitro* and its effect on the lungs and the heart in a PH animal model to address its applicability in the treatment of PAH.

References

1. Aird WC. Discovery of the cardiovascular system: from Galen to William Harvey. *J Thromb Haemost.* 2011;9 Suppl 1:118-29.
2. ElMaghawry M, Zanatta A, Zampieri F. The discovery of pulmonary circulation: From Imhotep to William Harvey. *Glob Cardiol Sci Pract.* 2014;2014(2):103-16.
3. Serageldin I. Ancient Alexandria and the dawn of medical science. *Glob Cardiol Sci Pract.* 2013;2013(4):395-404.
4. Lewis O. Praxagoras of Cos on Arteries, Pulse and Pneuma. *Fragments and Interpretation. Stud Anc Med.* 2017;48:1-375.
5. Akmal M, Zulkifile M, Ansari A. Ibn nafis - a forgotten genius in the discovery of pulmonary blood circulation. *Heart Views.* 2010;11(1):26-30.
6. Muresian H. The clinical anatomy of the right ventricle. *Clin Anat.* 2016;29(3):380-98.
7. Schulte K, Kunter U, Moeller MJ. The evolution of blood pressure and the rise of mankind. *Nephrol Dial Transplant.* 2015;30(5):713-23.
8. Simonneau G, Gatzoulis MA, Adatia I, Celermajer D, Denton C, Ghofrani A, et al. Updated clinical classification of pulmonary hypertension. *J Am Coll Cardiol.* 2013;62(25 Suppl):D34-41.
9. Foshat M, Boroumand N. The Evolving Classification of Pulmonary Hypertension. *Arch Pathol Lab Med.* 2017;141(5):696-703.
10. K. Grunberg WJM. A practical approach to vascular pathology in pulmonary hypertension. *Diagn Histopath.* 2013;19(8):298-310.
11. Wagenvoort CA. Vasoconstrictive primary pulmonary hypertension and pulmonary veno-occlusive disease. *Cardiovasc Clin.* 1972;4(2):97-113.
12. Potaris K, Athanasiou A, Konstantinou M, Zaglavira P, Theodoridis D, Syrigos KN. Pulmonary hypertension after pneumonectomy for lung cancer. *Asian Cardiovasc Thorac Ann.* 2014;22(9):1072-9.
13. Foroulis CN, Kotoulas CS, Kakouros S, Evangelatos G, Chassapis C, Konstantinou M, et al. Study on the late effect of pneumonectomy on right heart pressures using Doppler echocardiography. *Eur J Cardiothorac Surg.* 2004;26(3):508-14.
14. Dickinson MG, Bartelds B, Borgdorff MA, Berger RM. The role of disturbed blood flow in the development of pulmonary arterial hypertension: lessons from preclinical animal models. *Am J Physiol Lung Cell Mol Physiol.* 2013;305(1):L1-14.
15. Happe CM, Szulcek R, Voelkel NF, Bogaard HJ. Reconciling paradigms of abnormal pulmonary blood flow and quasi-malignant cellular alterations in pulmonary arterial hypertension. *Vascul Pharmacol.* 2016;83:17-25.
16. Rabinovitch M. Molecular pathogenesis of pulmonary arterial hypertension. *J Clin Invest.* 2008;118(7):2372-2379.
17. Davies PF. Flow-mediated endothelial mechanotransduction. *Physiol Rev.* 1995;75(3):519-60.
18. Chiu JJ, Chien S. Effects of disturbed flow on vascular endothelium: pathophysiological basis and clinical perspectives. *Physiol Rev.* 2011;91(1):327-87.
19. Hierck BP, Van der Heiden K, Alkemade FE, Van de Pas S, Van Thienen JV, Groenendijk BC, et al. Primary cilia sensitize endothelial cells for fluid shear stress. *Dev Dyn.* 2008;237(3):725-35.
20. Wann AK, Knight MM. Primary cilia elongation in response to interleukin-1 mediates the inflammatory response. *Cell Mol Life Sci.* 2012;69(17):2967-77.
21. Guignabert C, Tu L, Girerd B, Ricard N, Huertas A, Montani D, et al. New molecular targets of pulmonary vascular remodeling in pulmonary arterial hypertension: importance of endothelial communication. *Chest.* 2015;147(2):529-37.
22. Lane KB, Machado RD, Pauciulo MW, Thomson JR, Phillips JA, 3rd, Loyd JE, et al. Heterozygous germline mutations in BMPR2, encoding a TGF-beta receptor, cause familial primary pulmonary hypertension. *Nat Genet.* 2000;26(1):81-4.

23. Deng Z, Morse JH, Slager SL, Cuervo N, Moore KJ, Venetos G, et al. Familial primary pulmonary hypertension (gene PPH1) is caused by mutations in the bone morphogenetic protein receptor-II gene. *Am J Hum Genet.* 2000;67(3):737-44.
24. Cogan JD, Pauciulo MW, Batchman AP, Prince MA, Robbins IM, Hedges LK, et al. High frequency of BMPR2 exonic deletions/duplications in familial pulmonary arterial hypertension. *Am J Respir Crit Care Med.* 2006;174(5):590-8.
25. Aldred MA, Vijaykrishnan J, James V, Soubrier F, Gomez-Sanchez MA, Martensson G, et al. BMPR2 gene rearrangements account for a significant proportion of mutations in familial and idiopathic pulmonary arterial hypertension. *Hum Mutat.* 2006;27(2):212-3.
26. Tielemans B, Delcroix M, Belge C, Quarck R. TGFbeta and BMPRII signalling pathways in the pathogenesis of pulmonary arterial hypertension. *Drug Discov Today.* 2019;24(3):703-16.
27. Long L, Ormiston ML, Yang X, Southwood M, Graf S, Machado RD, et al. Selective enhancement of endothelial BMPR-II with BMP9 reverses pulmonary arterial hypertension. *Nat Med.* 2015;21(7):777-85.
28. Andruska A, Spiekerkoetter E. Consequences of BMPR2 Deficiency in the Pulmonary Vasculature and Beyond: Contributions to Pulmonary Arterial Hypertension. *Int J Mol Sci.* 2018;19(9).
29. Tu L, Desroches-Castan A, Mallet C, Guyon L, Cumont A, Phan C, et al. Selective BMP-9 Inhibition Partially Protects Against Experimental Pulmonary Hypertension. *Circ Res.* 2019;124(6):846-55.
30. Hassoun PM, Mouthon L, Barbera JA, Eddahibi S, Flores SC, Grimminger F, et al. Inflammation, growth factors, and pulmonary vascular remodeling. *J Am Coll Cardiol.* 2009;54(1 Suppl):S10-9.
31. Voelkel NF, Gomez-Arroyo J, Abbate A, Bogaard HJ, Nicolls MR. Pathobiology of pulmonary arterial hypertension and right ventricular failure. *Eur Respir J.* 2012;40(6):1555-65.
32. Godinas L, Guignabert C, Seferian A, Perros F, Bergot E, Sibille Y, et al. Tyrosine kinase inhibitors in pulmonary arterial hypertension: a double-edge sword? *Semin Respir Crit Care Med.* 2013;34(5):714-24.
33. Gomez-Arroyo J, Sakagami M, Syed AA, Farkas L, Van Tassell B, Kraskauskas D, et al. Iloprost reverses established fibrosis in experimental right ventricular failure. *Eur Respir J.* 2015;45(2):449-62.
34. Wollin L, Maillet I, Quesniaux V, Holweg A, Ryffel B. Antifibrotic and anti-inflammatory activity of the tyrosine kinase inhibitor nintedanib in experimental models of lung fibrosis. *J Pharmacol Exp Ther.* 2014;349(2):209-20.
35. Wollin L, Wex E, Pautsch A, Schnapp G, Hostettler KE, Stowasser S, et al. Mode of action of nintedanib in the treatment of idiopathic pulmonary fibrosis. *Eur Respir J.* 2015;45(5):1434-45.
36. Inomata M, Nishioka Y, Azuma A. Nintedanib: evidence for its therapeutic potential in idiopathic pulmonary fibrosis. *Core Evid.* 2015;10:89-98.

2

Chapter 2

Pathophysiology and treatment of Pulmonary Arterial Hypertension

Rol N, Guignabert C, Bogaard HJ

Introduction

Pulmonary hypertension (PH) is not a single disease, but a haemodynamic feature found in a rather large group of diseases. PH is defined as a mean pulmonary artery pressure (mPAP) above 25 mmHg at rest. Based on current aetiological perceptions of the condition, PH is classified into five clinical groups (Table 1). Increasing resistance in the pulmonary vasculature (PVR) leads to a high right ventricular (RV) afterload, and the RV either adapts to the high pressures with hypertrophy or dilates and fails. RV failure is the cause of death in the vast majority of patients (2).

Patients present with nonspecific symptoms, like breathlessness, fatigue, weakness, angina and syncope (3). The New York Heart Association (NYHA) Functional Class (Table 2), based on clinical symptoms, is a strong predictor of survival (4, 5). At physical examination, a left parasternal heave can be felt and auscultation may demonstrate an accentuated pulmonary component of the second heart sound, a pansystolic murmur of tricuspid regurgitation, a diastolic murmur of pulmonary insufficiency or a RV third sound. Different imaging techniques, including electrocardiography, chest radiography, echocardiography and cardiac magnetic resonance imaging, may raise the suspicion of the existence of PH, and these tests are also useful to identify possible underlying causes and to monitor treatment responses. Right heart catheterisation (RHC) is always needed to confirm the diagnosis, to evaluate the severity of the disease and to determine the effectiveness of drug therapy. The acute vasoreactivity test aids in determining drug therapy (2).

The current PH clinical classification gathers groups of PH that share similar haemodynamic criteria and types of pulmonary vascular lesions to optimise therapeutic approaches, predict patient outcomes and facilitate research strategies (Table 1) (1). Group 1 PH corresponds to pulmonary arterial hypertension (PAH). PAH is characterised by precapillary PH (mPAP \geq 25 mmHg, with a normal pulmonary capillary wedge pressure \leq 15 mmHg) due to major pulmonary arterial remodelling. The lowest reported prevalence and incidence of PAH are 15 cases/million adult population and 2.4 cases/million adult population/year, respectively.

Table 1 – Clinical classification of pulmonary hypertension based on 5th WSPH Nice 2013

| |
|---|
| 1 Pulmonary arterial hypertension (PAH) |
| 1.1 Idiopathic |
| 1.2 Heritable |
| 1.2.1 BMPR2 |
| 1.2.2 ALK1, ENG, Smad9, Cav1, KCNK3 |
| 1.2.3 Unknown |
| 1.3 Drug and toxin induced |
| 1.4 Associated with |
| 1.4.1 Connective tissue disease |
| 1.4.2 HIV infection |
| 1.4.3 Portal infection |
| 1.4.4 Congenital heart disease |
| 1.4.5 Schistosomiasis |
| 1.5 Pulmonary Hypertension of the newborn |
| 1° Pulmonary veno-occlusive disease and/or pulmonary capillary haemangiomatosis |
| 1° Persistent pulmonary hypertension of the newborn (PPHN) |
| 2 Pulmonary hypertension due to left heart disease |
| 2.1 Systolic dysfunction |
| 2.2 Diastolic dysfunction |
| 2.3 Valvular disease |
| 2.4 Congenital/acquired left heart inflow/outflow tract obstruction and congenital cardiomyopathies |
| 3 Pulmonary hypertension due to lung disease and/or hypoxia |
| 3.1 Chronic obstructive pulmonary disease |
| 3.2 Interstitial lung disease |
| 3.3 Other pulmonary diseases with mixed restrictive and obstructive pattern |
| 3.4 Sleep-disordered breathing |
| 3.5 Alveolar hypoventilation disorders |
| 3.6 Chronic exposure to high altitude |
| 3.7 Developmental abnormalities |
| 4 Chronic thromboembolic pulmonary hypertension (CTEPH) |
| 5 PH with unclear multifactorial mechanisms |
| 5.1 Haematological disorders: chronic haemolytic anaemia, myeloproliferative disorders, splenectomy |
| 5.2 Systemic disorders: sarcoidosis, pulmonary histiocytosis, lymphangioleiomyomatosis |
| 5.3 Metabolic disorders: glycogen storage disease, Gaucher disease, thyroid disorders |
| 5.4 Others: tumoral obstruction, fibrosis mediastinitis, chronic renal failure, segmental PH |

Adapted from Simonneau et al. (1)

ALK1 activin receptor-like kinase 1 gene, *APAH* associated pulmonary arterial hypertension, *BMPR2* bone morphogenetic protein receptor, type 2, *Cav1* caveolin-1, *ENG* endoglin, *HIV* human immunodeficiency virus, *KCNK3* potassium channel, subfamily K, member 3, *PAH* pulmonary arterial hypertension

Table 2 Pulmonary hypertension New York Heart Association (NYHA) Functional Classification (FC) (75)

| | |
|------------|--|
| I | Patients with PH but without resulting limitation of physical activity. Ordinary physical activity does not cause undue dyspnea or fatigue, chest pain or near syncope |
| II | PH patients with slight limitation of physical activity. They are comfortable at rest. Ordinary physical activity causes undue dyspnea or fatigue, chest pain or near syncope |
| III | PH patients with marked limitation of physical activity. They are comfortable at rest. Less than ordinary activity causes undue dyspnea or fatigue, chest pain or near syncope |
| IV | PH patients with inability to carry out any physical activity without symptoms. These patients manifest signs of right heart failure. Dyspnea and/or fatigue may even be present at rest. Discomfort is increased by any physical activity |

The prevalence of PAH in Europe is estimated between 15 and 50 subjects/million population (6). In 70 % of the heritable PAH cases, a germ line mutation of the bone morphogenetic protein receptor 2 (BMPR2) is found (7, 8). The same mutation is found in 11–40% of sporadic PAH patients, indicating the genetic predisposing factor for PAH (9).

In the year 2000, exonic mutations in the gene encoding for bone morphogenetic protein receptor type 2 (BMPR2) were found in 54% of PAH patients, or more specifically 58–74% of patients with heritable PAH (hPAH) and in 3.5–40% of patients with sporadic PAH (8, 10 – 14). BMPR2 is a member of the receptor family of transforming growth factor- β (TGF- β). The penetrance of mutations of BMPR2 is below 20%, indicating that the BMPR2 gene is not the only gene responsible for PAH and that the pathophysiology of this disease is multifactorial. Therefore, many laboratories have investigated possible mutations in other members involved in the signalling cascade of TGF- β , and two genes were found mutated: ACVRL1 (activating A receptor type II - like kinase 1) and ENG (endoglin). However, these mutations account for only a small proportion of cases of hPAH. Recently, mutations have also been described in Smad 1, Smad 4, Smad 8 and Smad 9 (15, 16). All these mutations disrupt the BMP/Smad signalling pathway and promote endothelial and smooth muscle apoptosis and proliferation, resulting in loss of the endothelial barrier function and pulmonary vascular remodelling. These mutations could also increase the susceptibility to inflammatory stimuli (17). Recently, Ma et al. (18) demonstrated the involvement of the potassium channel subfamily K member 3 (KCNK3) missense mutations in the pathophysiology of PAH. Indeed, mutations in this gene were identified in six unrelated patients with PAH (three patients displaying heritable form of PAH out of 93 patients [3.2%] and three patients with sporadic PAH out of 230 patients [1.3%]) (18). To date, all identified KCNK3 mutations are missense mutations and are responsible for a loss of function of the two-pore-domain potassium channel TASK-1 and its signalling pathway in PAH. The reduction in potassium channel activity may enhance calcium channel-mediated vasoconstriction and vascular remodelling (19, 20).

Pulmonary vascular remodelling, occurring mostly in the small- to mid-sized pulmonary arterioles ($\leq 500 \mu\text{m}$), is a hallmark of most forms of PH. This process is ascribed to the increased proliferation, migration and survival of pulmonary vascular cells within the pulmonary artery wall, i.e. pulmonary vascular smooth muscle cells (SMCs), endothelial cells (ECs), myofibroblasts and pericytes. PAH is associated with excessive production of vasoconstrictive mediators such as endothelin (ET)-1 concurrent with a reduced bioavailability of vasodilator molecules nitric oxide (NO) and prostacyclin (PGI₂). Pulmonary vascular remodelling is also under the control of various key growth factors such as platelet-derived growth factor (PDGF), serotonin (5-hydroxytryptamine; 5-HT) and fibroblast growth factor (FGF)-2. Abnormalities in the expression and function of calcium and potassium channels are also involved in pulmonary vasoconstriction and remodelling of the pulmonary vasculature. Recent findings highlight the critical role of the close and complex relationship between the pulmonary vascular endothelium and inflammation/autoimmunity in PAH. Indeed, circulating levels of certain cytokines and chemokines are abnormally elevated, and some have been reported to correlate with a worse clinical outcome in patients with PAH (21 – 24). Altered regulatory T (Treg) cell function has been demonstrated in patients with PAH, a phenomenon that has been demonstrated to be partly leptin-dependent (25, 26). Similarly, natural killer (NK) cells have recently been implicated (27). An accumulation of immature dendritic cells (DCs) has been demonstrated, suggesting that they may contribute to PAH immunopathology (28). Furthermore, ectopic lymphoid follicles that develop in contact with remodelled pulmonary arteries could be the site of a local autoimmune reaction, leading to the production of autoantibodies directed notably against pulmonary vascular cells. Circulating autoantibodies are commonly detected in idiopathic PAH (iPAH) patients without evidence of an associated autoimmune condition (29 – 32). However, despite the many arguments supporting a role of inflammation in the pathogenesis of PAH, only some patients respond to anti-inflammatory and/or immunosuppressive therapy. It is therefore necessary to understand the complexity of the immune mechanisms of PAH to improve the transfer of knowledge to the clinic.

Although PAH is still a disease without a cure, there are approved drug therapies that at least temporarily stabilise or improve the symptoms in the majority of patients. In this chapter, we will first outline the pathophysiological mechanisms that underlie PAH and PAH-associated RV failure. Subsequently, we will discuss the major therapeutic targets which are currently available or under development.

Pathophysiology of PAH

The extensive structural and functional remodelling of the vasculature in lungs of patients with PAH takes place sequentially and includes medial hypertrophy, muscularisation of small arterioles, intimal thickening and the formation of plexiform

lesions. These processes involve changes in all three layers (intima, media and adventitia) of the vessel wall and are the consequence of cellular hypertrophy, hyperplasia, inflammation, apoptosis, migration and accumulation of extracellular matrix (ECM).

Pulmonary endothelial cell dysfunction

Pulmonary endothelial dysfunction is a critical element in the development and progression of PH, irrespective of disease origin. In PAH, the dysfunctional endothelium shows several abnormalities: (a) a transition from a quiescent state (having no adhesiveness) to an activated state, expressing specific markers and proteins, such as E-selectin and key adhesion molecules [e.g. intercellular adhesion molecule (ICAM-1) and vascular adhesion molecule (VCAM-1)] (submitted data); (b) a reduced ability to produce vasodilatory mediators such as NO and PGI₂; (c) an excessive production and release of vasoconstrictive mediators such as 5-HT, ET-1 and Ang II (33); (d) an important qualitative and quantitative remodelling of components of the ECM; and (e) an increased production of various factors affecting the control of proliferation, differentiation and migration of pulmonary vascular cells such as FGF-2 (basic), interleukin (IL)-6 and leptin (26, 34 – 36). Furthermore, the pulmonary ECs derived from iPAH patients exhibit an aberrant cell phenotype which is characterised by an excessive proliferation and resistance to apoptosis induction (35, 37). Tu et al. (35) have demonstrated that an excessive FGF-2 autocrine loop is one of the mechanisms involved in this aberrant endothelial phenotype, explaining the constitutive activation of the mitogen-activated protein kinase (MAPK) signalling pathway and the overexpression of two key anti-apoptotic factors B-cell lymphoma 2 (BCL2) and B-cell lymphoma-extra large (BCL-xL).

In PAH pulmonary ECs, many other intrinsic abnormalities were also described including p130 cas overexpression, a key amplifier of receptor tyrosine kinase (RTK) downstream signals, altered energy metabolism and a constitutive activation of hypoxia-inducible factors (HIF)-1 α (38, 39). In addition, the abnormal cellular crosstalk between ECs and the other pulmonary vascular cells in the pulmonary vascular wall in PAH represent a key feature of PAH pathogenesis. We have shown that dysfunctional pulmonary ECs from patients with iPAH, through an aberrant release of FGF-2 and IL-6, contribute to increased pericyte coverage of distal pulmonary arteries in PAH, an abnormality that is a potential source of smooth musclelike cells (36). Indeed, activated TGF- β in pulmonary arterial walls in PAH can promote human pulmonary pericyte differentiation into contractile smooth musclelike cells. Multiple lines of evidence therefore suggest that neutralisation of FGF-2, IL-6 and TGF- β 1 may be beneficial against the progression of PAH. A better understanding of the underlying mechanisms is critical to slow down and reverse this obliterative pulmonary vascular remodelling

in PAH. Experimental work strongly supports the fact that the obstructive vascular remodelling may be limited by strategies which, at a time, promote vasodilation and inhibit cell proliferation/survival and inflammation. Because many of these tools have been developed and are available

through cancer treatment, there is a growing interest for the transfer of these tools to PAH. However, several studies are needed not only to identify the best strategies/ molecules for use in PAH but also to better understand the risk/benefit of these anti-proliferative treatments, especially vis-à-vis the maintenance of cardiac function.

Pulmonary smooth muscle hyperplasia

Mechanisms underlying the excessive pulmonary vascular SMC proliferation in PAH are partially understood and result from two complementary mechanisms: inherent characteristics and dysregulation of molecular events that govern SMC growth, including signals originating from pulmonary ECs. Cultured pulmonary arterial SMCs from patients with iPAH grew faster than SMCs from controls at basal conditions or when stimulated by 5-HT, FGF-2, epidermal growth factor (EGF), PDGF or fetal calf serum (FCS). For example, 5-HT transporter (5-HTT) activity is associated with pulmonary artery smooth muscle cell proliferation, and the L-allelic variant of the 5-HTT gene promoter, which is associated with increased expression of 5-HTT, is present in homozygous form in 65% of patients with iPAH compared with 27% of controls (40).

These observations explain the fact that interest has been growing in the potential use of anti-proliferative approaches in PAH (41). Excessive release of various growth factors that are encrypted in the ECM and/or modification of growth factor production, receptor expression and/or alterations in the intracellular mitogenic signals have also been reported to contribute to this excessive smooth muscle migration, proliferation and survival. Inhibition of various RTK signalling pathways by specific inhibitors, such as imatinib, gefitinib and dovitinib, have been shown to exert beneficial effects in animal models of PH (34, 39, 42, 43). However, further efforts still need to be made in order to establish the long-term safety and efficacy of these anti-proliferative approaches in PAH and their potential additive benefit with other drugs. Recent investigations also suggest that a chronic shift in energy production from mitochondrial oxidative phosphorylation to glycolysis (the Warburg effect) of pulmonary vascular cells is present and may participate in the pathogenesis (44 – 46). Mechanistic studies focusing on cell metabolism and its interface with the genetic basis of PAH and inflammation are needed for a better appreciation of its role in the promotion of SMC proliferation and survival and to the disease progression.

Perivascular inflammatory cell accumulation

In the past two decades, understanding of inflammation associated to PAH has moved from a common histopathological curiosity to a key pathomechanism that could be detrimental both in terms of disease susceptibility and development of pulmonary vascular remodelling. Histopathologically, pulmonary vascular lesions occurring in patients with PAH as well as in animal models of PH are characterized by varying degrees of perivascular inflammatory infiltrates, comprising of T and B lymphocytes, macrophages, DCs and mast cells. Recently, correlations were found between the average perivascular inflammation score and the intima plus media and adventitia thickness or mPAP, supporting a role of perivascular inflammation in the processes of pulmonary vascular remodelling (47). In addition, inflammation precedes pulmonary vascular remodelling in animal models of PH, strongly supporting the notion that increased perivascular immune cell infiltration around lung vessels plays a key role in PAH development and progression (25). As previously discussed, circulating levels of certain cytokines and chemokines are abnormally elevated and can directly control cell proliferation, migration and differentiation of pulmonary vascular cells.

There seems to be a particular role for IL-6 in the pathogenesis of PAH. Delivery of recombinant IL-6 protein in rodents is sufficient to cause pulmonary vascular remodelling and PH or to exaggerate the pulmonary hypertensive response to chronic hypoxia (48, 49). Furthermore, IL-6-overexpressing mice spontaneously develop PH and pulmonary vascular remodelling, whereas IL-6 knockout mice are more resistant to the development of PH induced by chronic hypoxia (50, 51). Recent data from our group demonstrated that the overabundance of macrophage migration inhibitory factor (MIF) plays a pivotal role in the pathogenesis of PAH. MIF is a critical upstream inflammatory mediator with pleiotropic actions partly explained by its binding to the extracellular domain of the endothelial CD74. In endothelial cells, activation of the CD74 can lead to activation of Srcfamily kinase and MAPK/ERK, PI3K/Akt and nuclear factor-kappa B (NF- κ B) pathways and to apoptotic resistance by increasing the anti-apoptotic factors BCL2 and BCL-xL and by inhibiting p53 (submitted data). In addition, MIF can bind to C-X-C chemokine receptor type 2 (CXCR2) and type 4 (CXCR4), lead to the proliferation of pulmonary artery smooth muscle cells and contribute to hypoxic PH (52 – 54). While this body of knowledge provides a preliminary understanding, it also highlights subtleties and complexities that require further investigation to determine whether anti-inflammatory strategies will be useful in PAH treatment in the future.

Impaired pulmonary angiogenesis

Multiple lines of evidence suggest that angiogenesis is clearly disturbed in experimental and human PAH with loss and progressive obliteration of precapillary arteries leading

to a pattern of vascular rarefaction (“dead-tree” picture). However, high levels of different angiogenic factor including FGF-2 and VEGF are present in patients with iPAH, strongly supporting the notion that this phenomenon is probably due to signalling defects in the endothelium in PAH. Cool et al. demonstrated exuberant expression of the VEGF receptor KDR, coupled with a reduced expression of p27/kip1 (a cell cycle inhibitory protein) in the pulmonary ECs of plexiform lesions (55). Since increased pericyte coverage in iPAH has been recently reported, another explanation might be related to abnormal pericyte recruitment or to intrinsic abnormalities in pulmonary pericytes in PAH (36). A greater understanding of the role of pulmonary pericytes in vascular homeostasis and remodelling is needed.

In situ thrombosis

PAH pathological specimens often display thrombotic lesions in the absence of clinical or pathological evidence of pulmonary embolism, suggesting an in situ clotting phenomenon (56, 57). In addition, PH is associated with a hypercoagulable phenotype that includes vascular upregulation of tissue factor and an increase in circulating levels of von Willebrand factor or plasma fibrinopeptide A (58 – 60).

Development of right heart failure

Despite its meagre ability to respond to a rapid increase in pressure, the RV is usually able to adapt to a gradually increasing afterload by augmenting its contractility and wall thickness. The one metric which best describes RV adaptation in PAH is ventriculo-arterial coupling, which takes into account both contractility and afterload. When the increased afterload is matched by an adaptive increase in RV contractility and mass, the RV is said to be coupled to the pulmonary arterial circulation (61). However, in the majority of patients with PAH, the severity and chronicity of the afterload increase ultimately overwhelm the increases in RV mass and contractility. The final course of PAH is therefore characterised by RV dilatation and failure, and eventually death (see figure 1). It has been speculated that, as in LV failure, neurohormonal activation may be central in the transition from RV adaptation to RV failure (63). Indeed, sympathetic nervous system activity is increased in PAH patients, which finding has prognostic significance (64). Likewise, an increased renin-angiotensin-aldosterone system (RAAS) activity reflects PAH disease severity (65).

A typical feature of RV failure is the prolongation of the systolic contraction time in comparison to the left ventricular contraction time, leading to a leftward shift of the septum at the end of RV contraction (during which time the LV is already in its relaxing phase) and impaired LV filling (66). In addition to a systolic functional impairment, RV

failure is characterised by diastolic dysfunction, which probably comes about through a combination of intrinsic stiffness and fibrotic replacement of RV cardiomyocytes (67, 68). The transition from RV adaptation to RV failure is further characterised by reduced myocardial perfusion, which may not only reflect reduced coronary perfusion due to, e.g. systemic hypotension, but also an impairment in angiogenesis relative to the degree of hypertrophy (69, 70). Metabolic remodelling is another recently highlighted characteristic of RV failure and includes a decreased uptake of fatty acids and an increased generation of ATPs through glycolysis rather than through glucose oxidation (71, 72).

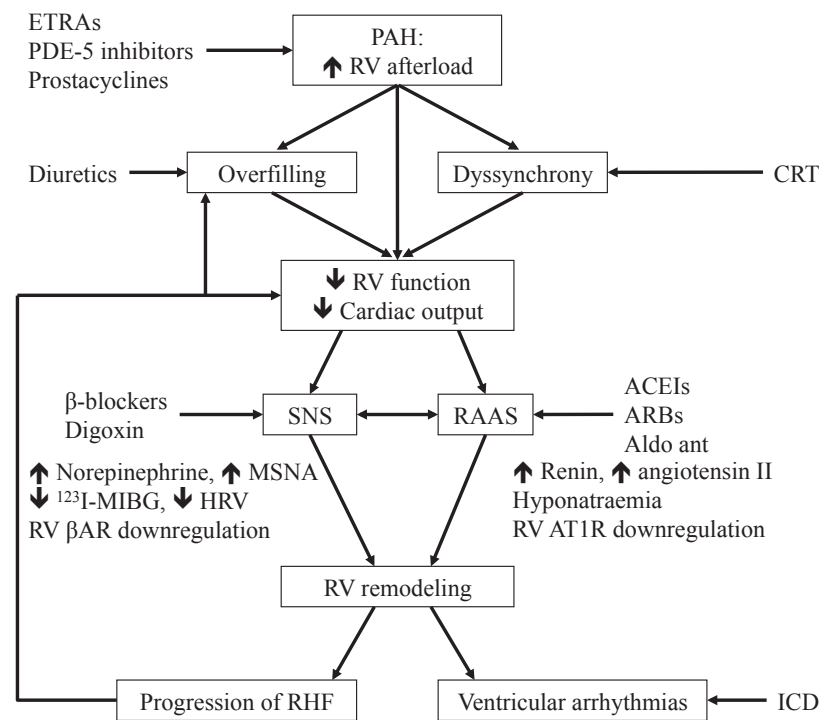


Figure 1 - Schematic overview of hypothetical pathophysiological mechanisms in PAH-related right heart failure, showing the multiple interactions between mechanical events (pressure overload, dilatation), electrophysiological changes (dyssynchrony, arrhythmias) and neurohormonal activation (Reproduced with permission from ref (62)). *RV* right ventricular, *ETRA*s endothelin receptor antagonists, *PDE-5* phosphodiesterase-5, *CRT* cardiac resynchronisation therapy, *SNS* sympathetic nervous system, *RAAS* renin-angiotensin-aldosterone system, *ACEIs* angiotensin-converting enzyme inhibitors, *ARBs* angiotensin receptor blockers, *MSNA* muscle sympathetic nervous activity, *HRV* heart rate variability, *βAR* cardiomyocyte β 1 -adrenergic receptor, *AT1R* cardiomyocyte angiotensin type 1 receptor, *Aldo ant* aldosterone antagonist, *RHF* right heart failure, *ICD* implantable cardioverter defibrillator

Specific drug therapy

To facilitate a treatment plan, it is important to rule out all the possible underlying causes that could induce and cause progression of PAH. In addition to treating the underlying cause, when such a treatment is not available in the cases of idiopathic and heritable PAH, there are PAH-specific approved drugs which aim to dilate pulmonary vessels. In vitro and animal studies suggest that these drugs also have inhibitory effects on vascular remodelling (73). Long-term treatment in patients has not led to a demonstrable regression of vascular remodelling (47). Novel therapies in development (discussed later) show promising results with regard to inhibition of cell proliferation and inducing apoptosis, thereby limiting the progressive changes in morphometry (74).

Drugs targeting the pulmonary vasculature

The currently available drugs for PAH treatment mainly target vasoconstriction via three biochemical pathways: ET-1, NO and PGI₂ (Figure 2) (76). Experimentally, these therapies have some anti-proliferative effects (77, 78). Table 3 shows FDA-approved therapeutics intervening in these three major pathways.

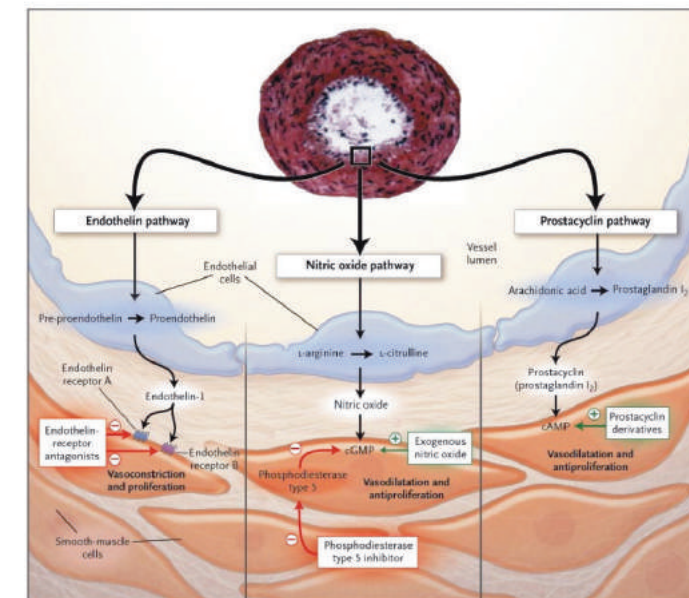


Figure 2 - The pathways involved in contraction and proliferation of pulmonary arterial smooth muscle cells and the endothelium. The four biggest groups of drugs available for PAH that target these pathways are endothelin receptor antagonists, nitric oxide, phosphodiesterase type 5 inhibitor and prostacyclin derivatives (Reproduced with permission from ref. (75))

Table 3 - FDA-approved drug therapies in PAH tested in randomised clinical trials

| Drug | Study + reference | Improvement of | | | Serious adverse effects | |
|-----------------------------------|---|------------------------|---------------|----|--------------------------------|---|
| | | 6MWD/Exercise capacity | Hemo-dynamics | FC | | Survival |
| CCB^a | | | | | | |
| Amlodipine, Diltiazem, Nifedipine | Rich (77), Sitbon (79) | + | + | + | + | Systemic hypotension, bradycardia, edema, headache, nausea |
| NO/cGMP | | | | | | |
| Riociguat | PATENT (80) | + | + | + | + | Hypotension, syncope |
| Sildenafil | SUPER-1 (81), Sastry (82), Singh (83), PACES (84), Iversen (85) | + | + | + | + | Headache, flushing, epistaxis |
| Tadalafil | PHIRST (86, 87) | + | + | + | + | Headache, flushing, epistaxis |
| PGI2 | | | | | | |
| Beraprost | ALPHABET (88), Barst (89) | + ^b | | | | Headache, flushing, jaw pain, diarrhea, approved in Japan/south Korea |
| Epoprostenol | Rubin (90), Barst (91) | + | + | + | + | Local site infection, catheter obstruction and sepsis (pump related) |
| Iloprost (inhal) | AIR (92), STEP ^c (93), COMBI ^c (94) | + | + | + | + | Flushing, jaw pain |
| Treprostinil | Simonneau (s.c.) (95), TRIUMPH (inh.) (96), Freedom C1, C2 and M (oral) (97-99) | + ^d | + | | | Infusion site pain |

Table 3 Continued.

| Drug | Study + reference | Improvement of | | | Serious adverse effects | |
|--------------------|---|------------------------|---------------|----|--------------------------------|------------------|
| | | 6MWD/Exercise capacity | Hemo-dynamics | FC | | Survival |
| ET-1 | | | | | | |
| Ambrisentan | ARIES-1, ARIES-2 (100) Study-351 (101-102), BREATHE-1 (103), BREATHE-2 (104), EARLY (105) | + | | + | | Peripheral edema |
| Bosentan | | + | + | + | | |
| Macitentan | SERAPHI (106) | + | | | + | |
| Combination | | | | | | |
| Initial | Galiè (107) BREATHE-2 (104), Kemp (108), AMBITION (NCT01178073) | + | + | | | |
| Sequential | | + | + | | | |

Modified after Galiè et al. (109) with regard to improvement in 6MWD/exercise capacity, haemodynamics, functional class, survival, time to clinical worsening and the most prominent adverse effects observed; ^aIf prescribed after positive acute vasodilator test; ^b Temporal effect of 3–6 months; ^c Conflicting results with AIR study; ^d Not significantly different in Freedom C1 and C2

Calcium channel blockers

Intracellular calcium levels are elevated in pulmonary arterial SMCs of PAH patients, leading to contraction of the muscular layer in the vessels. Less than 10% of the patients with iPAH respond to an acute vasodilator, like inhaled NO or iloprost. This small group harbours patients who obtain improvement of symptoms after treatment with calcium channel blockers such as long-acting nifedipine, diltiazem or amlodipine. The patients who respond to long-term calcium channel blocker therapy exhibit a more pronounced reduction in mPAP, reaching an absolute mPAP of 33 ± 8 mmHg with acute vasodilator testing. As a result, the consensus definition of a response is now defined as a fall in mPAP of ≥ 10 mmHg, to an mPAP ≤ 40 mmHg, with an unchanged or increased cardiac output. Patients with iPAH who meet these criteria may be treated with calcium channel blockers (79, 110). Owing to potential negative inotropic effects, verapamil should be avoided (111). If the patient does not respond well to the calcium channel blockers (CCB), medication directing the NO, PGI₂ or ET-1 pathway should be added or replace the current treatment (77).

Nitric oxide pathway

NO produced in ECs is translocated to the SMCs to bind to soluble guanylyl cyclase (sGC). This process leads to activation of cyclic guanosine monophosphate (cGMP), which has a strong vasodilatory and a mild anti-proliferative effect on the pulmonary vessels. In PAH, NO production is decreased, with a consequential decrease in cGMP levels resulting in vasoconstriction. Phosphodiesterase type 5 (PDE-5) inhibitors antagonise cGMP degradation by inhibiting PDE-5 and thereby increase cGMP availability. Tadalafil and sildenafil, also prescribed for erectile dysfunction, are effective PDE-5 inhibitors in PAH. The latter, a potent and highly specific PDE-5 inhibitor, was shown to improve exercise capacity, FC and haemodynamics in PAH in the Sildenafil Use in Pulmonary Hypertension (SUPER) trial (81). Because the effectiveness of a PDE-5 inhibitor is determined by the amount of NO available, the new drugs developed are higher in the NO-sGC-cGMP chain. Riociguat is a new drug that increases sGC activity and thereby accelerates cGMP production. This balances the NO pathway, with vasodilatory and anti-proliferative effects as a consequence of a PDE-5 inhibitor is determined by the amount of NO available, the new drugs developed are higher in the NO-sGC-cGMP chain. Riociguat is a new drug that increases sGC activity and thereby accelerates cGMP production. This balances the NO pathway, with vasodilatory and anti-proliferative effects as a consequence.

Prostacyclin pathway

PGI₂, produced by ECs, has antithrombotic, anti-proliferative, anti-mitogenic, immunomodulatory and vasodilating effects. PGI₂ and its downstream targets are downregulated in PAH patients. Drugs directed on this shortage are prostacyclin analogues and prostacyclin receptor agonists, the latter group including selexipag, which is currently tested for effectiveness in PAH. The first specific drug for PAH was the prostanoid epoprostenol, which has to be administered (in a formulation, Flolan) continuously via a central venous catheter because of its short half-life (<5 min). Recently, a more stable form of epoprostenol, Veletri, is available and is more patient compliant (112). Epoprostenol is the only treatment that has shown a reduction in mortality in a randomised controlled trial (91, 109). Treprostinil, another prostacyclin analogue, is more stable and has a longer half-life (4 h) than epoprostenol and can be administered subcutaneously, intravenously (i.v.), orally and by inhalation. The FDA approved subcutaneous treprostinil in 2002 for use in FC II, III, and IV PAH. The possibilities of subcutaneous implantation of an i.v. pump system are now being researched to avoid limitations of an external pump system, as risk of infections, catheter-related embolism and thrombosis (113). Iloprost, a chemically stable prostacyclin analogue, can also be administered by inhalation. Beraprost, an orally active prostacyclin analogue with a short half-life of 35–40 min only, is currently approved for PAH in Japan and South Korea.

Endothelin pathway

ET-1 binds to the ET-A receptors located on vascular SMCs and exerts vasoconstrictive and proliferative effects. Binding of ET-1 to ET-B receptors on ECs and SMCs antagonises vasodilation by NO and prostacyclin. Although assumed that ET-A selective inhibitors (bosentan) would be more effective in PAH treatment, there is no evidence that those treatments are more effective than nonselective (ambrisentan, macitentan) endothelin receptor antagonist (ERAs). It is important to monitor liver functions monthly when ERA treatment is prescribed, because this group of drugs can induce liver toxicity. Haemoglobin and haematocrit levels should also be monitored on a quarterly basis. The potential side effect of lower extremity oedema, particularly within the first several weeks after initiation of therapy, may need to be treated with diuretics. Sitaxentan, a nonselective ERA, has been withdrawn from the market due to two cases of fatal liver injury (2, 109).

Combination therapy (initial, sequential)

When the results of monotherapy are not satisfying, combination therapy is usually started (sequential combination therapy). In patients who have been receiving monotherapy, combination therapy appears to be moderately more effective than continuation of monotherapy with regard to 6 minute walk distance (6MWD), with a magnitude of effect that is approximately equal to the estimated minimal important difference for PAH of 33 m. Several clinical trials of combination therapy, targeting two or more pathways, have also shown clinical benefit when used as upfront combination therapy (109). The results from the recent AMBITION study still have to be published, but this randomised, double-blind, multicenter study with initial combination therapy with ambrisentan and tadalafil in NYHA classes II and III PAH patients showed a delayed time to hospitalisation by 63% (NCT01178073).

Transplantation

All of the drugs mentioned above are able to lower pulmonary vascular resistance to some extent, but long-term outcomes of PAH patients remain uncertain. Singlelung, double-lung and heart–lung transplantations can improve the patient's condition. Lung transplantation is generally reserved for those failing the best available medical therapy. It is shown that RV function can recover fast after lung transplantation, even in severe conditions preoperatively (114, 115). Median survival of iPAH patients is 5.2 years after lung transplantation (116). Combined heart and lung transplantation is generally reserved for those with complex congenital heart disease.

Additional advice and treatment options

The PAH treatment guideline of the European Society of Cardiology gives general advice with regard to daily living and exercise. Physical activity should be encouraged with exercise rehabilitation, as long as it does not lead to severe breathlessness. Exercise training improves endothelial dysfunction, exercise capacity and quality of life (117). Pregnancy is associated with a mortality rate of 30–60% and should therefore be avoided (118, 119). Psychosocial support is important since many PAH patients suffer from anxiety and depression (120). Infection prevention could be considered, because PAH patients are prone to pneumonia and is the cause of death in 7% of the patients (2).

Besides PAH-specific drugs, oral anticoagulants can be part of the PAH treatment plan. Patients suffering from right heart failure with fluid retention benefit from diuretic treatment. Oxygen supplementation should be considered for PAH in NYHA FC III and IV during long flights (2). Although there is no proof for longterm effects,

oxygen administration can lower the PVR in PAH patients, which may be beneficial. Ambulatory additional oxygen could improve symptoms and help with desaturation during exercise.

Atrial Septostomy: Atrial septostomy involves the creation of a right-to-left interatrial shunt to increase cardiac output, which, despite reduction in systemic arterial oxygen saturation, may increase systemic oxygen transport, thus reducing the signs and symptoms of right heart failure. Where advanced medical therapies are available, atrial septostomy is used as a palliative measure or a bridge to lung transplantation in appropriately selected patients with refractory right heart failure or syncope/near syncope despite therapy. In regions of the world without access to current medical therapies, atrial septostomy is sometimes used as a primary therapy (109, 117).

Future therapeutic options

As discussed before, perivascular inflammatory cell accumulation is frequently observed in all forms of PAH. Preclinical studies show beneficial effects in preventing and sometimes even reversing PH symptoms with treatments targeting the immunity. FK506 (calcineurin inhibitor) and anakinra (IL-1 receptor antagonist) are investigated in ongoing clinical trials after promising results in the preclinical setting (24). In addition, a randomised clinical trial testing the safety and efficacy of the monoclonal antibody anti-CD20, a B-lymphocyte protein, is in phase 2 studies in patients with PAH with systemic sclerosis (NCT01086540). Tyrosine kinase inhibitors (TKI) as imatinib, sorafenib and nilotinib showed encouraging results in preclinical studies with regard to vascular and cardiac function, with improvement of functional parameters such as exercise capacity. Unfortunately, these compounds are also associated with serious adverse events and raise safety concerns that limit their use in PAH. Indeed, several lines of evidence suggested that most of these molecules may induce cardiotoxicity (121).

Recent pharmacological studies suggest that activation of RhoA/ROCK signaling system is an important event in the pathogenesis of PH. In vivo, beneficial effects of treatment with Rho kinase inhibitor fasudil have been demonstrated in several animal models of PH (122 – 129). In addition, the beneficial effect of sildenafil I on PH is mediated, at least in part, by the inhibition of the RhoA/Rho kinase pathway (130). Serotonylation of RhoA by intracellular type 2 transglutaminase (TG2), leading to constitutive RhoA activation, is also proposed as a possible risk factor of pulmonary vascular remodelling in PH (128, 131). Similarly, findings from another recent study from Wei et al. indicate increased serotonylation of fibronectin in human and experimental PH (132).

Discovery of the mutations in the BMP/Smad signalling pathway has led to a new range of therapeutic targets in PAH treatment. In fact, restoration of the BMPR2 is a

promising therapeutic strategy. A high-throughput screening on 3,756 drugs approved by the FDA has led to the identification of FK506 (tacrolimus) as an activator of this pathway *in vitro*. FK506 was subsequently shown to be effective in reducing the experimental PH induced in rodents (133), but as mentioned above, these effects may also have been the result of immune modulation.

Drugs targeting the heart

It is important to improve right ventricle function, because patients with persistent low RV ejection fraction despite effective vasodilator treatment have worse prognosis (134). Digoxin increases myocardial contractility but does not show beneficial short-term effects in PAH treatment (135). Beta-adrenoreceptor blockers are currently contraindicated in the treatment of PAH because there is a risk of lowering cardiac output and reducing myocardial contractility. However, reduced myocardial oxygen consumption could also have beneficial effects on the heart and they could also help prevent arrhythmias. After positive results in experimental studies, the effectiveness and patient safety of carvedilol and bisoprolol are now being studied (136 – 138). In addition, the use of angiotensin-converting enzyme (ACE) inhibitors and angiotensin II receptor antagonists remains debatable. Drugs targeting reactive oxygen species (ROS) are also possible therapeutics in PAH since they reduce damage to the RV and thereby prevent reduction of RV contractility. Both are being preclinically studied.

Concluding remarks

PAH is a devastating disease characterised by sustained remodelling of the lung vasculature leading to increased vascular resistance. The adaptive response of the RV to the increased load critically determines clinical outcome. Pulmonary vasodilators have been the cornerstone of PAH therapy and induce calcium channel blockers and more than ten different drugs that modulate nitric oxide, prostacyclin and endothelin pathways. Although the use of these drugs has resulted in improved outcomes for patients, there is an urgent need for new therapies that reverse pulmonary vascular remodelling or directly target the heart, thereby improving right heart function and survival.

References

1. Simonneau G, Gatzoulis MA, Adatia I, Celermajer D, Denton C, Ghofrani A, et al. Updated clinical classification of pulmonary hypertension. *J Am Coll Cardiol*. 2013;62(25): D34–41.
2. Authors/Task Force Members, Galie N, Hoeper MM, Humbert M, Torbicki A, Vachiery J-L, et al. Guidelines for the diagnosis and treatment of pulmonary hypertension: The Task Force for the Diagnosis and Treatment of Pulmonary Hypertension of the European Society of Cardiology (ESC) and the European Respiratory Society (ERS), endorsed by the International Society of Heart and Lung Transplantation (ISHLT). *Eur Heart J*. 2009;30(20):2493–537.
3. Rich S, Dantzker DR, Ayres SM, Bergofsky EH, Brundage BH, Detre KM, et al. Primary pulmonary hypertension a national prospective study. *Ann Intern Med*. 1987;107(2): 216–23.
4. McLaughlin VV, Presberg KW, Doyle RL, Abman SH, McCrory DC, Fortin T, et al. Prognosis of pulmonary arterial hypertension* ACCP evidence-based clinical practice guidelines. *CHEST J*. 2004;126(1_Suppl):78S–92.
5. Barst RJ, McGoon M, Torbicki A, Sitbon O, Krowka MJ, Olschewski H, et al. Diagnosis and differential assessment of pulmonary arterial hypertension. *J Am Coll Cardiol*. 2004;43(12): S40–7.
6. Peacock AJ, Murphy NF, McMurray JJV, Caballero L, Stewart S. An epidemiological study of pulmonary arterial hypertension. *Eur Respir J*. 2007;30(1):104–9.
7. Machado RD, Aldred MA, James V, Harrison RE, Patel B, Schwalbe EC, et al. Mutations of the TGF- β type II receptor BMPR2 in pulmonary arterial hypertension. *Hum Mutat*. 2006;27(2):121–32.
8. Machado RD, Eickelberg O, Elliott CG, Geraci MW, Hanaoka M, Loyd JE, et al. Genetics and genomics of pulmonary arterial hypertension. *J Am Coll Cardiol*. 2009;54(1):S32–42.
9. Sztrymf B, Coulet F, Girerd B, Yaici A, Jais X, Sitbon O, et al. Clinical outcomes of pulmonary arterial hypertension in carriers of BMPR2 mutation. *Am J Respir Crit Care Med*. 2008;177(12):1377–83.
10. Deng Z, Morse JH, Slager SL, Cuervo N, Moore KJ, Venetos G, et al. Familial primary pulmonary hypertension (gene PPH1) is caused by mutations in the bone morphogenetic protein receptor-II gene. *Am J Hum Genet*. 2000;67(3):737–44.
11. Lane KB, Machado RD, Pauciulo MW, Thomson JR, Phillips JA, Loyd JE, et al. Heterozygous germline mutations in BMPR2, encoding a TGF- β receptor, cause familial primary pulmonary hypertension. *Nat Genet*. 2000;26(1):81–4.
12. Cogan JD, Pauciulo MW, Batchman AP, Prince MA, Robbins IM, Hedges LK, et al. High frequency of BMPR2 exonic deletions/duplications in familial pulmonary arterial hypertension. *Am J Respir Crit Care Med*. 2006;174(5):590–8.
13. Thomson JR, Machado RD, Pauciulo MW, Morgan NV, Humbert M, Elliott GC, et al. Sporadic primary pulmonary hypertension is associated with germline mutations of the gene encoding BMPR-II, a receptor member of the TGF- β family. *J Med Genet*. 2000;37(10): 741–5.
14. Humbert M. Update in pulmonary arterial hypertension 2007. *Am J Respir Crit Care Med*. 2008;177(6):574–9.
15. Shintani M, Yagi H, Nakayama T, Saji T, Matsuoka R. A new nonsense mutation of SMAD8 associated with pulmonary arterial hypertension. *J Med Genet*. 2009;46(5):331–7.
16. Nasim MT, Ogo T, Ahmed M, Randall R, Chowdhury HM, Snape KM, et al. Molecular genetic characterization of SMAD signaling molecules in pulmonary arterial hypertension. *Hum Mutat*. 2011;32(12):1385–9.
17. Hagen M, Fagan K, Steudel W, Carr M, Lane K, Rodman DM, et al. Interaction of interleukin-6 and the BMP pathway in pulmonary smooth muscle. *Am J Physiol Lung Cell Mol Physiol*. 2007;292(6):L1473–9.
18. Ma L, Roman-Campos D, Austin ED, Eyries M, Sampson KS, Soubrier F, et al. A novel channelopathy in pulmonary arterial hypertension. *N Engl J Med*. 2013;369(4):351–61.
19. Austin ED, Loyd JE. The genetics of pulmonary arterial hypertension. *Circ Res*. 2014;115(1):189–202.
20. Kuhr FK, Smith KA, Song MY, Levitan I, Yuan JX-J. New mechanisms of pulmonary arterial hypertension: role of Ca²⁺ signaling. *Am J Physiol Heart Circ Physiol*. 2012;302(8): H1546–62.

21. Soon E, Holmes AM, Treacy CM, Doughty NJ, Southgate L, Machado RD, et al. Elevated levels of inflammatory cytokines predict survival in idiopathic and familial pulmonary arterial hypertension. *Circulation*. 2010;122(9):920–7.
22. Cracowski JL, Chabot F, Labarère J, Faure P, Degano B, Schwebel C, et al. Proinflammatory cytokine levels are linked to death in pulmonary arterial hypertension. *Eur Respir J*. 2014;43(3):915–7.
23. Heresi GA, Aytekin M, Hammel JP, Wang S, Chatterjee S, Dweik RA. Plasma interleukin-6 adds prognostic information in pulmonary arterial hypertension. *Eur Respir J*. 2014;43(3): 912–4.
24. Rabinovitch M, Guignabert C, Humbert M, Nicolls MR. Inflammation and immunity in the pathogenesis of pulmonary arterial hypertension. *Circ Res*. 2014;115(1):165–75.
25. Tamosiuniene R, Tian W, Dhillon G, Wang L, Sung YK, Gera L, et al. Regulatory T cells limit vascular endothelial injury and prevent pulmonary hypertension. *Circ Res*. 2011;109(8):867–79.
26. Huertas A, Tu L, Gambaryan N, Girerd B, Perros F, Montani D, et al. Leptin and regulatory T-lymphocytes in idiopathic pulmonary arterial hypertension. *Eur Respir J*. 2012;40(4): 895–904.
27. Ormiston ML, Chang C, Long LL, Soon E, Jones D, Machado R, et al. Impaired natural killer cell phenotype and function in idiopathic and heritable pulmonary arterial hypertension. *Circulation*. 2012;126(9):1099–109.
28. Perros F, Dorfmueller P, Souza R, Durand-Gasselín I, Mussot S, Mazmanian M, et al. Dendritic cell recruitment in lesions of human and experimental pulmonary hypertension. *Eur Respir J*. 2007;29(3):462–8.
29. Dib H, Tamby MC, Bussone G, Regent A, Berezne A, Lafi ne C, et al. Targets of anti- endothelial cell antibodies in pulmonary hypertension and scleroderma. *Eur Respir J*. 2012;39(6):1405–14.
30. Tamby MC. Antibodies to fibroblasts in idiopathic and scleroderma-associated pulmonary hypertension. *Eur Respir J*. 2006;28(4):799–807.
31. Rich S, Kieras K, Hart K, Groves BM, Stobo JD, Brundage BH. Antinuclear antibodies in primary pulmonary hypertension. *J Am Coll Cardiol*. 1986;8(6):1307–11.
32. Rich S, Kieras K, Hart K, Groves BM, Stobo JD, Brundage BH. Antinuclear antibodies in primary pulmonary hypertension. *J Am Coll Cardiol*. 1986;8(6):1307–11.
33. Tamby MC. Anti-endothelial cell antibodies in idiopathic and systemic sclerosis associated pulmonary arterial hypertension. *Thorax*. 2005;60(9):765–72.
34. Dewachter L, Adnot S, Fadel E, Humbert M, Maitre B, Barlier-Mur A-M, et al. Angiotensin/Tie2 pathway influences smooth muscle hyperplasia in idiopathic pulmonary hypertension. *Am J Respir Crit Care Med*. 2006;174(9):1025–33.
35. Izikki M, Guignabert C, Fadel E, Humbert M, Tu L, Zadigue P, et al. Endothelial-derived FGF2 contributes to the progression of pulmonary hypertension in humans and rodents. *J Clin Invest*. 2009;119(3):512–23.
36. Tu L, Dewachter L, Gore B, Fadel E, Darteville P, Simonneau G, et al. Autocrine fibroblast growth factor-2 signaling contributes to altered endothelial phenotype in pulmonary hypertension. *Am J Respir Cell Mol Biol*. 2011;45(2):311–22.
37. Ricard N, Tu L, Le Hiress M, Huertas A, Phan C, Thuillet R, et al. Increased pericyte coverage mediated by endothelial-derived fibroblast growth factor-2 and interleukin-6 is a source of smooth muscle-like cells in pulmonary hypertension. *Circulation*. 2014;129(15):1586–97.
38. Masri FA, Xu W, Comhair SAA, Asosingh K, Koo M, Vasanji A, et al. Hyperproliferative apoptosis-resistant endothelial cells in idiopathic pulmonary arterial hypertension. *Am J Physiol Lung Cell Mol Physiol*. 2007;293(3):L548–54.
39. Bonnet S. An abnormal mitochondrial-hypoxia inducible factor-1 -Kv channel pathway disrupts oxygen sensing and triggers pulmonary arterial hypertension in fawn hooded rats: similarities to human pulmonary arterial hypertension. *Circulation*. 2006;113(22): 2630–41.
40. Tu L, De Man FS, Girerd B, Huertas A, Chaumais M-C, Lecerf F, et al. A critical role for p130 Cas in the progression of pulmonary hypertension in humans and rodents. *Am J Respir Crit Care Med*. 2012;186(7):666–76.
41. Eddahibi S, Humbert M, Fadel E, Raffestin B, Darmon M, Capron F, et al. Serotonin transporter overexpression is responsible for pulmonary artery smooth muscle hyperplasia in primary pulmonary hypertension. *J Clin Invest*. 2001;108(8):1141–50.
42. Humbert M, Evgenov OV, Stasch J-P, editors. *Pharmacotherapy of pulmonary hypertension*. Berlin/Heidelberg: Springer; 20[cited 2014 Aug 17]. Available from: <http://link.springer.com/10.1007/978-3-642-38664-0>.
43. Merklinger SL. Epidermal growth factor receptor blockade mediates smooth muscle cell apoptosis and improves survival in rats with pulmonary hypertension. *Circulation*. 2005;112(3):423–31.
44. Schermuly RT. Reversal of experimental pulmonary hypertension by PDGF inhibition. *J Clin Invest*. 2005;115(10):2811–21.
45. Xu W, Koeck T, Lara AR, Neumann D, DiFilippo FP, Koo M, et al. Alterations of cellular bioenergetics in pulmonary artery endothelial cells. *Proc Natl Acad Sci*. 2007;104(4): 1342–7.
46. Tuder RM, Davis LA, Graham BB. Targeting energetic metabolism: a New frontier in the pathogenesis and treatment of pulmonary hypertension. *Am J Respir Crit Care Med*. 2012;185(3):260–6.
47. Archer SL, Gomberg-Maitland M, Maitland ML, Rich S, Garcia JGN, Weir EK. Mitochondrial metabolism, redox signaling, and fusion: a mitochondria-ROS-HIF-1 -Kv1.5 O₂-sensing pathway at the intersection of pulmonary hypertension and cancer. *Am J Physiol Heart Circ Physiol*. 2008;294(2):H570–8.
48. Stacher E, Graham BB, Hunt JM, Gandjeva A, Groshong SD, McLaughlin VV, et al. Modern age pathology of pulmonary arterial hypertension. *Am J Respir Crit Care Med*. 2012;186(3):261–72.
49. Miyata M, Sakuma F, Yoshimura A, Ishikawa H, Nishimaki T, Kasukawa R. Pulmonary hypertension in rats. 2. Role of interleukin-6. *Int Arch Allergy Immunol*. 1995;108(3):287–91.
50. Golembeski SM, West J, Tada Y, Fagan KA. Interleukin-6 causes mild pulmonary hypertension and augments hypoxia-induced pulmonary hypertension in mice. *CHEST J*. 2005;128(6_Suppl):572S–3.
51. Savale L, Tu L, Rideau D, Izikki M, Maitre B, Adnot S, et al. Impact of interleukin-6 on hypoxia-induced pulmonary hypertension and lung inflammation in mice. *Respir Res*. 2009;10(1):6.
52. Steiner MK, Syrkinina OL, Kolliputi N, Mark EJ, Hales CA, Waxman AB. Interleukin-6 overexpression induces pulmonary hypertension. *Circ Res*. 2009;104(2):236–44.
53. Zhang Y, Talwar A, Tsang D, Bruchfeld A, Sadoughi A, Hu M, et al. Macrophage migration inhibitory factor mediates hypoxia-induced pulmonary hypertension. *Mol Med*. 2012;18(1):215.
54. Zhang B, Shen M, Xu M, Liu L-L, Luo Y, Xu D-Q, et al. Role of macrophage migration inhibitory factor in the proliferation of smooth muscle cell in pulmonary hypertension. *Mediators Inflamm*. 2012;1–10.
55. Bernhagen J, Krohn R, Lue H, Gregory JL, Zernecke A, Koenen RR, et al. MIF is a noncognate ligand of CXC chemokine receptors in inflammatory and atherogenic cell recruitment. *Nat Med*. 2007;13(5):587–96.
56. Cool CD, Stewart JS, Werahera P, Miller GJ, Williams RL, Voelkel NF, et al. Three-dimensional reconstruction of pulmonary arteries in plexiform pulmonary hypertension using cell-specific markers: evidence for a dynamic and heterogeneous process of pulmonary endothelial cell growth. *Am J Pathol*. 1999;155(2):411–9.
57. Pietra GG, Edwards WD, Kay JM, Rich S, Kernis J, Schloo B, et al. Histopathology of primary pulmonary hypertension. A qualitative and quantitative study of pulmonary blood vessels from 58 patients in the National Heart, Lung, and Blood Institute, Primary Pulmonary Hypertension Registry. *Circulation*. 1989;80(5):1198–206.
58. Bjornsson J, Edwards WD. Primary pulmonary hypertension: a histopathologic study of 80 cases. *Mayo Clin Proc*. 1985;60(1):16–25.
59. Schermuly RT, Ghofrani HA, Wilkins MR, Grimminger F. Mechanisms of disease: pulmonary arterial hypertension. *Nat Rev Cardiol*. 2011;8(8):443–55.
60. White RJ, Meoli DF, Swarthout RF, Kallop DY, Galaria II, Harvey JL, et al. Plexiform-like lesions and increased tissue factor expression in a rat model of severe pulmonary arterial hypertension. *Am J Physiol Lung Cell Mol Physiol*. 2007;293(3):L583–90.
61. Johnson SR, Granton JT, Mehta S. Thrombotic arteriopathy and anticoagulation in pulmonary hypertension. *CHEST J*. 2006;130(2):545–52.

61. Kuehne T. Magnetic resonance imaging analysis of right ventricular pressure-volume loops: in vivo validation and clinical application in patients with pulmonary hypertension. *Circulation*. 2004;110(14):2010–6.
62. Handoko ML, de Man FS, Allaart CP, Paulus WJ, Westerhof N, Vonk-Noordegraaf A. Perspectives on novel therapeutic strategies for right heart failure in pulmonary arterial hypertension: lessons from the left heart. *Eur Respir Rev*. 2010;19(115):72–82.
63. De Man FS, Handoko ML, Guignabert C, Bogaard HJ, Vonk-Noordegraaf A. Neurohormonal axis in patients with pulmonary arterial hypertension: friend or foe? *Am J Respir Crit Care Med*. 2013;187(1):14–9.
64. Ciarka A, Doan V, Velez-Roa S, Naeije R, van de Borne P. Prognostic significance of sympathetic nervous system activation in pulmonary arterial hypertension. *Am J Respir Crit Care Med*. 2010;181(11):1269–75.
65. De Man FS, Tu L, Handoko ML, Rain S, Ruiter G, François C, et al. Dysregulated renin-angiotensin-aldosterone system contributes to pulmonary arterial hypertension. *Am J Respir Crit Care Med*. 2012;186(8):780–9.
66. Marcus JT, Gan CT-J, Zwanenburg JJM, Boonstra A, Allaart CP, Götte MJW, et al. Interventricular mechanical asynchrony in pulmonary arterial hypertension. *J Am Coll Cardiol*. 2008;51(7):750–7.
67. Rain S, Handoko ML, Trip P, Gan CT-J, Westerhof N, Stienen GJ, et al. Right ventricular diastolic impairment in patients with pulmonary arterial hypertension. *Circulation*. 2013;128(18):2016–25.
68. Rain S, Bos Dda S, Handoko ML, Westerhof N, Stienen G, Ottenheijm C, et al. Protein changes contributing to right ventricular cardiomyocyte diastolic dysfunction in pulmonary arterial hypertension. *J Am Heart Assoc*. 2014;3(3):e000716.
69. Vogel-Claussen J, Skrok J, Shehata ML, Singh S, Sibley CT, Boyce DM, et al. Right and left ventricular myocardial perfusion reserves correlate with right ventricular function and pulmonary hemodynamics in patients with pulmonary arterial hypertension 1. *Radiology*. 2011;258(1):119–27.
70. Bogaard HJ, Natarajan R, Henderson SC, Long CS, Kraskauskas D, Smithson L, et al. Chronic pulmonary artery pressure elevation is insufficient to explain right heart failure. *Circulation*. 2009;120(20):1951–60.
71. Nagaya N, Goto Y, Satoh T, Uematsu M, Hamada S, Kuribayashi S, et al. Impaired regional fatty acid uptake and systolic dysfunction in hypertrophied right ventricle. *J Nucl Med*. 1998;39:1676–80.
72. Piao L, Fang YH, Cadete VJ, Wietholt C, Urboniene D, Toth PT, et al. The inhibition of pyruvate dehydrogenase kinase improves impaired cardiac function and electrical remodeling in two models of right ventricular hypertrophy: resuscitating the hibernating right ventricle. *J Mol Med*. 2010;88(1):47–60.
73. Schermuly RT, Stasch J-P, Pullamsetti SS, Middendorff R, Müller D, Schlüter K-D, et al. Expression and function of soluble guanylate cyclase in pulmonary arterial hypertension. *Eur Respir J*. 2008;32(4):881–91.
74. Morrell N, Archer S, DeFelice A, Evans S, Fiszman M, Martin T, et al. Anticipated classes of new medications and molecular targets for pulmonary arterial hypertension. *Pulm Circ*. 2013;3(1):226.
75. Humbert M, Sitbon O, Simonneau G. Treatment of pulmonary arterial hypertension. *N Engl J Med*. 2004;351(14):1425–36.
76. Wu Y, O'Callaghan DS, Humbert M. An update on medical therapy for pulmonary arterial hypertension. *Curr Hypertens Rep*. 2013;15(6):614–22.
77. Rich S, Kaufmann E, Levy PS. The effect of high doses of calcium-channel blockers on survival in primary pulmonary hypertension. *N Engl J Med*. 1992;327(2):76–81.
78. Tantini B, Manes A, Fiumana E, Pignatti C, Guarnieri C, Zannoli R, et al. Antiproliferative effect of sildenafil in human pulmonary artery smooth muscle cells. *Basic Res Cardiol*. 2005;100(2):131–8.
79. Sitbon O. Long-term response to calcium channel blockers in idiopathic pulmonary arterial hypertension. *Circulation*. 2005;111(23):3105–11.
80. Ghofrani H-A, Galiè N, Grimminger F, Grünig E, Humbert M, Jing Z-C, et al. Riociguat for the treatment of pulmonary arterial hypertension. *N Engl J Med*. 2013;369(4):330–40.
81. Galiè N, Ghofrani HA, Torbicki A, Barst RJ, Rubin LJ, Badesch D, et al. Sildenafil citrate therapy for pulmonary arterial hypertension. *N Engl J Med*. 2005;353(20):2148–57.
82. Sastry BKS, Narasimhan C, Reddy NK, Raju BS. Clinical efficacy of sildenafil in primary pulmonary hypertension. *J Am Coll Cardiol*. 2004;43(7):1149–53.
83. Singh TP, Rohit M, Grover A, Malhotra S, Vijayvergiya R. A randomized, placebo-controlled, double-blind, crossover study to evaluate the efficacy of oral sildenafil therapy in severe pulmonary artery hypertension. *Am Heart J*. 2006;151(4):851.e1–5.
84. Simonneau G, Rubin LJ, Galiè N, Barst RJ, Fleming TR, Frost AE, et al. Addition of sildenafil to long-term intravenous epoprostenol therapy in patients with pulmonary arterial hypertension A randomized trial. *Ann Intern Med*. 2008;149(8):521–30.
85. Iversen K, Jensen AS, Jensen TV, Vejstrup NG, Sondergaard L. Combination therapy with bosentan and sildenafil in Eisenmenger syndrome: a randomized, placebo-controlled, double-blind trial. *Eur Heart J*. 2010;31(9):1124–31.
86. Galiè N, Brundage BH, Ghofrani HA, Oudiz RJ, Simonneau G, Safdar Z, et al. Tadalafil therapy for pulmonary arterial hypertension. *Circulation*. 2009;119(22):2894–903.
87. Oudiz RJ, Brundage BH, Galiè N, Ghofrani HA, Simonneau G, Botros FT, et al. Tadalafil for the treatment of pulmonary arterial hypertension. *J Am Coll Cardiol*. 2012;60(8):768–74.
88. Galiè N, Humbert M, Vachiéry J-L, Vizza C, Kneussl M, Manes A, et al. Effects of beraprost sodium, an oral prostacyclin analogue, in patients with pulmonary arterial hypertension: a randomized, double-blind, placebo-controlled trial. *J Am Coll Cardiol*. 2002;39(9):1496–502.
89. Barst RJ, McGoan M, McLaughlin V, Tapson V, Oudiz R, Shapiro S, et al. Beraprost therapy for pulmonary arterial hypertension. *J Am Coll Cardiol*. 2003;41(12):2119–25.
90. Rubin LJ, Mendoza J, Hood M, McGoan M, Barst R, Williams WB, et al. Treatment of primary pulmonary hypertension with continuous intravenous prostacyclin (epoprostenol) results of a randomized trial. *Ann Intern Med*. 1990;112(7):485–91.
91. Barst RJ, Rubin LJ, Long WA, McGoan MD, Rich S, Badesch DB, et al. A comparison of continuous intravenous epoprostenol (prostacyclin) with conventional therapy for primary pulmonary hypertension. *N Engl J Med*. 1996;334(5):296–301.
92. Olschewski H, Simonneau G, Galiè N, Higenbottam T, Naeije R, Rubin LJ, et al. Inhaled iloprost for severe pulmonary hypertension. *N Engl J Med*. 2002;347(5):322–9.
93. McLaughlin VV, Oudiz RJ, Frost A, Tapson VF, Murali S, Channick RN, et al. Randomized study of adding inhaled iloprost to existing bosentan in pulmonary arterial hypertension. *Am J Respir Crit Care Med*. 2006;174(11):1257–63.
94. Hoeper MM. Combining inhaled iloprost with bosentan in patients with idiopathic pulmonary arterial hypertension. *Eur Respir J*. 2006;28(4):691–4.
95. Simonneau G, Barst RJ, Galiè N, Naeije R, Rich S, Bourge RC, et al. Continuous subcutaneous infusion of treprostinil, a prostacyclin analogue, in patients with pulmonary arterial hypertension: a double-blind, randomized, placebo-controlled trial. *Am J Respir Crit Care Med*. 2002;165(6):800–4.
96. McLaughlin VV, Benza RL, Rubin LJ, Channick RN, Voswinkel R, Tapson VF, et al. Addition of inhaled treprostinil to oral therapy for pulmonary arterial hypertension. *J Am Coll Cardiol*. 2010;55(18):1915–22.
97. Tapson VF, Torres F, Kermeen F, Keogh AM, Allen RP, Frantz RP, et al. Oral treprostinil for the treatment of pulmonary arterial hypertension in patients on background endothelin receptor antagonist and/or phosphodiesterase type 5 inhibitor therapy (the FREEDOM-C study): a randomized controlled trial. *CHEST J*. 2012;142(6):1383–90.
98. Tapson VF, Jing Z-C, Xu K-F, Pan L, Feldman J, Kiely DG, et al. Oral treprostinil for the treatment of pulmonary arterial hypertension in patients receiving background endothelin receptor antagonist and phosphodiesterase type 5 inhibitor therapy (the FREEDOM-C2 study) treprostinil for pulmonary arterial hypertension A randomized controlled trial. *CHEST J*. 2013;144(3):952–8.
99. Jing Z-C, Parikh K, Pulido T, Jerjes-Sanchez C, White RJ, Allen R, et al. Efficacy and safety of oral treprostinil monotherapy for the treatment of pulmonary arterial hypertension: a randomized. *Control Trial Circ*. 2013;127(5):624–33.

100. Galie N, Olschewski H, Oudiz RJ, Torres F, Frost A, Ghofrani HA, et al. Ambrisentan for the treatment of pulmonary arterial hypertension: results of the ambrisentan in pulmonary arterial hypertension, randomized, double-blind, placebo-controlled, multicenter, efficacy (ARIES) study 1 and 2. *Circulation*. 2008;117(23):3010–9.
101. Channick RN, Simonneau G, Sitbon O, Robbins IM, Frost A, Tapson VF, et al. Effects of the dual endothelin-receptor antagonist bosentan in patients with pulmonary hypertension: a randomized placebo controlled study. *Lancet*. 2001;358(9288):1119–23.
102. Sitbon O, Badesch DB, Channick RN, Frost A, Robbins IM, Simonneau G, et al. Effects of the dual endothelin receptor antagonist bosentan in patients with pulmonary arterial hypertension a 1-year follow-up study. *CHEST J*. 2003;124(1):247–54.
103. Rubin LJ, Badesch DB, Barst RJ, Galie N, Black CM, Keogh A, et al. Bosentan therapy for pulmonary arterial hypertension. *N Engl J Med*. 2002;346(12):896–903.
104. Humbert M. Combination of bosentan with epoprostenol in pulmonary arterial hypertension: BREATHE-2. *Eur Respir J*. 2004;24(3):353–9.
105. Galie N, Rubin LJ, Hoeper MM, Jansa P, Al-Hiti H, Meyer GMB, et al. Treatment of patients with mildly symptomatic pulmonary arterial hypertension with bosentan (EARLY study): a double-blind, randomised controlled trial. *Lancet*. 2008;371:2093–100.
106. Pulido T, Adzerikho I, Channick RN, Delcroix M, Galie N, Ghofrani H-A, et al. Macitentan and morbidity and mortality in pulmonary arterial hypertension. *N Engl J Med*. 2013;369(9):809–18.
107. Galie N, Palazzini M, Manes A. Pulmonary arterial hypertension: from the kingdom of the near-dead to multiple clinical trial meta-analyses. *Eur Heart J*. 2010;31(17):2080–6.
108. Kemp K, Savale L, O'Callaghan DS, Jaïs X, Montani D, Humbert M, et al. Usefulness of first-line combination therapy with epoprostenol and bosentan in pulmonary arterial hypertension: an observational study. *J Heart Lung Transplant*. 2012;31(2):150–8.
109. Galie N, Corris PA, Frost A, Girgis RE, Granton J, Jing ZC, et al. Updated treatment algorithm of pulmonary arterial hypertension. *J Am Coll Cardiol*. 2013;62(25):D60–72.
110. McLaughlin VV. Pulmonary arterial hypertension. *Circulation*. 2006;114(13):1417–31.
111. Packer M, Medina N, Yushak M, Wiener I. Detrimental effects of verapamil in patients with primary pulmonary hypertension. *Br Heart J*. 1984;52(1):106–11.
112. Chin KM, Badesch DB, Robbins IM, Tapson VF, Palevsky HI, Kim NH, et al. Two formulations of epoprostenol sodium in the treatment of pulmonary arterial hypertension: EPITOME-1 (epoprostenol for injection in pulmonary arterial hypertension), a phase IV, open-label, randomized study. *Am Heart J*. 2014;167(2):218–25.e1.
113. Desole S, Velik-Salchner C, Fraedrich G, Ewert R, Kähler CM. Subcutaneous implantation of a new intravenous pump system for prostacyclin treatment in patients with pulmonary arterial hypertension. *Heart Lung J Acute Crit Care*. 2012;41(6):599–605.
114. Katz WE, Gasior TA, Quinlan JJ, Lazar JM, Firestone L, Griffith BP, et al. Immediate effects of lung transplantation on right ventricular morphology and function in patients with variable degrees of pulmonary hypertension. *J Am Coll Cardiol*. 1996;27(2):384–91.
115. Ritchie M, Waggoner AD, Dávila-román VG, Barzilai B, Trulock EP, Eisenberg PR. Echocardiographic characterization of the improvement in right ventricular function in patients with severe pulmonary hypertension after single-lung transplantation. *J Am Coll Cardiol*. 1993;22(4):1170–4.
116. Yusef RD, Christie JD, Edwards LB, Kucheryavaya AY, Benden C, Dipchand AI, et al. The registry of the international society for heart and lung transplantation: thirtieth adult lung and heart-lung transplant report—2013; focus theme: age. *J Heart Lung Transplant*. 2013;32(10):965–78.
117. Gomez-Arroyo J, Sandoval J, Simon MA, Dominguez-Cano E, Voelkel NF, Bogaard HJ. Treatment for pulmonary arterial hypertension-associated right ventricular dysfunction. *Ann Am Thorac Soc*. 2014;11(7):1101–15.
118. Khan J, Idrees M. Saudi guidelines on the diagnosis and treatment of pulmonary hypertension: pregnancy in pulmonary hypertension. *Ann Thorac Med*. 2014;9(5):108.
119. Weiss BM, Zemp L, Seifert B, Hess OM. Outcome of pulmonary vascular disease in pregnancy: a systematic overview from 1978 through 1996. *J Am Coll Cardiol*. 1998;31(7):1650–7.
120. Harzheim D, Klose H, Pinado FP, Ehlken N, Nagel C, Fischer C, et al. Anxiety and depression disorders in patients with pulmonary arterial hypertension and chronic thromboembolic pulmonary hypertension. *Respir Res*. 2013;14:104.
121. Godinas L, Guignabert C, Seferian A, Perros F, Bergot E, Sibille Y, et al. Tyrosine kinase inhibitors in pulmonary arterial hypertension: a double-edge sword? *Semin Respir Crit Care Med*. 2013;34(05):714–24.
122. Nakagawa O, Fujisawa K, Ishizaki T, Saito Y, Nakao K, Narumiya S. ROCK-I and ROCK-II, two isoforms of Rho-associated coiled-coil forming protein serine/threonine kinase in mice. *Fed Eur Biochem Soc*. 1996;392(2):189–93.
123. Abe K. Long-term treatment with a Rho-kinase inhibitor improves monocrotaline-induced fatal pulmonary hypertension in rats. *Circ Res*. 2004;94(3):385–93.
124. Fagan KA. Attenuation of acute hypoxic pulmonary vasoconstriction and hypoxic pulmonary hypertension in mice by inhibition of Rho-kinase. *Am J Physiol Lung Cell Mol Physiol*. 2004;287(4):L656–64.
125. Nagaoka T. Rho/Rho kinase signaling mediates increased basal pulmonary vascular tone in chronically hypoxic rats. *Am J Physiol Lung Cell Mol Physiol*. 2004;287(4):L665–72.
126. Nagaoka T, Fagan KA, Gebb SA, Morris KG, Suzuki T, Shimokawa H, et al. Inhaled Rho kinase inhibitors are potent and selective vasodilators in rat pulmonary hypertension. *Am J Respir Crit Care Med*. 2005;171(5):494–9.
127. Oka M, Homma N, Taraseviciene-Stewart L, Morris KG, Kraskauskas D, Burns N, et al. Rho kinase-mediated vasoconstriction is important in severe occlusive pulmonary arterial hypertension in rats. *Circ Res*. 2007;100(6):923–9.
128. Guilluy C, Eddahibi S, Agard C, Guignabert C, Izikki M, Tu L, et al. RhoA and Rho kinase activation in human pulmonary hypertension: role of 5-HT signaling. *Am J Respir Crit Care Med*. 2009;179(12):1151–8.
129. Mouchaers KTB, Schaliij I, de Boer MA, Postmus PE, van Hinsbergh VWM, van Nieuw Amerongen GP, et al. Fasudil reduces monocrotaline-induced pulmonary arterial hypertension: comparison with bosentan and sildenafil I. *Eur Respir J*. 2010;36(4):800–7.
130. Guilluy C, Sauzeau V, Rolli-Derkinderen M, Guérin P, Sagan C, Pacaud P, et al. Inhibition of RhoA/Rho kinase pathway is involved in the beneficial effect of sildenafil I on pulmonary hypertension. *Br J Pharmacol*. 2005;146(7):1010–8.
131. Guilluy C, Rolli-Derkinderen M, Tharaux P-L, Melino G, Pacaud P, Loirand G. Transglutaminase-dependent RhoA activation and depletion by serotonin in vascular smooth muscle cells. *J Biol Chem*. 2007;282(5):2918–28.
132. Wei L, Warburton RR, Preston IR, Roberts KE, Comhair SAA, Erzurum SC, et al. Serotonylated fibronectin is elevated in pulmonary hypertension. *Am J Physiol Lung Cell Mol Physiol*. 2012;302(12):L1273–9.
133. Spiekerkoetter E, Tian X, Cai J, Hopper RK, Sudheendra D, Li CG, et al. FK506 activates BMPR2, rescues endothelial dysfunction, and reverses pulmonary hypertension. *J Clin Invest*. 2013;123(8):3600–13.
134. Van de Veerdonk MC, Kind T, Marcus JT, Mauritz G-J, Heymans MW, Bogaard H-J, et al. Progressive right ventricular dysfunction in patients with pulmonary arterial hypertension responding to therapy. *J Am Coll Cardiol*. 2011;58(24):2511–9.
135. Rich S, Seidlitz M, Dodin E, Osimani D, Judd D, Genthner D, et al. The short-term effects of digoxin in patients with right ventricular dysfunction from pulmonary hypertension. *Chest*. 1998;114(3):787–92.
136. Drake JJ, Bogaard HJ, Mizuno S, Clifton B, Xie B, Gao Y, et al. Molecular signature of a right heart failure program in chronic severe pulmonary hypertension. *Am J Respir Cell Mol Biol*. 2011;45(6):1239–47.
137. Bogaard HJ, Natarajan R, Mizuno S, Abbate A, Chang PJ, Chau VQ, et al. Adrenergic receptor blockade reverses right heart remodeling and dysfunction in pulmonary hypertensive rats. *Am J Respir Crit Care Med*. 2010;182(5):652–60.
138. De Man FS, Handoko ML, van Ballegoij JJM, Schaliij I, Bogaards SJP, Postmus PE, et al. Bisoprolol delays progression towards right heart failure in experimental pulmonary hypertension. *Circ Heart Fail*. 2012;5(1):97–105.

3

Chapter 3

Pneumonectomy combined with SU5416 induces severe pulmonary hypertension in rats

Happé CM, De Raaf MA, **Rol N**, Schalij I, Vonk Noordegraaf A, Westerhof N,
Voelkel N, de Man FS, Bogaard HJ

Abstract

Introduction

The SU5416+Hypoxia (SuHx) rat model a commonly used model of severe pulmonary arterial hypertension (PAH). Previous studies have shown that to induce PH in rats, administration of SU5416 alone is insufficient, but when administered together with a second hit such as hypoxia or immune modification, severe angioproliferative PH will ensue. Abnormal pulmonary blood flow (PBF) has since long been known to invoke pathological changes in the pulmonary vasculature. We tested the hypothesis that a combination of SU5416 administration and a left pneumonectomy (PNx) to induce an abnormal PBF in the contralateral lung is sufficient to induce severe PAH in rats. Disease progression over time was studied and compared with the SuHx model.

Methods

Sprague Dawley rats were subjected to standard SuHx protocol (SU5416 / 4 weeks of hypoxia) or SuPNx protocol (SU5416 + PNx). Comparisons between models were made at week 2 and 6 utilizing echocardiography to determine cardiac morphometry and function and right ventricle (RV) catheterization to determine RV pressures and function. Tissue and molecular analysis was performed to examine pulmonary vascular remodeling, proliferation, apoptosis and inflammation.

Results

Both SuHx and SuPNx models displayed extensive obliterative vascular remodeling leading to an increased right ventricular systolic pressure at week 6. Similar inflammatory response in the lung vasculature of both models was observed alongside increased endothelial cell proliferation and apoptosis.

Conclusion

This study described the SuPNx model which features severe PAH at 6 weeks and could serve as an alternative to the SuHx model. Our study together with previous studies on experimental models of pulmonary hypertension shows that the typical histopathological findings of PAH, including obliterative lesions, inflammation, increased cell turnover and ongoing apoptosis represent a final common pathway of a disease that can evolve as a consequence of a variety of insults to the lung vasculature.

Introduction

Pulmonary Arterial Hypertension (PAH) is a group of progressive diseases, characterized by obliteration of the small precapillary pulmonary vessels, termed angio-obliteration, resulting in increased pulmonary vascular resistance ultimately leading to right heart failure and death(31). The arterial changes are based on pathobiological mechanisms that are to some degree shared with cancer including hyperproliferative angiogenesis and altered endothelial cell biology(10, 25). At the same time it is well accepted that a disturbed blood flow may be important in the pathogenesis and pathobiology of PAH, in particular in those forms associated with congenital systemic to pulmonary shunts(3, 6) This concept is supported by animal studies based on disturbed blood flow, such as the monocrotaline (MCT) + pneumonectomy rat model(21, 42) and the MCT + aorta-caval shunt rat model(6, 38). A concept of 'wound healing gone awry' can connect the concepts of quasi-malignancy and flow-dependent alterations in the development of PAH(39).

Recently, we have characterized the Sugen-Hypoxia (SuHx) model by performing longitudinal histology and telemetric monitoring of the Right Ventricular Systolic Pressure (RVSP)(5, 36). We showed partial reversibility of pulmonary hypertension and RV hypertrophy in this model after return to a normoxic environment and also that subsequent disease progression in the model was not dependent on remodeling of the lung vascular media. As such, hypoxia-induced changes in pulmonary artery smooth muscle cells seemed not required to maintain the obliterative vascular phenotype in rats with advanced SuHx induced PAH(5). It has been hypothesized that the exuberant lumen obliterating cell growth in the SuHx lung vasculature is not fully dependent on the mechanism driven by hypoxia. Changes in pulmonary blood flow velocity, first driven by hypoxic vasoconstriction and later by vascular obliteration, may play an additional causative role in the evolution of abnormal vascular cell phenotypes in the SuHx model.

The fact that hypoxia is not an obligatory secondary hit in SU5416 induced angio-obliterative PAH is exemplified by the development of other SU5416 mediated animal models that lack the stimulus of hypoxia, such as the Sugen Ovalbumin model(20). The aim of the present study was to evaluate whether the combination of VEGF receptor blockade by SU5416 and an increase in pulmonary blood flow velocity, is sufficient to induce lung vascular cell proliferation and severe angioobliterative pulmonary lesions. To achieve this, the hypoxic component of the SuHx model was substituted by a left pneumonectomy, to create a Sugen Pneumonectomy (SuPNx) model. In addition to disease progression, functional endpoints were monitored and compared with the SuHx model.

Materials and methods

Animals

All experiments were approved by the Institutional Animal Care and Use Committee of the VU University and were conducted in accordance with the European Convention for the Protection of Vertebrate Animals used for Experimental and Other Scientific Purposes, and the Dutch Animal Experimentation Act. Male Sprague Dawley rats (n= 60, 6-8 weeks, Charles River, Sulzfeld, Germany) were housed in groups of 4 under controlled conditions (22°C, 12:12 h light/dark cycle). Food and water were available ad libitum in accordance with the animal care committee protocol (FYS12-18, FYS-13-01).

Study design

Rats were randomly divided between five groups: Control (Con), SU5416 (SU), Pneumonectomy (PNx), SU5416 + hypoxia (SuHx) and SU5416 + PNx (SuPNx) (fig1). The SuHx protocol was employed as previously described(5). Briefly, animals were injected with SU5416 (25 mg/kg, Tocris Bioscience, #3037, Bristol, United Kingdom) dissolved in carboxymethylcellulose (CMC) and exposed to hypoxia (10%) for four weeks followed by re-exposure to normoxia. PNx animals underwent a left pneumonectomy. Two days following PNx-surgery an injection of SU5416 was administered (25 mg/kg). The Con-group received only the solvent CMC. Echocardiography was utilized at baseline (pre-hypoxia/pre-surgery), week two and week six to determine cardiac morphometry and function. Two and six weeks post-surgery/post-hypoxia animals were anesthetized and right ventricle (RV) and left ventricle (LV) pressure measurements via catheterization were performed. Animals were killed via exsanguination and organs were weighed and processed for analysis.

Surgical Procedure

Thirty minutes prior to anaesthesia (Isoflurane; 4.0/2.5% induction/maintenance; 1:1 O₂/Air mix) and intubation (Teflon tube, 16 gauge) rats received an injection of buprenorphine analgesia (0,1 mg/kg). Rats were ventilated at a rate of 70/minute with a peak pressure of 10 cmH₂O and placed in half supine position on a heating pad. The surgical site was shaved and cleaned with chlorhexidine digluconate in 70% ethanol (Addedpharma, Oss, Netherlands). Heart rate, saturation and carbon dioxide levels were (measured via pulse oximetry) and temperatures were monitored at all times during the surgery. Thoracotomy was performed by opening the third intercostal space. Ventilation was briefly interrupted for a maximum of 30 seconds to fix the left lung outside the chest cavity with the use of Q-tips. Bronchus, artery and veins were ligated and the lung was removed. The thorax was closed by suturing of the muscular and dermal layers. After cessation of isoflurane administration animals were extubated and received an additional injection of sterile saline (3 ml) and Carprofen (4.0 mg/kg) subcutaneous (Rimdadyl, Pfizer, Capelle aan den IJssel, the Netherlands).

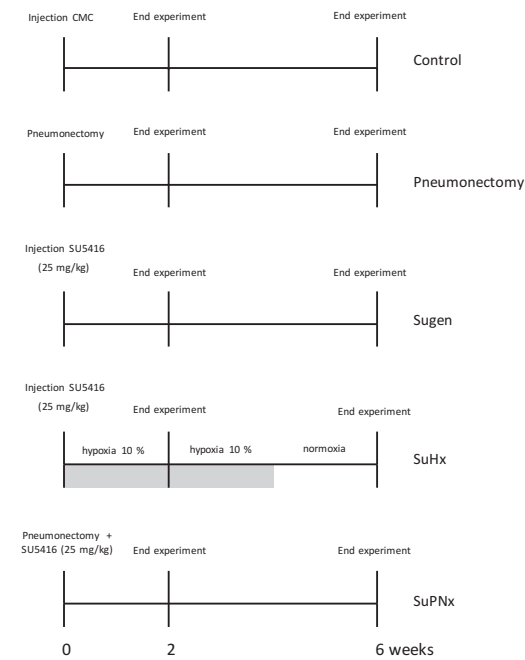


Figure 1 - Study design: 5 groups of n = 6 per time point. SuHx, SU5416 + hypoxia; SuPNx, SU5416 + pneumonectomy.

Echocardiography

Echocardiography was utilized at baseline, week two and week six. Measurements (ProSound SSD-4000, 13-MHz linear transducer #UST-5542, Aloka, Tokyo, Japan) were performed on anesthetized, spontaneously breathing rats (2,0% isoflurane, 1:1 O₂/Air mix). Time under anaesthesia was set to 15 minutes to minimise effects of isoflurane (12, 24). Measured parameters were pulmonary artery acceleration time (PAAT), right ventricular wall thickness (RVWT) and end diastolic diameter (RVEDD), cycle length (CL), tricuspid annular plane systolic excursion (TAPSE), cardiac output (CO), heart rate (HR) and stroke volume (SV). Non-invasive estimation of RV systolic pressures (eRVSP) and total pulmonary vascular resistance (TPR) was performed as described previously: $eRVSP = 142 \times e^{-11(p_{aat}/cl)}$; $TPR \approx [mean PAP]/[cardiac output] = (0.61 \times [eRVSP] + 2 \text{ mmHg})/[cardiac output]$ (13, 15, 11, 2, 30, 41). Analysis was performed offline (Tomtec Imaging systems, Unterschleissheim, Germany).

Right ventricle pressure measurements

At the end of the study protocol, open-chest RV catheterization was performed under general anesthesia in all animals (2.5% isoflurane, 1:1 O₂/air mix). Before the procedure, rats were intubated (Teflon tube, 16 gauge) and attached to a mechanical ventilator (Micro-Ventilator, UNO, Zevenaar, the Netherlands; ventilator settings: breathing

frequency, 70 breaths per minute; pressures, 12/0 cm H₂O; inspiratory/expiratory ratio, 1:1). RV pressures were recorded by use of a microtip pressure-volume conductance catheter (Millar Instruments, Houston, TX). Analyses were performed when steady state was reached over an interval of at least 10 seconds.

Histology and morphometry

Lungs were weighed and the airways of the right middle lobe were filled with 0.5% low-melt agarose in saline under constant pressure of 25 mmHg and stored in formaline (#4169-30, Klinipath BV, Duiven, the Netherlands). The remaining lobes were stored in liquid nitrogen for further processing. The heart was perfused with tyrode solution, weighed, dissected, snap-frozen in liquid nitrogen and stored in -80°C. Transversally cut lung sections (4µm) were stained with elastica van Gieson for analysis of vascular dimensions for week two and six. The degree of vascular occlusion was determined by counting 50 random vessels and expressing which percentage of these was categorized as occluded.

Immunofluorescent staining

Lungsections were deparaffinized and epitope retrieval was performed by immersing the slides in antigen unmasking solution (H3300, Vector Laboratories) for 40 minutes in a pressure cooker. Blocking steps with 1% bovine serum albumin were performed, before labeling with the primary antibody (PCNA, PC-10, sc-56), (Cleaved caspase 3, cell signaling, 9661), (CD08, sc-53063), (CD20, M-20, sc-7735), (CD68, abcam, ab31630) (1:250) O/N in 4°C, except for negative control. Subsequent labeling with appropriate secondary antibody, anti- α -smooth-muscle-actin – Cy3 (α -SMA, C6198, Sigma), Von Willebrand Factor (VWF, ab8822, Abcam) and 4'-diamidino-2-phenylindole (DAPI, H-1200, Vector Labs) counterstaining followed. Image acquisition was performed on a ZEISS Axiovert 200M Marianas inverted microscope.

Quantification of inflammation, proliferation and apoptotic activity

A minimum of 30 randomly selected vessels per sample was acquired via Slidebook imaging analysis software (SlideBook 5.5, Intelligent Imaging Innovations) Proliferation (PCNA) and apoptotic activity (CC3) was quantified by counting smooth muscle cell – or endothelial cells with a positive (PCNA or CC3) signal. Both values are expressed as number of positive (+) cells per vessel. Inflammation was quantified in a similar fashion, with the exception that positive cells in the lesions surrounding the vessel were included.

Statistical Analysis

All analyses were performed in a blinded fashion. All data were verified for normal distribution. A *p*-value <0,05 was considered significant. All data are presented as mean \pm SEM. Parameters were analysed by two-way ANOVA with Bonferroni post-hoc testing (GraphPad Prism for Windows 5.01, San Diego CA).

Results

Effect of SU5416- or pneumonectomy after 2 and 6 weeks

All animals survived the surgical procedure. No adverse effects of SU5416 with regard to post-operative wound healing were observed. Right lung mass was found to be increased in the pneumonectomy group compared to control both after 2 and 6 weeks of initiation experiment. Lung CD68 (macrophage) counts were found to be increased in the SU-group compared to control at week 2 (table 1 and 2) suggesting an inflammatory reaction to VEGFR inhibition. For ease of interpretation the following results will only include comparisons between control versus SuHx and SuPNx.

Table 1 - Characteristics of Sugen or pneumonectomy vs. control at 2 wk.

| | 2 weeks | | | | | | P-value |
|----------------------|---------|------------|-------|------------|-------|------------|---------|
| | CON | | SU | | PNX | | |
| PAAT/CL | 13,7 | \pm 4,9 | 16,9 | \pm 4,4 | 13,1 | \pm 2,1 | n.s. |
| RVWT (mm) | 1,0 | \pm 0,3 | 1,0 | \pm 0,1 | 0,9 | \pm 0,4 | n.s. |
| RVEDD (mm) | 2,3 | \pm 0,4 | 3,0 | \pm 0,3 | 2,8 | \pm 0,2 | n.s. |
| TAPSE (mm) | 3,2 | \pm 0,2 | 3,2 | \pm 0,3 | 2,9 | \pm 0,5 | n.s. |
| SV (ml) | 0,2 | \pm 0,06 | 0,2 | \pm 0,03 | 0,2 | \pm 0,06 | n.s. |
| HR (bpm) | 409,0 | \pm 23,6 | 384,7 | \pm 21,5 | 370,9 | \pm 23,0 | n.s. |
| CO (ml) | 88,2 | \pm 20,2 | 64,4 | \pm 10,4 | 80,3 | \pm 18,4 | n.s. |
| TPR (mmHg/ml.min) | 0,3 | \pm 0,1 | 0,3 | \pm 0,1 | 0,3 | \pm 0,1 | n.s. |
| eRVSP (mmHg) | 24,6 | \pm 2,2 | 26,9 | \pm 1,9 | 29,9 | \pm 2,0 | n.s. |
| RVSP (mmHg) | 25,4 | \pm 2,5 | 23,5 | \pm 1,9 | 29,6 | \pm 8,2 | n.s. |
| RV Ees (mmHg/ml) | 55,6 | \pm 22,2 | 52,3 | \pm 25,1 | 42,0 | \pm 17,3 | n.s. |
| RV Eed (mmHg/ml) | 3,1 | \pm 0,9 | 2,1 | \pm 0,9 | 3,4 | \pm 3,1 | n.s. |
| RV Ea (mmHg/ml) | 101,0 | \pm 33,0 | 143,0 | \pm 31,0 | 120,0 | \pm 32,5 | n.s. |
| Intima fraction (%) | 7,9 | \pm 1,3 | 10,1 | \pm 2,8 | 8,8 | \pm 0,5 | n.s. |
| Media fraction (%) | 10,5 | \pm 1,5 | 12,8 | \pm 1,3 | 14,1 | \pm 2,0 | n.s. |
| Right lung mass (gr) | 24,2 | \pm 3,1 | 41,9 | \pm 8,4 | 54,1 | \pm 13,5 | * 0,05 |
| Fulton/RV/(LV+S) | 0,3 | \pm 0,1 | 0,4 | \pm 0,2 | 0,4 | \pm 0,1 | n.s. |

CON, control; SU, SU5416; PNx, pneumonectomy; eRVSP, estimated right ventricle systolic pressure; PAAT/CL, pulmonary artery acceleration time/cycle length; RVWT, right ventricle wall thickness; RVEDD, right ventricle end diastolic diameter; TAPSE, tricuspid annular plane systolic excursion; SV, stroke volume; CO, cardiac output; TPR, total pulmonary resistance; Ees, RV contractility (end diastolic elastance); Eed, RV stiffness (end diastolic stiffness); Ea, RV afterload; n.s., not significant. **P* < 0.05 difference vs. control.

Table 2 - Characteristics of Sugen or pneumonectomy vs. control at 6 wk.

| | 6 weeks | | | P-VALUE |
|-----------------------|-------------|--------------|---------------|---------|
| | CON | SU | PNX | |
| PAAT/CL | 15,5 ± 3,5 | 11,8 ± 3,9 | 12,5 ± 2,2 | n.s. |
| RVWT (mm) | 1,1 ± 0,2 | 1,2 ± 0,3 | 1,4 ± 0,2 | n.s. |
| RVEDD (mm) | 3,9 ± 0,8 | 4,4 ± 0,9 | 4,9 ± 1,1 | n.s. |
| TAPSE (mm) | 2,6 ± 0,5 | 2,7 ± 0,6 | 2,7 ± 0,4 | n.s. |
| SV (ml) | 0,2 ± 0,05 | 0,2 ± 0,04 | 0,2 ± 0,03 | n.s. |
| HR (bpm) | 345,0 ± 8,0 | 333,0 ± 42,0 | 383,0 ± 23,0 | n.s. |
| CO (ml) | 80,9 ± 19,9 | 72,9 ± 15,6 | 69,7 ± 11,9 | n.s. |
| TPR (mmHg/ml.min) | 0,2 ± 0,1 | 0,3 ± 0,0 | 0,4 ± 0,1 | n.s. |
| eRVSP (mmHg) | 27,4 ± 4,0 | 24,4 ± 4,0 | 31,7 ± 2,1 | n.s. |
| RVSP (mmHg) | 22,9 ± 4,5 | 24,0 ± 6,3 | 25,2 ± 2,3 | n.s. |
| RV Ees (mmHg/ml) | 30,4 ± 10,0 | 33,9 ± 11,0 | 31,0 ± 11,8 | n.s. |
| RV Eed (mmHg/ml) | 2,3 ± 0,9 | 2,6 ± 0,8 | 1,8 ± 0,7 | n.s. |
| RV Ea (mmHg/ml) | 94,4 ± 52,9 | 112,3 ± 47,7 | 101,5 ± 24,4 | n.s. |
| Intima fraction (%) | 7,6 ± 0,1 | 12,0 ± 1,5 | 12,2 ± 1,6 | n.s. |
| Media fraction (%) | 12,0 ± 2,8 | 16,7 ± 2,4 | 21,2 ± 8,2 | n.s. |
| Right lung mass (gr) | 26,3 ± 2,2 | 30,5 ± 4,8 | 43,9 ± 12,5 * | 0,05 |
| Fulton/RV/(LV+S) | 0,2 ± 0,0 | 0,2 ± 0,1 | 0,3 ± 0,1 | n.s. |
| PCNA EC | 0,1 ± 0,1 | 0,1 ± 0,1 | 0,1 ± 0,1 | n.s. |
| PCNA SMC | 0,1 ± 0,1 | 0,2 ± 0,1 | 0,3 ± 0,1 | n.s. |
| Cleaved caspase-3 EC | 0,1 ± 0,1 | 0,2 ± 0,2 | 0,1 ± 0,1 | n.s. |
| Cleaved caspase-3 SMC | 0,3 ± 0,2 | 0,6 ± 0,2 | 0,4 ± 0,2 | n.s. |
| CD8 | 0,4 ± 0,2 | 0,6 ± 0,2 | 0,6 ± 0,2 | n.s. |
| CD20 | 0,3 ± 0,1 | 0,4 ± 0,2 | 0,4 ± 0,2 | n.s. |
| CD68 | 0,2 ± 0,1 | 0,9 ± 0,1* | 0,3 ± 0,1 | 0,05 |

CON, control; SU, SU5416; PNX, pneumonectomy; eRVSP, estimated right ventricle systolic pressure; PAAT/CL, pulmonary artery acceleration time/cycle length; RVWT, right ventricle wall thickness; RVEDD, right ventricle end diastolic diameter; TAPSE, tricuspid annular plane systolic excursion; SV, stroke volume; CO, cardiac output; TPR, total pulmonary resistance; Ees, RV contractility (end diastolic elastance); Eed, RV stiffness (end diastolic stiffness); Ea, RV afterload; PNCA, proliferating cell nuclear antigen; EC, endothelial cells; SMC, smooth muscle cells; n.s., not significant. * $P < 0.05$ difference vs. control.

Development of pulmonary hypertension in SuHx and SuPNx rats

RVSP was significantly elevated after two weeks in the SuHx model compared to Con, whereas no differences in RVSP were observed between SuPNx and control animals. However, Six weeks after initiation of the protocol, both SuHx and SuPNx demonstrated an elevated RVSP compared to Con (fig2A). RV afterload (Ea) was significantly increased in SuHx after two weeks. Ea was increased in both SuHx and SuPNx after 6 weeks

(fig2B). RV Contractility (Ees) increased in SuHx and SuPNx at week two compared to Con and remained so in at week 6 (fig2C). SuHx RV stiffness (Eed) was increased at week two, while no differences between groups were observed at week 6 (fig2D).

Total pulmonary resistance (TPR) was increased in SuHx after week two and in both SuHx and SuPNx at week six, which was in accordance with the increased Ea (fig3A). No significant differences in cardiac output (CO) were observed between groups (fig3B). RV wall thickness (RVWT) and end diastolic diameter (RVEDD) were increased at week two in SuHx rats when compared to both Con and SuPNx, whilst after six weeks, RVWT and RVEDD were increased in SuHx and SuPNx rats alike (fig3CD). Tricuspid annular plane excursion time (TAPSE) was decreased in SuHx at week two compared to Control animals. Both SuHx and SuPNx showed a decline in TAPSE at week 6 (fig3E). Pulmonary artery acceleration time / cycle length (PAAT/CL) was reduced in both SuHx and SuPNx at week six compared to control animals (fig 3F).

Right lung mass was increased at both time points in the SuPNx group, compared to Con and SuHx (fig4A). SuHx left lung mass was increased compared to Con at week two (Con: 16.8±.7 vs SuHx: 26.95±0.8; $p < 0.01$) and six (Con: 16.7±3 vs SuHx: 22.4±1.4; $p < 0.01$). At week two, the Fulton index in SuHx was higher when compared to Control and SuPNx animals. At week six both SuHx and SuPNx showed an increased Fulton index compared to Control animals (fig 4B). The hematocrit levels were increased in the SuHx model at week two (hypoxic period) (fig 4C). Bodymass of SuHx was lower compared to Con at week two. Both SuHx and SuPNx bodymass was decreased at week six compared to control (fig4D).

Increased intimal fraction accompanied by obliterative lesions in SuHx and SuPNx

Vascular wall media fraction was already increased in SuPNx at week two, when compared to Con and SuHx, with similar elevated fractions of both SuHx and SuPNx at week six. In contrast, intimal fraction increased in the SuHx group at week two, with similar fractions between SuHx and SuPNx at week six (fig5AB). An increase in occlusive lesions was observed in both SuHx and SuPNx at week 2 and week 6. Overviews (40x magnification) of lung morphology reveal obliterative lesions in SuHx and SuPNx at week six (fig5DE).

Increased proliferation, apoptosis and inflammation in both SuHx and SuPNx

Markers of cell proliferation and pro-apoptotic signaling (as assessed by immunofluorescence) at week six indicated increased proliferation of endothelial cells (EC) in SuHx and smooth muscle cells (SMC) in both SuHx and SuPNx (compared to control). The apoptotic signaling in both PH-models was similarly increased in ECs as well as SMCs compared to Con (fig 6AB). Cytotoxic T-cells (CD8), B-cells (CD20) and macrophage (CD68) count at- or near vessels was increased in both SuHx and SuPNx. Sugen increased CD68 compared to Con. The CD68 count was higher in SuPNx compared to SuHx (fig6E). Typical examples are shown (fig6BCDE).

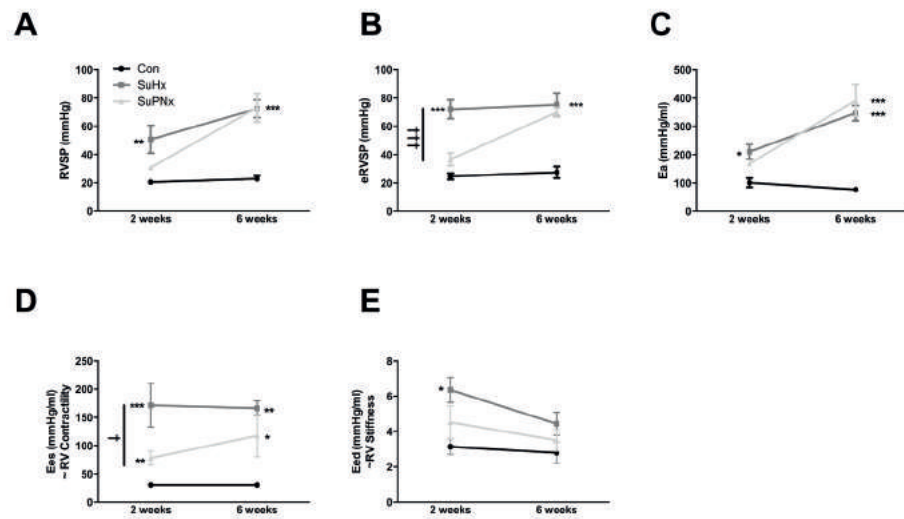


Figure 2 – Pressure-volume measurements. *A*: right ventricle systolic pressure (RVSP); *B*: estimated RVSP (eRVSP); *C*: RV afterload (Ea); *D*: RV contractility [end systolic elastance (Ees)]; *E*: RV stiffness [end diastolic stiffness (Eed)]; Con, control; SuHx, SU5416 + hypoxia; SuPNx, SU5416 + pneumonectomy. * $P < 0.05$, ** $P < 0.01$, *** $P < 0.001$, † $P < 0.05$, †† $P < 0.01$; (*differences between SuHx/SuPNx vs. control; †differences between SuHx vs. SuPNx).

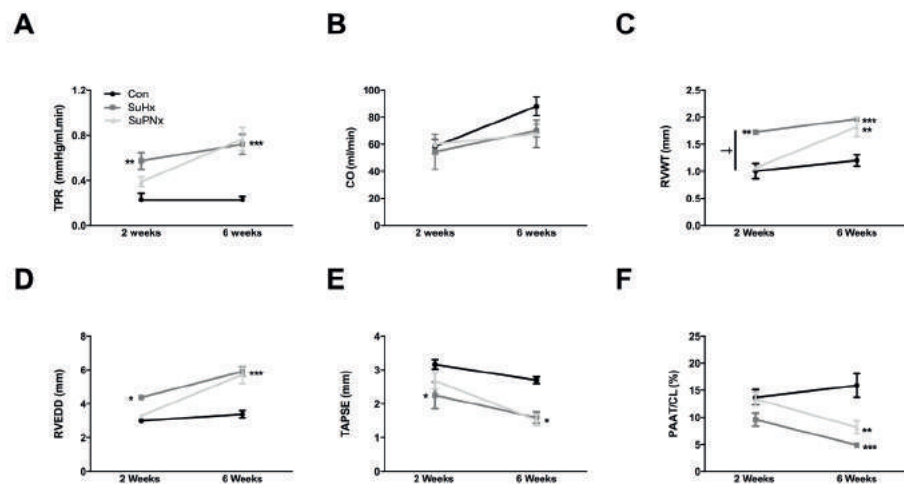


Figure 3 – Echocardiography parameters. *A*: total pulmonary resistance (TPR); *B*: cardiac output (CO); *C*: right ventricle wall thickness (RVWT); *D*: right ventricle end diastolic diameter (RVEDD); *E*: tricuspid annular plane systolic excursion (TAPSE); *F*: pulmonary artery acceleration time/cycle length (PAAT/CL). Con, control; SuHx, SU5416 + hypoxia; SuPNx, SU5416 + pneumonectomy. * $P < 0.05$; ** $P < 0.01$; *** $P < 0.001$; † $P < 0.05$ (*differences between SuHx/SuPNx vs. control; †differences between SuHx vs. SuPNx).

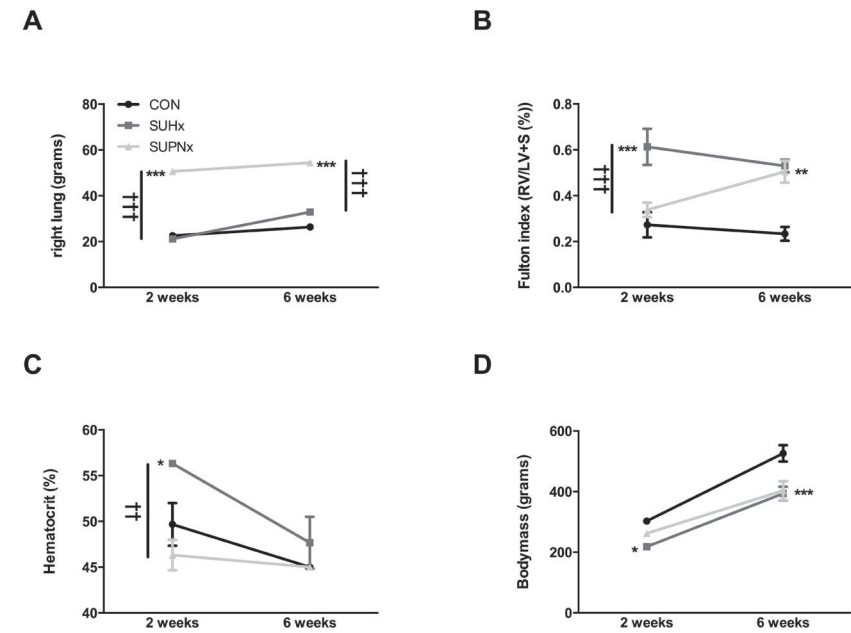


Figure 4 – Lung mass, Fulton index, hematocrit, and body mass. *A*: right lung mass. Left lung indicated by striped pattern; *B*: Fulton index (RV/LV+S)(%); *C*: hematocrit (%); *D*: body mass (g). Con, control; SuHx, SU5416 + hypoxia; SuPNx, SU5416 + pneumonectomy. * $P < 0.05$; ** $P < 0.01$; *** $P < 0.001$; † $P < 0.05$; †† $P < 0.01$; ††† $P < 0.001$ (*differences between SuHx/SuPNx vs. control; †differences between SuHx vs. SuPNx).

Discussion

To our knowledge this study is the first full report on the combined lung vascular effects of left pneumonectomy and SU5416 in rats. In the current study, several important hallmarks of human PAH were detected in the rat model that combines PNx and one single injection of the VEGF receptor antagonist SU5416. These include severe pulmonary hypertension, angio-obliterative vascular lesions and increased rates of proliferation and pro-apoptotic signaling of lung endothelial and smooth muscle cells and RV dysfunction. The present study confirms that an abnormal pulmonary blood flow (PBF), combined with VEGF receptor blockade, is sufficient to establish severe PAH in rats. Additionally, our study supports the two-hit hypothesis of severe PAH, similar to previous studies in which PNx was paired with the administration of MCT(8, 43). Our study extends previous findings by Sakao et al., who showed that in cultured endothelial cells, SU5416 and shear stress act to promote apoptosis resistance and cell proliferation(29). Additionally, this is the first report of ongoing pro-apoptotic signaling in developed PAH in two animal models.

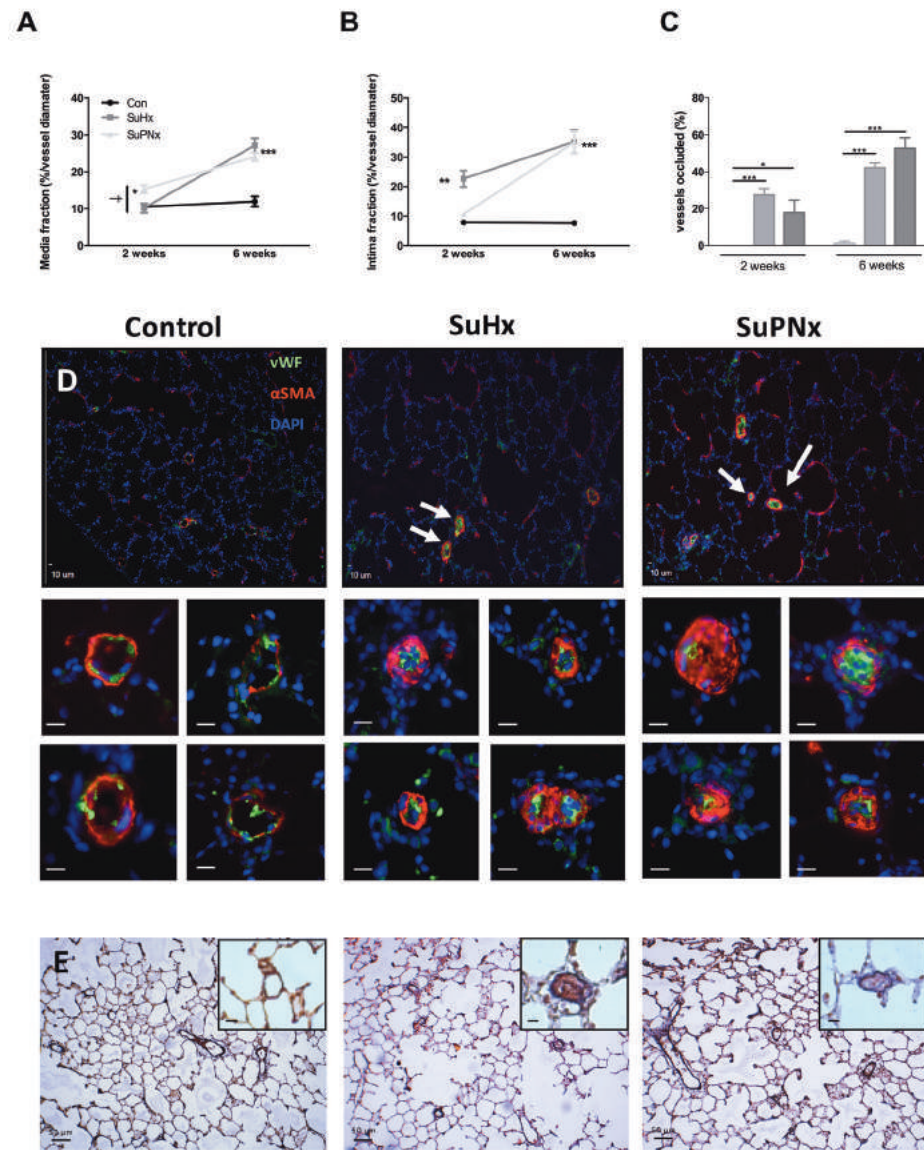


Figure 5 – Vascular remodeling. *A*: media fraction thickness. *B*: intima fraction thickness. *C*: vessels occluded (%). Con, control; SuHx, SU5416+hypoxia; SuPNx, SU5416+pneumonectomy. * $P < 0.05$; ** $P < 0.01$; *** $P < 0.001$; † $P < 0.05$. *D*: overview (magnification x 100 and x 400) of lung vasculature. Green, von Willebrand factor [endothelial cells (ECs)]; red, α-smooth muscle actin [smooth muscle cells (SMC)]; blue, 4=6-diamidino-2-phenylindole DAPI (nuclei). White arrows indicate occlusions. *E*: examples of histology (Elastica van Gieson) of pulmonary vessels in control, SuHx, and SuPNx (*differences between SuHx/SuPNx vs. control; †differences between SuHx vs. SuPNx).

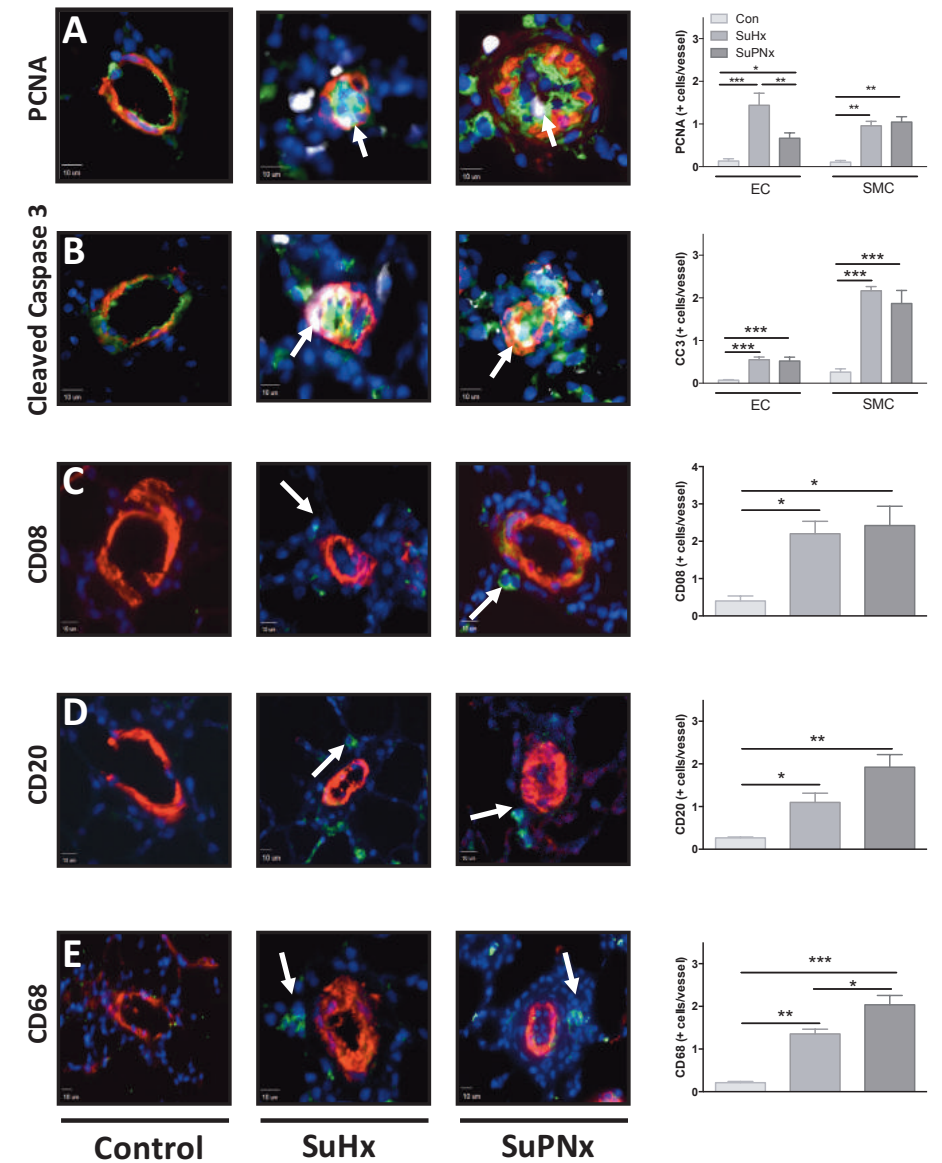


Figure 6 – Proliferation and apoptotic activity week 6. *A*: PCNA-positive cell count in ECs and SMCs. *B*: CC3-positive cell count in ECs and SMCs; characterization of inflammation of at week 6. *C*: CD08. *D*: CD20. *E*: CD68-positive cells at or near vessel. Green (*A*, *B*), von Willebrand factor (ECs); green (*C*, *D*, *E*), CD08/CD20/CD68; red, α-smooth muscle actin (SMC); blue, DAPI (nuclei). Con, control; SuHx, SU5416 + hypoxia; SuPNx, SU5416 + pneumonectomy. * $P < 0.05$; ** $P < 0.01$; *** $P < 0.001$. Scale bar = 10 μ m. *Differences between SuHx/SuPNx vs. control; †differences between SuHx vs. SuPNx.

SU5416 combined with left pneumonectomy induces severe PH

As determined by echocardiography and pressure-volume analysis of the RV, the combination of SU5416 and left PNx caused RV dysfunction as is frequently observed in severe PAH. Measurements of RVEDD and RVWT confirmed increased RV hypertrophy and dimensions, which findings were confirmed by an increase in RV/LV+S. In addition, the systolic function of the RV was affected as shown by a significant decrease in TAPSE. TPR was increased due to extensive pulmonary vascular changes. We found an increase in right lung mass in SuPNx which is possibly explained by compensatory lung growth, edema and/or influx of inflammatory cells after pneumonectomy(27, 28).

The increase in TPR in SuPNx model was associated with an increased pulmonary arteriolar mean wall thickness. The increased rates of proliferative and pro-apoptotic cells within and around the lung arterioles support the concept that apoptosis and proliferation are important factors promoting angioproliferation, the ongoing proliferation and proliferative activity in the pulmonary vasculature, in experimental models of pulmonary hypertension(14, 34). Increased proliferation, but not ongoing pro-apoptotic signaling has been reported before in an animal shunt model of PH(18), but in this model cell proliferation was restricted to the pulmonary vascular smooth muscle cells while no lumen obliteration was observed. Indeed, pneumonectomy combined with MCT induces neointimal proliferation as does the combination of MCT with an abdominal aortacaval shunt(8, 22, 7).

A hypothetical explanation for the similarities between the SuHx and SuPNx models is that pneumonectomy (through a reduction in pulmonary vascular bed) and hypoxic exposure (through vasoconstriction) both exert their effects via an increased pulmonary blood flow velocity. We propose that abnormal PBF induced activation and injury of lung vascular endothelial cells cannot be repaired when SU5416 impairs signaling via VEGF receptors, which is required for the homeostatic maintenance of lung vessels(40). Since VEGFR2 and VEGFR3 are both part of a mechanosensory complex in endothelial cells it can be argued that SU5416 interferes with this complex, thereby hampering EC mechanosensing (4, 37). A failure of normal adaptation to changes in PBF may be crucial in the development of pulmonary vascular remodeling. Indeed, recent findings indicate that late-stage inhibition of caspases can stabilize PECAM-1 levels thereby restoring endothelial shear-responsiveness and reverses remodeling in-vivo (32).

Comparison of SuHx versus SuPNx

The SuHx model is a now frequently utilized model of severe angio-obliterative PAH(5). In comparison to the SuHx-model, the combination of pneumonectomy with VEGF receptor blockade showed several important differences in disease progression. Although the vascular lesions in the SuPNx model are very similar to the SuHx-model, the hyperproliferation of endothelial cells and the resulting obliterative lesions as

a consequence of disturbed flow in the SuPNx model, indicate that the endothelial dysfunction and injury do not necessarily require metabolic pathways activated by hypoxia. This might suggest that the hypoxic exposure within the SuHx protocol is important for disturbing the blood flow by its mechanical loss of vascular lumen and explains the efficacy of monocrotaline or SU5416 in flow based animal models. As a pneumonectomy alone can elicit a hypoxic pathway response it will be of future interest to characterize the hypoxic response in both models in more detail(17). SU5416, by itself, damages endothelial cells, but without a second hit does not cause angio-obliterative luminal changes(14). The bodymass at week 6 is equally lowered in SuHx and SuPNx rats, although SuHx rats show a temporal more profound decline in bodymass in comparison to SuPNx rats in week two. This phenomenon is probably explained by a combination of hypoxia induced diuresis and anorexia which lowers bodymass(16). Inflammation, measured by presence of cytotoxic T-cells, B-cells and macrophages occurred in both SuHx and SuPNx models in comparison to control animals.

It appears that inflammatory components are important, perhaps necessary, for the development of angio-obliterative lesions in animal models of severe PAH. Indeed, in the rat model which combines SU5416 and the allergic inflammatory ovalbumin, the angio-obliterative PH could be prevented by anti-CD20 (anti-B lymphocyte) monoclonal antibody treatment(19). Athymic rats, characterized by their lack of regulatory T-cells (Treg), develop angio-obliterative PH with evidence of inflammatory cell infiltration, when SU5416 is administered(20, 35). Reconstitution of the Treg function after pulmonary vascular disease has developed reversed PAH and lung vessel inflammation(33). Our observation of the early stage (2 weeks) and the advanced stage (6 weeks) after the pneumonectomy and comparison with the similar time points in the SuHx model revealed that the onset of PAH is delayed in the SuPNx model.

As the SuHx model is a well-established and characterized animal model for PAH, subsequent studies characterizing the SuPNx model will have to show whether there are more similarities and-or differences between the models. This could include the exploration of the role of inflammation and of the immune disequilibrium in the pulmonary vascular remodeling that is triggered by increased pulmonary blood flow in the setting of an injured and inflamed endothelium. Also, vasoconstriction is a major factor that accounts for the increased PVR observed in the SuHx model, and can be relieved by intravenous Fasudil(23). It will be of interest to assess the vasoconstrictive component of the SuPNx model in the future. Finally, the future further characterization beyond six weeks will also be of interest to investigate whether the disease progression leads to right heart failure and-or the development of plexiform lesions, as observed in SuHx animals at week 14(1).

Perspectives and conclusion

In summary, we have shown that the combination of SU5416 and PNx causes severe angio-obliterative pulmonary hypertension associated with increased cell proliferation and pro-apoptotic signaling resulting in neointima and medial remodeling. Perhaps this SuPNx model can serve as an alternative model or complementary model of severe angio-obliterative PAH that can be employed to further study the detailed mechanisms underlying high pulmonary blood flow related vascular remodeling, including the study of endothelial mesenchymal transition and the specific interactions between apoptosis and proliferation of vascular wall cells (9, 26). Some of the advantages that SuPNx could offer over SuHx is that by design in the SuHx model, temporal exposure to hypoxia and reversal of hypoxic vasoconstriction and hemoconcentration upon return to normoxia results in a partial reversibility of pulmonary hypertension. This aspect of reversibility is reflected by some decrease in RVSP and RV hypertrophy after the hypoxic period and may complicate drug treatment studies when using the SuHx model. Because the SuPNx model lacks the element of hypoxic vasoconstriction and hemoconcentration, the RVSP after pneumonectomy increases gradually over time, which may favor the assessment of drug effects in preclinical trials.

Our study together with previous studies on experimental models of pulmonary hypertension shows that the typical histopathological findings of PAH, including obliterative lesions, inflammation, increased cell turnover and ongoing apoptosis represent a final common pathway of a disease that can evolve as a consequence of a variety of insults to the lung vasculature

Acknowledgements

We acknowledge the support from the Dutch Lung Foundation (Longfonds, grant number 3.3.12.036) and the Netherlands CardioVascular Research Initiative: the Dutch Heart Foundation, Dutch Federation of University Medical Centers, the Netherlands Organization for Health Research and Development, and the Royal Netherlands Academy of Sciences grant number 2012-08 awarded to the Phaedra consortium (www.phaedraresearch.nl)

References

1. Abe K, Toba M, Alzoubi A, Ito M, Fagan KA, Cool CD, Voelkel NF, McMurtry IF, Oka M. Formation of Plexiform Lesions in Experimental Severe Pulmonary Arterial Hypertension. *Circulation* 121: 2747–2754, 2010.
2. Chemla D, Castelain V, Humbert M, Hébert J-L, Simonneau G, Lecarpentier Y, Hervé P. New formula for predicting mean pulmonary artery pressure using systolic pulmonary artery pressure. *Chest* 126: 1313–1317, 2004.
3. Chiu J-J, Chien S. Effects of disturbed flow on vascular endothelium: pathophysiological basis and clinical perspectives. *Physiol Rev* 91: 327–387, 2011.
4. Coon BG, Baeyens N, Han J, Budatha M, Ross TD, Fang JS, Yun S, Thomas J-L, Schwartz MA. Intramembrane binding of VE-cadherin to VEGFR2 and VEGFR3 assembles the endothelial mechanosensory complex. *J Cell Biol* 208: 975–986, 2015.
5. de Raaf MA, Schalij I, Gomez-Arroyo J, Rol N, Happé C, de Man FS, Vonk-Noordegraaf A, Westerhof N, Voelkel NF, Bogaard HJ. SuHx rat model: partly reversible pulmonary hypertension and progressive intima obstruction. *Eur Respir J* 44: 160–168, 2014.
6. Dickinson MG, Bartelds B, Borgdorff MAJ, Berger RMF. The role of disturbed blood flow in the development of pulmonary arterial hypertension: lessons from preclinical animal models. *Am J Physiol - Lung Cell Mol Physiol* 305: L1–L14, 2013.
7. Dickinson MG, Bartelds B, Molema G, Borgdorff MA, Boersma B, Takens J, Weij M, Wichers P, Sietsma H, Berger RMF. Egr-1 Expression During Neointimal Development in Flow-Associated Pulmonary Hypertension. *Am J Pathol* 179: 2199–2209, 2011.
8. Dorfmueller P, Chaumais M-C, Giannakouli M, Durand-Gasselien I, Raymond N, Fadel E, Mercier O, Charlotte F, Montani D, Simonneau G, Humbert M, Perros F. Increased oxidative stress and severe arterial remodeling induced by permanent high-flow challenge in experimental pulmonary hypertension. *Respir Res* 12: 119, 2011.
9. Golpon HA, Fadok VA, Taraseviciene-Stewart L, Scerbavicius R, Sauer C, Welte T, Henson PM, Voelkel NF. Life after corpse engulfment: phagocytosis of apoptotic cells leads to VEGF secretion and cell growth. *FASEB J* 18: 1716–1718, 2004.
10. Guignabert C, Tu L, Le Hire M, Ricard N, Sattler C, Seferian A, Huertas A, Humbert M, Montani D. Pathogenesis of pulmonary arterial hypertension: lessons from cancer. *Eur Respir Rev Off J Eur Respir Soc* 22: 543–551, 2013.
11. Handoko ML, Man FS de, Happé CM, Schalij I, Musters RJP, Westerhof N, Postmus PE, Paulus WJ, Laarse WJ van der, Vonk-Noordegraaf A. Opposite Effects of Training in Rats With Stable and Progressive Pulmonary Hypertension. *Circulation* 120: 42–49, 2009.
12. Handoko ML, Schalij I, Kramer K, Sebkhii A, Postmus PE, van der Laarse WJ, Paulus WJ, Vonk-Noordegraaf A. A refined radio-telemetry technique to monitor right ventricle or pulmonary artery pressures in rats: a useful tool in pulmonary hypertension research. *Pflugers Arch* 455: 951–959, 2008.
13. Jones JE, Mendes L, Rudd MA, Russo G, Loscalzo J, Zhang Y-Y. Serial noninvasive assessment of progressive pulmonary hypertension in a rat model. *Am J Physiol Heart Circ Physiol* 283: H364–371, 2002.
14. Kasahara Y, Tuder RM, Taraseviciene-Stewart L, Le Cras TD, Abman S, Hirth PK, Waltenberger J, Voelkel NF. Inhibition of VEGF receptors causes lung cell apoptosis and emphysema. *J Clin Invest* 106: 1311–1319, 2000.
15. Kato Y, Iwase M, Kanazawa H, Kawata N, Yoshimori Y, Hashimoto K, Yokoi T, Noda A, Takagi K, Koike Y, Nishizawa T, Nishimura M, Yokota M. Progressive development of pulmonary hypertension leading to right ventricular hypertrophy assessed by echocardiography in rats. *Exp Anim Jpn Assoc Lab Anim Sci* 52: 285–294, 2003.
16. Kim N, Voicu L, Hare GMT, Cheema-Dhadli S, Chong CK, Chan SKW, Bichet DG, Halperin ML, Mazer CD. Response of the renal inner medulla to hypoxia: possible defense mechanisms. *Nephron Physiol* 121: p1–7, 2012.

17. Li D, Fernandez LG, Dodd-o J, Langer J, Wang D, Laubach VE. Upregulation of Hypoxia-Induced Mitogenic Factor in Compensatory Lung Growth after Pneumonectomy. *Am J Respir Cell Mol Biol* 32: 185–191, 2005.
18. Li F, Xia W, Li A, Zhao C, Sun R. Long-term inhibition of Rho kinase with fasudil attenuates high flow induced pulmonary artery remodeling in rats. *Pharmacol Res* 55: 64–71, 2007.
19. Mizuno S, Farkas L, Hussein AA, Farkas D, Gomez-Arroyo J, Kraskauskas D, Nicolls MR, Cool CD, Bogaard HJ, Voelkel NF. Severe Pulmonary Arterial Hypertension Induced by SU5416 and Ovalbumin Immunization. *Am J Respir Cell Mol Biol* 47: 679–687, 2012.
20. Nicolls MR, Mizuno S, Taraseviciene-Stewart L, Farkas L, Drake JI, Al Hussein A, Gomez-Arroyo JG, Voelkel NF, Bogaard HJ. New models of pulmonary hypertension based on VEGF receptor blockade-induced endothelial cell apoptosis. *Pulm Circ* 2: 434–442, 2012.
21. Okada K, Tanaka Y, Bernstein M, Zhang W, Patterson GA, Botney MD. Pulmonary hemodynamics modify the rat pulmonary artery response to injury. A neointimal model of pulmonary hypertension. *Am J Pathol* 151: 1019–1025, 1997.
22. Okada K, Tanaka Y, Bernstein M, Zhang W, Patterson GA, Botney MD. Pulmonary hemodynamics modify the rat pulmonary artery response to injury. A neointimal model of pulmonary hypertension. *Am J Pathol* 151: 1019–1025, 1997.
23. Oka M, Homma N, Taraseviciene-Stewart L, Morris KG, Kraskauskas D, Burns N, Voelkel NF, McMurtry IF. Rho Kinase-Mediated Vasoconstriction Is Important in Severe Occlusive Pulmonary Arterial Hypertension in Rats. *Circ Res* 100: 923–929, 2007.
24. Plante E, Lachance D, Roussel E, Drolet M-C, Arsenault M, Couet J. Impact of anesthesia on echocardiographic evaluation of systolic and diastolic function in rats. *J Am Soc Echocardiogr Off Publ Am Soc Echocardiogr* 19: 1520–1525, 2006.
25. Rai PR, Cool CD, King JAC, Stevens T, Burns N, Winn RA, Kasper M, Voelkel NF. The cancer paradigm of severe pulmonary arterial hypertension. *Am J Respir Crit Care Med* 178: 558–564, 2008.
26. Ranchoux B, Antigny F, Rucker-Martin C, Hautefort A, Péchoux C, Bogaard HJ, Dorfmueller P, Remy S, Lecerf F, Planté S, Chat S, Fadel E, Houssaini A, Anegon I, Adnot S, Simonneau G, Humbert M, Cohen-Kaminsky S, Perros F. Endothelial-to-Mesenchymal Transition in Pulmonary Hypertension. *Circulation* 131: 1006–1018, 2015.
27. Rannels DE, Rannels SR. Compensatory growth of the lung following partial pneumonectomy. *Exp Lung Res* 14: 157–182, 1988.
28. Ravikumar P, Yilmaz C, Bellotto DJ, Dane DM, Estrera AS, Hsia CCW. Separating in vivo mechanical stimuli for postpneumonectomy compensation: imaging and ultrastructural assessment. *J Appl Physiol* 114: 961–970, 2013.
29. Sakao S, Tatsumi K. The Effects of Antiangiogenic Compound SU5416 in a Rat Model of Pulmonary Arterial Hypertension. *Respiration* 81: 253–261, 2011.
30. Selimovic N, Rundqvist B, Bergh C-H, Andersson B, Petersson S, Johansson L, Bech-Hanssen O. Assessment of pulmonary vascular resistance by Doppler echocardiography in patients with pulmonary arterial hypertension. *J Heart Lung Transplant Off Publ Int Soc Heart Transplant* 26: 927–934, 2007.
31. Simonneau G, Robbins IM, Beghetti M, Channick RN, Delcroix M, Denton CP, Elliott CG, Gaine SP, Gladwin MT, Jing Z-C, Krowka MJ, Langleben D, Nakanishi N, Souza R. Updated clinical classification of pulmonary hypertension. *J Am Coll Cardiol* 54: S43–54, 2009.
32. Szulcek R, Happé CM, Rol N, Fontijn RD, Dickhoff C, Hartemink KJ, Grünberg K, Tu L, Timens W, Nossent GD, Paul MA, Leyen TA, Horrevoets AJ, de Man FS, Guignabert C, Yu PB, Vonk-Noordegraaf A, van Nieuw Amerongen GP, Bogaard HJ. Delayed Microvascular Shear-adaptation in Pulmonary Arterial Hypertension: Role of PECAM-1 Cleavage. *Am. J. Respir. Crit. Care Med.* (January 13, 2016). doi: 10.1164/rccm.201506-1231OC.
33. Tamosiuniene R, Nicolls MR. Regulatory T cells and Pulmonary Hypertension. *Trends Cardiovasc Med* 21: 166–171, 2011.
34. Taraseviciene-Stewart L, Kasahara Y, Alger L, Hirth P, Mc Mahon G, Waltenberger J, Voelkel NF, Tuder RM. Inhibition of the VEGF receptor 2 combined with chronic hypoxia causes cell death-dependent pulmonary endothelial cell proliferation and severe pulmonary hypertension. *FASEB J Off Publ Fed Am Soc Exp Biol* 15: 427–438, 2001.
35. Taraseviciene-Stewart L, Nicolls MR, Kraskauskas D, Scerbavicius R, Burns N, Cool C, Wood K, Parr JE, Boackle SA, Voelkel NF. Absence of T Cells Confers Increased Pulmonary Arterial Hypertension and Vascular Remodeling. *Am J Respir Crit Care Med* 175: 1280–1289, 2007.
36. Toba M, Alzoubi A, O'Neill KD, Gairhe S, Matsumoto Y, Oshima K, Abe K, Oka M, McMurtry IF. Temporal hemodynamic and histological progression in Sugen5416/hypoxia/normoxia-exposed pulmonary arterial hypertensive rats. *Am. J. Physiol. Heart Circ. Physiol.* (November 15, 2013). doi: 10.1152/ajpheart.00728.2013.
37. Tzima E, Irani-Tehrani M, Kiosses WB, Dejana E, Schultz DA, Engelhardt B, Cao G, DeLisser H, Schwartz MA. A mechanosensory complex that mediates the endothelial cell response to fluid shear stress. *Nature* 437: 426–431, 2005.
38. van Albada ME, Bartelds B, Wijnberg H, Mohaupt S, Dickinson MG, Schoemaker RG, Kooi K, Gerbens F, Berger RMF. Gene expression profile in flow-associated pulmonary arterial hypertension with neointimal lesions. *Am J Physiol Lung Cell Mol Physiol* 298: L483–491, 2010.
39. Voelkel NF, Gomez-Arroyo J, Abbate A, Bogaard HJ, Nicolls MR. Pathobiology of pulmonary arterial hypertension and right ventricular failure. *Eur Respir J* 40: 1555–1565, 2012.
40. Voelkel NF, Vandivier RW, Tuder RM. Vascular endothelial growth factor in the lung. *Am J Physiol - Lung Cell Mol Physiol* 290: L209–L221, 2006.
41. Westerhof N, Stergiopoulos N, Noble MIM. *Snapshots of Hemodynamics: An Aid for Clinical Research and Graduate Education.* Springer Science & Business Media, 2010.
42. White RJ, Meoli DF, Swarthout RF, Kallop DY, Galaria II, Harvey JL, Miller CM, Blaxall BC, Hall CM, Pierce RA, Cool CD, Taubman MB. Plexiform-like lesions and increased tissue factor expression in a rat model of severe pulmonary arterial hypertension. *Am J Physiol Lung Cell Mol Physiol* 293: L583–590, 2007.
43. White RJ, Meoli DF, Swarthout RF, Kallop DY, Galaria II, Harvey JL, Miller CM, Blaxall BC, Hall CM, Pierce RA, Cool CD, Taubman MB. Plexiform-like lesions and increased tissue factor expression in a rat model of severe pulmonary arterial hypertension. *Am J Physiol - Lung Cell Mol Physiol* 293: L583–L590, 2007.

4

Chapter 4

Vascular remodeling in the pulmonary circulation after major lung resection

RoI N, Happé CM, Belien JAM, de Man F, Westerhof N, Vonk Noordegraaf A, Grünberg K, Bogaard HJ

To the editor

Lung resection is standard treatment in clinical stages I and II and selected stage IIIA non-small cell lung cancer.[1] Major lung resections (MLR), such as (bi)lobectomy or pneumonectomy, occasionally lead to pulmonary hypertension (PH). Several studies report an increase in pulmonary artery pressures in about one third of patients up to 5 years postoperatively.[2-4] The development of PH after MLR may simply be explained by the fact that total cardiac output flows through a smaller vascular bed. Because histological studies were never performed after MLR, it remains unknown whether flow induced structural changes in the remaining lung vasculature lead to progressive increases in pulmonary vascular resistance.

The aim of the current study was to determine whether an altered pulmonary blood flow *per se* is associated with phenotypic changes in the lung vasculature akin to PH. In human, contralateral lung tissue obtained at least two years after pneumonectomy, bilobectomy or lobectomy of the left upper lobe. Control tissue was from people who died acutely due to a traumatic cause and are described in earlier histopathological studies.[5, 6] Samples were obtained from the biobank of the VUmc, Amsterdam, the Netherlands. In rats, wall thickness measurements in the unilateral lung 6 weeks post-pneumonectomy were compared to sham-operated animals.

Evaluation of vasculopathy was done according to previously described patterns.[7] Immunohistochemical staining with ki-67, histone H3 and cleaved caspase 3 was performed to determine proliferation and apoptosis of endothelial cells. For quantitative measurements the thickness of the intimal and medial layer of arterioles (attached to 4 septal walls) was determined and expressed as percentage of their external diameter. Vessels with an elliptical shape due to oblique sectioning were excluded. Animal experiments were permitted by the Institutional Animal Care and Use of the VU University and conducted in accordance with the European Convention for the Protection of Vertebrate Animals used for Experimental and Other Scientific Purposes, and the Dutch Animal Experimentation Act (FYS12-18, FYS13-01). Sprague Dawley rats (n=4 per group) were subjected to either pneumonectomy or sham operation. The animals were part of an earlier study, as described previously.[8]

Lung tissue specimens from thirteen MLR patients and six controls were obtained. Control subjects died at an age of 36±4 years old and were all male. MLR patients were 69±2 years, and 10 out of 13 were male. 10 MLR patients had a known history of smoking and the average survival after surgery was 4.8±0.9 years. The clinical history of four MLR patients was not available. Seven patients had received radiotherapy prior to MLR, three in combination with chemotherapy.

Predominant patterns observed in MLR patients while absent in controls were thrombotic arteriopathy (46%) and aselective intimal fibrosis (23%) (figure 1a). These patterns did not associate with the presence of inflammation. In half of the patients with thrombotic arteriopathy, vascular remodeling was mild with slight congestive features. In two patients diffuse congestion was more prominent and the last patient showed organising diffuse alveolar damage. The three patients with non-specific intimal fibrosis showed parenchymal intimal fibrosis, with involvement of the veins in two cases. Congestive vasculopathy was present in both MLR and controls. In two MLR patients this was paired with intimal fibrosis in arterial, parenchymal and venous vessels, medial hyperplasia in bronchiolar arteries and venous arterialisation. A very similar pattern was found in all controls with congestive structural changes. There is no conclusive diagnosis for the other two MLR patients with congestive vasculopathy.

The number of endothelial cells positively stained for the proliferative marker ki-67 was higher in the MLR group (p=0.01)(figure 1b), not correlating to inflammation (p=0.50). Histone H3 showed a similar pattern, although not statistically significant (p=0.18). No differences were found with regards to cleaved caspase 3 (p=0.81)(figure 1b).

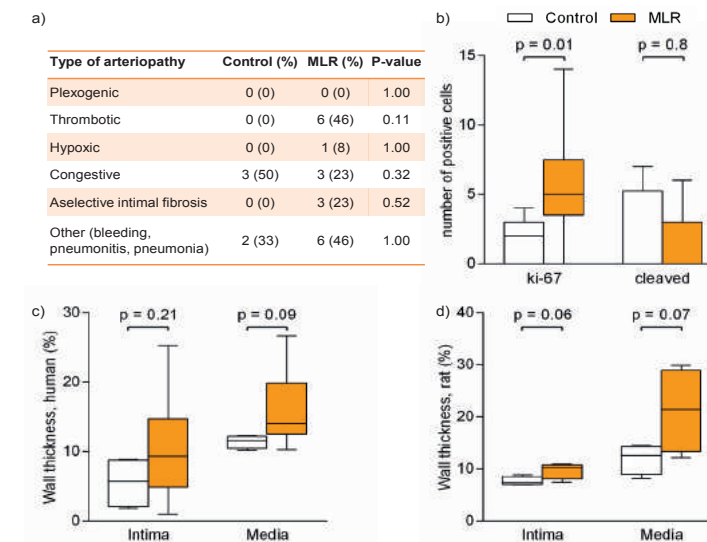


Figure 1 – Type of arteriopathy in major lung resection (MLR) and control lung tissue scored quantitatively, p-values calculated with Fisher's exact test. b) number of positively stained endothelial cells for ki-67 and cleaved caspase 3. c) Intimal and medial wall thickness in human and d) rat, expressed as percentage of outer diameter of the vessel. Data are reported as box and whisker plots, minimum to maximum. For statistical analysis unpaired t-tests (parametric data) and Mann-Whitney tests (non-parametric data) were used.

In the human pulmonary vasculature, the outer diameter of the arterioles ranged between 27-178µm, with a mean distance of 69 and 76µm in control and MLR subjects, respectively (p=0.33). There was no significant increase of the intima in MLR lung tissue, the media showed a tendency towards thickening (figure 1c). Thickening of the intimal and medial wall was not different with and without inflammation. In rats, the outer diameter was 40±1.3 µm (sham) and 43±2.6 µm (MLR)(p=0.32). Both vascular layers showed a tendency towards thickening (figure 1d).

The small cohort and random selection of tissue blocks limits the generalization of our findings. Other limitations are possible confounding by differences in age, smoking history, or cancer treatment. Thickening of the intima is often seen in older subjects[9] and smokers[10, 11]. Both features apply to patients undergoing MLR for lung cancer. Chemo- and radiotherapy are also associated with vascular, mostly intimal, remodeling[12, 13]. Increased presence of inflammation in MLR patients was probably related to illness at the end of life. However, inflammation was not associated with vasculopathy patterns or proliferation, suggesting these changes were not consequences of inflammatory activity. We observed increased ki-67 staining in the MLR group without changes in cleaved caspase 3, indicating ongoing proliferation in the pulmonary vasculature. However, we could not link this observation to a greater intimal thickness.

We hypothesized that hyperflow *per se* could induce remodeling in the pulmonary vasculature, even when no PH develops. Indeed, six MLR patients showed thrombotic arteriopathy, while controls did not present this predominant pattern. Intimal and medial thickness was not changed in human and rat lungs. Finally, MLR patients showed increased proliferation, without changes in apoptosis. Surprisingly, we observed a congestive arteriopathy in half of the control lung samples, indicating that these findings are common and probably non-specific rather than related to hyperflow.

The findings in our focused study of thirteen patients after MLR implicate that vascular changes in PH are perhaps partially explained by altered pulmonary blood flow, but further research is needed in a bigger cohort with more tissue to study which additional stimuli are needed to induce PH.

References

1. Manser R, Wright G, Hart D, Byrnes G, Campbell DA. Surgery for early stage non-small cell lung cancer. *Cochrane Database Syst Rev* 2005(1): CD004699.
2. Deslauriers J, Ugalde P, Miro S, Ferland S, Bergeron S, Lacasse Y, Provencher S. Adjustments in cardiorespiratory function after pneumonectomy: results of the pneumonectomy project. *J Thorac Cardiovasc Surg* 2011; 141(1): 7-15.
3. Foroulis CN, Kotoulas CS, Kakouros S, Evangelatos G, Chassapis C, Konstantinou M, Lioulias AG. Study on the late effect of pneumonectomy on right heart pressures using Doppler echocardiography. *Eur J Cardiothorac Surg* 2004; 26(3): 508-514.
4. Potaris K, Athanasiou A, Konstantinou M, Zaglavira P, Theodoridis D, Syrigos KN. Pulmonary hypertension after pneumonectomy for lung cancer. *Asian Cardiovasc Thorac Ann* 2014; 22(9): 1072-1079.
5. Overbeek MJ, Mouchaers KT, Niessen HM, Hadi AM, Kupreishvili K, Boonstra A, Voskuyl AE, Belien JA, Smit EF, Dijkmans BC, Vonk-Noordegraaf A, Grunberg K. Characteristics of interstitial fibrosis and inflammatory cell infiltration in right ventricles of systemic sclerosis-associated pulmonary arterial hypertension. *Int J Rheumatol* 2010: 2010.
6. Overbeek MJ, Boonstra A, Voskuyl AE, Vonk MC, Vonk-Noordegraaf A, van Berkel MP, Mooi WJ, Dijkmans BA, Hondema LS, Smit EF, Grunberg K. Platelet-derived growth factor receptor-beta and epidermal growth factor receptor in pulmonary vasculature of systemic sclerosis-associated pulmonary arterial hypertension versus idiopathic pulmonary arterial hypertension and pulmonary veno-occlusive disease: a case-control study. *Arthritis Res Ther* 2011; 13(2): R61.
7. Grünberg K, Mooi WJ. A practical approach to vascular pathology in pulmonary hypertension. Diagnostic histopathology, 2013.
8. Happe CM, De Raaf MA, Rol N, Schalij I, Vonk-Noordegraaf A, Westerhof N, Voelkel NF, de Man FS, Bogaard HJ. Pneumonectomy combined with SU5416 induces severe pulmonary hypertension in rats. *Am J Physiol Lung Cell Mol Physiol* 2016: ajplung.
9. Wagenvoort CA, Wagenvoort N. AGE CHANGES IN MUSCULAR PULMONARY ARTERIES. *Arch Pathol* 1965; 79: 524-528.
10. Chiu JJ, Chien S. Effects of disturbed flow on vascular endothelium: pathophysiological basis and clinical perspectives. *Physiol Rev* 2011; 91(1): 327-387.
11. Santos S, Peinado VI, Ramirez J, Melgosa T, Roca J, Rodriguez-Roisin R, Barbera JA. Characterization of pulmonary vascular remodelling in smokers and patients with mild COPD. *Eur Respir J* 2002; 19(4): 632-638.
12. Weintraub NL, Jones WK, Manka D. Understanding radiation-induced vascular disease. *J Am Coll Cardiol* 2010; 55(12): 1237-1239.
13. Sanchez-Gonzalez PD, Lopez-Hernandez FJ, Lopez-Novoa JM, Morales AI. An integrative view of the pathophysiological events leading to cisplatin nephrotoxicity. *Crit Rev Toxicol* 2011; 41(10): 803-821.

5

Chapter 5

Vascular narrowing in pulmonary arterial hypertension is heterogeneous: Rethinking resistance

RoI N, Timmer EM, Faes TJC, Vonk Noordegraaf A, Grünberg K, Bogaard HJ, Westerhof N.

Abstract

Background

In idiopathic pulmonary arterial hypertension (PAH), increased pulmonary vascular resistance is associated with structural narrowing of small (resistance) vessels and increased vascular tone. Current information on pulmonary vascular remodeling is mostly limited to averaged increases in wall thickness, but information on number of vessels affected and internal diameter decreases for vessels of different sizes is limited.

Aim

Our aim was to quantify numbers of affected vessels and their internal diameter decrease for differently sized vessels in PAH in comparison with non-PAH patients.

Methods

Internal and external diameters of transversally cut vessels were measured in 5 control subjects and 6 PAH patients. Resistance vessels were classified in Strahler orders, internal diameters 13 μ m (order 1) to 500 μ m (order 8). The number fraction, i.e. % affected vessels, and the internal diameter fraction, i.e. % diameter of normal diameter, were calculated.

Results

In PAH not all resistance vessels are affected. The number fraction is about 30%, i.e., 70% of vessels have diameters not different from vessels of control subjects. Within each order the decrease in diameter of affected vessels is variable with an averaged diameter fraction of 50-70%.

Conclusions

Narrowing of resistance vessels is heterogeneous: not all vessels are narrowed, and the decrease in internal diameters, even within a single order, vary largely. This heterogeneous narrowing alone cannot explain the large resistance increase in PAH. We suggest rarefaction could be an important contributor to the hemodynamic changes.

Introduction

Idiopathic pulmonary arterial hypertension (iPAH) is generally assumed to result from decreased internal diameters of the small vessels, often labelled as resistance vessels. Resistance may increase up to a factor ~4-5 and consequently mean pulmonary artery pressure may increase by a similar amount.(3; 10; 11; 13; 15-17) Internal diameters of these resistance vessels can be reduced by vasoconstriction or (concentric) remodeling, and because in only a minority of PAH patients acute vasodilator challenges result in a substantial pressure decrease, concentric remodeling is considered to be the major factor in vessel narrowing and augmentation of pulmonary vascular resistance.(15) Inhibition of vascular remodeling is considered as an effective therapeutic target.

However, quantitative information on remodeling of resistance vessels from iPAH patients, in comparison with non-PAH, is almost exclusively limited to the increase in relative wall thickness, expressed as $WT = (d_o - d_i)/d_o \times 100\%$, with d_o and d_i external and internal diameter. In general, wall thickness is most often presented in terms of average values, not discriminating between vessel size.(15; 17) Chazova et al. reported on averaged wall thickening in six diameter groups of arteries, and showed that the wall thickness increase in iPAH, and therefore the internal diameter change, may depend on vessel size. In the same study, wall thickening of the pulmonary veins is also reported.(3) Anderson et al. reported similar findings in 3 PAH patients.(1) However, only averaged data were reported, while the percentage of vessels affected and the possible variation in degree of vessels narrowing were not. Hence, to the best of our knowledge, in the published literature on PAH, very little quantitative information has been provided pertaining to the number of affected vessels and the degree of internal diameter decreases of differently sized vessels in the (peripheral) pulmonary vascular bed. Quantitative information on internal diameters is required to accurately estimate vascular resistance.

Therefore, we determined internal and external diameters of pulmonary resistance vessels (13 to 500 μ m; Strahler orders 1-8) and number of occluded vessels in histological slides of healthy subjects and PAH patients, and quantified the fraction of narrowed vessels and their degree of narrowing in each Strahler order. (6-8)

Methods

Internal and external diameters

Lung tissue was obtained from the biobank at the department of pathology of the VU University Medical Center, Amsterdam, the Netherlands. The study was approved by the Institutional Review Board on Research Involving Human Subjects of the VU University Medical Center. Tissue of control subjects was obtained from people who

died acutely due to traumatic causes (mean age: 40.8 (24-79) years; 100% male). Tissues were analyzed from 5 idiopathic PAH and one hereditary PAH patient (#2), all of whom were diagnosed following prevailing diagnostic criteria (three males, all normal BMI, 4 non-smokers). Diagnosis was confirmed at autopsy by histological observation of vascular remodeling and plexiform lesions (Figure 1). Mean age was 54 (45 – 57) years at death. The patient cases were part of an earlier study.(14) Lung parenchyma was perfused with and fixed in formalin and tissue from different lobes was embedded in paraffin. Serial sections of 4 μm thickness were subjected to conventional haematoxylin and eosin staining to confirm diagnosis and Elastica van Gieson staining for evaluation of structural changes. Per subject the external and internal diameter of all transversally cut vessels (arterial and venous, grouped) encountered in one tissue block with average size of $2,75 \text{ cm}^2 \pm 0,26 \text{ cm}^2$ between 13 to 500 μm were measured, by determining the mean distance between the lamina elastica externa and lumen in two perpendicular directions (see figure 1A). Number of vessels counted in each Strahler order is reported in the supplementary table 1.

By comparing PAH internal diameters with their normal values found in the controls, the number of narrowed PAH vessels and their degree of narrowing were determined. This was done per order for Strahler orders $m=1$ to $m=8$, i.e. resistance vessels with diameters of 13 μm to 500 μm (supplementary table 1).(7; 8) We introduced for each order m a number fraction $F_n(m)$, which is the fraction of narrowed vessels with respect to the total number of vessels, and a diameter fraction $F_d(m)$, which is the internal diameter as a fraction of the normal internal diameter. The diameter fraction $F_d(m)$ of a narrowed vessel thus expresses the percentage that is left of a narrowed vessel. On both number and diameter fraction linear regression analysis was performed.

Determinations of number fraction and diameter fraction

To determine $F_n(m)$ and $F_d(m)$, firstly, the internal diameters d_i were plotted as a function of the external diameters d_o . Subsequently, linear regression analysis was performed on the logarithmic diameter values of all control data to get a control relation between internal and external diameter for normal vessels. Furthermore, the iPAH data was categorized in orders based on external diameter, as follows: the categorization criteria were obtained from Horsfield, who labelled vessels based on internal diameter.(6, 7) These internal diameters were converted to external diameters using our control relation. Next, a one-sided 90% prediction interval for the control relation, called the prediction line, was determined to define normal and narrowed vessels in iPAH. Narrowed vessels were the iPAH vessels lying below this prediction line. In every order m , the number of narrowed vessels was counted and divided by the total number of vessels, to calculate the number fraction $F_n(m)$. Linear regression analysis was performed on $F_n(m)$ to construct a regression line of $F_n(m)$ as a function of order m with a 95% confidence interval.

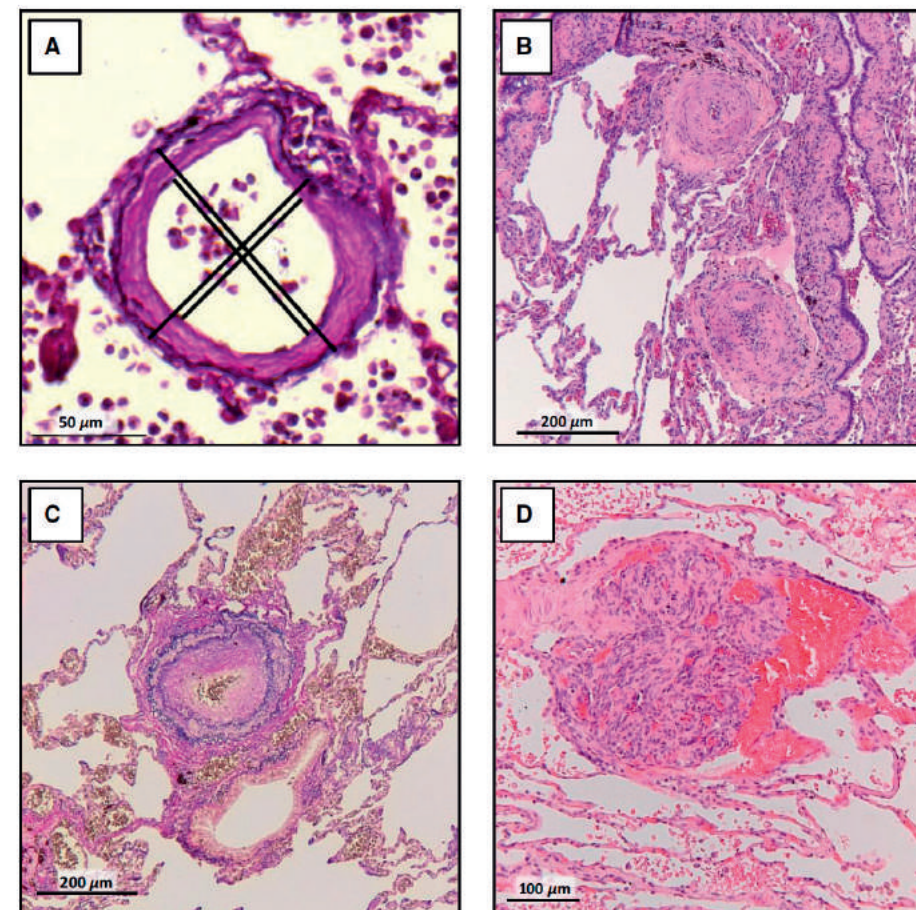


Figure 1 – Wall thickness measurement and vascular remodeling seen in PAH. (A) Example of determining the wall thickness of a pulmonary vessel by measuring the lamina elastica externa and lumen in two perpendicular directions in all transversally cut vessels between 13 and 500 μm encountered per slide. Examples of typical vascular remodeling observed in the lung tissue of pulmonary arterial hypertension patients in our study group, like intimal fibrosis (B; H&E staining) and medial thickening (C; Elastica van Gieson staining) in a pulmonary artery and a plexiform lesion (D; H&E staining). Scalebar indicates 100 μm .

To calculate one value of the diameter fractions $F_d(m)$ for each order m , first, the normal internal diameters of each narrowed vessel were obtained from the control relation. Second, their measured internal diameter was divided by their calculated normal internal diameter to calculate the diameter fraction of each narrowed vessel, and these were plotted per order. Next, linear regression analysis was performed on the diameter fractions to construct a regression line of the diameter fraction $F_d(m)$ as a function of order m with a 95% confidence interval.

Occluded vessels

Immunofluorescent staining with von Willebrand factor antibody conjugated to FITC (vWf, 1:200 dilution, overnight incubation at 4°C, Abcam, Ab8822) combined with α -smooth muscle actin conjugated to Cy3 (α -SMA, 1:200 dilution, 2 hours at room temperature, Sigma, C6198) was performed on control and PAH lung tissue to determine the number of occluded vessels as percentage of the total number of vessels. 30-68 vessels below 100 μ m were studied in 7-12 fields of view per subject. Occlusion was defined by vWf staining completely comprising the luminal surface of a vessel. Imaging was performed at 10x magnification with an Axiovert 200 Marianas inverted wide-field fluorescence microscope (Carl Zeiss Microscopy, Jena, Germany). These percentages were averaged for controls and patients and given as mean \pm SEM.

Table 1. General patient characteristics

| | |
|---|--------------------|
| Male/female, no | 3/3 |
| Age at death (years) | 54 (45 – 57) |
| mPAP (mmHg) | 59 (44 – 76) |
| PAWP (mmHg) | 6 (0 – 11) |
| PVR (dyn·s·cm ⁻⁵) | 856,6 (455 – 1587) |
| CO (L/min) | 4,8 (3,6 – 5,8) |
| CI (L/min/m ²) | 2,6 (1,9 – 3,5) |
| Smoking history (never/current/former, n) | 4/0/2 |
| Therapy | |
| Prostacyclin | 5 |
| ERA | 1 |
| PDE-5 inhibitor | 1 |
| ABS | 2 |

ABS: atrial balloon septostomy; CI: cardiac index; CO: cardiac output; ERA: endothelin receptor antagonist; mPAP: mean pulmonary artery pressure; PAWP: pulmonary artery wedge pressure; PDE-5: phosphodiesterase 5; PVR: pulmonary vascular resistance.

Results

Patient characteristics, including hemodynamic profiles, of the PAH patients are, when known, shown in table 1.

Internal and external diameters

Heterogeneous vascular remodeling was seen in PAH patients, with varying thickening of the intimal and medial vascular layers. PAH patients showed intimal fibrosis and medial thickening, but no significant increase in complete vascular occlusions. 10.4 \pm 2.3% of the vessels of PAH patients were occluded, compared to 6.6 \pm 3.5% in control subjects (Figure 2).

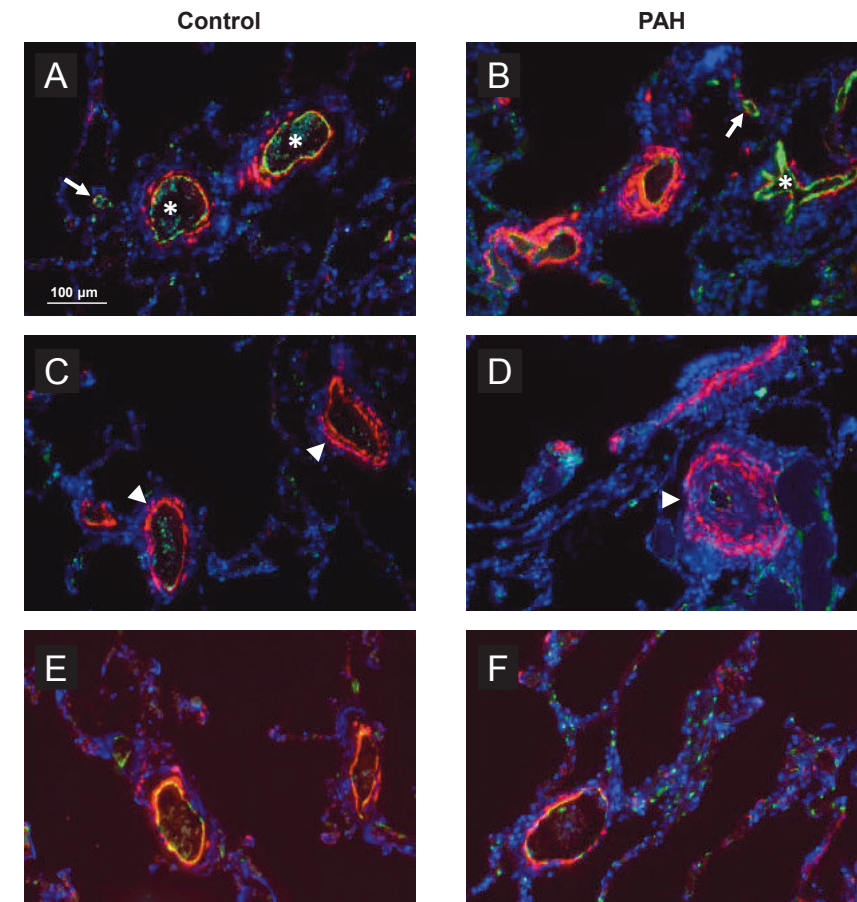


Figure 2 – Vascular occlusions assessed with immunofluorescent staining. Besides thickening of the intimal (B, asterix) and medial (D, arrowhead) vascular layer in pulmonary arterial hypertension compared with control (A, asterisks; C, arrowhead), a great number of vessels is not occluded (A and D, arrows) when assessed with immunofluorescent von Willebrand factor staining. Vascular remodeling does not occur in all vessels in PAH tissue (E) and still look similar to control vessels (F). Scale bar indicates 100 μ m.

Figures 3 and 4 show the relations between internal and external diameters of the control subjects and PAH patients, respectively, with their linear fits. The control data showed a clear linear relation (R^2 between 0.984 and 0.996). The mean relative wall thickness (WT) of all control vessels was about 16% (mean \pm 95% CI: 16.3% \pm 0.7%). Patient data showed a weaker relation between internal and external diameter (R^2 between 0.668 and 0.985) and a mean WT of all vessels of about 22% (22.0% \pm 1.2%). However, many PAH data points appeared to follow the control regression line indicating unaffected vessels.

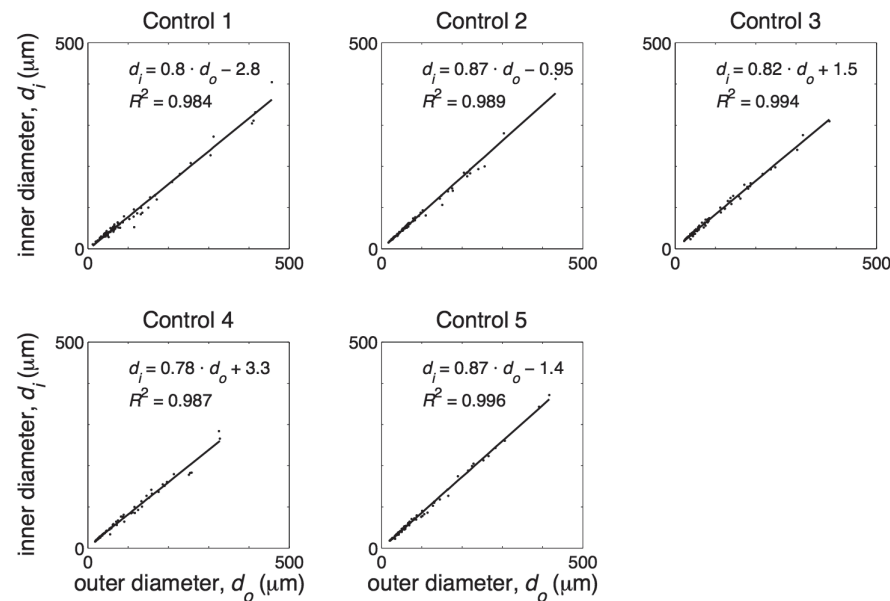


Figure 3 – Internal diameter (d_i) as a function of external diameter (d_o) as measured in five control subjects. Regression line is depicted with black line.

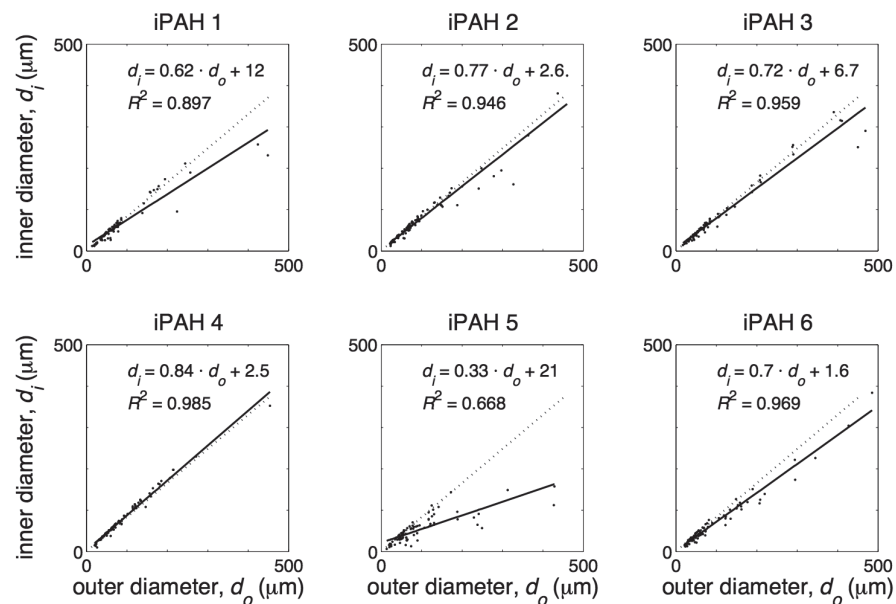


Figure 4 – Internal diameter (d_i) as a function of external diameter (d_o) as measured in six PAH patients. Regression line, depicted with black line, and the averaged control regression line (all control data of taken together, dotted line): $d_i = 0.824 d_o + 0.260$, $R^2 = 0.993$.

Figure 5 shows the diameter relations on a log-log scale. Diagram A shows the data of all controls with the control regression line and the lower 90% control prediction line. Panel B shows the data of all PAH patients with the control regression line and lower 90% control prediction line. About 70% of the PAH data points are above this prediction line and are considered as vessels with a non-reduced internal diameter, while 30% (in grey) are below the prediction line and thus have a significantly reduced inner diameter. The normal vessels had a mean WT of $14\% \pm 0.6\%$, and the narrowed vessels had a mean WT of $39\% \pm 2\%$.

The number fractions $F_n(m)$ (diagram A) and the diameter fractions (diagram B) of the PAH vessels are shown by order in figure 6. The linear regression lines of the data with the 95% CIs are shown.

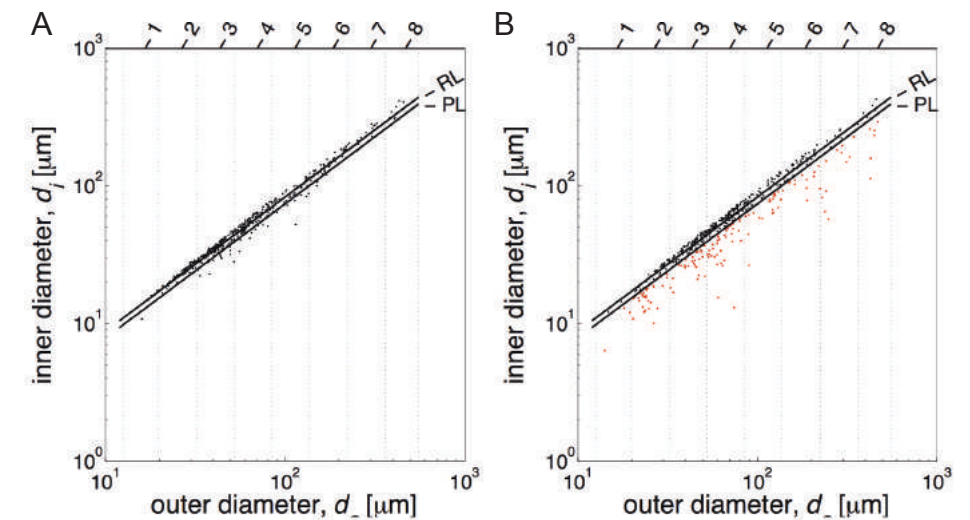


Figure 5 – Log-log plots of the diameters of control (A) and PAH (B) vessels per order (Strahler order numbers indicated on top), both with the regression line (RL) and the lower 90% prediction line (PL) of the control data. The vertical lines indicate the order limits. The PAH data points under the control PL are classified as narrowed vessels (red dots).

Discussion

We determined external and internal diameters of pulmonary vessels in the range of 13-500 μm , Strahler orders 1-8. The internal and external diameters of the control vessels were all located in a narrow range around the regression line (figure 5A), while in the PAH patients, on average, about 30% of the vessels were narrowed (figure 6A, number fraction), thus $\sim 70\%$ was in the range of the control subjects. This was the

first heterogeneity observed: not all vessels are narrowed. A second heterogeneity was that in each Strahler order, the affected vessels showed a large range of variation in internal diameter.

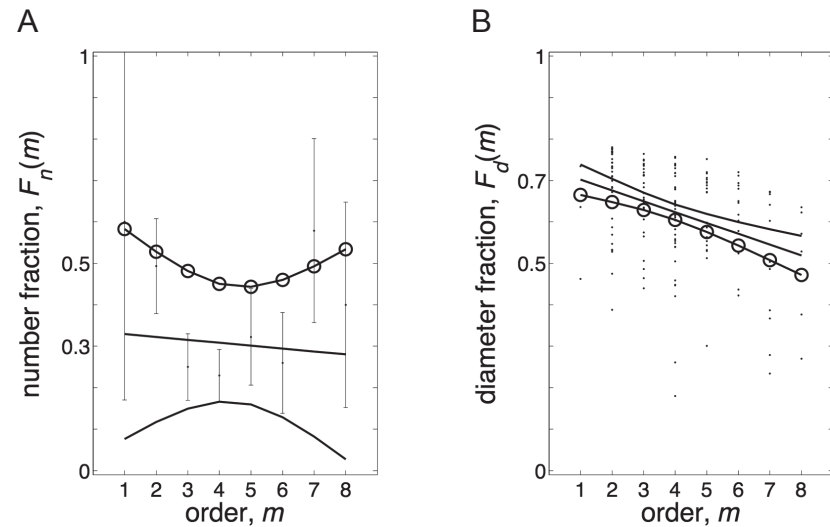


Figure 6 – Number and diameter fractions per order. (A) Number fractions $F_n(m)$ as function of order. (B) Diameter fractions of the vessels $F_d(m)$ per order. The regression lines with their 95% confidence intervals are shown. The slope of $F_n(m)$ is not significant ($P = 0.70$); the slope of $F_d(m)$ is significant ($P < 0.0001$). The circles on the upper and lower confidence limits indicate the values of $F_n(m)$ and $F_d(m)$ that predict the worst case that a maximal number of vessels are involved with a minimal inner diameter, thereby contributing maximally to the resistance increase.

Diameter and wall thickness

We here report data on internal and external diameters of the pulmonary vasculature, and thus were able to derive relative wall thickness from the slope of the relation between internal and external diameters (figures 3 and 4) as $WT = 1 - \text{slope}$. Only wall thickness (intima plus media) was studied, changes in wall composition (e.g., isolated media hypertrophy etc.), were not determined. To the best of our knowledge, number and diameter fractions, presented in figure 6, implying heterogeneous narrowing, are unique and a direct comparison with the literature is not possible.

In control subjects we find an average slope of 0.83, thus an average wall thickness of ~17%, which is close to wall thickness reported by Chazova (~18%).(3) Stacher et al., however, recently reported considerably thicker vessel walls in controls (about 30%).(17) Of all vessels studied 8.3% was occluded. Because vWF stains both endothelial cells and platelets, our histological analysis does not allow for a discrimination between occlusion due to thrombotic material and occlusion due to endothelial hyperproliferation.

In PAH we found the number of occluded vessels to be similar to control. Diameter relations vary greatly, but their average slope (figure 4) (when all vessels are included) is 0.66, resulting in an averaged wall thickness of 34%. Calculation of averaged wall thickness including the occluded vessels would only minimally increase the calculated average wall thickness, to about 39%. Chazova et al. report, at systolic/diastolic PAP 120/60 mmHg, thus estimated mPAP ~70 mmHg, a wall thickness of 50% for vessels between 25 and 250 μm .(3) Stacher et al. report wall thickness in hypertension at a mPAP ~58 mmHg about 60%.(17) However, it is not entirely clear if all vessels are included in Chazova's (3) and Stachers(17) studies. Palevsky et al. use wall area, with $WA = 100 \times \text{wall area} / \text{total vessel cross-sectional area}$ and found 64%, and thus wall thickness equaling $\sqrt{1 - \text{fractional WA}}$ is about 60% with range 40% - 75%, at a mPAP of ~60 mmHg.(15)

Can vascular changes predict Pulmonary Vascular Resistance?

Calculation of PVR, to estimate the contribution of vascular remodeling to resistance increase, requires the determination of the total number and internal diameters of all vessels in the entire lung. This data is not available. However, a relative increase in PVR from control to PAH can be obtained as follows. We found a number fraction of 30% (figure 6A), i.e., 70% of normal vessels remain. When we assume that in controls and PAH patients the percentage of occluded vessels are similar, that length changes do not occur and that all narrowed vessels are completely closed (i.e., thus not contributing to flow; this leads to an overestimation of the actual resistance), 30% of abnormal vessels would result in an $1/0.7 = 1.4$ fold increase in PVR in PAH. Maximal PVR in healthy individuals, within the limits of normal is 99 $\text{dyne} \cdot \text{s} \cdot \text{cm}^{-5}$.(16) Thus the value of $1.4 \cdot 99 = 138,6$ $\text{dyne} \cdot \text{s} \cdot \text{cm}^{-5}$, is far lower than the resistance in our patient group, which is 857 $\text{dyne} \cdot \text{s} \cdot \text{cm}^{-5}$ (table 1). This can partly be explained by the vascular reservoir capacity and blood flow recruitment the lung has, strengthened by the finding of Burrowes *et al.* who calculated that more than 50% of the vessels have to be obstructed to increase PVR.(2)

The number of occluded vessels we found and the small number of affected vessels between control and PAH, is considerably smaller than the 65% of mechanical obstruction that Burrowes et al. calculated to be required to increase the mPAP above 25 mmHg.(2)

The relatively large number of vessels with the same diameter as control vessels, if still functional, would suggest considerable effect of vasodilation. Since this is not the case, the vessels with normal wall thickness are either not functioning normally or pulmonary resistance is greatly affected by rarefaction or (changed) venous resistance.

Rarefaction has been debated.(12) In animal experiments the resistance of the venous system has been shown to be considerable.(5) An increased capillary pressure has been shown in patients with PAH, also suggesting a high venous resistance.(9) Recently Dorfmueller et al. showed venous involvement in chronic thromboembolic

pulmonary hypertension.(4) We therefore suggest that rarefaction and increased venous resistance should be studied in future research to determine their role in hemodynamic changes.

Limitations

Although studying pulmonary pathology in human tissue gives valuable insights, technical drawbacks are: Tissue blocks used in this study were retrospectively selected from the tissue biobank stored for diagnostic purposes. We randomly selected tissue blocks from unknown locations, but it cannot be guaranteed to be representative for the entire lung. That could also be true for the selection of rounded, transversally cut vessels. Also, longitudinal consistency of changes in the pulmonary vasculature has not been shown and could add another dimension of heterogeneity in vascular remodeling in PAH. Location of occlusive lesions in the pulmonary vasculature (proximal versus distal) could have a different impact on PVR. Studies on 3-dimensional vessel analyses and of the pulmonary vasculature below 25µm could improve understanding of the relation between vascular remodeling and PVR.

Diameters we been determined using samples of autopsy material where vessels are possibly (maximally) vasodilated and are therefore not necessarily representative of the *in vivo* situation. The possibility of differences in vasoactive state at death and potential differences of changes in vasodilation/constriction during fixation are, at present, not known. However, there is no reason to assume differences regarding to vasoconstriction and vasodilation between the control and PAH vessels after fixation and embedding.

Whether or not rarefaction of vessels exists could not be determined. To assess this phenomenon lengths and diameters and the total number of vessels or total endothelial surface area in control and PAH patients should be measured and compared in various regions of the lungs.

The presented data suggest that vascular remodeling results in a relatively small increase in PVR, which is insufficient to fully explain pulmonary vascular resistance as observed in PAH patients. Absolute numbers of vessels, wall thickness measurements of vessels below 25µm, and even information on the venous vasculature are required.

Conclusion

We show that structural changes in the pulmonary vasculature of PAH patients are heterogeneous: 70% of vessels is not altered and of the affected vasculature the degree of diameter decrease varies greatly. These diameter changes alone cannot explain the resistance increase in PAH (figure 7).

Perspectives

It is generally assumed that in pulmonary arterial hypertension (PAH), structural changes of the (small) pulmonary arteries in combination with vasoconstriction are the predominant cause of the increased resistance to blood flow and high pressure. We show that structural changes in the pulmonary arterial vasculature are heterogeneous: only 30 to 50% of the resistance arteries are narrowed and narrowing varies in vessel orders and possibly along vessel length. These changes cannot fully explain the resistance increase in PAH.

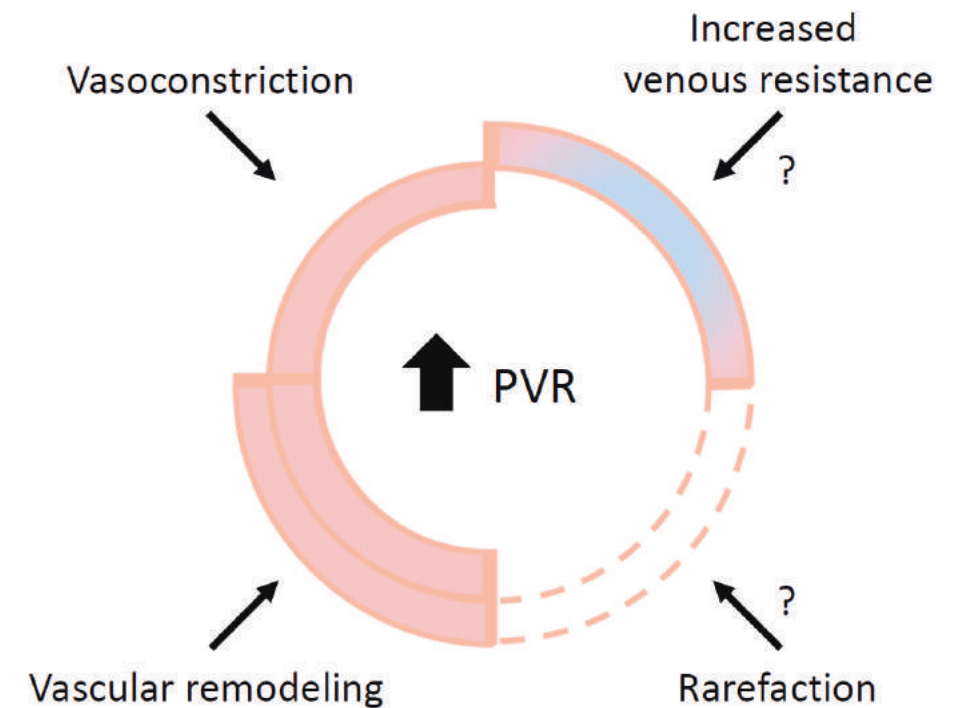


Figure 7 – Contributors to increased pulmonary vascular resistance. Increased pulmonary vascular resistance (PVR) can not only be attributed to vasoconstriction and pulmonary vascular remodeling; it is likely that increased venous resistance and rarefaction also contribute to hemodynamic changes seen in pulmonary arterial hypertension.

References

1. Anderson G, Reid L and Simon G. The radiographic appearances in primary and in thromboembolic pulmonary hypertension. *Clin Radiol* 24: 113-120, 1973.
2. Burrowes KS, Clark AR, Marcinkowski A, Wilsher ML, Milne DG and Tawhai MH. Pulmonary embolism: predicting disease severity. *Philos Trans A Math Phys Eng Sci* 369: 4255-4277, 2011.
3. Chazova I, Loyd JE, Zhdanov VS, Newman JH, Belenkov Y and Meyrick B. Pulmonary artery adventitial changes and venous involvement in primary pulmonary hypertension. *Am J Pathol* 146: 389-397, 1995.
4. Dorfmueller P, Gunther S, Ghigna MR, Thomas dM, V, Boulate D, Paul JF, Jais X, Decante B, Simonneau G, Dartevielle P, Humbert M, Fadel E and Mercier O. Microvascular disease in chronic thromboembolic pulmonary hypertension: a role for pulmonary veins and systemic vasculature. *Eur Respir J* 44: 1275-1288, 2014.
5. Hakim TS and Kelly S. Occlusion pressures vs. micropipette pressures in the pulmonary circulation. *J Appl Physiol (1985)* 67: 1277-1285, 1989.
6. Horsfield K. Morphometry of the small pulmonary arteries in man. *Circ Res* 42: 593-597, 1978.
7. Huang W, Yen RT, McLaurine M and Bledsoe G. Morphometry of the human pulmonary vasculature. *J Appl Physiol (1985)* 81: 2123-2133, 1996.
8. Huang W, Zhou Q, Gao J and Yen RT. A continuum model for pressure-flow relationship in human pulmonary circulation. *Mol Cell Biomech* 8: 105-122, 2011.
9. Kafi SA, Melot C, Vachiere JL, Brimiouille S and Naeije R. Partitioning of pulmonary vascular resistance in primary pulmonary hypertension. *J Am Coll Cardiol* 31: 1372-1376, 1998.
10. Lankhaar JW, Westerhof N, Faes TJ, Gan CT, Marques KM, Boonstra A, van den Berg FG, Postmus PE and Vonk-Noordegraaf A. Pulmonary vascular resistance and compliance stay inversely related during treatment of pulmonary hypertension. *Eur Heart J* 29: 1688-1695, 2008.
11. Lankhaar JW, Westerhof N, Faes TJ, Marques KM, Marcus JT, Postmus PE and Vonk-Noordegraaf A. Quantification of right ventricular afterload in patients with and without pulmonary hypertension. *Am J Physiol Heart Circ Physiol* 291: H1731-H1737, 2006.
12. Mooi W and Wagenvoort CA. Decreased numbers of pulmonary blood vessels: reality or artifact? *J Pathol* 141: 441-447, 1983.
13. Overbeek MJ, Lankhaar JW, Westerhof N, Voskuyl AE, Boonstra A, Bronzwaer JG, Marques KM, Smit EF, Dijkmans BA and Vonk-Noordegraaf A. Right ventricular contractility in systemic sclerosis-associated and idiopathic pulmonary arterial hypertension. *Eur Respir J* 31: 1160-1166, 2008.
14. Overbeek MJ, Vonk MC, Boonstra A, Voskuyl AE, Vonk-Noordegraaf A, Smit EF, Dijkmans BA, Postmus PE, Mooi WJ, Heijdra Y and Grunberg K. Pulmonary arterial hypertension in limited cutaneous systemic sclerosis: a distinctive vasculopathy. *Eur Respir J* 34: 371-379, 2009.
15. Palevsky HI, Schloo BL, Pietra GG, Weber KT, Janicki JS, Rubin E and Fishman AP. Primary pulmonary hypertension. Vascular structure, morphometry, and responsiveness to vasodilator agents. *Circulation* 80: 1207-1221, 1989.
16. Peacock AJ, Naeije R and Rubin LJ. *Pulmonary circulation: diseases and their treatment*. London: Arnold, 2011.
17. Stacher E, Graham BB, Hunt JM, Gandjeva A, Groshong SD, McLaughlin VV, Jessup M, Grizzle WE, Aldred MA, Cool CD and Tuder RM. Modern age pathology of pulmonary arterial hypertension. *Am J Respir Crit Care Med* 186: 261-272, 2012.

Supplemental material

Supplementary Table 1 – Number of vessels counted in each Strahler order

| Strahler order | Number of measurements | |
|----------------|------------------------|-------------|
| | Control (n = 5) | PAH (n = 6) |
| 1 | 7 | 5 |
| 2 | 71 | 73 |
| 3 | 120 | 110 |
| 4 | 101 | 170 |
| 5 | 44 | 62 |
| 6 | 43 | 48 |
| 7 | 21 | 19 |
| 8 | 8 | 15 |

6

Chapter 6

Endothelial dysfunction in pulmonary arterial hypertension: loss of cilia length regulation upon cytokine stimulation

RoI N, Dummer A, Szulcek R, Kurakula K, Pan X, Visser BI, Bogaard HJ, DeRuiter MC, Goumans MJ, Hierck BP.

Abstract

Pulmonary arterial hypertension (PAH) is a syndrome characterized by progressive lung vascular remodelling, endothelial cell (EC) dysfunction, and excessive inflammation. The primary cilium is a sensory antenna that integrates signalling and fine tunes EC responses to various stimuli. Yet, cilia function in the context of deregulated immunity in PAH remains obscure. We hypothesized that cilia function is impaired in ECs from patients with PAH due to their inflammatory status and tested whether cilia length changes in response to cytokines. Primary human pulmonary and mouse embryonic EC were exposed to pro- (TNF α , IL1 β , and IFN γ) and/or anti-inflammatory (IL-10) cytokines and cilia length was quantified. Chronic treatment with all tested inflammatory cytokines led to a significant elongation of cilia in both control human and mouse EC (by ~ 1 μ m, $P < 0.001$). This structural response was PKA/PKC dependent. Intriguingly, withdrawal of the inflammatory stimulus did not reduce cilia length. IL-10, on the other hand, blocked and reversed the pro-inflammatory cytokine-induced cilia elongation in healthy ECs, but did not influence basal length. Conversely, primary cilia of ECs from PAH patients were significantly longer under basal conditions compared to controls (1.86 ± 0.02 vs. 2.43 ± 0.08 μ m, $P = 0.002$). These cilia did not elongate further upon pro-inflammatory stimulation and anti-inflammatory treatment did not impact cilia length. The missing length modulation was specific to cytokine stimulation, as application of fluid shear stress led to increased cilia length in the PAH endothelium. We identified loss of cilia length regulation upon cytokine stimulation as part of the endothelial dysfunction in PAH.

Introduction

Pulmonary arterial hypertension (PAH) represents a group of lung diseases characterized by high pulmonary artery pressure (PAP) (>25 mmHg) eventually leading to right heart failure.(1,2) Blood vessels in the lungs of PAH patients are highly remodeled due to genetic changes, altered cellular signaling, metabolic changes, aberrant pressures, and chronic inflammation.(2–4)

PAH patients have a high inflammatory status both in the systemic circulation and in the lung vasculature.(4) Vascular inflammation involves various cytokines, including the pro-inflammatory TNF α , IL1 β , and IFN γ , as well as the anti-inflammatory cytokine IL10. Under the influence of pro-inflammatory cytokines, endothelial cells (ECs) express proteins, such as cell adhesion molecules, for the recruitment of blood borne inflammatory cells into the vessel wall.(5,6) Chronic or dysregulated inflammation leads to EC dysfunction involving a number of factors, such as loss of barrier integrity.(5,7)

As with most mammalian cell types, ECs carry primary cilia. The main structural part of the cilium is the rigid axoneme consisting of 9+0 microtubule doublets, which protrudes from the cellular membrane into the lumen or extracellular space.(8) The base of the cilium, the transition zone, functions as an active barrier for both the cytoplasmic and membrane content preventing free exchange and contributing to a unique subcellular environment.(9) The endothelial primary cilium is a highly regulated and specified antenna that senses and orchestrates responses to chemical and mechanical cues from the flowing blood.(10,11) Emerging data further identify the primary cilium as a specialized organelle involved in intracellular signaling processes from hedgehog proteins, growth factors, calcium, and others.(12–19) Furthermore, EC primary cilia are important for vascular integrity and homeostasis, since absence of primary cilia has been shown to promote endothelial-to-mesenchymal transition (EndoMT).(20) In accordance, primary cilia were found in areas of disturbed flow and are therefore suggested to protect against shear-induced EndoMT.(21,22)

Cilia length is instrumental for cilia function and is controlled by intraflagellar transport (IFT). Cilia length itself can regulate cargo loading of the IFT particles (e.g. with receptors), suggesting that signaling directly links to cilia length.(23) In addition, many signaling pathways have been shown to influence cilia length.(24–26) As such, cilia length increases in response to pro-inflammatory cytokines and was thereby proposed to mediate inflammatory responses.(27)

In diseases with dysregulated vascular inflammation, such as PAH, ECs are chronically exposed to vast amounts of pro-inflammatory cytokines. Hence, we hypothesized that the loss of cytokine-induced cilia length control is part of the EC dysfunction in PAH and tested whether cytokines can affect cilia length of human pulmonary microvascular EC from patients.

Methods

Cell culture

Cells were grown on 0.1% gelatin coated eight-chamber slides (BD Biosciences) until confluency. Ciliated mouse embryonic endothelial cells (MEC) were cultured as previously described.(20, 28) Primary human pulmonary microvascular endothelial cells (MVEC) were obtained from end-stage PAH patients and healthy tissues of lobectomy donors, as described before.(29) The tissue harvest and MVEC isolations were approved by the IRB of the VU University Medical Center (VUmc, Amsterdam, The Netherlands) and consent was given. MVEC were cultured in complete ECM medium supplemented with 1% pen/strep, 1% endothelial cell growth supplement, and 5% FCS (ScienceCell). Shear stress was applied, as previously described, by culturing cells on m-slides I Luer (ibidi) and applying medium flow at 15 dyn/cm² over the adherent cells with the ibidi pump system for five days.(29)

Treatments

Treatments were performed in starvation medium with 1% FCS and pen/strep. Stimuli were provided in fresh medium for 24 h. The following concentrations were used: TNF α 10 ng/mL, IL1 β 10 ng/mL, IFN γ 100 U/mL, and IL10 10 ng/mL. Forskolin (FK) was used in a concentration of 100 μ M (Sigma-Aldrich). H89 and Gö6983 (Sigma-Aldrich) were applied at 10 μ M and 2 μ M, respectively. The NF κ B inhibitor BAY 11-7085 (Cayman Chemicals) was applied at 1 μ M final concentration.

Cilia immunostaining

Cells were fixed in 4% paraformaldehyde (Merck) in PBS for 10 min at room temperature (RT). Fixed cells were permeabilized with 0.05% Tween 20 (Merck) in PBS. Incubation with the primary antibody against acetylated- α -tubulin (6-11B-1, 1:2000, Sigma-Aldrich) was performed overnight at 4°C. This was followed by 1 h incubation with secondary Cy3-labeled goat-anti-mouse antibody (1:500, Vector Laboratories) and DAPI nuclear counterstaining (1:1000, Molecular Probes) for 5 min at RT. Samples were mounted in Prolong Gold (Molecular Probes).

Cilia length measurements

Confocal z-stacks were taken with a fixed step distance of 0.25 μ m using a SP5 confocal microscope (Leica). Image acquisition and cilia length measurements were performed as described previously.(30) In short, a random population of at least ten cilia per condition were measured using the Pythagoras (PyT) method. Herefore, cilium length was determined in the xy- as well as in z-direction with ImageJ (NIH) and the three-dimensional length was calculated based on the Pythagorean theorem $a^2+b^2=c^2$, with a being the xy-length based on a maximum intensity projection (MIP) and b the z-length (Fig. 1, schematic). With the PyT method, the spatial orientation of the cilium is accounted for, wherefore selection bias and standard deviation are minimized.

Statistics

Experiments in MEC were performed in duplicate and repeated three times, experiments with MVEC were performed in duplicate in at least three donors. Statistics were calculated based on the averaged cilia length per donor with the total number of donors used as independent n . Data visualization and statistics were generated with GraphPad Prism 7. Data are presented as mean \pm SEM. Samples were tested for Gaussian distribution by D'Agostino-Pearson omnibus normality test. If not otherwise indicated, significance was determined by one-way ANOVA with Kruskal-Wallis test and Dunn's post hoc test. * $P = 0.033$, ** $P = 0.002$, *** $P < 0.001$

Results

TNF α induces sustained cilia elongation

We sought to determine whether TNF α influences cilia length dose dependently. Therefore, different concentrations of TNF α were tested on MEC (Fig. 1a). A low concentration of 2.5 ng/mL TNF α induced significant cilia elongation compared to unstimulated controls (1.96 ± 0.04 to 2.37 ± 0.05 mm, $P = 0.002$). Cilia length plateaued at an average length of approximately 3 mm with a concentration of 10 ng/mL or higher ($P < 0.001$). An additional increase in TNF α concentration did not further increase cilia length.

To examine the time course of cilia elongation upon TNF α stimulation, cilia length was measured at various time points (Fig. 1b). Indeed, cilia elongation upon TNF α stimulation was time-dependent. At 2 h after treatment, cilia elongation was visible, although not significant. Length was significantly increased 4 h after treatment ($P < 0.001$) and reaches a plateau after 8 h. The stimulation with TNF α caused sustained elongation and no significant differences in cilia length were found between 8 h and 48 h after treatment.

Additionally, we tested whether the removal of TNF α would reverse cilia length (Fig. 1c). To our surprise, washing steps after 16 h, 24 h, or 48 h did not alter cilia length. Moreover, additive treatment after 16 h, 24 h, or 48 h with TNF α did not show an extra effect on cilia length. Taken together, 8 h of TNF α treatment with a concentration of 10 ng/mL is sufficient to reach TNF α -induced maximal average cilia length and retain cilia elongation for at least 48 h.

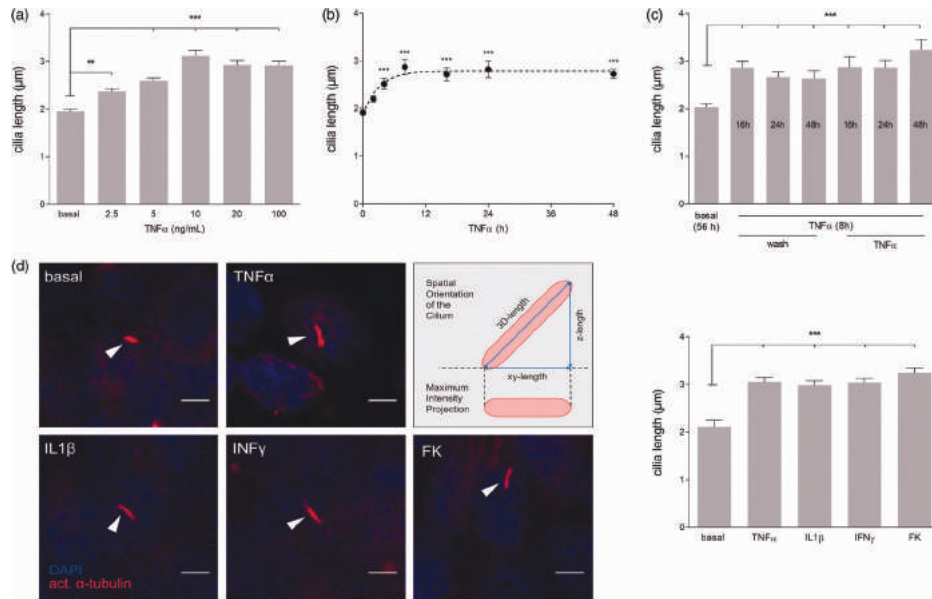


Figure 1 – Various pro-inflammatory cytokines elongate primary cilia permanently. (a) TNF α was applied to MEC in different concentrations for 24 h ($n \geq 100$ per concentration). (b) Time course of cilia elongation was quantified in MEC after addition of 10 ng/mL TNF α ($n \geq 43$ cilia per time point). (c) Cilia length was determined after an initial trigger of 8 h TNF α (10 ng/mL) followed by additional stimulation or an alternative wash step after 16 h, 24 h, or 48h. All conditions were fixed and quantified after 56 h ($n \geq 34$ cilia per condition). (d) Maximum intensity projections (MIP) of representative (flat) cilia (arrow heads) upon 24 h treatment with TNF α (10 ng/mL), IL1 β (10 ng/mL), IFN γ (100 U/mL), or the positive control FK (100 μ M) (scale bar = 5 μ m). Schematic depicts differences between MIP used to determine xy-length and three-dimensional (3D) length calculation applied for cilia length analysis and statistics. Quantification of average 3D cilia length is shown to the right ($n \geq 53$ per condition).

Various pro-inflammatory cytokines stimulate cilia elongation

To investigate whether various pro-inflammatory cytokines stimulate cilia elongation, MEC were exposed to either TNF α , IL1 β , or IFN γ (Fig. 1d). In general, cilia length significantly increased from approximately 2 μ m to approximately 3 μ m after stimulation ($P < 0.001$). FK was used as elongation as the inflammatory cytokines.

Since cells responding to stimulation have considerable cilia length variations, their frequency distribution was analyzed (Suppl. Fig. 1). The cytokine and FK stimulated samples showed a shift in frequency distribution towards longer cilia compared to controls. Cilia of 2 μ m were still present, indicative for cells that did not respond to stimulation, but the majority elongated to approximately 3 μ m and some individual cilia even up of 7 μ m.

Cytokine-induced cilia elongation is dependent on PKCdependent/ PKC signaling

It has been shown that primary cilia elongate upon direct stimulation of cyclic AMP with concomitant activation of PKC-dependent.(31) Involvement of PKC-dependent/PKC signaling in ciliary extension upon TNF α was tested by chemical inhibition with H89 or Gö6983 (Fig. 2). H89 and Gö6983 alone did not alter cilia length in MEC compared to basal condition. In agreement with the previous experiments, cilia length significantly increased to an average of approximately 3 μ m upon TNF α stimulation ($P < 0.001$). Importantly, inhibition of PKA and PKC prevented TNF α -induced elongation. Similar results were obtained with IL1 β , IFN γ , or the direct PKA activator FK (Suppl. Fig. 2A). In the presence of the inhibitors, none of the tested stimuli altered cilia length suggesting that cilia elongation by inflammatory cytokines is transduced through PKA/PKC dependent signaling.

To confirm the importance of PKC signaling more specifically, PKC knockdown was performed by shRNA. The knockdown was sufficient to prevent TNF α -induced elongation (Suppl. Fig. 2B). The use of the lentiviral construct resulted in viable cells with a 60% decrease in PKC mRNA levels (Suppl. Fig. 2C).

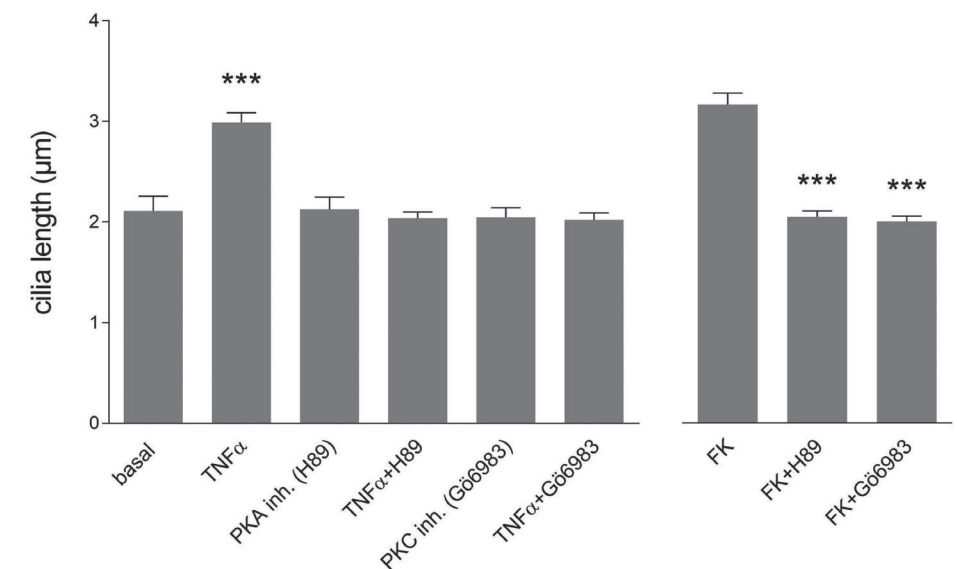


Figure 2 - Cilia elongation upon inflammatory cytokines is PKA/PKC-dependent. MEC were stimulated for 24 h with different combinations of TNF α (10 ng/mL) and/or the PKA inhibitor H89 (10 μ M) or PKC inhibitor Gö6983 (2 μ M) ($n \geq 43$ cilia per condition). The PKA activator FK was used as positive control.

IL10 blocks and reverses cilia elongation upon cytokine stimulation

We reasoned that when cells react to inflammatory cytokines by elongating their primary cilia, anti-inflammatory stimuli might counteract this response. Therefore, we tested whether IL10 prevents and reverses pro-inflammatory cytokine-induced cilia elongation.

MVEC were treated with basal medium, TNF α , or IL10 alone for 12 h. Afterwards either IL10 or TNF α were added on top of the previous stimulus for additional 12 h (Fig. 3a). In agreement with our previous experiments, 12 h or 24 h of TNF α stimulation alone showed significant cilia elongation to $\sim 3 \mu\text{m}$ ($P < 0.001$). IL10 alone did not influence cilia length compared to basal condition. Importantly, application of IL10 to TNF α blocked cilia elongation and IL10 added after TNF α reversed cilia length back to basal levels. The effect of IL10 on cilia length was not exclusive to TNF α , but identical upon IL1 β , IFN γ , and IL10 blocked the effect of direct PKA activation by FK stimulation (Suppl. Fig. 3A). Interestingly, its inhibitory function was dependent on the actual presence of IL10. Pre-treatment with IL10 followed by FK without IL10 in the medium was not sufficient to prevent elongation (Suppl. Fig. 3B). In conclusion, IL10 blocked and reversed cilia elongation upon stimulation with various inflammatory cytokines.

Cilia cytokine responses are similar in mouse and human endothelial cells

Primary cilia are highly conserved among species, wherefore their mechanisms might be as well. To examine, whether the primary cilia of human lung EC react in a similar manner to the pro-inflammatory TNF α and anti-inflammatory IL10 as mouse EC, we repeated the combination treatments in MVEC from healthy control lungs (Fig. 3b and c). Indeed, 12 h and 24 h of TNF α showed a significant cilia elongation to approximately $3 \mu\text{m}$ ($P < 0.001$) compared to basal length of $\sim 2 \mu\text{m}$. Again, IL10 alone had no effect on basal cilia length. When combined with TNF α , IL10 blocked cilia elongation, while IL10 applied 12 h after TNF α reversed cilia length back to basal levels.

Endothelial cells of PAH patients display elongated cilia

To test, whether cilia length differs between patient and control MVEC, cilia were quantified in samples of three control and three donors with PAH (Fig. 4a). Under basal conditions the average length of cilia on EC from PAH patients was significantly increased to $2.43 \pm 0.08 \mu\text{m}$ compared to $1.86 \pm 0.02 \mu\text{m}$ of the controls ($P = 0.002$).

TNF α and IL10 do not affect cilia length in PAH cells

Healthy MEC and MVEC showed cilia elongation upon stimulation with inflammatory cytokines to $\sim 3 \mu\text{m}$. IL10 could shorten cilia and block the effects of TNF α . PAH patient-derived MVEC exerted elongated cilia under basal conditions already (Fig. 4a), wherefore we tested cilia length responses in these patient cells (Fig. 4b). To our surprise, treatment with TNF α had no additional effect on cilia length and IL10 treatment of PAH MVEC did neither reduce basal cilia length nor affected the response

to TNF α . To answer whether specifically the response to IL10 was lost or if cilia of PAH cells are generally unresponsive to anti-inflammatory treatment, the NF κ B inhibitor BAY 11-7085 was tested. BAY 11-7085 showed similar responses like IL10 blocking the effects of TNF α in controls but leaving elongated basal PAH cilia unchanged.

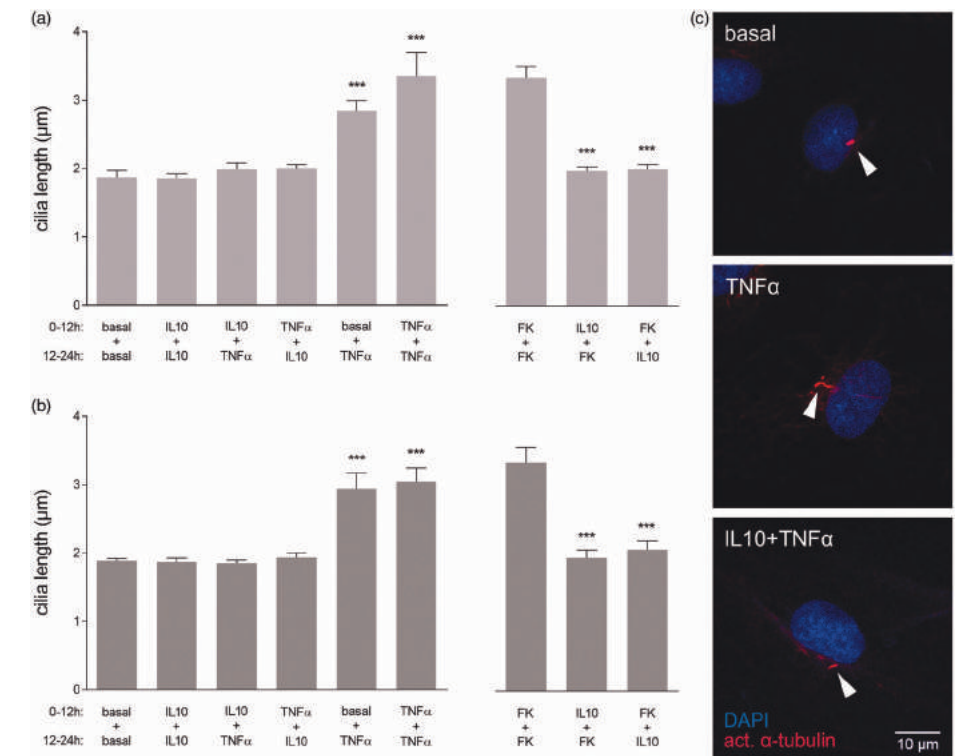


Figure 3 - IL10 blocks and reverses cilia elongation upon inflammatory cytokine stimulation in mouse and human endothelial cells. (a) MEC were either incubated with IL10 (10 ng/mL), TNF α (10 ng/mL), or left untreated for 12 h. Subsequently, different combinations of TNF or IL10 were added directly into the previous conditions and incubated for another 12 h ($n \geq 26$ cilia per condition). (b) The combination treatments were repeated in human pulmonary MVEC of healthy individuals (donor = 3, $n \geq 28$ cilia per condition). (c) MIP of representative cilia (arrowheads) on MVEC under the different conditions.

The sheared PAH endothelium shows increased cilia length

To further elucidate, if PAH MVEC have completely lost their cilia length regulation ability, fluid shear stress was tested as trigger (Fig. 4c). Primary cilia of PAH MVEC were found significantly elongated to $4.87 \pm 0.46 \mu\text{m}$ compared to $2.09 \pm 0.17 \mu\text{m}$ of controls ($P < 0.001$) after five days of high shear stress. Additionally, while cilia of the sheared controls were localized towards the leading edge of the cells in the direction of flow and migration, cilia of PAH MVEC were found randomly positioned around the nucleus.

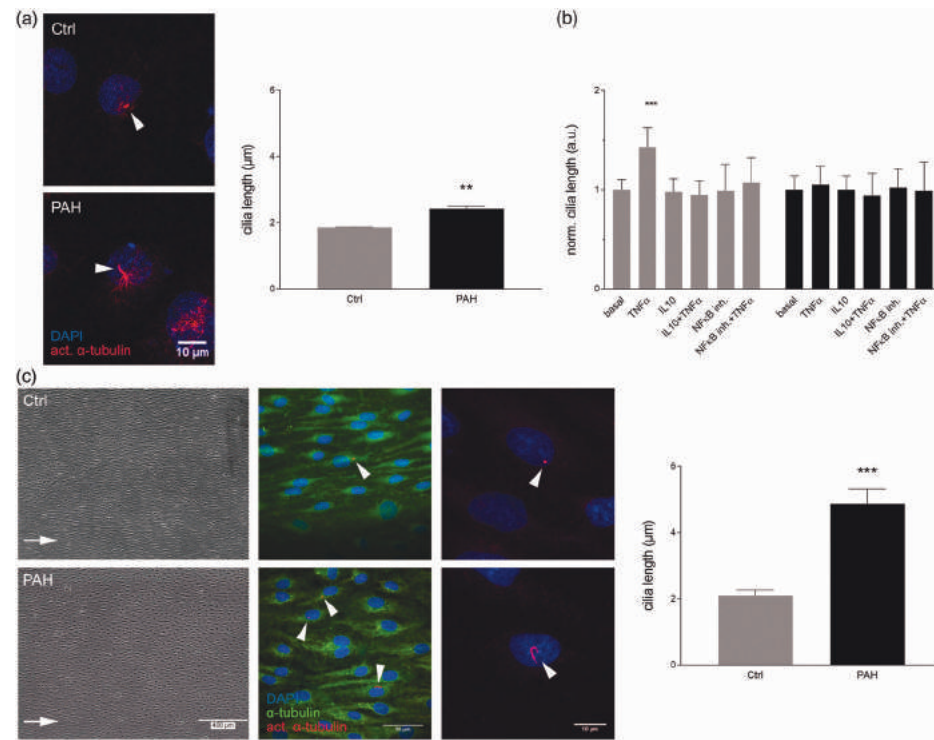


Figure 4 - PAH patient-derived endothelial cells exert elongated cilia that are non-responsive to pro- and anti-inflammatory treatment but respond to fluid shear stress. (a) MVEC from controls and PAH lungs were grown to confluency and did not receive additional treatment. Cilia length was quantified. Samples were normally distributed and significance was calculated using an unpaired student's t-test on their average lengths (donor = 3, $n \geq 10$ per donor). (b) Healthy controls (gray) and PAH-derived MVEC (black) were stimulated with TNF α , IL10 (both 10 ng/mL), Nf κ B inhibitor (1 μ M) alone, or a combination of TNF α and a inhibitor. Cilia length was normalized to intra-experimental controls (basal) (donor ≥ 3 , $n \geq 10$ per donor and condition). (c) Control and PAH MVEC were subjected to high fluid shear stress (15 dyn/cm²) for five days and cilia length was quantified. Representative phase-contrast and fluorescence staining are shown. Arrows indicate direction of flow. Cilia length was quantified and differences were calculated with an unpaired student's t-test.

Discussion

Microvascular EC from lungs of patients with PAH display elongated cilia. These cells are incapable to adapt their cilia length in response to pro- and anti-inflammatory cytokine stimulation.

Primary cilia play a pivotal role in vascular integrity and homeostasis. Cilia dysfunction is implicated in several pathologies, such as atherosclerosis and developmental diseases. Among the variety of ciliopathies, cilia can be elongated, truncated, less present, or completely absent.(26) In the Joubert syndrome, patients show less and shortened cilia.(32) In contrast, the phenotype of Meckel-Gruber syndrome is elongated cilia. Most patients with Bardet-Biedl syndrome show truncated cilia, although patients with one specific subtype have elongated renal epithelial cilia.(26, 33) In addition to variations in cilia form across different ciliopathies, there is considerable heterogeneity in cilia function dependent on host cell and vascular bed. Renal cilia play a part in repair processes; they elongate upon renal injury and decrease in length during renal repair.(34) In chondrocytes, cilia shorten upon mechanical loading to minimize cell sensitivity to prolonged activation.(35) In mesenchymal stem cells, cilia elongation has been shown important for differentiation.(36) Taken together, cells change their cilia length in response to environmental cues. When this process is dysfunctional, initial adaptation is disturbed and homeostasis and repair impaired.

PAH is a fatal group of diseases with a high inflammatory status.(4) Cilia length increases in response to pro-inflammatory cytokines and was thereby proposed to mediate inflammatory responses.(27) Hence, we tested the pro-inflammatory cytokines TNF α , IL1 β , and IFN γ on healthy EC and all three cytokines provoked a similar increase in average cilia length to ~ 3 μ m. Thereby, not only the increase in length but also the length distribution was comparable between the various cytokines. This indicates a generic mechanism for cilia elongation upon inflammatory stimuli, since the cytokines themselves act through unique receptors and signaling pathways.(5) Moreover, similar effects were observed between mouse and human ECs, which point towards a conserved mechanism among species.

Chondrocytes have been shown to elongate cilia upon IL1 β stimulation in a PKA/PKC-dependent manner.(27) In line with this finding, we show that PKA and PKC inhibition prevented cilia elongation after stimulation with the inflammatory cytokines. Interestingly, PKA/PKC signaling was not necessary to express cilia and basal length was not affected by PKA or PKC inhibition. Therefore, PKA/PKC signaling is predominantly needed for cilia elongation and might present a common integrator for various stimuli.

To consider, the individual stimuli might cause subtle differences in absolute cilia length. Using the PyT method to determine average cilia length keeps selection bias minimal. However, subtle length differences $<0.2 \mu\text{m}$ might be underestimated.(30) What controls maximal cilia length and what absolute minimal change of length is functionally important remains to be resolved.

To reverse cilia length, removing the inflammatory stimulus was not sufficient, but application of the anti-inflammatory cytokine IL10 was needed to shorten the extended cilia back to basal levels demonstrating the need for active cues to switch EC from a pro- to anti-inflammatory state. In addition, IL10 (or NF κ B inhibition) could block cilia elongation upon inflammatory cytokines and FK. Here, the effect was direct and reversible and left basal cilia length unaffected. Interestingly, the effect of IL10 was general for all tested cytokines and conserved in mouse and human EC. The precise mechanism of IL10 regulating cilia length remains to be determined. A direct effect of IL10 on PKA/PKC was not yet shown, while PKA itself is involved in IL10 production. (37) Recent literature showed that the effects of TNF α , INF γ , and IL10 might, at least in part, be regulated independent of PKA via the SOCS (suppressor of cytokine signaling) pathway.(37) The authors found a synergistic activation of SOCS-3 when combining IL10 and cyclic AMP treatment that was independent from PKA activation.

When repeating the stimulations in MVEC from patients with PAH, we found that cilia were already elongated under basal conditions compared to controls. Therefore, we assumed that treatment with IL10 would reduce cilia length. To our surprise, PAH ECs did neither respond to pro- nor anti-inflammatory cytokines with a variation of cilia length. The basal elongation and loss of TNF α response might be an adaptation to the excessive amounts of pro-inflammatory cytokines produced by the diseased cells and the chronic state of inflammation in patient lungs.(4) However, the failure of IL10 to reduce cilia length might alternatively indicate that the basal elongation is independent from inflammatory signaling but rather due to metabolic changes.(38) Of interest, longer cilia are known to be associated with decreased proliferation and thereby might be the cells attempt to counteract the hyper-proliferative phenotype characteristic to the PAH endothelium.(39, 40) In accordance with this line of reasoning, PAH patients with high levels of IL10 have a worse prognosis.(41) On the contrary, higher IL10 levels are also suggested as compensatory mechanism in more advanced stages of the disease. In addition, administration of IL10 prevented development of PH in the monocrotaline rat model a model characterized by severe inflammation.(42)

Application of fluid shear stress (instead of cytokines) significantly altered cilia length of PAH cells, wherefore the loss of cilia length control seems specific to cytokine stimulation. Nevertheless, cilia of sheared PAH cells were longer than of controls and randomly localized around the nucleus, although they should be oriented towards the leading edge of the shear adapted cells, such as seen in the controls. This indicates

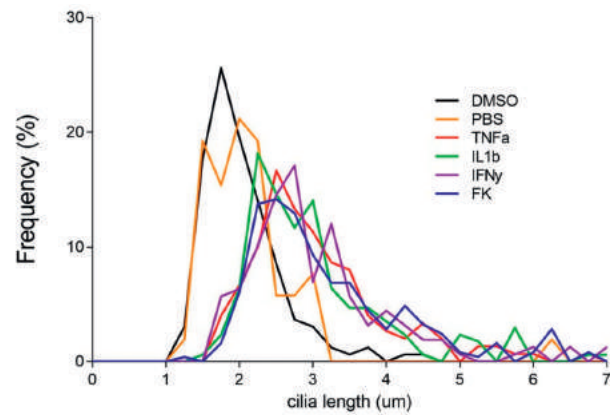
defective mechano-responses and cell polarity in the sheared PAH cells, which might be a consequence of the defective shear sensing and delayed morphological adaptation that we reported earlier.(29) However, mono-motile cilia are linked to cell polarity, directed migration, and wound repair pointing towards a generally dysfunctional PAH endothelial responsiveness to microenvironmental cues that might manifest through or, at least partly, be caused by the dysfunctional cilium.(43)

To summarize, longer cilia are an inherent feature of PAH MVEC. The sustained elongation of primary cilia and a loss of length regulation function upon cytokine stimulation might represent an adaptive response to the chronic inflammation and act as a rescue mechanism to prevent further recruitment of blood-borne inflammatory cells into the vessel wall of patient lungs and decrease EC proliferative rates. However, the functional consequences of cilia non-responsiveness on intra-endothelial signaling and the surrounding tissue remain subject to further studies. Here, investigating defective cilia elongation in response to inflammatory cytokines might reveal downstream cellular changes contributing to disease progression. Additionally, restoring cilia responses to anti-inflammatory treatment in ECs from PAH patients might decelerate disease progression by maintaining the EC phenotype.

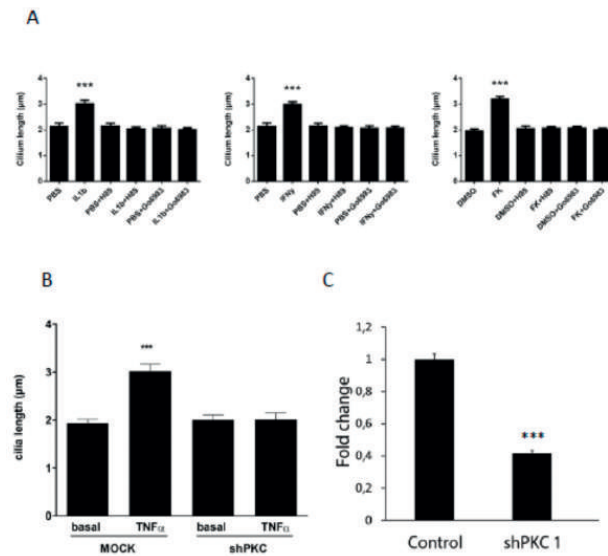
References

1. Galiè N, Humbert M, Vachiery J-L, et al. 2015 ESC/ERS Guidelines for the diagnosis and treatment of pulmonary hypertension: The Joint Task Force for the Diagnosis and Treatment of Pulmonary Hypertension of the European Society of Cardiology (ESC) and the European Respiratory Society (ERS); Endor. *Eur Respir J* 2015; 46: 903–975. 2.
2. Guignabert C and Dorfmüller P. Pathology and pathobiology of pulmonary hypertension. *Semin Respir Crit Care Med* 2013; 34: 551–559.
3. Dickinson MG, Kowalski PS, Bartelds B, et al. A critical role for Egr-1 during vascular remodelling in pulmonary arterial hypertension. *Cardiovasc Res* 2014; 103: 573–584.
4. Groth A, Vrugt B, Brock M, et al. Inflammatory cytokines in pulmonary hypertension. *Respir Res* 2014; 15: 47.
5. Kindt TJ, Goldsby RAR and Osborne BA. *Kuby Immunology*, 6th ed. New York: W.H. Freeman, 2007.
6. Carbone F and Montecucco F. Inflammation in arterial diseases. *IUBMB Life* 2015; 67: 18–28.
7. Sprague AH and Khalil RA. Inflammatory cytokines in vascular dysfunction and vascular disease. *Biochem Pharmacol* 2009; 78: 539–552.
8. Van der Heiden K, Groenendijk BCW, Hierck BP, et al. Monocilia on chicken embryonic endocardium in low shear stress areas. *Dev Dyn* 2006; 235: 19–28.
9. Takao D and Verhey KJ. Gated entry into the ciliary compartment. *Cell Mol Life Sci* 2016; 73: 119–127.
10. Praetorius HA. The primary cilium as sensor of fluid flow: new building blocks to the model. A review in the theme: cell signaling: proteins, pathways and mechanisms. *Am J Physiol Cell Physiol* 2015; 308: C198–208.
11. Poelmann RE, Van der Heiden K, Gittenberger-de Groot A, et al. Deciphering the endothelial shear stress sensor. *Circulation* 2008; 117: 1124–1126.
12. Satir P, Pedersen LB and Christensen ST. The primary cilium at a glance. *J Cell Sci* 2010; 123: 499–503.
13. Clement CA, Ajbro KD, Koefoed K, et al. TGF- β signaling is associated with endocytosis at the pocket region of the primary cilium. *Cell Rep* 2013; 3: 1806–1814.
14. Christensen ST, Clement CA, Satir P, et al. Primary cilia and coordination of receptor tyrosine kinase (RTK) signalling. *J Pathol* 2012; 226: 172–184.
15. May-Simera HL and Kelley MW. Cilia, Wnt signaling, and the cytoskeleton. *Cilia* 2012; 1: 7.
16. Satir P and Christensen ST. Overview of structure and function of mammalian cilia. *Annu Rev Physiol* 2007; 69: 377–400.
17. Egorova ADD, Van der Heiden K, Van de Pas S, et al. Tgfb/ Alk5 signaling is required for shear stress induced klf2 expression in embryonic endothelial cells. *Dev Dyn* 2011; 240: 1670–1680.
18. Basten SG and Giles RH. Functional aspects of primary cilia in signaling, cell cycle and tumorigenesis. *Cilia* 2013; 2: 6.
19. Mick DU, Rodrigues RB, Leib RD, et al. Proteomics of primary cilia by proximity labeling. *Dev Cell* 2015; 35: 497–512.
20. Egorova AD, Khedoe PPSJ, Goumans M-JTH, et al. Lack of primary cilia primes shear-induced endothelial-to-mesenchymal transition. *Circ Res* 2011; 108: 1093–1101.
21. Van der Heiden K, Hierck BP, Krams R, et al. Endothelial primary cilia in areas of disturbed flow are at the base of atherosclerosis. *Atherosclerosis* 2008; 196: 542–550.
22. Dinsmore C and Reiter JF. Endothelial primary cilia inhibit atherosclerosis. *EMBO Rep* 2016; 17: 156–166.
23. Wren KN, Craft JM, Tritschler D, et al. A differential cargo-loading model of ciliary length regulation by IFT. *Curr Biol* 2013; 23: 2463–2471.
24. Keeling J, Tsiokas L and Maskey D. Cellular Mechanisms of Ciliary Length Control. *Cells* 2016; 5: 6.
25. Miyoshi K, Kasahara K, Miyazaki I, et al. Factors that influence primary cilium length. *Acta Med Okayama* 2011; 65: 279–285.
26. Avasthi P and Marshall WF. Stages of ciliogenesis and regulation of ciliary length. *Differentiation* 2012; 83: 30–42.
27. Wann AKT and Knight MM. Primary cilia elongation in response to interleukin-1 mediates the inflammatory response. *Cell Mol Life Sci* 2012; 69: 2967–2977.
28. Nauli SM, Kawanabe Y, Kaminski JJ, et al. Endothelial cilia are fluid shear sensors that regulate calcium signaling and nitric oxide production through polycystin-1. *Circulation* 2008; 117: 1161–1171.
29. Szulcek R, Hapke CM, Rol N, et al. Delayed microvascular shear adaptation in pulmonary arterial hypertension. role of platelet endothelial cell adhesion molecule-1 cleavage. *Am J Respir Crit Care Med* 2016; 193: 1410–1420.
30. Dummer A, Poelma C, DeRuiter MC, et al. Measuring the primary cilium length: improved method for unbiased highthroughput analysis. *Cilia* 2016; 5: 7.
31. Besschetnova TY, Kolpakova-Hart E, Guan Y, et al. Identification of signaling pathways regulating primary cilium length and flow-mediated adaptation. *Curr Biol* 2010; 20: 182–187.
32. Malicdan MCV, Vilboux T, Stephen J, et al. Mutations in human homologue of chicken talpid3 gene (KIAA0586) cause a hybrid ciliopathy with overlapping features of Jeune and Joubert syndromes. *J Med Genet* 2015; 52: 830–839.
33. Mokrzan EM, Lewis JS and Mykytyn K. Differences in renal tubule primary cilia length in a mouse model of Bardet-Biedl syndrome. *Nephron Exp Nephrol* 2007; 106: e88–96.
34. Verghese E, Ricardo SD, Weidenfeld R, et al. Renal primary cilia lengthen after acute tubular necrosis. *J Am Soc Nephrol* 2009; 20: 2147–2153.
35. McGlashan SR, Knight MM, Chowdhury TT, et al. Mechanical loading modulates chondrocyte primary cilia incidence and length. *Cell Biol Int* 2010; 34: 441–446.
36. Dalbay MT, Thorpe SD, Connelly JT, et al. Adipogenic differentiation of hMSCs is mediated by recruitment of IGF-1r onto the primary cilium associated with cilia elongation. *Stem Cells* 2015; 33: 1952–1961.
37. Gasperini S, Crepaldi L, Calzetti F, et al. Interleukin-10 and cAMP-elevating agents cooperate to induce suppressor of cytokine signaling-3 via a protein kinase A-independent signal. *Eur Cytokine Netw* 2002; 13: 47–53.
38. Rabinovitch M, Guignabert C, Humbert M, et al. Inflammation and immunity in the pathogenesis of pulmonary arterial hypertension. *Circ Res* 2014; 115: 165–175.
39. Kim S, Zaghoul NA, Bubenshchikova E, et al. Nde1-mediated inhibition of ciliogenesis affects cell cycle re-entry. *Nat Cell Biol* 2011; 13: 351–360.
40. Sakao S, Tatsumi K and Voelkel NF. Endothelial cells and pulmonary arterial hypertension: apoptosis, proliferation, interaction and transdifferentiation. *Respir Res* 2009; 10: 95.
41. Soon E, Holmes AM, Treacy CM, et al. Elevated levels of inflammatory cytokines predict survival in idiopathic and familial pulmonary arterial hypertension. *Circulation* 2010; 122: 920–927.
42. Ito T, Okada T, Miyashita H, et al. Interleukin-10 expression mediated by an adeno-associated virus vector prevents monocrotaline-induced pulmonary arterial hypertension in rats. *Circ Res* 2007; 101: 734–741.
43. Veland IR, Lindbæk L and Christensen ST. Linking the primary cilium to cell migration in tissue repair

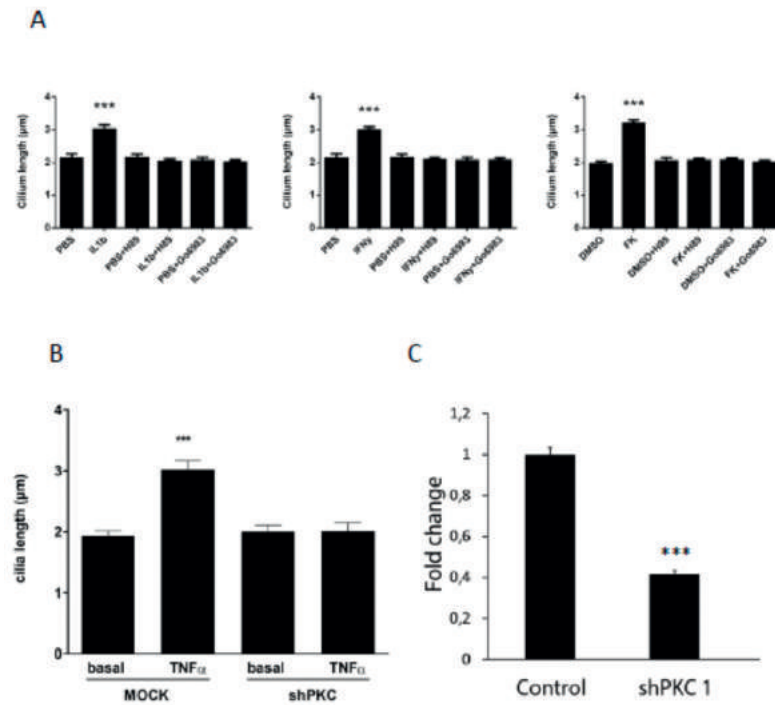
Supplemental figures



Supplemental Figure 1 – Frequency distributions of cilia length in stimulated and unstimulated MEC. Represented are the hull curves of the histograms ($n > 53$ cilia per condition). PBS and DMSO controls show similar length distributions with a maximum at around $1.8 \mu\text{m}$. $\text{TNF}\alpha$, $\text{IL1}\beta$, $\text{IFN}\gamma$ and forskolin (FK) show a shift in cilia length distribution towards in average longer cilia at 24 h after stimulation.



Supplemental Figure 2 – A) Pharmacological inhibition of PKA with H89 and PKC signaling by Gö6983 blocks cilia elongation upon stimulation with $\text{IL1}\beta$, $\text{IFN}\gamma$, or FK in MEC. B) Lenti-viral knockdown of PKCeta prevents $\text{TNF}\alpha$ induced cilia elongation in MEC. shRNA against GFP was used as control. C) PKCeta knockdown shows 60% efficiency on mRNA level.



Supplemental Figure 3 – A) IL10 blocks and reverses cilia elongation upon stimulation with $\text{IL1}\beta$, $\text{IFN}\gamma$, or FK in MEC. B) IL10 needs to be combined with FK to block FK induced cilia elongation. Pre-treatment with IL10 alone is not sufficient.

Supplemental methods

Knockdown

MEC were grown to 60% confluency and treated with lenti-viral constructs containing shRNA against PKCeta (SHCLNG_NM_008856, Sigma Aldrich, Table 1). Selection was done with 3 ng/mL puromycin (Sigma-Aldrich).

qPCR

RNA was isolated using the RNeasy Micro Kit (Qiagen). cDNA synthesis was performed using the iScript™ cDNA Synthesis Kit (Biorad) with 500 ng total RNA input. Real-time qPCR was performed by using iQ SYBR Green Supermix (Biorad) in a Mx3000 real-time thermocycler (Stratagene). Primers are listed in Table 2. No-template controls were used as negative controls. mRNA expression levels were calculated relative compared to the housekeeping gene GAPDH.

Table 1 - ID and sequences of shRNAs

| Target | shRNA clone | sequence |
|--------|--------------------------------|---|
| shPKC | NM_008856.2-933s1c1 | CCGGCGACAAGGACTTCAGTGTAACCTCGAGTTTACTACTGAA-GTCCTTGTCGTTTTT |
| MOCK | MISSION pLKO.1-puro eGFP shRNA | CCGGTACAACAGCCACAACGTCTATCTCGAGATAGACGTTGTG-GCTGTTGTATTTTT |

Table 2 - qPCR primers

| Target | Primer sequence |
|----------------|----------------------|
| GAPDH forward | TTGATGGCAACAATCTCCAC |
| GAPDH reverse | CGTCCCGTAGACAAAATGGT |
| PKCeta forward | GCATCCGCCTTAGAACACC |
| PKCeta reverse | CCTGGGGACTTGAGAGAGC |

7

Chapter 7

TGF-beta and BMPR2 signaling in PAH: two black sheep in one family

Roel N., Kurakula K, Happé CM, Bogaard HJ, Goumans MJ

Abstract

Knowledge pertaining to the involvement of transforming growth factor β (TGF- β) and bone morphogenetic protein (BMP) signaling in pulmonary arterial hypertension (PAH) is continuously increasing. There is a growing understanding of the function of individual components involved in the pathway, but a clear synthesis of how these interact in PAH is currently lacking. Most of the focus has been on signaling downstream of BMPR2, but it is imperative to include the role of TGF- β signaling in PAH. This review gives a state of the art overview of disturbed signaling through the receptors of the TGF- β family with respect to vascular remodeling and cardiac effects as observed in PAH. Recent (pre)-clinical studies in which these two pathways were targeted will be discussed with an extended view on cardiovascular research fields outside of PAH, indicating novel future perspectives.

Introduction

Pulmonary arterial hypertension (PAH) is a condition defined by an increase in mean pulmonary artery pressure and characterized by remodeling of the pulmonary vasculature (1). Abnormalities in vessel functionality and responses to stressors culminate in aberrant growth of endothelial cells (ECs) and smooth muscle cells (SMCs), leading to vascular obstruction and the formation of plexiform lesions. The increased pulmonary vascular resistance enhances the load upon the right ventricle (RV). The RV will compensate with hypertrophy, which progresses to RV-failure and death. Current available therapies for PAH mainly target vasoconstriction to reduce pressures and relieve the load, with some showing anti-proliferative effects in vitro. These drugs decelerate, but do not stop disease progression (2,3).

The transforming growth factor- β (TGF- β) family plays a major role in the initiation and progression of PAH. TGF- β is not only an important regulator of vascular remodelling and inflammation in the lung, but also of hypertrophy and fibrosis in the heart (4,5,6,7,8). Of all receptors belonging to the TGF- β family (Figure 1), the bone morphogenetic protein type 2 receptor (BMPR2) is the most relevant for PAH. Mutations in the BMPR2 gene were the first discovered and most studied mutations underlying hereditary PAH to date (9,10). BMPR2 is closely entangled with other members of the TGF- β family, but the roles of many of the ligands and receptors in the TGF- β family are still underappreciated in PAH. Although bone morphogenetic protein (BMP) ligands and their receptors play an important role in disease progression and could function as therapeutic targets (11), agents effectively decreasing TGF- β 1 activity, together with selective TGF- β ligand traps open up new treatment possibilities (12,13,14,15,16).

Here, we give a comprehensive update on TGF- β signaling in PAH, summarized in Table 1. Furthermore, we provide insights into current (pre)-clinical studies targeting the TGF- β pathway in other diseases that may be useful in designing therapeutic strategies for the deadly condition of PAH.

TGF- β signaling

Members of the TGF- β family are widely expressed in diverse tissues and play an essential role throughout life, starting from gastrulation and the onset of body axis asymmetry to organ-specific morphogenesis and adult tissue homeostasis (55,56,57,58). At the cellular level, TGF- β family members regulate fundamental processes important for tissue homeostasis and embryogenesis, such as cell proliferation, differentiation, apoptosis, migration, adhesion, cytoskeletal organization, extracellular matrix production, in a context- and cell type-dependent manner. Consistent with this pleiotropic activity, disrupted TGF- β signaling is associated with

several developmental disorders, cancer, auto-immune, cardiovascular and fibrotic diseases (55,56,57,59,60).

The TGF- β family members are subdivided into two functional groups: the TGF- β group that comprises the three mammalian TGF- β isoforms, activins, nodals and some growth and differentiation factors (GDFs) and the BMP group that includes all BMPs and most GDFs (Figure 1) (57,59). TGF- β family members form functional dimers, bind to heterotetrameric complex of type I and type II serine/threonine kinase transmembrane receptors and signal through both Smad-dependent and Smad-independent pathways (57,58,61,62) (Figure 2). In mammals, seven type I receptors, also known as activin receptor-like kinases (ALKs), and five type II receptors have been reported so far. To control duration and intensity of TGF- β signaling, agonists, antagonists, co-receptors and intracellular signaling play key roles in ligand access and posttranslational modification of the receptors and downstream mediators in a cell- and context-dependent manner (60,61,63). TGF- β is secreted in its latent form and needs to be proteolytically processed before being able to bind to signaling receptors (4). This complex activation mechanism could open up new therapeutic targets. TGF- β signals in most cells by binding to β RII forming a complex with β RI (or ALK5). Activins bind to activin receptor type IIA (ActRIIA) or ActRIIB in a complex with ALK4, while BMPs signal via BMP type II receptor (BMPRII), ActRIIA or ActRIIB, in combination with ALK1, 2, 3 or 6. Although β RII/ β RI is the preferable high affinity signaling complex, in endothelial cells, TGF- β can also signal through β RII/ALK1/ALK5 (64,65).

Upon complex formation, the activated type I receptor kinase will transduce the signal from the membrane to the nucleus by phosphorylating Smad transcription factors (61). Smads are divided into three major classes: receptor-regulated Smads (R-Smads), common mediator Smad (co-Smad) and the inhibitory Smads (I-Smads). R-Smads (Smad1, Smad2, Smad3, Smad5 and Smad8) function as direct substrates for specific type I receptor kinases. ALK4, -5 and -7 phosphorylate Smad2 and Smad3, whereas Smad1, Smad5 and Smad8 become phosphorylated by the BMP type I receptors ALK1, -2, -3 and -6 (66). Upon phosphorylation, R-Smads form a complex with the co-Smad, Smad4, and translocate to the nucleus. In the nucleus, Smad complexes engage in cooperative interactions with DNA and other DNA-binding proteins such as FAST1, FAST2, Fos/Jun and ATF2 to mediate the transcription of specific target genes (60,67). The two I-Smads, Smad6 and Smad7, first identified in 1997 as vascular Smads, can compete with and inhibit R-Smads for type I interaction preventing phosphorylation (61,68). Furthermore, they can induce proteasomal degradation of the type I receptor by recruiting Smurf1/2 E3 ubiquitin ligases (55,56,57,59,60). For a more extensive description of TGF- β signaling, we refer to recent reviews (58,69,70,71,72,73,74,75,76,77).

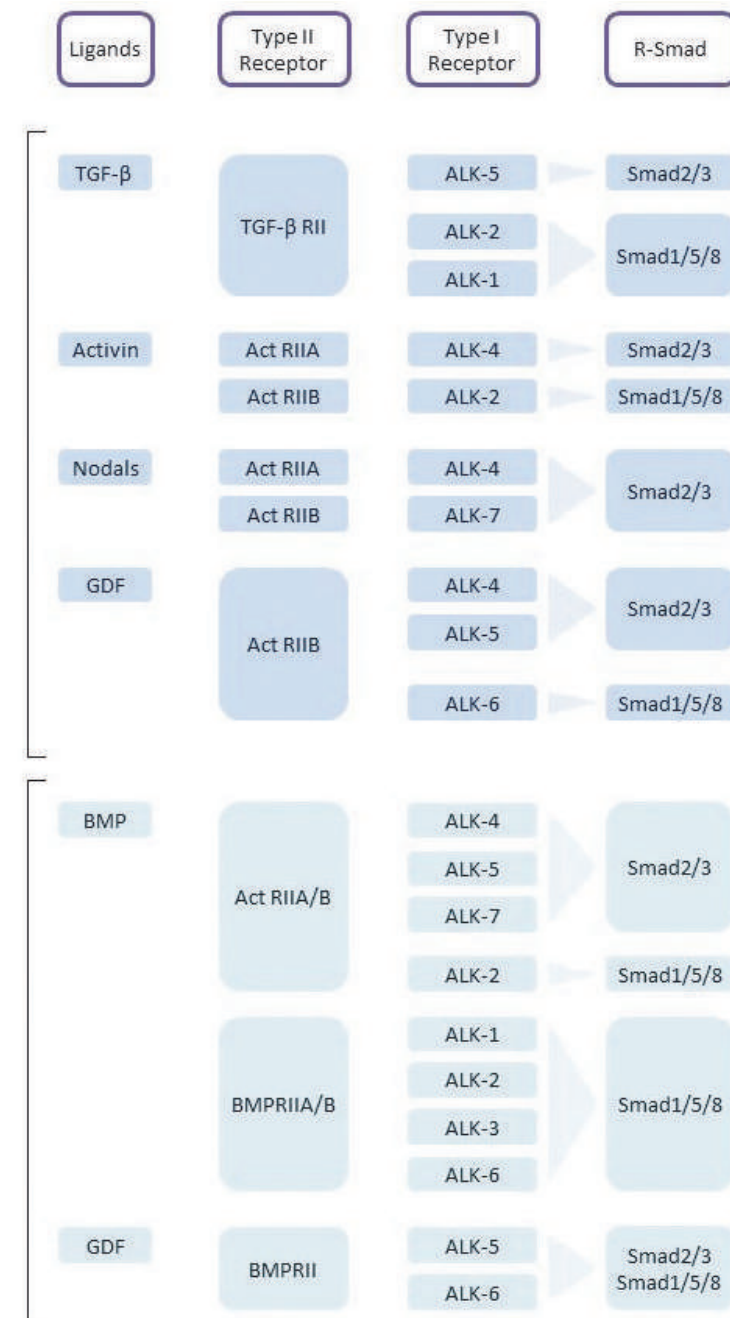


Figure 1 – TGF- β and BMP signaling. Receptors with evidence of mutations in pulmonary arterial hypertension (PAH) are underlined (17). Abbreviations: ActRII, activin receptor type II; ALK, activating receptor-like kinase; BMP, bone morphogenetic protein; GDF, growth/differentiation factor; TGF, transforming growth factor.

Role of TGF- β ligands in pulmonary arterial hypertension

The presence of different TGF- β isoforms in the pulmonary vascular wall in the context of tissue remodeling in PAH was already described in 1994. Particularly, TGF- β 3 is highly upregulated in both medial and intimal layers of remodeled pulmonary vessels (20). More recent studies report that the increased presence of active TGF- β ligands co-localizes with SMCs in pulmonary arterioles and a strong expression of TGF- β 1 in ECs and the interstitium of the plexiform lesions (46,78). TGF- β signaling can directly inhibit BMP-Smad signaling in SMCs, and ligands from this side of the signaling balance can function as antagonists by competing for type II receptor binding (79,80). Interestingly, pulmonary arterial ECs (PAECs) expressing a mutant BMPR2 release higher levels of TGF- β into the medium, thereby accelerating SMC growth (81). As the quiescent effect that TGF- β typically has on SMC growth is impaired in PAH, the elevated TGF- β levels cause medial hypertrophy (82,83,84). TGF- β -single nucleotide polymorphisms (SNP) on top of heterozygous BMPR2 mutation modulate the age of diagnosis and penetrance of familial PAH (45). Other circulating ligands, such as activins and GDFs, are increased in PAH, as well, possibly stimulating cell growth and thereby contributing to pulmonary vascular remodeling (18,19,31,32,33,38). The different animal models for pulmonary hypertension (PH) confirm the human pathology harboring more TGF- β and activins in the serum, pulmonary arteries and the RV in hypoxia or monocrotaline (MCT)-induced PH in rats (12,22,23,26). The imperative role of TGF- β in PAH development is also illustrated by the dependency on this ligand in PAH associated with schistosomiasis in rats and required enhanced TGF- β signaling in a mouse model of scleroderma-related PH (SSc-PH) (24,85,86). A recent study demonstrated that bone marrow-derived thrombospondin-1 causes *Schistosoma*- and hypoxia-induced pulmonary hypertension via activation of TGF- β (87).

Endothelial-to-mesenchymal transition in pulmonary arterial hypertension

ECs can change their endothelial cobblestone morphology to a mesenchymal phenotype, a process referred to as endothelial-to-mesenchymal transition (EndoMT). In this process, ECs progressively lose their characteristics, i.e., cell-cell junctions and specific markers such as CD31, VE-cadherin and CD34 and gain markers such as α -SMA, collagen-I and vimentin migrate and invade into the surrounding tissues (88,89). Although EndoMT takes place during embryogenesis where the transition contributes to the development of the valves of the heart, it does not occur under normal physiological circumstances (90). An imbalance in the TGF- β /BMP axis and disturbed inflammation contribute to the induction of EndoMT (91). EndoMT is stimulated by increased TGF- β receptor signaling and attenuated by intact BMPR2 signaling (21,92). This process has been reported in pathologies such as inflammatory bowel disease,

chronic kidney disease, cardiac fibrosis and portal hypertension (88,93,94,95). In vitro, TGF- β -induced EndoMT in PAECs leads to higher migration rates, lower proliferation rates and decreased barrier integrity (91).

Both pre-clinical and clinical studies demonstrate that EndoMT plays a role in the pathogenesis of PAH (89,96). EndoMT is also detected in the pulmonary vasculature of systemic sclerosis-associated PAH patients (91). This study additionally shows that in vitro-induced EndoMT leads to reduced barrier integrity of PAECs with the production of pro-inflammatory cytokines such as IL-6, IL-8 and TNF- α and high trans-endothelial migration of immune cells.

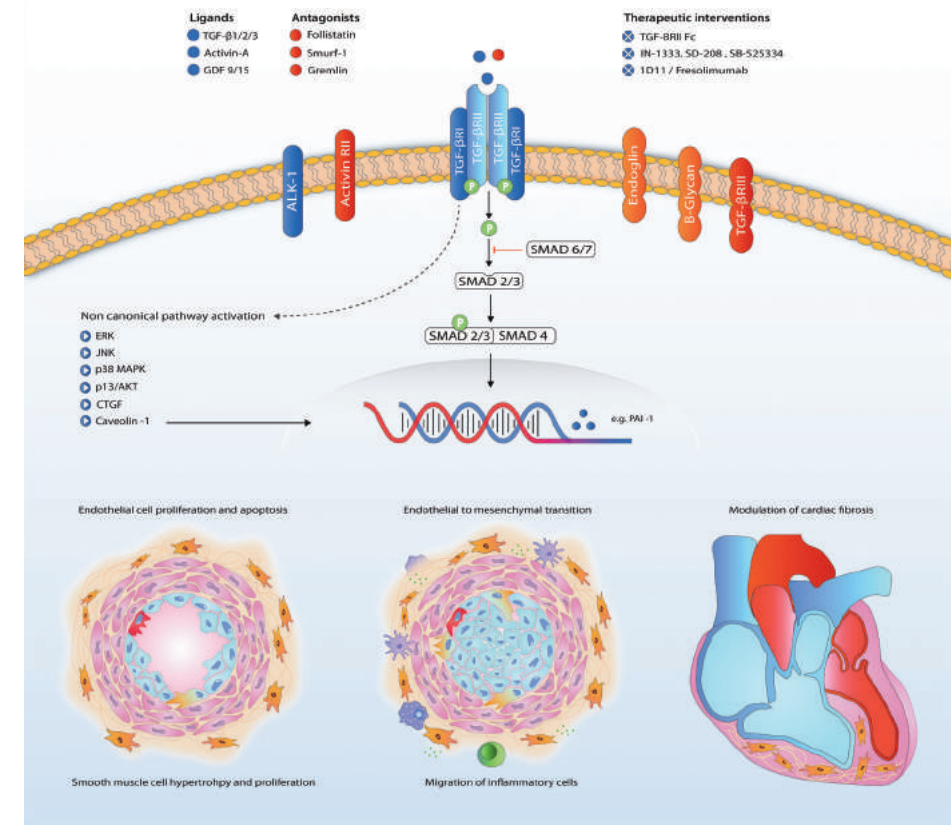


Figure 2 – Proposed mechanism of TGF- β signaling in the pathogenesis of pulmonary arterial hypertension. Abbreviations: ActRII, Activin receptor type II; AKT, protein kinase B; ALK1, activin receptor-like kinase 1; CTGF, connective tissue growth factor; ERK, extracellular signal-regulated kinases; GDF, growth/differentiation factor; JNK, c-Jun N-terminal kinases; MAPK, mitogen-activated protein kinase; PAI-1, plasminogen activator inhibitor-1; TGF- β , transforming growth factor β . TGFBR1, TGF- β receptor type I.

In the pulmonary vasculature of MCT rats, overexpression of Twist-1 and VE-cadherin and repression of p120-catenin indicate the induction of EndoMT (21). Rapamycin, an immunosuppressive drug, reverses experimental PH by inhibiting the migration of PAECs and reducing EndoMT markers. Ponatinib, a multi-target tyrosine-kinase inhibitor, attenuates TGF- β -induced EndoMT in human pulmonary microvascular ECs (96).

Receptors in pulmonary arterial hypertension

Besides BMPR2 mutations, rare variants in other TGF- β receptor superfamily member genes are also associated with autosomal dominant familial PAH. Mutations in the type I receptor ALK1 and co-receptor endoglin are found in hereditary hemorrhagic telangiectasia (HHT)-associated PAH (35,36). The increased prevalence of (h) PAH in HHT1 and HHT2 could be explained by the involvement of arteriovenous malformations, caused by ALK1 and ENG mutations, in the pathophysiology in both diseases (97,98,99). Interestingly, in idiopathic PAH (iPAH) mRNA and protein levels of ALK1 and endoglin are specifically increased in ECs, leading to enhanced Smad1/5 phosphorylation (pSmad1/5) when stimulated with TGF- β , indicating a disturbed TGF- β /BMP balance (19). In mice carrying a kinase-deficient T β RII in fibroblasts, the disturbed TGF- β signaling leads to pulmonary vasculopathy with medial thickening and mildly elevated pulmonary artery pressures (42). TGF- β type III receptor (T β RIII) or β -glycan, a co-receptor acting as a reservoir of TGF- β 2 for the type I and II receptors, is downregulated in familial PAH (28). The functional consequences of these changes for the pathogenesis of PAH are yet unknown.

Canonical TGF- β signaling in pulmonary arterial hypertension

In the pulmonary vasculature, Smad2 phosphorylation after TGF- β receptor activation is increased, even though mRNA expression of Smad2 and Smad3 is decreased in whole lung lysates of PAH patients (27,39,45). While pSmad2 (and not pSmad3) is likewise increased in the lungs of mice exposed to hypoxia, rats experimentally exposed to MCT develop PH 2–4 weeks after MCT injection, showing contrasting results with regards to canonical TGF- β signaling in the lung (25,31,46,100). Some studies report increased pSmad2, while others show no change or even a decrease in Smad2 phosphorylation using Western blot analysis (12,37,43,46). On the cellular level increased Smad2 levels, driven by Activin A activation, are found in cultured SSC-PAH fibroblasts, responsible for collagen production (101). Transgenic mice carrying an SMC specific dominant-negative BMPR2 gene do not show any alteration in Smad2 phosphorylation in lung tissue by Western blot analysis (102). Although this could be due to technical differences between studies, it is possible that a BMPR2 mutation alone is not sufficient to regulate Smad2 phosphorylation.

Table 1 – TGF-beta signaling in pulmonary arterial hypertension in human tissue and animal models

| | Serum | Lung tissue/ vessel | Heart tissue | EC | SMC | References |
|--------------------------------|------------------------------|---------------------------------------|---|--|-----------------|--|
| Ligands | | | | | | |
| TGF- β 1 | mRNA = Protein \uparrow | = \uparrow | \uparrow ^{a, b, d} \uparrow ^{a, b, d} | \uparrow ^b \uparrow ^b | = \uparrow | [12, 18, 19, 20, 21, 22, 23, 24, 25, 26] |
| TGF- β 2 | mRNA Protein | = = | \downarrow ^b | | | [12, 20] |
| TGF- β 3 | mRNA Protein | \downarrow \uparrow | \uparrow = ^{b, c} \uparrow ^a | | | [12, 20, 27, 28, 29, 30] |
| ActivinA | mRNA Protein | \uparrow \uparrow ^a | | | | [31] |
| GDF 9/15 | mRNA Protein | \uparrow \uparrow | | | | [32, 33, 34] |
| Type I receptors | | | | | | |
| ALK1 | mRNA Protein | \uparrow \uparrow | \uparrow \uparrow \downarrow ^b | \uparrow \uparrow | = = | [19, 35] |
| ALK5 | mRNA Protein | = \uparrow = | = | = = | = | [19, 21, 39, 40, 41] |
| Type II receptors | | | | | | |
| TGFBRII | mRNA Protein | | \downarrow ^b \uparrow ^{a, c} \downarrow ^b | = | = | [25, 42, 43, 44] |
| ActRII | mRNA Protein | | \uparrow ^a | | | [31] |
| Co-receptors | | | | | | |
| β -glycan | mRNA Protein | = \downarrow | | | | [28, 38] |
| Endoglin | mRNA Protein | = \uparrow | \downarrow ^b | \uparrow \uparrow | = = | [19, 43] |
| Canonical signaling | | | | | | |
| Smad2 | mRNA Protein | \downarrow | \downarrow \uparrow \downarrow ^{=a, b} | \downarrow | \uparrow | [12, 27, 31, 37, 39, 40, 41, 43, 44, 45, 46] |
| Smad3 | mRNA Protein | \downarrow | \downarrow ^b \uparrow ^{a, b} \downarrow ^b | | | [12, 13, 27, 31, 41, 43] |
| Smad4 | mRNA Protein | \downarrow | \downarrow ^b \downarrow ^b | = | = | [27, 37, 39, 43, 47, 48] |
| Smad6/7 | mRNA Protein | | \uparrow ^a \downarrow ^b \uparrow ^a | | | [37, 44, 48] |
| PAI-1 | mRNA Protein | \uparrow | \downarrow \downarrow | \uparrow ^b \uparrow ^b | | [12, 13, 49, 50] |
| Non-canonical signaling | | | | | | |
| MAPKs | mRNA Protein | | | \uparrow | | [51] |
| Cav1 | mRNA Protein | | \downarrow = ^b | | | [36, 37, 52] |
| CTGF | mRNA Protein | | \downarrow ^b \downarrow ^b | \uparrow ^{c, e} \uparrow ^{c, e} | | [43, 53, 54] |

Grey boxes indicate findings in tissue of Pulmonary Arterial Hypertension patients, white boxes indicate findings in experimental animal models. a) Hypoxia induced PH in rat, b) Monocrotalin induced PH in rat, c) Sugen hypoxia induced PH in rat, d) Schistosoma induced PH in mice, e) Pulmonary artery banding in rats. Increases in Smad protein is regarding phosphorylation. Abbreviations: ActRII, Activin receptor type II; ALK1, activin receptor-like kinase 1; ALK5, activin receptor-like kinase 5; Cav1, caveolin-1; CTGF, connective tissue growth factor; EC, endothelial cell; GDF, growth/differentiation factor; MAPKs, mitogen-activated protein kinase; PAI-1, plasminogen activator inhibitor-1; SMC, smooth muscle cell; TGF- β , transforming growth factor β . TGFBRII, TGF- β receptor type II.

Upon translocation into the nucleus, pSmad2 binds to the promoter of specific target genes like plasminogen activator inhibitor (PAI)-1, a well-acknowledged TGF- β target gene (103). Interestingly, mRNA and protein expression of PAI-1 are decreased in iPAH, while circulating levels of PAI-1 are increased in both primary (idiopathic) and secondary PAH (49,50). The latter is likely linked to the widespread development of thrombosis with intraluminal thrombin deposition (104). The two widely-used experimental PH rat models, MCT and SuHx (VEGF receptor inhibitor Sugen combined with hypoxia), show conflicting results compared to the human situation, with increased mRNA expression of PAI-1 (12).

The co-Smad, Smad4, forms an intracellular complex with the TGF- β and BMP-mediated phosphorylated R-Smads and is needed for nuclear translocation (60). Mutations in Smad4, together with ACVRL1 (ALK1) and ENG are causative of the vascular disorder HHT (105). Nasim et al. report two independent iPAH cases with a missense and splice site mutation in Smad4, but no differential protein expression was found in PAECs and SMCs of iPAH patients (39,47). In contrast with these human findings, Smad4 is reduced in MCT-induced PH on both the mRNA and protein level (43,48). Transcription of the I-Smads, Smad6 and Smad7, is also reduced in lung tissue of these animals (48). Differences in expression of I-Smads in human PAH tissue have not been reported to date. However, it has been shown that Smad6 is suppressed by the prostanoid Iloprost, thereby enhancing the intensity and duration of the TGF- β /Smad responses (106).

Non-canonical TGF- β signaling

Downstream signaling of TGF- β goes beyond phosphorylation of the Smad proteins. Activation of ERK, JNK/p38, Rho-like GTPases and PI3K/Akt is involved in the non-Smad pathway and also familiar in PAH research (Figure 2) (107,108,109,110). Upregulation of these proteins in PAH has been shown before, although only a few in the context of disturbed TGF- β signaling (13,51,111). Besides BMPR2 mutations, caveolin 1 (CAV1) mutations are a rare cause of PAH, influencing both canonical and non-canonical TGF- β /BMP signaling (36,52,112).

Downstream targets of TGF- β in the lung

Several reports demonstrated that vascular thrombosis plays an essential role in the pathophysiology of iPAH. Indeed, anticoagulation treatment confers a survival benefit in iPAH patients (113,114), perhaps because in situ thrombosis of pulmonary vessels may contribute to the pathogenesis of this disease (115,116). Transcriptional activity of PAI-1 is elevated in patients with PAH along with other coagulation-associated genes. This increase in PAI-1 activity may explain impaired fibrinolysis in iPAH patients

(116,117). In contrast, two other studies demonstrated no change in PAI-1 activity in the serum of iPAH and chronic thrombo-embolic pulmonary hypertension (CTEPH) patients at rest or after venous occlusion (118,119). However, the same group reported later that there is an increase in PAI-1 activity in female iPAH patients before and after venous occlusion (120). The discrepancies between these studies may be caused by the use of different assays, gender differences and a low sample size per group. Given the heterogeneity in PAH patients, more studies are warranted to unravel the true function of PAI-1 in the pulmonary vasculature in PAH.

The inhibitor of DNA binding family of proteins (ID proteins) is a major downstream transcriptional target of BMP signaling (121). In mammalian cells, four members of the Id family, Id1–4, have been identified so far. It has been reported that ID1, ID2 and ID3 are induced by BMPs in PAECs and SMCs through a canonical Smad-dependent pathway (11,106,121,122). In adult organs, ID4 is mostly expressed in testis, brain and kidney and left out of the scope of this review (123). Interestingly, BMP9 strongly induces the expression of ID proteins in PAECs, while BMP4 and BMP6 increase the expression of ID proteins in SMCs (121,124). Mutations in BMPR2 strongly reduced the expression of ID proteins in both PAECs and SMCs. Unexpectedly, the expression of ID proteins along with BMPR2 expression are also reduced in PAECs and SMCs of some iPAH patients. In line with these observations in cultured cells, the expression of ID proteins is attenuated in experimental MCT-PH lungs, as well as in human lungs (48). ID proteins also regulate the cell cycle and proliferation of SMCs in a BMP4-dependent manner (106,121). Recently, BMP9 has been shown to selectively increase BMPR2, ID1 and ID3 proteins in endothelial cells in vitro and thereby decrease experimental PH in vivo, suggesting the potential involvement of these genes in PAH (11).

TGF- β signaling in the heart in pulmonary arterial hypertension

Survival of PAH patients is determined by the ability of the RV to adapt to the increased pressures in the pulmonary vasculature (125). The challenged RV suffers from neurohormonal activation, capillary loss inflammation, apoptosis, oxidative stress and metabolic shifts leading to hypertrophy and fibrosis (126). Cardiac fibrosis is related to increased TGF- β signaling (127,128). In rat, cardiac fibrosis induced by increased RV afterload, as seen in PH, is likely to be mediated through TGF- β -induced connective tissue growth factor signaling (Figure 2) (53,54). The beneficial effects of carvedilol (β -blocker), iloprost (prostacyclin) and losartan (angiotensin receptor blocker) on RV function in animals are partly ascribed to attenuated TGF- β -mediated fibrosis (53,54,129). Furthermore, nintedanib, a tyrosine kinase inhibitor known to inhibit TGF- β -mediated fibrosis, attenuated cardiac fibrosis in experimental pulmonary hypertension (130,131)

Hemnes et al. showed an upregulation of the TGF- β pathway in the RV of PAH patients by increased transcription of TGF- β 3 (29). TGF- β inhibition by either pan-TGF β antibodies or specifically binding to TGF- β 1 and TGF- β 3 showed lowering of RV systolic pressures and attenuated RV hypertrophy in MCT and SuHx rat models (12,132). One of the few studies investigating downstream TGF- β signaling in the heart in the context of PAH showed decreased phosphorylation of Smad2 in both RV and LV. This observation was independent of the presence of a BMPR2 mutation (40).

Therapeutic interventions relevant in PAH

In 13 preclinical and nearly twenty phase I–III clinical trials, TGF- β signaling is targeted to treat cancer and fibrotic diseases (72,77,133). TGF- β signaling can be targeted mainly in three different ways in clinical trials: specific antibodies, antisense oligonucleotides and receptor kinase inhibitors. As ECs and SMCs in PAH produce excessive amounts of TGF- β , the use of these targets may decrease vascular remodeling through their inhibitory effect on these cells. In contrast to the clear role of TGF- β signaling in tumorigenesis, vascular diseases are more complex with simultaneous up- and down-regulation of the pathway and interactions with the BMP pathway (72).

Beneficial effects of inhibiting TGF- β ligands on pulmonary vascular and cardiac remodeling have previously been shown in experimental MCT- and hypoxia-induced rat PH models (12). Targeting the ALK5 kinase with SD208, a drug known to suppress tumor metastasis in rodent models, ameliorated MCT-induced PH (134). Beneficial anti-remodeling effects of prostacyclin analogues, used in PAH treatment strategies, can partly be explained by TGF- β inhibition (13,135). How these effects in rat models can provide implications for the human disease are uncertain; besides increased availability of TGF- β ligands, different regulation patterns are observed. As TGF- β signaling is crucial for many physiological functions, prolonged inhibition of this signaling might lead to harmful side effects. Preclinical studies in PAH patient-derived cells could give valuable information about expected responses, illustrated by different effects in ECs and SMCs upon TGF- β stimulation (19,82,83).

Conclusions

In PAH, several mutations in components of the TGF- β /BMP signaling pathway have been identified. However, most research over the years has focused on BMP signaling, in particular BMPR2. Enhanced expression of TGF- β has been found systemically (i.e., in serum) and locally (i.e., in ECs and SMCs of the pulmonary vasculature) in PH patients and animal models. Furthermore, TGF- β has been shown to be involved in proliferation, inflammation, angiogenesis and fibrosis in lungs in PAH. In addition, TGF- β

induces EndoMT, which is also involved in PAH, and as such, TGF- β could be interesting as a treatment target. Inhibition of TGF- β signaling, either directly or through targeting intermediates, may be a novel therapeutic strategy in PAH.

TGF- β signaling plays an essential role in vascular cells, immune cells and other cells such as epithelial cells in lungs. However, TGF- β signaling is very complex, as there are numerous ligands and diverse receptors that exhibit distinct functions in a cell- and context-dependent manner through interaction with other proteins, thereby affecting multiple signaling cascades. This intricate pathway is crucial for vessel wall homeostasis in many diseases, including PAH. Therefore, a deeper understanding of this pathway is necessary for the development of safer and efficient therapies for PAH.

In conclusion, overactive TGF- β signaling is an important regulator of pulmonary vascular remodelling in PAH, e.g., by balancing BMP signaling. TGF- β inhibitors have entered clinical trials for treatment of cancer and fibrotic diseases with encouraging first clinical results. The future of specific TGF- β inhibitors are promising and open new challenges in PAH research.

References

- Galie N., Humbert M., Vachieri J.L., Gibbs S., Lang I., Torbicki A., Simonneau G., Peacock A., Vonk N.A., Beghetti M., et al. 2015 ESC/ERS Guidelines for the diagnosis and treatment of pulmonary hypertension: The Joint Task Force for the Diagnosis and Treatment of Pulmonary Hypertension of the European Society of Cardiology (ESC) and the European Respiratory Society (ERS); Endorsed by: Association for European Paediatric and Congenital Cardiology (AEPC), International Society for Heart and Lung Transplantation (ISHLT) *Eur. Heart J.* 2016;37:67–119.
- Rich S., Kaufmann E., Levy P.S. The effect of high doses of calcium-channel blockers on survival in primary pulmonary hypertension. *N. Engl. J. Med.* 1992;327:76–81. doi: 10.1056/NEJM199207093270203.
- Tantini B., Manes A., Fiumana E., Pignatti C., Guarnieri C., Zannoli R., Branzi A., Galie N. Antiproliferative effect of sildenafil on human pulmonary artery smooth muscle cells. *Basic Res. Cardiol.* 2005;100:131–138.
- Ten D.P., Arthur H.M. Extracellular control of TGF β signalling in vascular development and disease. *Nat. Rev. Mol. Cell. Biol.* 2007;8:857–869.
- Ten D.P., Goumans M.J., Pardali E. Endoglin in angiogenesis and vascular diseases. *Angiogenesis.* 2008;11:79–89.
- Liang H., Zhang C., Ban T., Liu Y., Mei L., Piao X., Zhao D., Lu Y., Chu W., Yang B. A novel reciprocal loop between microRNA-21 and TGF β RIII is involved in cardiac fibrosis. *Int. J. Biochem. Cell. Biol.* 2012;44:2152–2160.
- Goumans M.J., Ten Dijke P. TGF- β signaling in control of cardiovascular function. *Cold Spring Harb Perspect. Biol.* 2018;10:a022210.
- Goumans M.J., Zwijsen A., Ten Dijke P., Bailly S. Bone morphogenetic proteins in vascular homeostasis and disease. *Cold Spring Harb. Perspect. Biol.* 2018;10:a031989.
- Lane K.B., Machado R.D., Pauculo M.W., Thomson J.R., Phillips J.A., III, Loyd J.E., Nichols W.C., Trembath R.C. Heterozygous germline mutations in BMPR2, encoding a TGF- β receptor, cause familial primary pulmonary hypertension. *Nat. Genet.* 2000;26:81–84.
- Deng Z., Morse J.H., Slager S.L., Cuervo N., Moore K.J., Venetos G., Kalachikov S., Cayanis E., Fischer S.G., Barst R.J., et al. Familial primary pulmonary hypertension (gene PPH1) is caused by mutations in the bone morphogenetic protein receptor-II gene. *Am. J. Hum. Genet.* 2000;67:737–744.
- Long L., Ormiston M.L., Yang X., Southwood M., Graf S., Machado R.D., Mueller M., Kinzel B., Yung L.M., Wilkinson J.M., et al. Selective enhancement of endothelial BMPR-II with BMP9 reverses pulmonary arterial hypertension. *Nat. Med.* 2015;21:777–785.
- Yung L.M., Nikolic I., Paskin-Flerlage S.D., Pearsall R.S., Kumar R., Yu P.B. A Selective TGF β Ligand Trap Attenuates Pulmonary Hypertension. *Am. J. Respir. Crit. Care Med.* 2016;134:A19307.
- Ogo T., Chowdhury H.M., Yang J., Long L., Li X., Torres Cleuren Y.N., Morrell N.W., Schermuly R.T., Trembath R.C., Nasim M.T. Inhibition of overactive transforming growth factor- β signaling by prostacyclin analogs in pulmonary arterial hypertension. *Am. J. Respir. Cell Mol. Biol.* 2013;48:733–741.
- Zabini D., Granton E., Hu Y., Miranda M.Z., Weichelt U., Breuils Bonnet S., Bonnet S., Morrell N.W., Connelly K.A., Provencher S., et al. Loss of SMAD3 Promotes Vascular Remodeling in Pulmonary Arterial Hypertension via MRTF Disinhibition. *Am. J. Respir. Crit. Care Med.* 2018;197:244–260. doi: 10.1164/rccm.201702-0386OC.
- Bellay P.S., Yanagihara T., Granton E., Sato S., Shimbori C., Upagupta C., Imani J., Hambly N., Ask K., Gaudie J., et al. Macitentan reduces progression of TGF- β 1-induced pulmonary fibrosis and pulmonary hypertension. *Eur. Respir. J.* 2018;2018:1701857.
- Lu A., Zuo C., He Y., Chen G., Piao L., Zhang J., Xiao B., Shen Y., Tang J., Kong D., et al. EP3 receptor deficiency attenuates pulmonary hypertension through suppression of Rho/TGF- β 1 signaling. *J. Clin. Investing.* 2015;125:1228–1242.
- Garcia-Rivas G., Jerjes-Sanchez C., Rodriguez D., Garcia-Pelaez J., Trevino V. A systematic review of genetic mutations in pulmonary arterial hypertension. *BMC Med. Genet.* 2017;18:82. doi: 10.1186/s12881-017-0440-5.
- Selimovic N., Bergh C.H., Andersson B., Sakiniene E., Carlsten H., Rundqvist B. Growth factors and interleukin-6 across the lung circulation in pulmonary hypertension. *Eur. Respir. J.* 2009;34:662–668.
- Gore B., Izikki M., Mercier O., Dewachter L., Fadel E., Humbert M., Darteville P., Simonneau G., Naeije R., Lebrin F., et al. Key role of the endothelial TGF- β /ALK1/endoglin signaling pathway in humans and rodents pulmonary hypertension. *PLoS ONE.* 2014;9:e100310.
- Botney M.D., Bahadori L., Gold L.I. Vascular remodeling in primary pulmonary hypertension. Potential role for transforming growth factor- β . *Am. J. Pathol.* 1994;144:286–295.
- Ranchoux B., Antigny F., Rucker-Martin C., Hautefort A., Pechoux C., Bogaard H.J., Dorfmüller P., Remy S., Lecerf F., Plante S., et al. Endothelial-to-mesenchymal transition in pulmonary hypertension. *Circulation.* 2015;131:1006–1018.
- Wang X.B., Wang W., Zhu X.C., Ye W.J., Cai H., Wu P.L., Huang X.Y., Wang L.X. The potential of asiaticoside for TGF- β 1/Smad signaling inhibition in prevention and progression of hypoxia-induced pulmonary hypertension. *Life Sci.* 2015;137:56–64.
- Dong L., Li Y., Hu H., Shi L., Chen J., Wang B., Chen C., Zhu H., Li Y., Li Q., et al. Potential therapeutic targets for hypoxia-induced pulmonary artery hypertension. *J. Transl. Med.* 2014;12:39.
- Graham B.B., Chabon J., Gebreab L., Poole J., Debella E., Davis L., Tanaka T., Sanders L., Dropcho N., Bandeira A., et al. Transforming growth factor- β signaling promotes pulmonary hypertension caused by *Schistosoma mansoni*. *Circulation.* 2013;128:1354–1364.
- Long L., Crosby A., Yang X., Southwood M., Upton P.D., Kim D.K., Morrell N.W. Altered bone morphogenetic protein and transforming growth factor- β signaling in rat models of pulmonary hypertension: Potential for activin receptor-like kinase-5 inhibition in prevention and progression of disease. *Circulation.* 2009;119:566–576.
- Ahmed L.A., Obaid A.A., Zaki H.F., Agha A.M. Role of oxidative stress, inflammation, nitric oxide and transforming growth factor- β in the protective effect of diosgenin in monocrotaline-induced pulmonary hypertension in rats. *Eur. J. Pharmacol.* 2014;740:379–387.
- Rajkumar R., Konishi K., Richards T.J., Ishizawa D.C., Wiechert A.C., Kaminski N., Ahmad F. Genomewide RNA expression profiling in lung identifies distinct signatures in idiopathic pulmonary arterial hypertension and secondary pulmonary hypertension. *Am. J. Physiol. Heart Circ. Physiol.* 2010;298:H1235–H1248.
- Geraci M.W., Moore M., Gesell T., Yeager M.E., Alger L., Golpon H., Gao B., Loyd J.E., Tuder R.M., Voelkel N.F. Gene expression patterns in the lungs of patients with primary pulmonary hypertension: A gene microarray analysis. *Circ. Res.* 2001;88:555–562.
- Hemnes A.R., Brittain E.L., Trammell A.W., Fessel J.P., Austin E.D., Penner N., Maynard K.B., Gleaves L., Talati M., Absi T., et al. Evidence for right ventricular lipotoxicity in heritable pulmonary arterial hypertension. *Am. J. Respir. Crit. Care Med.* 2014;189:325–334.
- Moreno-Vinasco L., Gomberg-Maitland M., Maitland M.L., Desai A.A., Singleton P.A., Sammani S., Sam L., Liu Y., Husain A.N., Lang R.M., et al. Genomic assessment of a multikinase inhibitor, sorafenib, in a rodent model of pulmonary hypertension. *Physiol. Genom.* 2008;33:278–291.

31. Yndestad A., Larsen K.O., Oie E., Ueland T., Smith C., Halvorsen B., Sjaastad I., Skjonsberg O.H., Pedersen T.M., Anfinson O.G., et al. Elevated levels of activin A in clinical and experimental pulmonary hypertension. *J. Appl. Physiol.* 2009;106:1356–1364.
32. Nickel N., Kempf T., Tapken H., Tongers J., Laenger F., Lehmann U., Golpon H., Olsson K., Wilkins M.R., Gibbs J.S., et al. Growth differentiation factor-15 in idiopathic pulmonary arterial hypertension. *Am. J. Respir. Crit. Care Med.* 2008;178:534–541.
33. Rhodes C.J., Wharton J., Howard L.S., Gibbs J.S., Wilkins M.R. Red cell distribution width outperforms other potential circulating biomarkers in predicting survival in idiopathic pulmonary arterial hypertension. *Heart.* 2011;97:1054–1060.
34. Nickel N., Jonigk D., Kempf T., Bockmeyer C.L., Maegel L., Rische J., Laenger F., Lehmann U., Sauer C., Greer M., et al. GDF-15 is abundantly expressed in plexiform lesions in patients with pulmonary arterial hypertension and affects proliferation and apoptosis of pulmonary endothelial cells. *Respir. Res.* 2011;12:62.
35. Eyries M., Coulet F., Girerd B., Montani D., Humbert M., Lacombe P., Chinet T., Gouya L., Roume J., Axford M.M., et al. ACVRL1 germinal mosaic with two mutant alleles in hereditary hemorrhagic telangiectasia associated with pulmonary arterial hypertension. *Clin. Genet.* 2012;82:173–179. doi: 10.1111/j.1399-0004.2011.01727.x.
36. Austin E.D., Loyd J.E. The genetics of pulmonary arterial hypertension. *Circ. Res.* 2014;115:189–202.
37. Ramos M.F., Lame M.W., Segall H.J., Wilson D.W. Smad signaling in the rat model of monocrotaline pulmonary hypertension. *Toxicol. Pathol.* 2008;36:311–320.
38. Jachec W., Foremny A., Domal-Kwiatkowska D., Smolik S., Tomasik A., Mazurek U., Wodniecki J. Expression of TGF- β 1 and its receptor genes (T β R I, T β R II, and T β R III- β glycan) in peripheral blood leucocytes in patients with idiopathic pulmonary arterial hypertension and Eisenmenger's syndrome. *Int. J. Mol. Med.* 2008;21:99–107.
39. Richter A., Yeager M.E., Zaiman A., Cool C.D., Voelkel N.F., Tuder R.M. Impaired transforming growth factor- β signaling in idiopathic pulmonary arterial hypertension. *Am. J. Respir. Crit. Care Med.* 2004;170:1340–1348.
40. Van der Bruggen C.E., Happe C.M., Dorfmueller P., Trip P., Spruijt O.A., Rol N., Hoevenaars F.P., Houweling A.C., Girerd B., Marcus J.T., et al. Bone Morphogenetic Protein Receptor Type 2 Mutation in Pulmonary Arterial Hypertension: A View on the Right Ventricle. *Circulation.* 2016;133:1747–1760.
41. Thomas M., Docx C., Holmes A.M., Beach S., Duggan N., England K., Leblanc C., Leuret C., Schindler F., Raza F., et al. Activin-like kinase 5 (ALK5) mediates abnormal proliferation of vascular smooth muscle cells from patients with familial pulmonary arterial hypertension and is involved in the progression of experimental pulmonary arterial hypertension induced by monocrotaline. *Am. J. Pathol.* 2009;174:380–389.
42. Derrett-Smith E.C., Dooley A., Gilbane A.J., Trinder S.L., Khan K., Baliga R., Holmes A.M., Hobbs A.J., Abraham D., Denton C.P. Endothelial injury in a transforming growth factor β -dependent mouse model of scleroderma induces pulmonary arterial hypertension. *Arthritis Rheum.* 2013;65:2928–2939.
43. Zakrzewicz A., Kouri F.M., Nejman B., Kwapiszewska G., Hecker M., Sandu R., Dony E., Seeger W., Schermuly R.T., Eickelberg O., et al. The transforming growth factor- β /Smad2,3 signalling axis is impaired in experimental pulmonary hypertension. *Eur. Respir. J.* 2007;29:1094–1104.
44. Yu H., Xu M., Dong Y., Liu J., Li Y., Mao W., Wang J., Wang L. 1,25(OH) $_2$ D $_3$ attenuates pulmonary arterial hypertension via microRNA-204 mediated Tgfb β 2/Smad signaling. *Exp. Cell Res.* 2018;362:311–323.
45. Phillips J.A., III, Poling J.S., Phillips C.A., Stanton K.C., Austin E.D., Cogan J.D., Wheeler L., Yu C., Newman J.H., Dietz H.C., et al. Synergistic heterozygosity for TGF β 1 SNPs and BMPR2 mutations modulates the age at diagnosis and penetrance of familial pulmonary arterial hypertension. *Genet. Med.* 2008;10:359–365.
46. Ma W., Han W., Greer P.A., Tuder R.M., Toque H.A., Wang K.K., Caldwell R.W., Su Y. Calcipain mediates pulmonary vascular remodeling in rodent models of pulmonary hypertension, and its inhibition attenuates pathologic features of disease. *J. Clin. Investig.* 2011;121:4548–4566.
47. Nasim M.T., Ogo T., Ahmed M., Randall R., Chowdhury H.M., Snape K.M., Bradshaw T.Y., Southgate L., Lee G.J., Jackson I., et al. Molecular genetic characterization of SMAD signaling molecules in pulmonary arterial hypertension. *Hum. Mutat.* 2011;32:1385–1389.
48. Morty R.E., Nejman B., Kwapiszewska G., Hecker M., Zakrzewicz A., Kouri F.M., Peters D.M., Dumitrascu R., Seeger W., Knaus P., et al. Dysregulated bone morphogenetic protein signaling in monocrotaline-induced pulmonary arterial hypertension. *Arterioscl. Thromb. Vasc. Biol.* 2007;27:1072–1078.
49. Kouri F.M., Queisser M.A., Konigshoff M., Chrobak I., Preissner K.T., Seeger W., Eickelberg O. Plasminogen activator inhibitor type 1 inhibits smooth muscle cell proliferation in pulmonary arterial hypertension. *Int. J. Biochem. Cell Biol.* 2008;40:1872–1882.
50. Welsh C.H., Hassell K.L., Badesch D.B., Kressin D.C., Marlar R.A. Coagulation and fibrinolytic profiles in patients with severe pulmonary hypertension. *Chest.* 1996;110:710–717.
51. Szulcek R., Happe C.M., Rol N., Fontijn R.D., Dickhoff C., Hartemink K.J., Grunberg K., Tu L., Timens W., Nossent G.D., et al. Delayed Microvascular Shear-adaptation in Pulmonary Arterial Hypertension: Role of PECAM-1 Cleavage. *Am. J. Respir. Crit. Care Med.* 2016;193:1410–1420.
52. Ma L., Chung W.K. The role of genetics in pulmonary arterial hypertension. *J. Pathol.* 2017;241:273–280.
53. Friedberg M.K., Cho M.Y., Li J., Assad R.S., Sun M., Rohailla S., Honjo O., Apitz C., Redington A.N. Adverse biventricular remodeling in isolated right ventricular hypertension is mediated by increased transforming growth factor- β 1 signaling and is abrogated by angiotensin receptor blockade. *Am. J. Respir. Cell Mol. Biol.* 2013;49:1019–1028.
54. Gomez-Arroyo J., Sakagami M., Syed A.A., Farkas L., Van T.B., Kraskauskas D., Mizuno S., Abbate A., Bogaard H.J., Byron P.R., et al. Iloprost reverses established fibrosis in experimental right ventricular failure. *Eur. Respir. J.* 2015;45:449–462.
55. Heldin C.H., Miyazono K., Ten D.P. TGF- β signalling from cell membrane to nucleus through SMAD proteins. *Nature.* 1997;390:465–471.
56. Heldin C.H., Moustakas A. Role of Smads in TGF β signaling. *Cell. Tissue Res.* 2012;347:21–36.
57. Goumans M.J., Liu Z., Ten D.P. TGF- β signaling in vascular biology and dysfunction. *Cell Res.* 2009;19:116–127.
58. Kurakula K., Goumans M.J., Ten D.P. Regulatory RNAs controlling vascular (dys)function by affecting TGF- β family signalling. *EXCLI J.* 2015;14:832–850.
59. Schmierer B., Hill C.S. TGF β -SMAD signal transduction: Molecular specificity and functional flexibility. *Nat. Rev. Mol. Cell Biol.* 2007;8:970–982.
60. Shi Y., Massague J. Mechanisms of TGF- β signaling from cell membrane to the nucleus. *Cell.* 2003;113:685–700.
61. Hata A., Chen Y.G. TGF- β Signaling from Receptors to Smads. *Cold Spring Harb. Perspect. Biol.* 2016;8:a022061.
62. Heldin C.H., Moustakas A. Signaling Receptors for TGF- β Family Members. *Cold Spring Harb. Perspect. Biol.* 2016;8:a022053.
63. Wong S.H., Hamel L., Chevalier S., Philip A. Endoglin expression on human microvascular endothelial cells association with β glycan and formation of higher order complexes with TGF- β signalling receptors. *Eur. J. Biochem.* 2000;267:5550–5560.
64. Goumans M.J., Valdimarsdottir G., Itoh S., Rosendahl A., Sideras P., Ten D.P. Balancing the activation state of the endothelium via two distinct TGF- β type I receptors. *EMBO J.* 2002;21:1743–1753.
65. Oh S.P., Seki T., Goss K.A., Imamura T., Yi Y., Donahoe P.K., Li L., Miyazono K., Ten D.P., Kim S., et al. Activin receptor-like kinase 1 modulates transforming growth factor- β 1 signaling in the regulation of angiogenesis. *Proc. Natl. Acad. Sci. USA.* 2000;97:2626–2631.
66. Kretzschmar M., Doody J., Massague J. Opposing BMP and EGF signalling pathways converge on the TGF- β family mediator Smad1. *Nature.* 1997;389:618–622.

67. Labbe E., Silvestri C., Hoodless P.A., Wrana J.L., Attisano L. Smad2 and Smad3 positively and negatively regulate TGF β -dependent transcription through the forkhead DNA-binding protein FAST2. *Mol. Cell.* 1998;2:109–120.
68. Topper J.N., Cai J., Qiu Y., Anderson K.R., Xu Y.Y., Deeds J.D., Feeley R., Gimeno C.J., Woolf E.A., Tayber O., et al. Vascular MADs: Two novel MAD-related genes selectively inducible by flow in human vascular endothelium. *Proc. Natl. Acad. Sci. USA.* 1997;94:9314–9319.
69. Hata A., Lieberman J. Dysregulation of microRNA biogenesis and gene silencing in cancer. *Sci. Signal.* 2015;8:re3.
70. Euler G. Good and bad sides of TGF β -signaling in myocardial infarction. *Front. Physiol.* 2015;6:66.
71. Cai J., Pardali E., Sanchez-Duffhues G., Ten D.P. BMP signaling in vascular diseases. *FEBS Lett.* 2012;586:1993–2002.
72. Akhurst R.J., Hata A. Targeting the TGF β signalling pathway in disease. *Nat. Rev. Drug Discov.* 2012;11:790–811.
73. Hinck A.P., Mueller T.D., Springer T.A. Structural Biology and Evolution of the TGF- β Family. *Cold Spring Harb. Perspect. Biol.* 2016;8:a021907.
74. Haque S., Morris J.C. Transforming growth factor- β : A therapeutic target for cancer. *Hum. Vaccin. Immunother.* 2017;13:1741–1750.
75. Xu X., Zheng L., Yuan Q., Zhen G., Crane J.L., Zhou X., Cao X. Transforming growth factor- β in stem cells and tissue homeostasis. *Bone Res.* 2018;6:2.
76. Robertson I.B., Rifkin D.B. Regulation of the Bioavailability of TGF- β and TGF- β -Related Proteins. *Cold Spring Harb. Perspect. Biol.* 2016;8:a022103.
77. Caja L., Dituri F., Mancarella S., Caballero-Diaz D., Moustakas A., Giannelli G., Fabregat I. TGF- β and the Tissue Microenvironment: Relevance in Fibrosis and Cancer. *Int J. Mol. Sci.* 2018;19:1294.
78. Jonigk D., Golpon H., Bockmeyer C.L., Maegel L., Hoeper M.M., Gottlieb J., Nickel N., Hussein K., Maus U., Lehmann U., et al. Plexiform lesions in pulmonary arterial hypertension composition, architecture, and microenvironment. *Am. J. Pathol.* 2011;179:167–179.
79. Upton P.D., Davies R.J., Tajsic T., Morrell N.W. Transforming growth factor- β (1) represses bone morphogenetic protein-mediated Smad signaling in pulmonary artery smooth muscle cells via Smad3. *Am. J. Respir. Cell Mol. Biol.* 2013;49:1135–1145.
80. Aykul S., Martinez-Hackert E. Transforming Growth Factor- β Family Ligands Can Function as Antagonists by Competing for Type II Receptor Binding. *J. Biol. Chem.* 2016;291:10792–10804.
81. Yang X., Long L., Reynolds P.N., Morrell N.W. Expression of mutant BMPR-II in pulmonary endothelial cells promotes apoptosis and a release of factors that stimulate proliferation of pulmonary arterial smooth muscle cells. *Pulm. Circ.* 2011;1:103–110.
82. Morrell N.W., Yang X., Upton P.D., Jourdan K.B., Morgan N., Sheares K.K., Trembath R.C. Altered growth responses of pulmonary artery smooth muscle cells from patients with primary pulmonary hypertension to transforming growth factor- β (1) and bone morphogenetic proteins. *Circulation.* 2001;104:790–795.
83. Davies R.J., Holmes A.M., Deighton J., Long L., Yang X., Barker L., Walker C., Budd D.C., Upton P.D., Morrell N.W. BMP type II receptor deficiency confers resistance to growth inhibition by TGF- β in pulmonary artery smooth muscle cells: Role of proinflammatory cytokines. *Am. J. Physiol. Lung Cell. Mol. Physiol.* 2012;302:L604–L615.
84. Liu Y., Cao Y., Sun S., Zhu J., Gao S., Pang J., Zhu D., Sun Z. Transforming growth factor- β 1 upregulation triggers pulmonary artery smooth muscle cell proliferation and apoptosis imbalance in rats with hypoxic pulmonary hypertension via the PTEN/AKT pathways. *Int J. Biochem. Cell Biol.* 2016;77:141–154.
85. Graham B.B., Kumar R. Schistosomiasis and the pulmonary vasculature (2013 Grover Conference series) *Pulm. Circ.* 2014;4:353–362.
86. Gilbane A.J., Derrett-Smith E., Trinder S.L., Good R.B., Pearce A., Denton C.P., Holmes A.M. Impaired bone morphogenetic protein receptor II signaling in a transforming growth factor- β -dependent mouse model of pulmonary hypertension and in systemic sclerosis. *Am. J. Respir. Crit. Care Med.* 2015;191:665–677.
87. Kumar R., Mickael C., Kassa B., Gebreab L., Robinson J.C., Koyanagi D.E., Sanders L., Barthel L., Meadows C., Fox D., et al. TGF- β activation by bone marrow-derived thrombospondin-1 causes Schistosoma- and hypoxia-induced pulmonary hypertension. *Nat. Commun.* 2017;8:15494.
88. Frid M.G., Kale V.A., Stenmark K.R. Mature vascular endothelium can give rise to smooth muscle cells via endothelial-mesenchymal transdifferentiation: In vitro analysis. *Circ. Res.* 2002;90:1189–1196.
89. Arciniegas E., Frid M.G., Douglas I.S., Stenmark K.R. Perspectives on endothelial-to-mesenchymal transition: Potential contribution to vascular remodeling in chronic pulmonary hypertension. *Am. J. Physiol. Lung Cell. Mol. Physiol.* 2007;293:L1–L8.
90. Kruithof B.P., Duim S.N., Moerkamp A.T., Goumans M.J. TGF β and BMP signaling in cardiac cushion formation: Lessons from mice and chicken. *Differentiation.* 2012;84:89–102.
91. Good R.B., Gilbane A.J., Trinder S.L., Denton C.P., Coghlan G., Abraham D.J., Holmes A.M. Endothelial to Mesenchymal Transition Contributes to Endothelial Dysfunction in Pulmonary Arterial Hypertension. *Am. J. Pathol.* 2015;185:1850–1858.
92. Diez M., Musri M.M., Ferrer E., Barbera J.A., Peinado V.I. Endothelial progenitor cells undergo an endothelial-to-mesenchymal transition-like process mediated by TGF β RI. *Cardiovasc. Res.* 2010;88:502–511.
93. Zeisberg E.M., Tarnavski O., Zeisberg M., Dorfman A.L., McMullen J.R., Gustafsson E., Chandraker A., Yuan X., Pu W.T., Roberts A.B., et al. Endothelial-to-mesenchymal transition contributes to cardiac fibrosis. *Nat. Med.* 2007;13:952–961.
94. He J., Xu Y., Koya D., Kanasaki K. Role of the endothelial-to-mesenchymal transition in renal fibrosis of chronic kidney disease. *Clin. Exp. Nephrol.* 2013;17:488–497.
95. Kitao A., Sato Y., Sawada-Kitamura S., Harada K., Sasaki M., Morikawa H., Shiomi S., Honda M., Matsui O., Nakanuma Y. Endothelial to mesenchymal transition via transforming growth factor- β 1/Smad activation is associated with portal venous stenosis in idiopathic portal hypertension. *Am. J. Pathol.* 2009;175:616–626.
96. Kang Z., Ji Y., Zhang G., Qu Y., Zhang L., Jiang W. Ponatinib attenuates experimental pulmonary arterial hypertension by modulating Wnt signaling and vasohibin-2/vasohibin-1. *Life Sci.* 2016;148:1–8.
97. Vorselaars V., Velthuis S., van Gent M., Westermann C., Snijder R., Mager J., Post M. Pulmonary Hypertension in a Large Cohort with Hereditary Hemorrhagic Telangiectasia. *Respiration.* 2017;94:242–250.
98. Mahmoud M., Borthwick G.M., Hislop A.A., Arthur H.M. Endoglin and activin receptor-like-kinase 1 are co-expressed in the distal vessels of the lung: Implications for two familial vascular dysplasias, HHT and PAH. *Lab. Investig.* 2009;89:15–25.
99. Trembath R.C., Thomson J.R., Machado R.D., Morgan N.V., Atkinson C., Winship I., Simonneau G., Galie N., Loyd J.E., Humbert M., et al. Clinical and molecular genetic features of pulmonary hypertension in patients with hereditary hemorrhagic telangiectasia. *N. Engl. J. Med.* 2001;345:325–334.
100. Upton P.D., Morrell N.W. The transforming growth factor- β -bone morphogenetic protein type signalling pathway in pulmonary vascular homeostasis and disease. *Exp. Physiol.* 2013;98:1262–1266.
101. Takagi K., Kawaguchi Y., Kawamoto M., Ota Y., Tochimoto A., Gono T., Katsumata Y., Takagi M., Hara M., Yamanaka H. Activation of the activin A-ALK-Smad pathway in systemic sclerosis. *J. Autoimmun.* 2011;36:181–188.
102. Yasuda T., Tada Y., Tanabe N., Tatsumi K., West J. Rho-kinase inhibition alleviates pulmonary hypertension in transgenic mice expressing a dominant-negative type II bone morphogenetic protein receptor gene. *Am. J. Physiol. Lung Cell. Mol. Physiol.* 2011;301:L667–L674.

103. Ha H., Oh E.Y., Lee H.B. The role of plasminogen activator inhibitor 1 in renal and cardiovascular diseases. *Nat. Rev. Nephrol.* 2009;5:203–211.
104. Hassell K.L. Altered hemostasis in pulmonary hypertension. *Blood Coagul. Fibrinolysis.* 1998;9:107–117.
105. Gallione C.J., Richards J.A., Letteboer T.G., Rushlow D., Prigoda N.L., Leedom T.P., Ganguly A., Castells A., Ploos van Amstel J.K., Westermann C.J., et al. SMAD4 mutations found in unselected HHT patients. *J. Med. Genet.* 2006;43:793–797.
106. Yang J., Li X., Al-Lamki R.S., Southwood M., Zhao J., Lever A.M., Grimminger F., Schermuly R.T., Morrell N.W. Smad-dependent and smad-independent induction of id1 by prostacyclin analogues inhibits proliferation of pulmonary artery smooth muscle cells in vitro and in vivo. *Circ. Res.* 2010;107:252–262.
107. Pardali E., Goumans M.J., ten Dijke P. Signaling by members of the TGF- β family in vascular morphogenesis and disease. *Trends Cell. Biol.* 2010;20:556–567.
108. Zhang Y.E. Non-Smad pathways in TGF- β signaling. *Cell Res.* 2009;19:128–139.
109. Zhang Y.E. Non-Smad Signaling Pathways of the TGF- β Family. *Cold Spring Harb. Perspect. Biol.* 2016;9:a022129.
110. Awad K.S., Elinoff J.M., Wang S., Gairhe S., Ferreyra G.A., Cai R., Sun J., Solomon M.A., Danner R.L. Raf/ERK drives the proliferative and invasive phenotype of BMPR2-silenced pulmonary artery endothelial cells. *Am. J. Physiol Lung Cell. Mol. Physiol.* 2016;310:L187–L201.
111. Lambers C., Roth M., Zhong J., Campregher C., Binder P., Burian B., Petkov V., Block L.H. The interaction of endothelin-1 and TGF- β 1 mediates vascular cell remodeling. *PLoS ONE.* 2013;8:e73399.
112. Razani B., Zhang X.L., Bitzer M., von Gersdorff G., Bottinger E.P., Lisanti M.P. Caveolin-1 regulates transforming growth factor (TGF)- β /SMAD signaling through an interaction with the TGF- β type I receptor. *J. Biol. Chem.* 2001;276:6727–6738.
113. Olsson K.M., Delcroix M., Ghofrani H.A., Tiede H., Huscher D., Speich R., Grunig E., Staehler G., Rosenkranz S., Halank M., et al. Anticoagulation and survival in pulmonary arterial hypertension: Results from the Comparative, Prospective Registry of Newly Initiated Therapies for Pulmonary Hypertension (COMPETE). *Circulation.* 2014;129:57–65.
114. Preston I.R., Roberts K.E., Miller D.P., Sen G.P., Selej M., Benton W.W., Hill N.S., Farber H.W. Effect of Warfarin Treatment on Survival of Patients With Pulmonary Arterial Hypertension (PAH) in the Registry to Evaluate Early and Long-Term PAH Disease Management (REVEAL). *Circulation.* 2015;132:2403–2411.
115. Hoepfer M.M., Sosada M., Fabel H. Plasma coagulation profiles in patients with severe primary pulmonary hypertension. *Eur. Respir. J.* 1998;12:1446–1449.
116. Johnson S.R., Granton J.T., Mehta S. Thrombotic arteriopathy and anticoagulation in pulmonary hypertension. *Chest.* 2006;130:545–552.
117. Eisenberg P.R., Lucore C., Kaufman L., Sobel B.E., Jaffe A.S., Rich S. Fibrinopeptide A levels indicative of pulmonary vascular thrombosis in patients with primary pulmonary hypertension. *Circulation.* 1990;82:841–847.
118. Huber K., Beckmann R., Frank H., Kneussl M., Mlczoch J., Binder B.R. Fibrinogen, t-PA, and PAI-1 plasma levels in patients with pulmonary hypertension. *Am. J. Respir. Crit. Care Med.* 1994;150:929–933.
119. Olman M.A., Marsh J.J., Lang I.M., Moser K.M., Binder B.R., Schleeff R.R. Endogenous fibrinolytic system in chronic large-vessel thromboembolic pulmonary hypertension. *Circulation.* 1992;86:1241–1248.
120. Christ G., Graf S., Huber-Beckmann R., Zorn G., Lang I., Kneussi M., Binder B.R., Huber K. Impairment of the plasmin activation system in primary pulmonary hypertension: Evidence for gender differences. *Thromb. Haemost.* 2001;86:557–562.
121. Yang J., Li X., Li Y., Southwood M., Ye L., Long L., Al-Lamki R.S., Morrell N.W. Id proteins are critical downstream effectors of BMP signaling in human pulmonary arterial smooth muscle cells. *Am. J. Physiol Lung Cell. Mol. Physiol.* 2013;305:L312–L321.
122. Yang J., Davies R.J., Southwood M., Long L., Yang X., Sobolewski A., Upton P.D., Trembath R.C., Morrell N.W. Mutations in bone morphogenetic protein type II receptor cause dysregulation of Id gene expression in pulmonary artery smooth muscle cells: Implications for familial pulmonary arterial hypertension. *Circ. Res.* 2008;102:1212–1221.
123. Riechmann V., van Cruchten I., Sablitzky F. The expression pattern of Id4, a novel dominant negative helix-loop-helix protein, is distinct from Id1, Id2 and Id3. *Nucleic Acids Res.* 1994;22:749–755.
124. Upton P.D., Davies R.J., Trembath R.C., Morrell N.W. Bone morphogenetic protein (BMP) and activin type II receptors balance BMP9 signals mediated by activin receptor-like kinase-1 in human pulmonary artery endothelial cells. *J. Biol. Chem.* 2009;284:15794–15804.
125. Van de Veerdonk M.C., Kind T., Marcus J.T., Mauritz G.J., Heymans M.W., Bogaard H.J., Boonstra A., Marques K.M., Westerhof N., Vonk-Noordegraaf A. Progressive right ventricular dysfunction in patients with pulmonary arterial hypertension responding to therapy. *J. Am. Coll. Cardiol.* 2011;58:2511–2519.
126. Naeije R., Manes A. The right ventricle in pulmonary arterial hypertension. *Eur. Respir. Rev.* 2014;23:476–487.
127. Bogaard H.J., Abe K., Vonk N.A., Voelkel N.F. The right ventricle under pressure: Cellular and molecular mechanisms of right-heart failure in pulmonary hypertension. *Chest.* 2009;135:794–804.
128. Khan R., Sheppard R. Fibrosis in heart disease: Understanding the role of transforming growth factor- β in cardiomyopathy, valvular disease and arrhythmia. *Immunology.* 2006;118:10–24.
129. Okumura K., Kato H., Honjo O., Breitling S., Kuebler W.M., Sun M., Friedberg M.K. Carvedilol improves biventricular fibrosis and function in experimental pulmonary hypertension. *J. Mol. Med.* 2015;93:663–674.
130. Wollin L., Wex E., Pautsch A., Schnapp G., Hostettler K.E., Stowasser S., Kolb M. Mode of action of nintedanib in the treatment of idiopathic pulmonary fibrosis. *Eur. Respir. J.* 2015;45:1434–1445.
131. Rol N., de Raaf M.A., Sun X., Kuiper V.P., da Silva Goncalves Bos D., Happe C., Kurakula K., Dickhoff C., Thuillet R., Tu L., et al. Nintedanib improves cardiac fibrosis but leaves pulmonary vascular remodeling unaltered in experimental pulmonary hypertension. *Cardiovasc. Res.* 2018
132. Megalou A.J., Glava C., Oikonomidis D.L., Vilaeti A., Agelaki M.G., Baltogiannis G.G., Papalois A., Vlahos A.P., Kolettis T.M. Transforming growth factor- β inhibition attenuates pulmonary arterial hypertension in rats. *Int. J. Clin. Exp. Med.* 2010;3:332–340.
133. De Gramont A., Faivre S., Raymond E. Novel TGF- β inhibitors ready for prime time in onco-immunology. *Oncoimmunology.* 2017;6:e1257453.
134. Zaiman A.L., Podowski M., Medicherla S., Gordy K., Xu F., Zhen L., Shimoda L.A., Neptune E., Higgins L., Murphy A., et al. Role of the TGF- β /Alk5 signaling pathway in monocrotaline-induced pulmonary hypertension. *Am. J. Respir. Crit. Care Med.* 2008;177:896–905.
135. Schermuly R.T., Yilmaz H., Ghofrani H.A., Woyda K., Pullamsetti S., Schulz A., Gessler T., Dumitrascu R., Weissmann N., Grimminger F., et al. Inhaled iloprost reverses vascular remodeling in chronic experimental pulmonary hypertension. *Am. J. Respir. Crit. Care Med.* 2005;172:358–363.

8

Chapter 8

BMP9 pushes lung vasculature endothelial cells of pulmonary arterial hypertension patients into a mesenchymal phenotype

Szulcek R, Sanchez-Duffhues G, **RoI N**, Pan X, Tsonaka R, Dickhoff C, Ming Yung L, Manz XD, Kurakula K, Kielbasa SM, Mei H, Timens W, Yu PB, Bogaard HJ, Goumans MJTH

Submitted

Abstract

Introduction

Disbalanced bone morphogenetic protein (BMP) signaling is postulated to favor a pathological pulmonary endothelial cell (pEC) phenotype in pulmonary arterial hypertension (PAH). BMP9 has beneficial effects in experimental animal models and patient-derived circulating endothelial cells. Yet, BMP9 responses of diseased human pEC remained unknown, wherefore we tested BMP9 on primary pEC from PAH patients.

Methods

Pulmonary microvascular endothelial cells (MVEC) were isolated from patients with PAH, stimulated with BMP9 (1 ng/mL) for different time intervals (90 min, 24 h, 72 h), and signaling and cell phenotype were compared with controls.

Results

Repetitive BMP9 stimulation of PAH MVEC, every 24 h for three days, caused a total loss of endothelial barrier function that was driven by gradually decreasing integrity of cell-cell interactions. In accordance, long-term BMP9 treatment induced a significant loss of junctional VE-cadherin in the diseased pEC (1.00 ± 0.07 vs. 0.64 ± 0.22 , $p < 0.001$), while controls increased peripheral VE-cadherin significantly compared to unstimulated samples (1.00 ± 0.16 vs. 1.45 ± 0.17 , $p < 0.001$). Further, BMP9 treated PAH MVEC gained SM22 α expression (1.00 ± 0.38 vs. 2.62 ± 0.42 , $p < 0.001$) and reorganized their F-actin cytoskeleton indicative for endothelial-to-mesenchymal transition (EndoMT). EndoMT was not detected in controls. Global transcriptome analysis revealed that BMP9 activates EndoMT signaling following 90 min stimulation. This activation was short-lived in controls, while in PAH MVEC the master EndoMT transcription factors *SNAI1* and *SNAI2* remained significantly four-fold increased 24 h after stimulation ($p \leq 0.02$). The prolonged EndoMT signaling in PAH MVEC coincided with persistent pro-inflammatory, pro-hypoxic, and pro-apoptotic pathway activation. Detailed gene expression analysis identified IL6 as the common denominator between these pathways. Elevated levels of IL6 (98.5 ± 14.8 vs. 365.4 ± 130.6 pg/mL, $p = 0.05$) were found to drive EndoMT in an autocrine manner, since application of an IL6-capturing antibody normalized *SNAI1/2* levels in BMP9 treated PAH MVEC and prevented mesenchymal trans-differentiation.

Conclusions

We show that BMP9 acutely triggers EndoMT signaling whereas sustained IL6-dependent signaling is the presumed driver in a two-step process causing full trans-differentiation of PAH pEC. Our study suggests that investigations of the therapeutic use for BMP9 should be pursued with attention to levels of IL6 and features of EndoMT as a possible indicator of long-term impact.

Introduction

Progressive occlusive remodeling of the distal pulmonary vasculature is the hallmark of pulmonary arterial hypertension (PAH), a heterogenous group of deadly lung disorders clinically defined by a mean pulmonary artery pressure above 20 to 25 mmHg with pulmonary vascular resistance ≥ 3 Wood Units at rest in the absence of other causes of pre-capillary pulmonary hypertension (PH) (Galiè et al., 2016; Simonneau et al., 2019). The etiology of PAH ranges from drugs and toxins, to comorbidities, and inherited gene mutations (Galiè et al., 2016). However, a shift towards increased transforming growth factor beta (TGF β)-dependent signaling at the expense of decreased bone morphogenetic protein (BMP)-dependent signaling in pulmonary endothelial cells (pEC) is indicated as a common denominator in all disease sub-types (Atkinson et al., 2002). This shift is characterized by decreased expression and signaling of the BMP type-II receptor (BMPR2) in mutation positive and negative cases, and potentiated TGF β -mediated signaling that in return antagonizes BMP signaling further (Ogo et al., 2013). Consequently, novel experimental treatment efforts aim to restore BMPR2 levels and consecutive downstream signaling by selective inhibition or enhancement of associated ligands and receptors to re-establish TGF β /BMP balance (Morrell et al., 2016).

A currently explored therapeutic strategy consists of the administration of recombinant BMP9, a circulating ligand of the TGF β -family, aiming to selectively enhance pEC BMPR2 expression and signaling. In accordance, BMP9 reinstates BMPR2 levels in blood derived circulating endothelial cells from PAH patients carrying different heterozygous *BMPR2* mutations and has beneficial hemodynamic and anti-remodeling effects in several animal models when applied preventively or therapeutically (Long et al., 2015). Yet, BMP9 responses of primary endothelial cells from lungs of patients with PAH are unknown.

The BMP-family encompasses cytokines that have initially been discovered as potent inducers of ectopic bone formation (Urist, 1965; Rider and Mulloy, 2010). Meanwhile, BMPs were shown to play a central role in organogenesis, vascular development, cell differentiation, and vascular homeostasis (Goumans et al., 2018). The BMP9 homodimer is generally described as a circulating vascular quiescence and maintenance factor that can exert hematopoietic, hepato-, osteo-, chondro-, and adipogenic functions in a highly context and concentration-dependent manner (David et al., 2008). As such, BMP9 appears to exert anti-angiogenic and anti-apoptotic effects in the mature endothelium (David et al., 2008; Long et al., 2015). Yet, BMP9 also serves as a pro-angiogenic and pro-tumorigenic factor in cancer cells demonstrating pleiotropic roles in health and disease (Brand et al., 2016).

Phenotypically altered, de-differentiated, or transitional pEC are postulated to contribute to the occlusive vascular remodeling in PAH both directly by transforming into smooth muscle (SM)-like cells as well as indirectly through paracrine effects

(Ranchoux et al., 2015; Stenmark et al., 2016; Suzuki et al., 2018). Endothelial-to-mesenchymal transition (EndoMT), an essential developmental process, by which mature endothelial cells lose their specific protein expression, morphology, and polarity to acquire mesenchymal characteristics, has moved into focus as a possible source of these highly proliferative SM-like mesenchymal cells (Lamouille et al., 2014). BMP9 is a known inducer of EndoMT and thereby for instance controls vascular remodeling and vascular wall-thickening during embryonic development (Ricard et al., 2012; Levet et al., 2015).

Because the effects of BMPs on the endothelium are highly context-dependent (García de Vinuesa et al., 2016), it is difficult to predict whether the beneficial effects of BMP9 seen in PH animal models and circulating cells can be translated to the functionally altered pEC of patients suffering from PAH (Szulcek et al., 2016). The concern that the same ligand might have opposite effects is illustrated by contradicting reports showing that deletion or inhibition of BMP9 protects rodents from experimental PH (Tu et al., 2019) while a case study associates a homozygous nonsense mutation in *GDF2* (encoding for BMP9) with the development of PAH in infants (Wang et al., 2016).

We examined the therapeutic potential of BMP9 in pEC of patients with PAH and its effect on their cell phenotype to gain greater insight into how the pleiotropic roles of BMP9 as both an endothelial differentiation or quiescence factor may impact pulmonary vascular disease.

Material and Methods

Cell cultures and in-vitro assays

Microvascular endothelial cells (MVEC) were isolated from pleura-free peripheral lung tissues, as described previously (Szulcek et al., 2016). Human tissues were obtained from end-stage PAH patients undergoing lung transplantations or from autopsies. Control tissues originated from lobectomies for suspected or proven non-small cell lung cancer (NSCLC) without PH. Patient characteristics can be found in table 1. Tissue collection and cell isolations were approved by the IRB of the VU University Medical Center, Amsterdam, the Netherlands (non-WMO, 2012/306) and written informed consent was provided by the participants. Cells were cultured on 0.1% gelatin coated standard cultureware (Corning) in ECM medium supplemented with 1% pen/strep, 1% endothelial cell growth supplement, 5% FCS (all ScienCell), and 1% non-essential amino acids (Biowest).

Barrier function was determined by impedance spectroscopy with ECIS (Applied Biophysics) and analyzed as previously described (Szulcek et al., 2014). Treatments were performed after 5 h preparative serum starvation with 1% FCS and without

additional growth factors. Stimuli were prepared fresh in final concentrations of 1 ng/mL BMP9 (R&D Systems), 1 ng/mL TGF β 1 (Sigma), 10 ng/mL IL6 (BD Biosciences), and 10 ng/mL anti-IL6 blocking antibody (mabg-hil6-3, InvivoGen). ELISAs for IL6 on cell-free supernatants were carried out with the BD OptEIA human IL6 kit (BD Bioscience) following manufacturer's instructions.

Immunofluorescence staining

Human EC were fixed in warm 4% paraformaldehyde for 20 min at room temperature (RT), quenched with 2 mg/mL glycine, permeabilized with 0.2% Triton X-100 for 10 min at RT, blocked with 5% BSA, and labeled with VE-cadherin (1:500, 2158, Cell Signaling), SM22 α (1:500, ab14106, Abcam) specific antibodies, and/or Rhodamine-Phalloidin (1:1000, R415, Invitrogen). Samples were preserved in ProLong Gold anti-fading agent with DAPI (Thermo Fisher). Imaging was done on a Nikon A1 confocal laser microscope at 60x magnification. Image quantification was performed with ImageJ (NIH) by measuring VE-cadherin and SM22 α intensity of a total of nine individual cells per donor at three random locations in the culture well. The resulting intensity values were normalized to the mean intensity of the unstimulated controls within one experiment. F-actin orientation was analyzed using the directionality analyze-function of ImageJ on images from three random locations in the culture.

Global transcriptomics (RNA-seq) and analysis

Serum starved MVEC (5 h at 1% FCS, no growth factors) were either stimulated with BMP9 (for 90 min or 24 h) or left untreated. RNA was isolated with the miRNAeasy mini kit (Qiagen). Total RNA was purified using MagMAX-96 total RNA isolation kit (Ambion), in which genomic DNA was removed. mRNA was purified from total RNA using Dynabeads mRNA purification kit (Invitrogen). Strand-specific RNA sequencing libraries were prepared using ScriptSeq mRNA-seq library preparation kit (Epicentre). Sequencing was performed on HiSeq2000 (Illumina) by a multiplexed, single-read run with 33 cycles. Reads were mapped to the human genome hg38. Differential gene expression analysis was performed by the Medical Statistics and Bioinformatics core at LUMC using normalized log-transformed counts per gene with appropriate weights per observation in a *fdr* multiple testing corrected multivariate regression model. The model tested, which genes are differentially expressed between the three conditions (starved, 90 min, or 24 h stimulation) in at least one donor group (control vs. PAH). Gene ontology (GO) term enrichment analysis was performed on the unranked genes passing the log₂-threshold of ± 1 versus the complete background dataset (p-value threshold 10^{-3}) using Gorilla (Eden et al., 2009). Gene Set Enrichment Analysis (GSEA) was run with the pre-ranked tool (Subramanian et al., 2005) on the adjusted log₂-fold gene lists. Pathway enrichment was defined by FDR < 0.05 and p < 0.001. Enrichment map visualization (network graph) was done with the Enrichment Map Pipeline collection in Cytoscape version 3.6.1.

Table 1. Patient characteristics.

| MVEC used in the control group | | | | | | | | | | | | |
|---------------------------------------|------------------------------|--------------------------------|-------------|-------------|---------|-----|-----|-----------|--------|------------------------------------|--|--|
| ID | Assays | Diagnosis | FVC | FEV1 | Dyspnea | Sex | Age | Ethnicity | Source | Echo/CT | | |
| Ctrl01 | PCR, RNAseq, IF, ELISA, ECIS | NSCLC, adenocarcinoma | - | - | No | F | 55 | Caucasian | Lob | No dilation of RV, RA, or LV | | |
| Ctrl02 | PCR, RNAseq, IF, ELISA | NSCLC, squamous cell carcinoma | 3.11 (100%) | 2.31 (98%) | No | M | 79 | Caucasian | Lob | No dilation of RV, RA, or LV | | |
| Ctrl03 | PCR, RNAseq, IF, ECIS | NSCLC | 5.3 (96%) | 4.39 (98%) | No | M | 42 | Caucasian | Lob | No dilation of RV, RA, or LV | | |
| Ctrl04 | IF, ELISA, ECIS | NSCLC | 4.13 (110%) | 3.23 (110%) | No | F | 60 | Caucasian | Lob | No dilation of RV, RA, or LV | | |
| Ctrl05 | PCR, RNAseq | NSCLC, squamous cell carcinoma | 2.75 (100%) | 1.17 (50%) | No | F | 61 | Caucasian | Lob | No dilation of RV, RA, or LV | | |
| Ctrl06 | PCR, RNAseq | Tumoral obstruction | - | - | Yes | M | 42 | Caucasian | Lob | Enlarged RV, small LV, enlarged RA | | |
| MVEC used in the PAH group | | | | | | | | | | | | |
| ID | Assays | Diagnosis | mPAP | PVR | CI | Sex | Age | Ethnicity | Source | Treatment | | |
| PAH01 | PCR, RNAseq, ELISA | iPAH | 54 | - | 2.1 | F | 54 | Caucasian | Obd | PDE5-I, ERA, PGI2 | | |
| PAH02 | PCR, RNAseq, IF, ELISA, ECIS | hPAH (BMPR2) | 68 | - | 1.6 | F | 40 | Caucasian | Ltx | PDE5-I, ERA, PGI2 | | |
| PAH03 | PCR, RNAseq, ELISA, ECIS | iPAH | 43 | 620 | 2.1 | F | 42 | Caucasian | Ltx | PDE5-I, PGI2 | | |
| PAH04 | PCR, RNAseq, IF, ELISA | iPAH | 89 | 1527 | 1.9 | F | 22 | Caucasian | Ltx | PDE5-I, ERA, PGI2 | | |
| PAH05 | PCR, RNAseq, IF, ELISA, ECIS | iPAH | 102 | 1375 | 3.4 | M | 21 | Caucasian | Ltx | PDE5-I, ERA, PGI2 | | |

ECIS = barrier function; IF = immunofluorescence; MVEC = lung microvascular endothelial cells; NSCLC = non-small-cell lung carcinoma; FVC = forced vital capacity (L); FEV1 = first second of forced expiration (L); Lob = lobectomy; RV = right ventricle; RA = right atrium; LV = left ventricle; iPAH = idiopathic pulmonary arterial hypertension; hPAH = hereditary PAH; mPAP = mean pulmonary artery pressure (mmHg); PVR = pulmonary vascular resistance (WU); CI = cardiac index (l/min/m²); PDE5-I = phosphodiesterase type 5 inhibitor; PGI2 = prostacyclin; ERA = endothelin receptor antagonist; Obd = autopsy; Ltx = lung transplantation.

Real-time polymerase chain reaction (RT-PCR)

RNA was isolated with the miRNeasy mini kit (Qiagen), cDNA synthesis performed with the iScript cDNA synthesis kit (Bio-Rad) on a 2720 Thermal Cycler (Applied Biosystems), and RT-PCR carried out with iQ SYBR green supermix on a CFX384 Real-Time System (all Bio-Rad) following manufacturer's instructions. Primer details (Sigma) can be found in table 2.

Statistics

Individual cell culture experiments were repeated at least three times, with different combinations of available donors (indicated by donor number n). Experimental data were analyzed using either unpaired two-tailed student's t-test, one-way analysis of variance with post-hoc Dunnett's, or two-way ANOVA with Tukey multiple comparison post-hoc test. The applied test is specified in the figure legends. Data were considered significantly different at p-values ≤ 0.05 . Data were visualized using GraphPad Prism version 7 (GraphPad Software). If not indicated differently, data are presented as mean \pm standard deviation.

Results

Long-term BMP9 treatment causes loss of endothelial barrier function in the PAH lung endothelium

Smaller pulmonary arteries are the principal sites of vascular remodeling in PAH (Rabinovitch, 2012). Previous studies used blood derived, circulating endothelial cells as a surrogate for lung MVEC and reported BMP9 to increase basal monolayer integrity, to prevent LPS-induced hyper-permeability over a time course of two hours, and to maintain VE-cadherin-based cell junctions after 24 h LPS stimulation (Long et al., 2015). We aimed to reproduce these findings in primary lung MVEC of PAH patients.

Electrical resistance was measured to quantify changes in endothelial barrier function in real-time (Fig. 1a). The cells were cultured under low serum-containing conditions and both untreated controls and PAH MVEC maintained an intact barrier over 72 h (on average 1685 vs. 2024 Ohms). The mechanical stimulation, and changes in temperature and pH during medium changes caused a drop in resistance that the cells recovered from after an adjustment period. BMP9 treated controls significantly improved their barrier at 48 h (1709 \pm 31 vs. 2323 \pm 127 Ohms, $p < 0.001$) and 72 h after stimulation (1629 \pm 41 vs. 1994 \pm 97 Ohms, $p < 0.001$) compared to unstimulated samples and thereby confirmed previous reports. On the contrary, BMP9 caused a significant drop in PAH MVEC resistance to ca. 50% of its basal value (2154 \pm 95 vs. 1124 \pm 14 Ohm, $p < 0.001$) which plateaued at 12 h. The cells were initially able to recover their barrier to basal levels at 24 h. However, the second stimulation with BMP9 caused a complete loss of PAH pEC barrier function at 48 h.

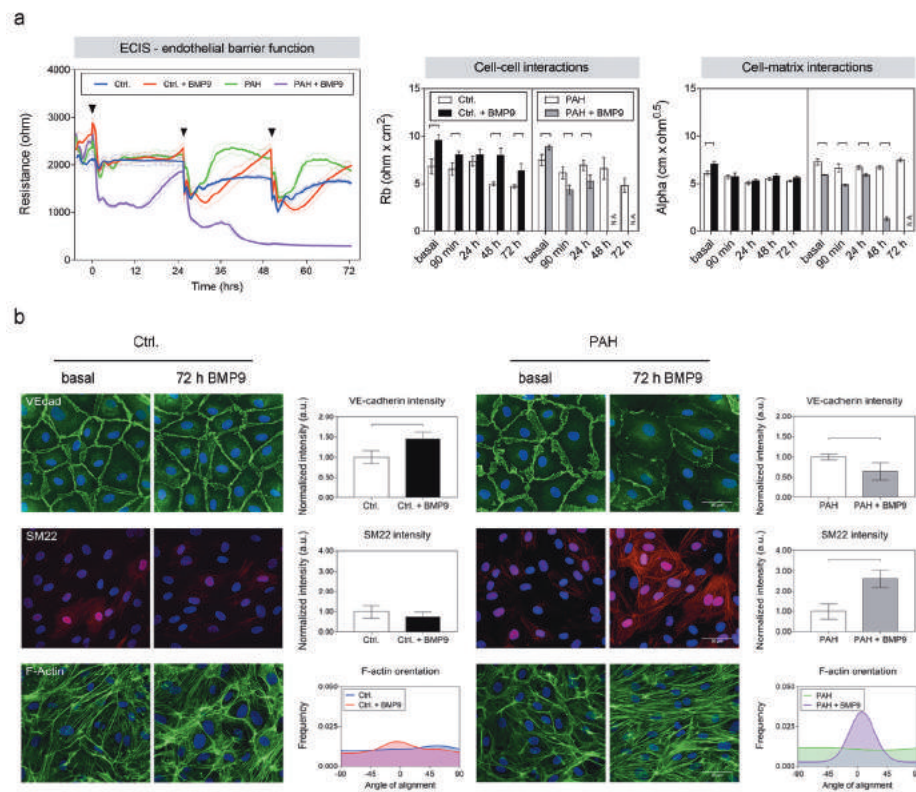


Figure 1 – Repetitive, long-term BMP9 treatment pushes the diseased lung microvascular lung endothelium into a mesenchymal phenotype. a) Representative, time-resolved, impedance spectroscopic quantification of endothelial barrier function (resistance), strength of cell-cell interactions (Rb), and cell-matrix interactions (Alpha). BMP9 administration was started 5 h after preparative serum starvation at 1% FCS (no growth factors). BMP9 was applied every 24 h (arrow heads) for a total duration of 72 h. Significance is based on multiple t-tests corrected for multiple comparisons using the Holm-Sidak method. b) Representative immunostaining for the endothelial marker VE-cadherin, the mesenchymal marker SM22 α , and cytoskeletal protein F-actin. MVEC were stimulated with BMP9 every 24 h for a total duration of 72 h. VE-cadherin and SM22 intensity as well as F-actin fiber orientation were quantified and compared between controls and PAH samples ($n = 3$). Statistical differences were determined by unpaired t-tests.

Detailed analysis of the electrical parameters confirmed that in controls BMP9 had improved strength of cell-cell interactions significantly after 48 h (4.97 ± 0.19 vs. 7.98 ± 0.77 , $p < 0.001$) and 72 h (4.73 ± 0.16 vs. 6.36 ± 0.72 , $p = 0.004$) and left cell-matrix adhesions unchanged. In PAH samples, BMP9 had opposite effects and triggered an immediate decrease in Rb at 90 min (6.15 ± 0.65 vs. 4.35 ± 0.49 , $p = 0.026$) and a complete loss of cell-cell contacts at the 48 h time-point followed by a gradual decreasing cell-matrix interactions.

We repeated this experiment with three different donors per group and although the BMP9 response of PAH cells always resulted in a loss of barrier function, the time-courses per donor were very varied. In some donors the loss of barrier was detected after 48 h and in others after 120 h stimulation.

PAH MVEC receiving long-term treatment with BMP9 show signs of EndoMT

Because of the loss of barrier function in response to BMP9, we initially assumed that the PAH cells went into apoptosis but upon microscopic inspection realized that cell morphology had changed. To test the impact of BMP9 on phenotypic plasticity, human MVEC received daily BMP9 supplementation for a total duration of three days and were fluorescently labeled for endothelial and mesenchymal markers (Fig. 1b). In alignment with the barrier function measurements, control cells in response to BMP9 significantly increased peripheral expression of endothelial VE-cadherin (1.00 ± 0.16 vs. 1.45 ± 0.17 , $p < 0.001$), retained low levels of SM22 α , and maintained cobble stone morphology with well-organized peripheral F-actin. PAH patient-derived MVEC effectively lost VE-cadherin expression from cell-cell junctions (1.00 ± 0.07 vs. 0.64 ± 0.22 , $p < 0.001$) and displayed an elongated morphology with F-actin stress fibers spanning the entire cell body and gaining collective directionality consistent with a contractile phenotype. In a sub-set of the stimulated PAH cells, SM22 α expression increased significantly (1.00 ± 0.38 vs. 2.62 ± 0.42 , $p < 0.001$) and co-localized with the cell cytoskeleton, a characteristic of mesenchymal cells.

BMP9 is a potent inducer of EndoMT signalling

The BMP9-induced loss of endothelial-specific protein expression, altered cytoskeletal organization, and gain of mesenchymal marker expression in patient-derived pEC pointed us towards the hypothesis that BMP9 pushes PAH MVEC into a mesenchymal phenotype.

To proof activation of transcriptional EndoMT signaling, RNA sequencing was carried out on pEC after 90 min and 24 h BMP9 stimulation. The transcriptome of controls and PAH samples overlapped substantially at 90 min stimulation with 54% of all genes that passed the log₂-threshold of ± 1 intersecting. The number of intersecting genes decreased to 25% at 24 h with 172 fewer genes passing the threshold in the PAH dataset compared to controls pointing towards altered long-term homeostatic responses. To test for a mesenchymal signature, focused Gene Ontology (GO) enrichment analysis was performed for the biological process of epithelial-to-mesenchymal transition (EMT) that shares preserved signaling and activators with EndoMT (Saito, 2013). Directly related mother terms were included in the analysis (Fig. 2a) and showed similarly strong enrichment in controls and patient cells at 90 min that did not perpetuate to the 24 h time-point (Fig. 2b). Application of a previously published EMT/EndoMT signature gene panel (Evrard et al., 2016), to determine directionality of regulation, uncovered the activation of an EndoMT gene set comprising a three to six log₂-fold induction of the

EndoMT transcription factors *SNAI1*, *SNAI2*, *HEY1* and *HEY2* compared to unstimulated samples (Fig. 2c). The EndoMT gene set got enriched in both control and PAH MVEC at the 90 min time-point and returned to basal values after 24 h confirming the results of the GO analysis. The mesenchymal markers *CDH2*, *PLAU*, *CDH11* and *PLEK2* were found decreased by two log₂-fold in controls after 24 h, whereas levels in PAH samples did not change compared to basal values or were even slightly elevated.

RT-PCR verification was carried out (Fig. 2d) together with TGFβ stimulation for its well-known role in EndoMT and PAH development (Cooley et al., 2014). The PCR corroborated the transcriptomic analysis of a robust elevation in *SNAI1* (3.2 ± 1.3 vs. 5.0 ± 1.0 , $p = 0.039$) and *SNAI2* (2.8 ± 2.0 vs. 4.6 ± 1.7 , not significant) expression in both donor groups early after stimulation. Subsequently, control cells returned to basal values, while *SNAI1* (-0.1 ± 0.6 vs. 2.1 ± 1.4 , $p = 0.017$) and *SNAI2* (-1.9 ± 1.1 vs. 2.6 ± 0.9 , $p < 0.001$) remained significantly elevated in PAH MVEC at the 24 h time-point. No statistically significant differences between controls and PAH samples were found in the tested genes upon TGFβ stimulation.

PAH pulmonary endothelial cells exert sustained pro-hypoxic, pro-apoptotic, and pro-inflammatory signaling upon BMP9 stimulation

EndoMT is a highly integrative process that involves various, context and stimulus-dependent combinations of signal transduction pathways (Sánchez-Duffhues et al., 2017). BMP9 application persuaded a transient EndoMT gene signature in both control and PAH donor groups, but only in PAH cells led to the development of a mesenchymal phenotype. To identify pathway interactions and regulatory patterns that might provide a second hit and drive the phenotypic change, unbiased Gene Set Enrichment Analysis (GSEA) was performed. Illustrated by the GSEA pathways enrichment map (Fig. 3a), BMP9 generally causes downregulation of signaling in controls after 24 h, whereas in PAH samples individual pathways show differential regulation patterns. To highlight pathways associated with the pathogenesis of the disease, the STRING database (Szklarczyk et al., 2015) was queried for “Pulmonary Hypertension” and the resulting gene list overlaid onto the network map (cut-off ≥ 5 overlapping genes). Comparing enrichment of the seven disease-specific pathways between control and PAH samples (Fig. 3b) revealed missing enrichment of hypoxia, apoptosis, and IL6, JAK, STAT3 pathways suggesting a partial loss of PAH MVEC suppressor function upon long-term BMP9 stimulation. Causative for the missing enrichment were several genes inversely regulated in PAH samples compared to controls (Fig. 3c). Analysis of leading-edge genes in all negatively enriched pathways identified interleukin-6 (IL6) as common denominator.

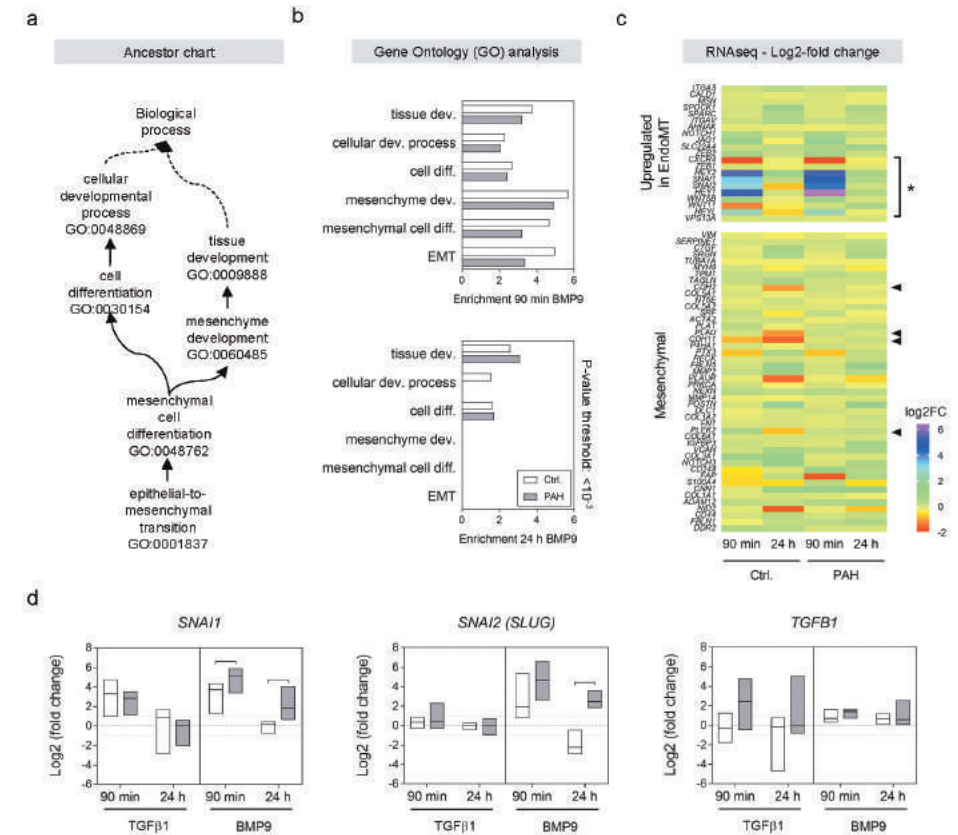


Figure 2 – BMP9 causes prolonged activation of the EndoMT master transcription factors *SNAI1* and *SNAI2*. a) Ancestor chart of selected Gene Ontology (GO) terms related to epithelial-to-mesenchymal transition (EMT) used for focused GO analysis. b) Time-resolved (90 min and 24 h) GO enrichment analysis on control and PAH samples for biological processes related to EMT. Analysis is based on global transcriptomics (RNA-seq, log₂-fold changes (FC) vs. unstimulated conditions, $n = 5$). Average enrichment scores that passed the p-value threshold are shown. c) Heat-map of known mesenchymal cell markers and modulators of endothelial-to-mesenchymal transition (EndoMT). Shown are log₂FC in transcript levels following 90 min or 24 h BMP9 stimulation compared to unstimulated samples. Asterix highlights cluster of EndoMT genes, and arrow heads individual genes differentially regulated, between the two donor groups. d) RT-PCR expression validation of the EndoMT master transcription factors *SNAI1* and *SNAI2*, and the well-known EndoMT inducer *TGFβ1*. Box plots represent min, max, and median log₂FC compared to unstimulated conditions ($n = 5$). Multiple t-tests corrected for multiple comparisons using the Holm-Sidak method were used to calculate p-values. Immunostaining for the endothelial marker VE-cadherin, the mesenchymal marker SM22 α , and cytoskeletal protein F-actin. MVEC were stimulated with BMP9 every 24 h for a total duration of 72 h. VE-cadherin and SM22 intensity as well as F-actin fiber orientation were quantified and compared between controls and PAH samples ($n = 3$). Statistical differences were determined by unpaired t-tests.

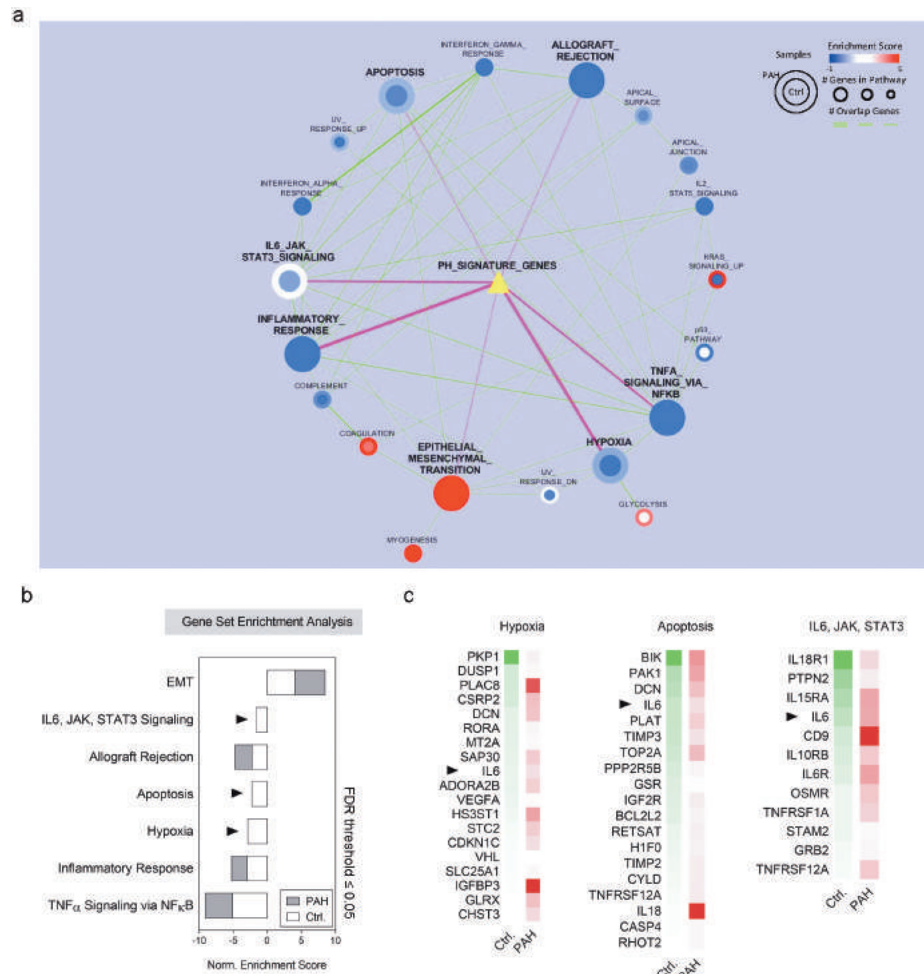


Figure 3 – BMP9-induced EndoMT signaling is accompanied by persistent pro-inflammatory, pro-apoptotic, and pro-hypoxic signaling in the PAH endothelium. a) Network graph resulting from unbiased Gene Set Enrichment Analysis (GSEA) of the sequenced control and PAH MVEC 24 h after BMP9 stimulation. Represented are positive (upregulated, red), negative (downregulated, blue), and non-enriched (white) pathways (circles) compared to unstimulated samples. Number of overlapping genes in between pathways (green lines) and gene overlap with a pulmonary hypertension (PH) signature gene set (yellow triangle with magenta lines) are shown (cut-off ≥ 5 genes). b) Average enrichment scores of the EndoMT and the six identified PH signature pathways. Arrowheads point out pathways that did not pass the enrichment threshold (FDR ≤ 0.05) 24 h after BMP9 treatment. c) Switch gene analysis per non-enriched pathway and per donor group-based on RNA-seq. Pseudo colors represent log₂-FC decrease (green) or increase (red) compared to non-stimulated samples. Arrow heads highlight interleukin-6 (*IL6*) as a common denominator between the non-enriched pathways identified by leading-edge analysis.

BMP9-induced EndoMT and IL6-dependent signaling collude in the mesenchymal switch of the PAH lung endothelium

IL6 was pointed out by the global transcriptome analysis as a key factor in the BMP9-induced PAH pEC phenotype change. In accordance, we found *IL6* gene levels increased under basal and BMP9-containing conditions in PAH MVEC compared to controls (Fig. 4a). ELISA measurements (Fig. 4b) showed a significant four-fold increased *IL6* concentration (1.1 ± 0.48 vs. 4.1 ± 1.95 , $p = 0.003$) in the supernatants of PAH MVEC compared to controls at 24 h, but not 90 min, of BMP9 stimulation. The *IL6* levels could be restored to levels of controls when using an *IL6*-capturing antibody (*αIL6*) in combination with the BMP9 treatment.

To prove the integrative role of *IL6* as the driver for the mesenchymal change, MVEC were again treated with daily addition of BMP9, *IL6*, *αIL6* or combinations thereof (Fig. 4c-d). After three days, control cells treated with the combination of BMP9 plus *IL6* had lost peripheral VE-cadherin and gained SM22 α protein expression that colocalized with the cytoskeleton (Fig. 4c). Single BMP9 treatment of controls, in-line with previous experiments, induced a more closed or quiescent confirmation of cell junctions with VE-cadherin tightly organizing at the cell periphery. In PAH MVEC in contrast (Fig. 4d), BMP9 treatment alone as well as the combination of BMP9 and *IL6* resulted in EndoMT evident by the previously described changes in marker expression. Conversely, exposing the PAH MVEC to BMP9 in the presence of the *IL6*-capturing antibody preserved cobble stone morphology and cytoskeletal arrangement with sustained expression and junctional organization of VE-cadherin. This finding taken together with the ELISA data suggest an autocrine mechanism of *IL6*.

RT-PCR confirmed that BMP9 did not directly induced transcription of *IL6* but caused long-term activation of *SNAI1* and *SNAI2* for 24 h in PAH pEC compared to controls. Treatment with the *IL6*-capturing antibody prevented continued induction of *SNAI1* (2.09 ± 1.43 vs. 0.23 ± 0.42 , $p = 0.047$) and *SNAI2* (1.80 ± 1.31 vs. 0.13 ± 0.15 , $p = 0.012$) and normalized signaling to levels of unstimulated controls.

Discussion

In summary, we provide proof for BMP9 being a potent inducer of EndoMT in the lung microvascular endothelium of patients with PAH. This function is highly context-dependent, as BMP9 stimulation alone was not sufficient to change the phenotype of control pEC, wherefore additional mechanisms in MVEC of PAH patients must drive the phenotypic change. Our study provides evidence that sustained pro-apoptotic, pro-hypoxic, and pro-inflammatory signaling mediated through *IL6*-dependent signaling in conjunction with the BMP9-induced expression of EndoMT promoting transcription

factors causes the trans-differentiation of the PAH endothelium, which can be inhibited by IL6-based antibody therapy (Fig. 5).

Postnatally, EMT and EndoMT are parts of a general lung repair program (Chapman, 2012) but EndoMT is also frequently implicated in numerous pathogenesis including fibrotic diseases, cancer, atherosclerosis, and heterotopic ossification (Lin et al., 2012; Evrard et al., 2016; Sánchez-Duffhues et al., 2017). In PAH specifically, EndoMT was shown to potentially give rise to transitional cells co-expressing endothelial and mesenchymal markers that are found in up to 5% of the diseased lungs and abundantly within the typical vascular lesions (Good et al., 2015; Ranchoux et al., 2015). The transitional cells exert high proliferation rates with a migratory or even invasive phenotype that weakens the endothelial barrier (Suzuki et al., 2018). Yet, if this transition is temporally and the cells attempt to initiate vascular repair and restore physiological function or if these cells fully transform into smooth muscle cells or fibroblasts that contribute to the progression of lung vascular remodeling is unclear (Jolly et al., 2018).

EndoMT is a highly integrative process that can result from pathway crosstalk-induced by TGF β family members, Notch and Wnt ligands, mechanical forces, growth factors, hypoxia, and inflammation (Sánchez-Duffhues et al., 2017). The relative importance and order of activation depend on stimulus and/or underlying (patho)biology. We demonstrate that BMP9 or IL6 alone are not sufficient to drive the mesenchymal change in MVEC to a higher level, but in accordance with literature need input from other signaling to induce full mesenchymal trans-differentiation (Sakao et al., 2007; Good et al., 2015; Hopper et al., 2016). In line, we recently showed that TNF α and IL-1 β induce EndoMT in human primary aortic endothelial cells and thereby sensitizing the cells for BMP9-induced osteogenic differentiation (Sánchez-Duffhues et al., 2019). Similarly, BMP9 alone was reported to have no effect on monocyte and neutrophil recruitment to the vascular endothelium but amplifies the effects of inflammatory stimuli like TNF α and LPS by priming the endothelial response (Appleby et al., 2016; Mitrofan et al., 2017). We and others thereby collectively hypothesize that imbalanced TGF β /BMP signaling reactivates developmental programs that in the diseased *milieu* of a PAH patient lung continuously switches the EC phenotype between different precursor states (Cooley et al., 2014). These transitional cells can easily be tipped towards one cell fate or another in response to injury or other triggers, as in this case BMP9. Here again, the question remains, if this is an attempt to compensate and repair the lung or if it represents a non-adaptive, pathological transformation of the cells (Jolly et al., 2018)?

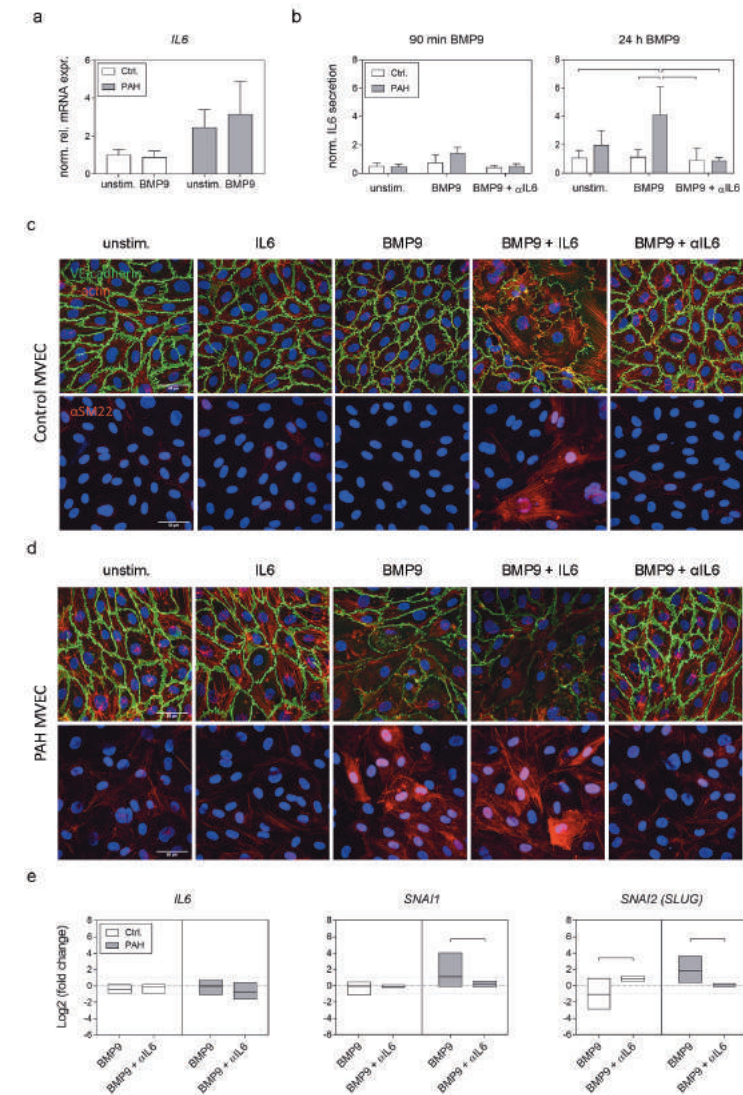


Figure 4 – The BMP9-induced phenotypic change of the PAH endothelium is mediated through IL6-dependent signaling and can be therapeutically impeded. a) Normalized relative *IL6* mRNA expression in human lung endothelium after 24 h BMP9 stimulation ($n = 5$), and b) *IL6* protein concentration in cell culture supernatants after different combination treatments with BMP9 and *IL6*-capturing antibody (α IL6). Statistics were calculated by two-way ANOVA multiple comparison with Tukey correction ($n = 5$). c) Representative immunostaining of endothelial VE-cadherin, mesenchymal SM22 α , and cytoskeletal F-actin in control and d) PAH MVEC after combination treatments with BMP9, *IL6*, and α IL6. Stimuli were applied every 24 h for a total of 72 h. e) RT-PCR validation of *IL6*, *SNAI1*, and *SNAI2* transcription levels after 24 h treatment with BMP9 or BMP9 in combination with α IL6. Log₂FC are calculated compared to unstimulated conditions. Box plots represent min, max, and median log₂FC compared to unstimulated conditions ($n = 5$). P-values were determined by unpaired student's t-tests.

Our pathway analysis revealed that BMP9 initiates anti-inflammatory, anti-hypoxic, and anti-apoptotic signaling in control cells, while this effect is astray in PAH patient cells. We found that the loss of suppressor function is caused by genes inversely regulated in PAH MVEC compared to controls, of which *IL6* is the most common gene between these pathways. The role of sustained inflammation, and IL6 in particular, as histopathological cause and contributor to PAH is studied comprehensively and is a known treatment target. For review see (Huertas et al., 2014). As such, IL6 was shown to induce PH by commanding a proliferative and apoptosis resistant pulmonary vasculature phenotype, to decrease BMPR2 levels, to exaggerate effects of chronic hypoxia, and to worsen vascular remodeling in BMPR2 deficient animals (Pickworth et al., 2017; Tamura et al., 2018). Increased IL6 protein levels are found across the systemic and lung circulation of PAH patients and are correlated with worse clinical outcomes (Selimovic et al., 2009). In a previous study we have shown that pro- and anti-inflammatory cytokine responses in MVEC of PAH patients are impaired (Dummer et al., 2018) and in agreement with this finding detected that PAH MVEC secrete higher levels of IL6 within 24 h of BMP9 stimulation. We postulate that the increased IL6 secretion could initiate an autocrine loop that impairs negative feedback signaling, as unexpectedly strong ectopic levels of membrane bound IL6 receptors were recently found to cause a apoptosis resistant cell phenotype in the remodeled SM-layer of distal pulmonary arteries (Tamura et al., 2018). Hence, sustained IL6-dependent signaling is the presumed driver in the two-step process required for full mesenchymal trans-differentiation of pEC, whereas BMP9 is the acute trigger initiating EndoMT signaling. How IL6 expression and signaling is activated precisely and why the cells have a dysfunctional response to BMP9 remains to be further explored.

However, our data suggest that the mechanism for EndoMT in the PAH MVEC is controlled through increased *SNAI1/2* transcription levels. These transcription factors together with *ZEB1/2*, *JAG1*, *HEY1/2* and others belong to a group of EndoMT master regulators that get activated in the initial phases of the EndoMT process and their contributions are dependent on cell or tissue type and the pathway that induces EndoMT. See (Lamouille et al., 2014) for review. We found early activation of *SNAI1* family transcription factors upon BMP9, which are reported to directly repress genes encoding VE-cadherin and PECAM-1, while zinc-finger E-box binding (*ZEB*) transcription factors are known to get activated later in the EndoMT process and control SM22 α and SMA protein expression (Lamouille et al., 2014; Levet et al., 2015). Excitingly, capturing IL6 from the endothelial interstitium prevents the activation of *SNAI1/2* upon BMP9 and thereby blocks the phenotypic change of the diseased cells.

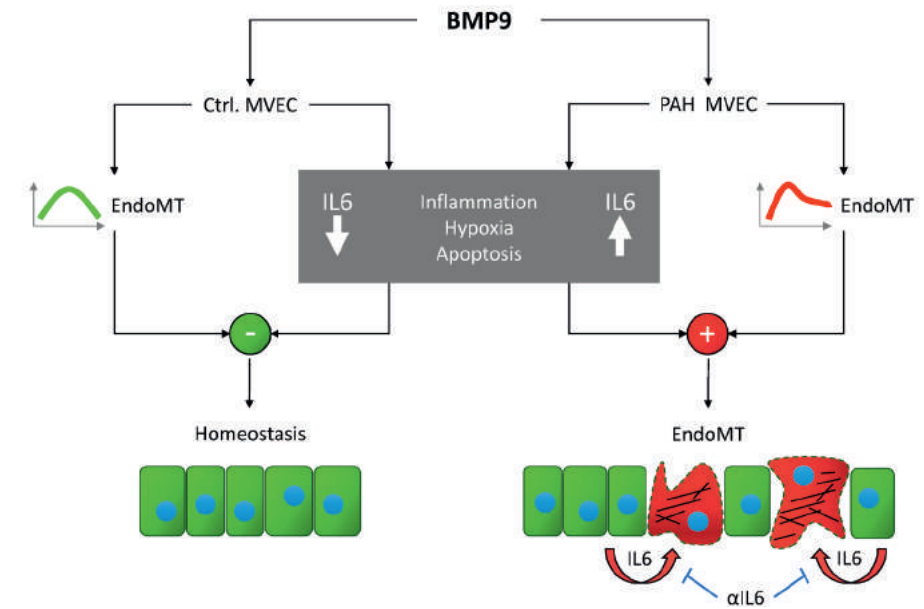


Figure 5 – Explanatory model. BMP9 transiently activates EndoMT signaling in the pulmonary endothelium. In the healthy lung this response is short-lived and on the long run coincides with a downregulation of other pathways including inflammatory, hypoxic, and apoptotic signaling. In the microvascular lung endothelium of patients with PAH the suppression of pro-inflammatory, pro-hypoxic, and pro-apoptotic signaling upon BMP9 is dysfunctional causing persistent pathway activation and EndoMT signaling. The loss of suppressor function is mediated and exacerbated through high transcriptional levels of *IL6* and autocrine activation of the PAH endothelium by IL6, which in conjunction with the BMP9-induced EndoMT program causes the diseased lung endothelium to lose endothelial specific markers and gain mesenchymal characteristics. The mesenchymal change upon BMP9 can be prevented by capturing extracellular IL6 with an antibody (α IL6).

As is mostly the case for this rare disease, number of donors is limited, and we must deal with considerable donor-to-donor variability just like not all PAH MVEC show high levels of IL6 and *SNAI1/2*, wherefore generalization to all patients and all disease subtypes should be done with caution.

In conclusion, we provide evidence that the phenotypic transformation of the PAH lung endothelium is the consequence of combined BMP9-induced EndoMT signaling and sustained pro-inflammatory, pro-hypoxic, and pro-apoptotic signaling mediated (in part) through IL6-dependent signaling. Accordingly, our study suggests that further investigations for the therapeutic use of BMP9 in PAH should be pursued with attention to the features of EndoMT as a possible indicator of long-term impact. Given the current findings, co-administration of anti-inflammatory therapy, such as an IL6 neutralizing antibody, could potentially mitigate inadvertent side-effects and might be considered for a sub-group of patients.

References

- Appleby, S. L., Mitrofan, C.-G., Crosby, A., Hoenderdos, K., Lodge, K., Upton, P. D., et al. (2016). Bone morphogenetic protein 9 enhances lipopolysaccharide-induced leukocyte recruitment to the vascular endothelium. *J Immunol* 197, 3302–3314. doi: 10.4049/jimmunol.1601219
- Atkinson, C., Stewart, S., Upton, P. D., Machado, R., Thomson, J. R., Trembath, R. C., et al. (2002). Primary pulmonary hypertension is associated with reduced pulmonary vascular expression of type II bone morphogenetic protein receptor. *Circulation* 105, 1672–1678. doi: 10.1161/01.CIR.0000012754.72951.3D
- Brand, V., Christian Lehmann, Christian Umkehrer, Stefan Bissinger, Martina Thier, Mariana de Wouters, et al. (2016). Impact of selective anti-BMP9 treatment on tumor cells and tumor angiogenesis. *Mol Oncol* 10, 1603–1620. doi: 10.1016/j.molonc.2016.10.002
- Chapman, H. A. (2012). Epithelial responses to lung injury: Role of the extracellular matrix. *Proc Am Thorac Soc* 9, 89–95. doi: 10.1513/pats.201112-053AW
- Cooley, B. C., Nevado, J., Mellad, J., Yang, D., Hilaire, C. S., Negro, A., et al. (2014). TGF- β signaling mediates endothelial-to-mesenchymal transition (EndMT) during vein graft remodeling. *Sci Transl Med* 6, 227ra34. doi: 10.1126/scitranslmed.3006927
- David, L., Mallet, C., Keramidas, M., Lamandé, N., Gasc, J.-M., Dupuis-Girod, S., et al. (2008). Bone morphogenetic protein-9 is a circulating vascular quiescence factor. *Circ Res* 102, 914–922. doi: 10.1161/CIRCRESAHA.107.165530
- Dummer, A., Rol, N., Szulcek, R., Kurakula, K., Pan, X., Visser, B. I., et al. (2018). Endothelial dysfunction in pulmonary arterial hypertension: Loss of cilia length regulation upon cytokine stimulation. *Pulm Circ* 8, 1-9. doi: 10.1177/2045894018764629
- Eden, E., Navon, R., Steinfeld, I., Lipson, D., and Yakhini, Z. (2009). GOrilla: A tool for discovery and visualization of enriched GO terms in ranked gene lists. *BMC Bioinformatics* 10, 48. doi: 10.1186/1471-2105-10-48
- Evrard, S. M., Lecce, L., Michelis, K. C., Nomura-Kitabayashi, A., Pandey, G., Purushothaman, K.-R., et al. (2016). Endothelial to mesenchymal transition is common in atherosclerotic lesions and is associated with plaque instability. *Nat Commun* 7, 11853. doi: 10.1038/ncomms11853
- Galiè, N., Humbert, M., Vachiery, J.-L., Gibbs, S., Lang, I., Torbicki, A., et al. (2016). 2015 ESC/ERS Guidelines for the diagnosis and treatment of pulmonary hypertension: The Joint Task Force for the Diagnosis and Treatment of Pulmonary Hypertension of the European Society of Cardiology (ESC) and the European Respiratory Society (ERS): Endorsed by: Association for European Paediatric and Congenital Cardiology (AEPC), International Society for Heart and Lung Transplantation (ISHLT). *Eur Heart J* 37, 67–119. doi: 10.1093/eurheartj/ehv317
- García de Vinuesa, A., Abdelilah-Seyfried, S., Knaus, P., Zwijsen, A., and Bailly, S. (2016). BMP signaling in vascular biology and dysfunction. *Cytokine Growth Factor Rev* 27, 65–79. doi: 10.1016/j.cytogfr.2015.12.005
- Good, R. B. B., Gilbane, A. J. J., Trinder, S. L. L., Denton, C. P. P., Coghlan, G., Abraham, D. J. J., et al. (2015). Endothelial to mesenchymal transition contributes to endothelial dysfunction in pulmonary arterial hypertension. *Am J Pathol* 185, 1850–1858. doi: 10.1016/j.ajpath.2015.03.019
- Goumans, M.-J. T. H., Zwijsen, A., Dijke, P. ten, and Bailly, S. (2018). Bone morphogenetic proteins in vascular homeostasis and disease. *Cold Spring Harb Perspect Biol* 10. doi: 10.1101/cshperspect.a031989
- Hopper, R. K., Moonen, J.-R. A. J., Diebold, I., Cao, A., Rhodes, C. J., Tojais, N. F., et al. (2016). In pulmonary arterial hypertension, reduced BMPR2 promotes endothelial-to-mesenchymal transition via HMGA1 and its target Slug. *Circulation* 133, 1783–1794. doi: 10.1161/CIRCULATIONAHA.115.020617
- Huertas, A., Perros, F., Tu, L., Cohen-Kaminsky, S., Montani, D., Dorfmüller, P., et al. (2014). Immune dysregulation and endothelial dysfunction in pulmonary arterial hypertension: a complex interplay. *Circulation* 129, 1332–1340. doi: 10.1161/CIRCULATIONAHA.113.004555
- Jolly, M. K., Ward, C., Eapen, M. S., Myers, S., Hallgren, O., Levine, H., et al. (2018). Epithelial-mesenchymal transition, a spectrum of states: Role in lung development, homeostasis, and disease. *Dev Dyn* 247, 346–358. doi: 10.1002/dvdy.24541
- Lamouille, S., Xu, J., and Derynck, R. (2014). Molecular mechanisms of epithelial-mesenchymal transition. *Nat Rev Mol Cell Biol* 15, 178–196. doi: 10.1038/nrm3758
- Levet, S., Ouarne, M., Ciais, D., Coutton, C., Subileau, M., Mallet, C., et al. (2015). BMP9 and BMP10 are necessary for proper closure of the ductus arteriosus. *Proc Natl Acad Sci U S A* 112, E3207–15. doi: 10.1073/pnas.1508386112
- Lin, F., Wang, N., and Zhang, T.-C. (2012). The role of endothelial-mesenchymal transition in development and pathological process. *IUBMB Life* 64, 717–723. doi: 10.1002/iub.1059
- Long, L., Ormiston, M. L., Yang, X., Southwood, M., Gräf, S., Machado, R. D., et al. (2015). Selective enhancement of endothelial BMPR-II with BMP9 reverses pulmonary arterial hypertension. *Nat Med* 21, 777–785. doi: 10.1038/nm.3877
- Mitrofan, C.-G., Appleby, S. L., Nash, G. B., Mallat, Z., Chilvers, E. R., Upton, P. D., et al. (2017). Bone morphogenetic protein 9 (BMP9) and BMP10 enhance tumor necrosis factor- α -induced monocyte recruitment to the vascular endothelium mainly via activin receptor-like kinase 2. *J Biol Chem* 292, 13714–13726. doi: 10.1074/jbc.M117.778506
- Morrell, N. W., Bloch, D. B., Dijke, P. ten, Goumans, M.-J. T. H., Hata, A., Smith, J., et al. (2016). Targeting BMP signalling in cardiovascular disease and anaemia. *Nat Rev Cardiol* 13, 106–120. doi: 10.1038/nrcardio.2015.156
- Ogo, T., Chowdhury, H. M., Yang, J., Long, L., Li, X., Torres Cleuren, Y. N., et al. (2013). Inhibition of overactive transforming growth factor- β signaling by prostacyclin analogs in pulmonary arterial hypertension. *Am J Respir Cell Mol Biol* 48, 733–741. doi: 10.1165/rcmb.2012-0049OC
- Pickworth, J., Rothman, A., Iremonger, J., Casbolt, H., Hopkinson, K., Hickey, P. M., et al. (2017). Differential IL-1 signaling induced by BMPR2 deficiency drives pulmonary vascular remodeling. *Pulm Circ* 7, 768–776. doi: 10.1177/2045893217729096
- Rabinovitch, M. (2012). Molecular pathogenesis of pulmonary arterial hypertension. *J Clin Invest* 122, 4306–4313. doi: 10.1172/JCI60658
- Ranchoux, B., Antigny, F., Rucker-Martin, C., Hautefort, A., Péchoux, C., Bogaard, H. J., et al. (2015). Endothelial-to-mesenchymal transition in pulmonary hypertension. *Circulation* 131, 1006–1018. doi: 10.1161/CIRCULATIONAHA.114.008750
- Ricard, N., Ciais, D., Levet, S., Subileau, M., Mallet, C., Zimmers, T. A., et al. (2012). BMP9 and BMP10 are critical for postnatal retinal vascular remodeling. *Blood* 119, 6162–6171. doi: 10.1182/blood-2012-01-407593
- Rider, C. C., and Mulloy, B. (2010). Bone morphogenetic protein and growth differentiation factor cytokine families and their protein antagonists. *Biochem J* 429, 1–12. doi: 10.1042/BJ20100305
- Saito, A. (2013). EMT and EndMT: Regulated in similar ways? *J Biochem* 153, 493–495. doi: 10.1093/jb/mvt032
- Sakao, S., Taraseviciene-Stewart, L., Cool, C. D., Tada, Y., Kasahara, Y., Kurosu, K., et al. (2007). VEGF-R blockade causes endothelial cell apoptosis, expansion of surviving CD34+ precursor cells and transdifferentiation to smooth muscle-like and neuronal-like cells. *FASEB J* 21, 3640–3652. doi: 10.1096/fj.07-8432com
- Sánchez-Duffhues, G., García de Vinuesa, A., and Dijke, P. ten (2017). Endothelial to mesenchymal transition in cardiovascular diseases: Developmental signalling pathways gone awry. *Dev Dyn*. doi: 10.1002/dvdy.24589
- Sánchez-Duffhues, G., García de Vinuesa, A., van de Pol, V., Geerts, M. E., Vries, M. R. de, Janson, S. G., et al. (2019). Inflammation induces endothelial-to-mesenchymal transition and promotes vascular calcification through downregulation of BMPR2. *J Pathol* 247, 333–346. doi: 10.1002/path.5193

- Selimovic, N., Bergh, C.-H., Andersson, B., Sakiniene, E., Carlsten, H., and Rundqvist, B. (2009). Growth factors and interleukin-6 across the lung circulation in pulmonary hypertension. *Eur Respir J* 34, 662–668. doi: 10.1183/09031936.00174908
- Simonneau, G., Montani, D., Celermajer, D. S., Denton, C. P., Gatzoulis, M. A., Krowka, M., et al. (2019). Haemodynamic definitions and updated clinical classification of pulmonary hypertension. *Eur Respir J* 53. doi: 10.1183/13993003.01913-2018
- Stenmark, K. R., Frid, M., and Perros, F. (2016). Endothelial-to-mesenchymal transition: An evolving paradigm and a promising therapeutic target in PAH. *Circulation* 133, 1734–1737. doi: 10.1161/CIRCULATIONAHA.116.022479
- Subramanian, A., Tamayo, P., Mootha, V. K., Mukherjee, S., Ebert, B. L., Gillette, M. A., et al. (2005). Gene set enrichment analysis: a knowledge-based approach for interpreting genome-wide expression profiles. *Proc Natl Acad Sci U S A* 102, 15545–15550. doi: 10.1073/pnas.0506580102
- Suzuki, T., Carrier, E. J., Talati, M. H., Rathinasabapathy, A., Chen, X., Nishimura, R., et al. (2018). Isolation and characterization of endothelial-to-mesenchymal transition cells in pulmonary arterial hypertension. *Am J Physiol Lung Cell Mol Physiol* 314, L118-L126. doi: 10.1152/ajplung.00296.2017
- Szklarczyk, D., Franceschini, A., Wyder, S., Forslund, K., Heller, D., Huerta-Cepas, J., et al. (2015). STRING v10: Protein-protein interaction networks, integrated over the tree of life. *Nucleic Acids Res* 43, D447-52. doi: 10.1093/nar/gku1003
- Szulcek, R., Bogaard, H. J., and van Nieuw Amerongen, G. P. (2014). Electric cell-substrate impedance sensing for the quantification of endothelial proliferation, barrier function, and motility. *J Vis Exp*. doi: 10.3791/51300
- Szulcek, R., Happe, C. M., Rol, N., Fontijn, R. D., Dickhoff, C., Hartemink, K. J., et al. (2016). Delayed microvascular shear adaptation in pulmonary arterial hypertension. Role of platelet endothelial cell adhesion molecule-1 cleavage. *Am J Respir Crit Care Med* 193, 1410–1420. doi: 10.1164/rccm.201506-1231OC
- Tamura, Y., Phan, C., Tu, L., Le Hiress, M., Thuillet, R., Jutant, E.-M., et al. (2018). Ectopic upregulation of membrane-bound IL6R drives vascular remodeling in pulmonary arterial hypertension. *J Clin Invest* 128, 1956–1970. doi: 10.1172/JCI96462
- Tu, L., Desroches-Castan, A., Mallet, C., Guyon, L., Cumont, A., Phan, C., et al. (2019). Selective BMP-9 inhibition partially protects against experimental pulmonary hypertension. *Circ Res* 124, 846–855. doi: 10.1161/CIRCRESAHA.118.313356
- Urist, M. R. (1965). Bone: Formation by autoinduction. *Science (New York, N.Y.)* 150, 893–899. doi: 10.1126/science.150.3698.893
- Wang, G., Fan, R., Ji, R., Zou, W., Penny, D. J., Varghese, N. P., et al. (2016). Novel homozygous BMP9 nonsense mutation causes pulmonary arterial hypertension: A case report. *BMC Pulm Med* 16, 17. doi: 10.1186/s12890-016-0183-7

9

Chapter 9

Nintedanib improves cardiac fibrosis but leaves pulmonary vascular remodeling unaltered in experimental pulmonary hypertension

Rol N, de Raaf MA, Sun XQ, Kuiper VP, da Silva Goncalves Bos D, Happé CM, Kurakula K, Dickhoff C, Thuillet R, Tu L, Guignabert C, Schlij I, Lodder K, Pan X, Herrmann FE, van Nieuw Amerongen GP, Koolwijk P, Vonk-Noordegraaf A, de Man FS, Wollin L, Goumans MJ, Szulcek R, Bogaard HJ.

Abstract

Aims

Pulmonary arterial hypertension (PAH) is associated with increased levels of circulating growth factors and corresponding receptors, such as PDGF, FGF and VEGF. Nintedanib, a tyrosine kinase inhibitor targeting primarily these receptors, is approved for the treatment of patients with idiopathic pulmonary fibrosis. Our objective was to examine the effect of nintedanib on proliferation of human pulmonary microvascular endothelial cells (MVEC) and assess its effects in rats with advanced experimental pulmonary hypertension (PH).

Methods and results

Proliferation was assessed in control and PAH MVEC exposed to nintedanib. PH was induced in rats by subcutaneous injection of Sugen (SU5416) and subsequent exposure to 10% hypoxia for 4 weeks (SuHx model). Four weeks after re-exposure to normoxia, nintedanib was administered once daily for three weeks. Effects of the treatment were assessed with echocardiography, right heart catheterization and histological analysis of the heart and lungs. Changes in extracellular matrix production was assessed in human cardiac fibroblasts stimulated with nintedanib.

Decreased proliferation with nintedanib was observed in control MVEC, but not in PAH patient derived MVEC. Nintedanib treatment did not affect right ventricular systolic pressure or total pulmonary resistance index in SuHx rats and had no effects on pulmonary vascular remodeling. However, despite unaltered pressure overload, the right ventricle showed less dilatation and decreased fibrosis, hypertrophy and collagen type III with nintedanib treatment. This could be explained by less fibronectin production by cardiac fibroblasts exposed to nintedanib.

Conclusions

Nintedanib inhibits proliferation of pulmonary MVECs from controls, but not from PAH patients. While in rats with experimental PH nintedanib has no effects on the pulmonary vascular pathology, it has favorable effects on right ventricular remodeling.

Introduction

Pulmonary Arterial Hypertension (PAH) is a devastating condition of increased pulmonary vascular resistance attributed to vasoconstriction and vascular remodeling, such as intimal thickening, medial hyperplasia, and muscularization of the small pulmonary arteries. Right ventricular (RV) hypertrophy, fibrosis and dilatation lead to heart failure and death in PAH patients. Dysregulated signaling by growth factors including platelet derived growth factor (PDGF), fibroblast growth factor (FGF), vascular endothelial growth factor (VEGF), and transforming growth factor- β (TGF- β) contribute to remodeling in PAH in both the pulmonary vasculature and the heart.¹⁻⁵ Until now, treatment success of vasodilating therapy is limited as it does not reverse the vascular alterations. Interest has shifted to therapies targeting growth factor receptors to mitigate or even reverse vascular remodeling.⁶⁻⁸

Circulating PDGF and its receptors are upregulated in endothelial cells (EC) and smooth muscle cells in PAH patients and contribute to right ventricular fibrosis.^{5, 9, 10} Although imatinib, primarily a PDGF receptor antagonist, had positive results in animal models, clinical studies showed mixed results with some hemodynamic improvement, unchanged exercise capacity and serious side-effects.^{11, 12} Perhaps one explanation for persistent pulmonary vascular remodeling after imatinib treatment is ongoing deregulated signaling through the VEGF and FGF receptors.¹³ Production of basal FGF by EC is increased in idiopathic PAH (iPAH) patients and also serum levels are elevated.¹⁴⁻¹⁶ Likewise, VEGF, together with its receptor, is abundantly expressed in ECs of plexiform lesions and circulating VEGF is also increased in PAH.^{10, 17-19} On the other hand, inhibition of the VEGF receptor (combined with hypoxia, as in the SuHx model) can also be used to induce pulmonary hypertension (PH) in animal models and reflects intimal remodeling as observed in human disease. The paradoxical effects of blocking the VEGF receptor as a potential treatment and a possible inducer in PAH is still an enigma.¹⁷

Nintedanib is a tyrosine kinase inhibitor (TKI) that has been approved for the treatment of idiopathic pulmonary fibrosis (IPF). Nintedanib targets primarily PDGF-, FGF- and VEGF-mediated proliferation in pulmonary fibroblasts, and possibly TGF- β -mediated transformation to myofibroblasts.²⁰⁻²² Experimentally and clinically nintedanib has been proven to attenuate lung fibrosis, while reports of development of PH are lacking.^{23, 24} The anti-proliferative properties of nintedanib have a potential beneficial effect on pulmonary vascular remodeling by reversing the associated PH in patients with IPF. Nintedanib might even have the potential of being a new treatment option for group 1 PH. In contrast, given the fact that TKIs with inhibiting properties on the VEGF receptor are associated with the development of clinical (dasatinib) and experimental (SU5416) PH,^{6, 25} it could also be postulated that nintedanib triggers the development of PAH or worsens IPF associated PH.

We hypothesized that the inhibitive properties of nintedanib on proliferation could have favorable effects on PH by reducing vascular remodeling. Therefore we studied the functional effect of nintedanib in primary pulmonary microvascular endothelial cells (MVEC) and in the SuHx rat model in an advanced stage of PH.

Material and methods

Reagents

The ethanesulfonate of nintedanib (Methyl (3Z)-3-[[[4-(methyl(4-methylpiperazin-1-yl)acetyl]amino)phenyl]amino](phenyl)methylidene}-2-oxo-2,3-dihydro-1H-indole-6-carboxylate) (Boehringer Ingelheim Pharma, Biberach, Germany) was dissolved in deionized water. For use in animal models, nintedanib was administered at a dose of 41.5 mg/kg (50.0 mg/kg with ethanesulfonate) once daily by oral gavage for 21 days, at a safe dose level based on the available results of 28-day or 90-day repeated dose toxicity studies (according ICH guidelines).

Cell culture

Cell isolation and culture were performed as previously described.²⁶ In brief, control pulmonary MVEC were isolated from patients that underwent lobectomy for suspected or proven lung malignancy. PAH MVEC were isolated from lung tissue obtained during lung transplantation. Patient characteristics are reported in table 1. The study was reviewed by the Institutional Review Board (IRB) of the VU University Medical Center (Amsterdam, the Netherlands) and decided that consent was not necessary because of use of rest material. The study was performed conform the declaration of Helsinki regarding ethical principles for medical research involving human subjects. All experiments were performed following unbiased approach and according recommendations recently proposed by Provencher *et al.*²⁷ Endothelial cell isolation and culture of the smallest pulmonary vessels was performed as previously described. Purity of cell isolations was confirmed by immunofluorescent staining.^{26, 28} The cells of five controls and four PAH patients were stimulated with VEGF₁₆₅ (25 ng/ml, ReliaTech GmbH, Wolfenbuttel, Germany) for 20 minutes to induce phosphorylation of Erk1/2 (pErk1/2) and lysed for Western blot analysis.

Human cardiac fibroblasts were cultured in DMEM with 10% FCS. When confluent, medium was changed to DMEM with 1% FCS and supplemented with 1 μ M Nintedanib for 24 hours.

Table 1 – Patient characteristics

| Donor | mPAP (mmHg) | Etiology | Gender | Age (yr) |
|-------|-------------|----------|--------|----------|
| 1 | 43 | iPAH | F | 42 |
| 2 | 89 | iPAH | F | 22 |
| 3 | 85 | iPAH | M | 21 |
| 4 | 94 | iPAH | F | 30 |

iPAH = idiopathic pulmonary arterial hypertension; mPAP = mean pulmonary artery pressure.

Proliferation

The effect of nintedanib on the proliferation rate of MVEC was measured by 5-ethynyl-2'-deoxyuridine (EdU) thymidine analogue incorporation (Click-It EdU Alexa Fluor 488 Imaging Kit, C10337, Invitrogen, Carlsbad, CA, USA). Cells were seeded at a density of 7×10^3 cells/cm² and attached overnight. MVEC were pre-incubated with nintedanib (0.3 μ M) in presence of 1% human serum albumin for two hours and stimulated with VEGF₁₆₅ (25 ng/ml, ReliaTech GmbH, Wolfenbuttel, Germany) and EdU nucleotides were added. After 24 hours cells were fixed and protocol was performed according to the manufacturer's instructions. Per condition 5 pictures were taken at a magnification of 20x by an Axiovert 200 Marianas inverted wide-field fluorescence microscope (Carl Zeiss Microscopy, Jena, Germany) and the number of proliferating nuclei was counted.

Extracellular matrix production

To study the influence of nintedanib on matrix production in the heart, human cardiac fibroblasts derived from two patients were treated with nintedanib (1 μ M) for 24 hours in DMEM with 1% FCS were lysed in RIPA supplemented with protease inhibitors. Fibronectin, as a measure of fibrosis, was determined by Western blot twice. Membranes were incubated with α -Fibronectin antibody (Sigma F7387) and α -Vinculin as loading control (Sigma V9131).

Animal model

This study was approved by the local Animal Welfare committee (VU-Fys 13-14) and performed conform the guidelines from directive 2010/63/EU of the European Parliament on the protection of animals used for scientific purposes. Progressive pressure-overload in conjunction with angioproliferative pulmonary vascular remodeling was induced by the combined exposure to SU5416 and hypoxia, as previously characterized by our group.²⁹ Sample sizes were based on our experience with pharmacological studies in SuHx rats and were chosen to provide sufficient numbers of animals for the different hemodynamic, histological and molecular studies. Twentyone male Sprague-Dawley rats weighing 200 g received a single subcutaneous injection of SU5416 (25 mg/kg, Tocris) and were exposed to a simulated altitude of 5000 meters in a nitrogen dilution chamber for 4 weeks; thereafter the animals were

kept at the sea level for another 7 weeks. Rats were randomly assigned to nintedanib or vehicle treatment. Twelve animals were treated with nintedanib for 3 weeks, starting in week 8, at an advanced stage of PH in the SuHx model. Dose calculation was adjusted to the individual body weights twice weekly and administered by oral gavage (50mg/kg). Nine animals received vehicle as a control group to nintedanib treatment. Clinical signs and body weights were measured daily. Experimental protocol is depicted in figure 2 A.

Echocardiography and hemodynamics

On the day of necropsy, animals were anesthetized (isoflurane; 4.0/2.5% induction/maintenance; 1:1 O₂/air mix) followed by an injection of buprenorphine analgesia (0.1mg/kg). After intubation, echocardiography was performed using a ProSound system (Prosound SSD-4000) equipped with a 13-Mhz linear transducer (UST-5542, Aloka, Tokyo, Japan), as described previously.²⁹ Hemodynamic measurements were performed with a 4.5-mm Millar conductance catheter in opened chest, which was inserted in the right ventricular outflow tract to acquire the right ventricular systolic pressure (RVSP), used for total pulmonary resistance index calculations (TPRI). Pressure-volume loop analyses were performed as described previously. Animals were killed via exsanguination and organs were weighed and processed for analysis. End experiments were performed unblinded, following experiments were performed blinded to treatment group.

Histology and immunofluorescent staining

Tissues were fixed in formalin, embedded in paraffin and 4 µm thick sections were prepared for histology and immunofluorescent staining. Lung tissue was stained with Elastica van Gieson and scanned (3DHISTECH, Budapest, Hungary). Averaged media and intima wall thickness were measured as described previously.^{29,30}

Total collagen content of the right ventricle (RV) was assessed by picrosirius red staining. Distinction between collagen type I (Southern Biotech, 1310-01, 1:100) and type III (Southern Biotech1330-01, 1:100) was made with immunofluorescent staining. Therefore, slides were fixed in acetone at 4°C, permeabilized with 0.2% Triton, and blocked with 1% BSA. Slides were incubated overnight with primary antibodies for collagen type I and III with co-staining for PECAM-1 (Santa Cruz, sc-1506-R). Alexa Fluor conjugated secondary species-specific secondary antibodies (dilution 1:250) were added and slides were covered with Prolong Gold Antifade Reagent with DAPI (Thermo Fisher Scientific, P36931). Three pictures of the right ventricle were taken with an Axiovert 200 Marianas inverted wide-field fluorescence microscope (Carl Zeiss Microscopy) at 10X magnification. Area of collagen was measured around transversally cut cardiomyocytes, excluding regions around vessels, using ImageJ.

Western blot

For Western blot analysis MVEC and RV lysates were processed as described by Szulcek, *et al.*²⁶ Membranes were blocked in 5% BSA (Sigma-Aldrich) in Tris-buffered saline (pH=7.6) with 0.1% tween for 1 hour at room temperature, membranes were incubated overnight at 4°C with primary antibodies: phosphor-p44/42 MAPK (Cell Signaling, 9106S, 1:1000), p44/42 MAPK (Cell Signaling, 9102S, 1:1000) and β-actin (Sigma-Aldrich, A3854, 1:50 000). After 1 hour incubation with horseradish peroxidase (HRP) conjugated species-specific secondary antibodies (Dako, 1:1000 for cell lysates, 1:5000 for RV lysates) blots were visualized with chemiluminescence with the LAS-3000 (Fujifilm, Tokyo, Japan). Phosphorylated protein was normalized to total protein and β-actin was used as loading control.

RT-PCR

RNA was isolated from rat RV tissue (1 µg of total RNA). cDNA generation was performed using iScript cDNA synthesis kit (Bio-Rad, #170-8891). For PCR reactions FAST SYBR Green Master Mix (Thermo Fisher Scientific, 4385612). With a cDNA pool of all samples best annealing temperatures and standard curve were optimized for the following primers: collagen I, collagen III, connective tissue growth factor (CTGF), osteopontin-1, and brain natriuretic peptide (BNP) (sequences shown in table 2).

Table 2 – Primer sequences

| | | |
|--|---------|--------------------------------|
| Connective tissue growth factor (CTGF) | Forward | 5'-CTGTTCCAAGACCTGTGGGAT-3' |
| | Reverse | 5'-TTTGGCCCTTCTTAATGTTCT-3' |
| Collagen I | Forward | 5'- GAACGGAGATGATGGGGAAG-3' |
| | Reverse | 5'- CCAAACCACTGAAACCTCTG-3' |
| Collagen III | Forward | 5'- AGTGCCATAATGGGGAACG-3' |
| | Reverse | 5'- ATGAATTGGGATGCAACTAC -3' |
| BNP | Forward | 5'- GCTGCTTTGGGCAGAAGATAGA -3' |
| | Reverse | 5'- GCCAGGAGGTCTTCTAAAACA -3' |
| Osteopontin-1 | Forward | 5'- CCCATCTCAGAAGCAGAATCTT -3' |
| | Reverse | 5'- GTCATGGCTTTCATTGGAGTTG -3' |
| 18S | Forward | 5'-GCAATAACAGGTCTGTGATGCC-3' |
| | Reverse | 5'-CACGAATGGGGTTCAACG-3' |

Statistics

Statistical analysis was performed using Graphpad Prism 6.0. Differences between two groups was assessed with paired (*in vitro*) and unpaired (*in vivo*) t-tests (parametric) or Mann-Whitney tests (nonparametric). Multiple comparisons were tested by one-way ANOVA, followed by the suitable post-hoc tests for between-group differences. All data are reported as mean ± SEM. No retrieved data points were excluded from statistical analysis. RT-PCR data are shown as Log 2 fold change, statistical analysis was performed on Log 2 fold change.

Results

Nintedanib inhibits VEGF induced proliferation of pulmonary MVEC

To assess the minimal effective dose of nintedanib, we examined the inhibitory effects of different concentrations of nintedanib on the phosphorylation of Erk1/2 upon VEGF stimulation, a downstream target involved in VEGF driven proliferation of endothelial cells.³¹ Nintedanib inhibited VEGF-induced pErk1/2 in control MVECs in a concentration-dependent manner ($p = 0.005$) (figure 1 A-B). At 0.3 μM , a concentration not resulting in morphological changes,²⁰ pErk1/2 levels were similar to non-stimulated conditions ($p = 0.02$). This concentration was used for all subsequent experiments. VEGF-induced proliferation of control MVECs, assessed by EdU incorporation, was reduced by nintedanib ($p = 0.02$) (figure 1 C). While nintedanib inhibited VEGF stimulated ERK1/2 phosphorylation in PAH MVEC, it had no significant effect on the proliferation of PAH patients derived MVEC ($p = 0.15$) (figure 1 A-C).

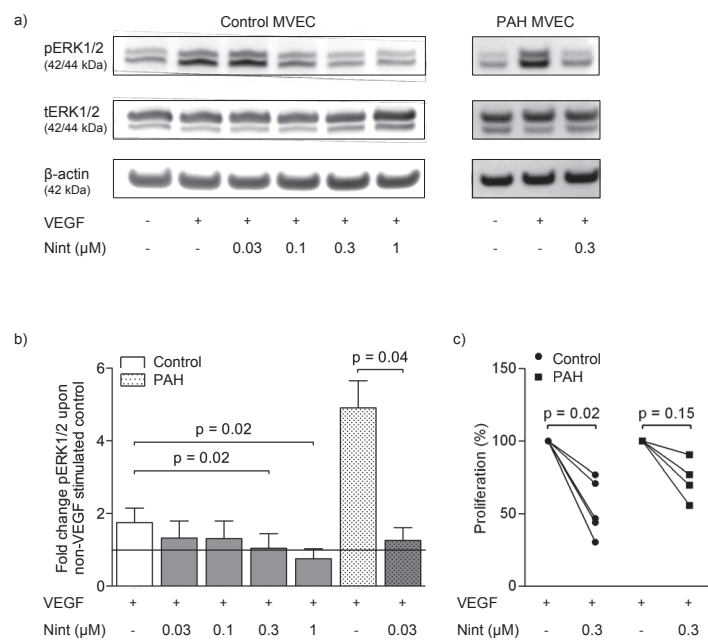


Figure 1 – Nintedanib attenuates VEGF induced proliferation of microvascular endothelial cells. Human primary microvascular endothelial cells (MVEC) were incubated with nintedanib at the concentrations indicated and stimulated with vascular endothelial growth factor (VEGF). Phosphorylated Erk1/2 (pErk1/2), total ERK1/2 (tErk1/2), and b-actin were quantified by western blot. A representative blot is shown in (A). The densitometric quantification of the ratio pErk1/2/tErk1/2 (control $n=5$, PAH $n=4$) depicted as fold increase upon non-stimulated MVEC is depicted in (B). One-way ANOVA was used to determine statistical significance. Data shown as mean \pm SEM. MVEC proliferation after VEGF stimulation in combination with pretreatment with or without 0.3 mM nintedanib was assessed with EdU staining (control $n=5$, PAH $n=4$), ratio paired t-test was performed (C).

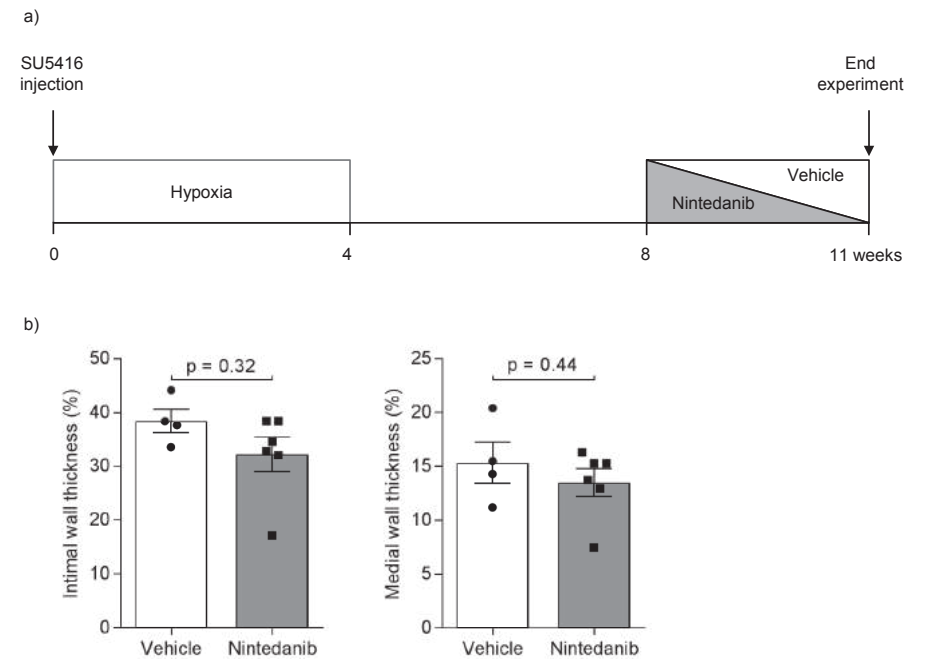


Figure 2 – Nintedanib did not reduce pulmonary vascular remodelling in experimental PH. Pulmonary hypertension was induced in rats (vehicle $n=4$, nintedanib $n=6$) by SU5416 injection in combination with 4 weeks hypoxia (10% O_2). At week eight, when advanced pulmonary lesions are formed, rats were treated with vehicle or nintedanib (50 mg/kg) for 3 weeks (A). Intimal and medial wall thickness of the pulmonary vasculature was not changed. A total of 19–50 vessels per rat were measured. Data shown as mean \pm SEM (B). Data shown as mean \pm SEM (B-E).

Nintedanib does not affect pulmonary vascular remodeling

To assess *in vivo* effects, we treated SuHx rats for three weeks with nintedanib starting in week 8. RV end diastolic diameter (RVEDD) was decreased after nintedanib treatment ($p = 0.002$), with a trend towards less RV stiffness (Eed, $p = 0.07$) and an increased pulmonary artery acceleration time corrected for cycle length (PAAT/cl, $p = 0.07$) (table 3). However, right ventricular end systolic pressure, total pulmonary resistance index, stroke volume index and tricuspid annular plan systolic excursion (TAPSE) were not different between vehicle and nintedanib treated rats (Table 3). Heart weight and Fulton index (RV/(LV \pm S)) were not different between vehicle and nintedanib treated animals (table 3). Hematocrit was decreased in nintedanib treated animals ($p = 0.03$). Our histological analysis in the lung, intimal and medial wall thickness was not different between vehicle and nintedanib treated animals (figure 2 B).

Nintedanib improves RV adaptation in SuHx rats

Cardiac fibrosis, detected by increasing RV diastolic stiffness, is suggested to contribute to right ventricular failure in PAH patients.^{32,33} Because the antifibrotic effect of nintedanib on the heart is still unknown, we assessed whether nintedanib treatment would result in less RV fibrosis. In the animal model total collagen was measured with picrosirius red staining. We observed a decrease of total collagen in the RV of nintedanib treated rats (figure 3 B). To assess collagen deposition, we quantified collagen I and III in the RV by RT-PCR and immunofluorescent staining. Collagen I was significantly lowered at mRNA level. Less collagen III was observed with immunofluorescent staining, without affecting the collagen I/III ratio (figure 3 A, C, D). To explore the TGF- β mediated anti-fibrotic properties of nintedanib on the RV of pulmonary hypertensive rats, we quantified connective tissue growth factor mRNA levels in the RV-tissue. Connective tissue growth factor was not inhibited by nintedanib treatment (figure 3 A).

Cardiomyocyte hypertrophy, another contributor to RV diastolic stiffness, was also decreased in the nintedanib group, compared to vehicle ($p = 0.009$) (Figure 3 E). Osteopontin-1 and BNP, prognostic markers in heart failure, were decreased after treatment with nintedanib ($p = 0.008$ and $p = 0.07$, respectively) (Figure 3 A).

Cardiac fibroblasts treated with nintedanib showed reduced fibronectin production ($p = 0.002$), indicating a role for nintedanib in decreased fibrosis in the heart (Figure 4).

Discussion

We have shown in our study that nintedanib inhibits proliferation of primary pulmonary microvascular endothelial cells from normal subjects, but not from PAH patients. In rats with experimentally induced PH, nintedanib treatment did not result in a reversal of pulmonary vascular remodeling, but did improve RV adaptation. Nintedanib improved RV contractility, decreased RV dilatation and reduced RV hypertrophy and collagen content.

A recent publication showed that inhibition of pErk1/2 by nintedanib regulated proliferation of macrovascular endothelial cells of the lung indicating therapeutic potential for the treatment of PAH.³⁴ In line with this study, we demonstrated the inhibitory effects of nintedanib on pErk1/2 and proliferation rate in control MVEC. Nintedanib showed a heterogeneous effect in the PAH donor group and could thereby not significantly reduce proliferation in patient endothelial cells. This could explain the lack of effect on pulmonary vascular remodeling observed in our *in vivo* experiment. While acute vasodilating effects of TKIs have been reported, we did not observe reductions in pulmonary or systemic pressures.^{35,36}

Paradoxically, TKI drugs that interfere with growth factor receptor signaling can also trigger endothelial proliferation and the development of pulmonary vascular remodeling and PAH.⁶ A series of case reports described PAH induced by dasatinib^{6,8} and it was suggested that Src kinase inhibition played a causative role⁶.

Table 3 – Characteristics of vehicle and nintedanib treated SuHx rats. Overview of body weight, catheterization, echocardiographic, and ex-vivo measurements comparing SuHx rats after 3 weeks of treatment with vehicle or nintedanib. For parametric data unpaired t-test was used, for non-parametric data Mann-Whitney U test was performed. Data shown as mean \pm SEM. (vehicle $n = 9$, nintedanib $n = 12$) Data shown as mean \pm SEM (B-E). Vehicle $n = 9$, nintedanib $n = 12$ (A-E).

| | SuHx + vehicle ($n = 12$) | SuHx + Nintedanib ($n = 9$) | p-value |
|------------------------------------|--------------------------------|----------------------------------|---------|
| Terminal body weight (g) | 466 \pm 20.2 | 423 \pm 16.5 | 0.12 |
| RVSP (mmHg) | 61.6 \pm 7.4 | 66.8 \pm 4.6 | 0.39 |
| dP/dt max (mmHg/s) | 2600 \pm 336 | 2970 \pm 294 | 0.42 |
| SVI (mL/cm ²) | 0.44 \pm 0.05 | 0.52 \pm 0.05 | 0.28 |
| TPRI (mmHg/mL/min/m ²) | 0.94 \pm 0.24 | 0.73 \pm 0.07 | 0.59 |
| Eed | 15.7 \pm 3.4 | 8.3 \pm 1.3 | 0.07 |
| TAPSE (mm) | 1.9 \pm 0.1 | 2.0 \pm 0.1 | 0.78 |
| RVEDD (mm) | 7.2 \pm 0.2 | 6.4 \pm 0.1 | 0.002 |
| PAAT/cl (%) | 7.4 \pm 0.6 | 8.5 \pm 0.3 | 0.07 |
| Hematocrit (%) | 44.3 \pm 0.8 | 40.0 \pm 1.5 | 0.03 |
| Heart weight (g) | 2.3 \pm 0.1 | 2.2 \pm 0.1 | 0.53 |
| Fulton index (RV/(LV+S)) | 0.60 \pm 0.05 | 0.66 \pm 0.04 | 0.36 |

Abbreviations: dP/dt, delta pressure/delta time; Eed, end-diastolic elastance; LV, left ventricle; PAAT/cl, pulmonary artery acceleration time divided by the cycle length; RV, right ventricle; RVEDD, right ventricular end diastolic diameter; RVSP, right ventricular systolic pressure; RVWT, right ventricular wall thickness; S, septum; SVI, stroke volume index; TPRI, total pulmonary resistance index; TAPSE, tricuspid annular plane systolic excursion;

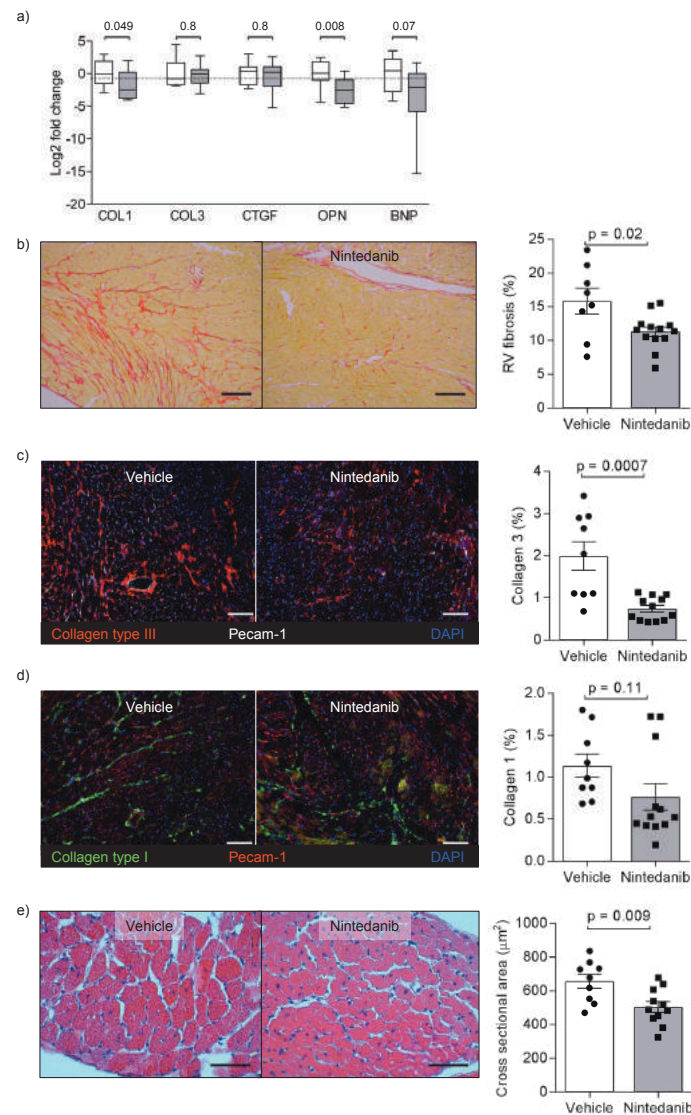


Figure 3 – Nintedanib inhibits cardiac fibrosis, osteopontin-1 and hypertrophy in experimental PH. In the right ventricle nintedanib (vehicle $n = 9$ white bars, nintedanib $n = 12$ grey bars) treatment showed a significant four fold decrease in collagen type I and osteopontin-1 transcriptional levels. Data shown as mean values, bars represent min to max. (A) Nintedanib treated rats showed a significant ($p = 0.02$) decrease in picosirius red staining in the right ventricle. Scale bar indicates $150 \mu\text{m}$ (B). Immunofluorescent staining for collagen type III proved a significant decrease ($p < 0.001$) in the nintedanib group. Scale bar indicates $100 \mu\text{m}$ (C). Collagen level type I was unchanged (three pictures of the RV per animal). Scale bar indicates $100 \mu\text{m}$ (D). Less hypertrophy of the right ventricle was observed ($p = 0.009$). Scale bar indicates $150 \mu\text{m}$ (E). For parametric data unpaired t-test was used, for non-parametric data Mann-Whitney U test was performed. Data shown as mean \pm SEM (B-E). Vehicle $n = 9$, nintedanib $n = 12$ (A-E).

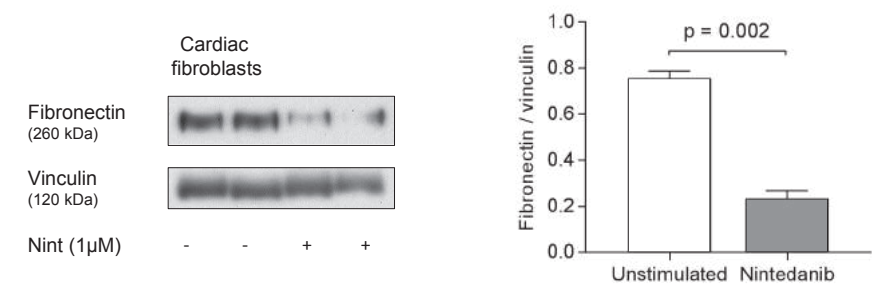


Figure 4 – Effect of nintedanib on fibronectin in cardiac fibroblasts. Two human cardiac fibroblast cell lines were treated with nintedanib ($1 \mu\text{M}$, 24 hours) and the effect of this compound on fibronectin production was determined. Representative Western blot of two experiments is shown. Vinculin was used as a loading control for quantification by Western Blot. Densitometric quantification of the blots showed that fibronectin, a measure of fibrosis, was significantly reduced by nintedanib ($p = 0.002$). Paired t-test was performed ($n = 4$). Data shown as mean \pm SEM.

Experimentally, the TKI Sugen causes endothelial apoptosis, an effect which has been explained by inhibition of the VEGF receptor and observations that the healthy lung endothelium is dependent on the presence of VEGF for its survival.³⁷ Upon exposure to a second hit, such as hypoxia³⁸ or a high shear stress^{39, 40}, the initial phase of apoptosis is followed by uncontrolled endothelial proliferation. In the rat model, Sugen is administered only once at the beginning of the protocol, and at the time of progressive lung vascular remodeling Sugen is no longer present. Therefore, lung vascular remodeling in the later stages of the Sugen hypoxia model, which closely resembles remodeling in human PAH, could be partly dependent on intact VEGF-R signaling, thus providing the rationale for our study. The fact that Nintedanib did not reverse remodeling, suggests that intimal proliferation in the remodeled Sugen hypoxia lung has to a certain degree become independent from growth factor receptor signaling. The same seems to be true for microvascular endothelial cells from PAH patients.

Despite suggestions that TKIs may provide a beneficial therapy in PAH, there is also concern that these drugs may have cardiotoxic effects. Previously, we reported no negative effects on capillary density and right ventricular pressure adaptation in rats after pulmonary artery banding treated with BIBF1000, a close structural analogue to nintedanib. Even though decreased VEGF signaling is linked to capillary rarefaction in the heart and thereby to RV heart failure⁴¹, we found no loss in capillaries but decreased dilatation, fibrosis and hypertrophy in the right ventricle of nintedanib treated rats. Other parameters potentially indicating worsening of right ventricular dysfunction, such as decreased TAPSE or cardiac index, were unchanged.⁴² Our data suggest that nintedanib prevented RV fibrosis by direct inhibition of cardiac fibroblast activation, leading to a decreased production of fibronectin.

In conclusion we found beneficial effects of nintedanib on control pulmonary endothelium in vitro and favorable effects on the right ventricle in rats with PH. A clinical trial might confirm that nintedanib may safely be administered to IPF patients with associated PH and might confirm or refute the absence of changes in pulmonary vascular remodeling by nintedanib in our rat model of PH.

Funding

This work was financially supported by Boehringer Ingelheim. We acknowledge the support from the Netherlands CardioVascular Research Initiative; the Dutch Heart Foundation, Dutch Federation of University Medical Centres, the Netherlands Organisation for Health Research and Development and the Royal Netherlands Academy of Sciences. Grant number: 2012-08

Acknowledgments

We would like to acknowledge M. H. van Wijhe (VU University Medical Center) for his input to this study and M.A. Paul (VU University Medical Center) and K.J. Hartemink (Antoni van Leeuwenhoek Hospital) for their contribution to tissue collection.

Conflict of interest

None declared

References

- Hassoun PM, Mouthon L, Barbera JA, Eddahibi S, Flores SC, Grimminger F, Jones PL, Maitland ML, Michelakis ED, Morrell NW, Newman JH, Rabinovitch M, Schermuly R, Stenmark KR, Voelkel NF, Yuan JX, Humbert M. Inflammation, growth factors, and pulmonary vascular remodeling. *J Am Coll Cardiol* 2009;54:S10-S19.
- Voelkel NF, Gomez-Arroyo J, Abbate A, Bogaard HJ, Nicolls MR. Pathobiology of pulmonary arterial hypertension and right ventricular failure. *Eur Respir J* 2012;40:1555-1565.
- Godinas L, Guignabert C, Seferian A, Perros F, Bergot E, Sibille Y, Humbert M, Montani D. Tyrosine kinase inhibitors in pulmonary arterial hypertension: a double-edge sword? *Semin Respir Crit Care Med* 2013;34:714-724.
- Guignabert C, Tu L, Girerd B, Ricard N, Huertas A, Montani D, Humbert M. New molecular targets of pulmonary vascular remodeling in pulmonary arterial hypertension: importance of endothelial communication. *Chest* 2015;147:529-537.
- Gomez-Arroyo J, Sakagami M, Syed AA, Farkas L, Van TB, Kraskauskas D, Mizuno S, Abbate A, Bogaard HJ, Byron PR, Voelkel NF. Iloprost reverses established fibrosis in experimental right ventricular failure. *Eur Respir J* 2015;45:449-462.
- Montani D, Bergot E, Gunther S, Savale L, Bergeron A, Bourdin A, Bouvaist H, Canuet M, Pison C, Macro M, Poubeau P, Girerd B, Natali D, Guignabert C, Perros F, O'Callaghan DS, Jais X, Tubert-Bitter P, Zalcman G, Sitbon O, Simonneau G, Humbert M. Pulmonary arterial hypertension in patients treated by dasatinib. *Circulation* 2012;125:2128-2137.
- Guignabert C, Phan C, Seferian A, Huertas A, Tu L, Thuillet R, Sattler C, Le Hiress M, Tamura Y, Jutant EM, Chaumais MC, Bouchet S, Maneglier B, Molimard M, Rousselot P, Sitbon O, Simonneau G, Montani D, Humbert M. Dasatinib induces lung vascular toxicity and predisposes to pulmonary hypertension. *J Clin Invest* 2016;126:3207-3218.
- Weatherald J, Chaumais MC, Savale L, Jais X, Seferian A, Canuet M, Bouvaist H, Magro P, Bergeron A, Guignabert C, Sitbon O, Simonneau G, Humbert M, Montani D. Long-term outcomes of dasatinib-induced pulmonary arterial hypertension: a population-based study. *Eur Respir J* 2017;50.
- Perros F, Montani D, Dorfmueller P, Durand-Gasselin I, Tcherakian C, Le PJ, Mazmanian M, Fadel E, Mussot S, Mercier O, Herve P, Emilie D, Eddahibi S, Simonneau G, Souza R, Humbert M. Platelet-derived growth factor expression and function in idiopathic pulmonary arterial hypertension. *Am J Respir Crit Care Med* 2008;178:81-88.
- Selimovic N, Bergh CH, Andersson B, Sakiniene E, Carlsten H, Rundqvist B. Growth factors and interleukin-6 across the lung circulation in pulmonary hypertension. *Eur Respir J* 2009;34:662-668.
- Schermuly RT, Dony E, Ghofrani HA, Pullamsetti S, Savai R, Roth M, Sydykov A, Lai YJ, Weissmann N, Seeger W, Grimminger F. Reversal of experimental pulmonary hypertension by PDGF inhibition. *J Clin Invest* 2005;115:2811-2821.
- Ghofrani HA, Seeger W, Grimminger F. Imatinib for the treatment of pulmonary arterial hypertension. *N Engl J Med* 2005;353:1412-1413.
- Casanovas O, Hicklin DJ, Bergers G, Hanahan D. Drug resistance by evasion of antiangiogenic targeting of VEGF signaling in late-stage pancreatic islet tumors. *Cancer Cell* 2005;8:299-309.
- Benisty JI, McLaughlin VV, Landzberg MJ, Rich JD, Newburger JW, Rich S, Folkman J. Elevated basic fibroblast growth factor levels in patients with pulmonary arterial hypertension. *Chest* 2004;126:1255-1261.
- Tu L, Dewachter L, Gore B, Fadel E, Dartevelle P, Simonneau G, Humbert M, Eddahibi S, Guignabert C. Autocrine fibroblast growth factor-2 signaling contributes to altered endothelial phenotype in pulmonary hypertension. *Am J Respir Cell Mol Biol* 2011;45:311-322.

16. Izikki M, Guignabert C, Fadel E, Humbert M, Tu L, Zadigue P, Dartevielle P, Simonneau G, Adnot S, Maitre B, Raffestin B, Eddahibi S. Endothelial-derived FGF2 contributes to the progression of pulmonary hypertension in humans and rodents. *J Clin Invest* 2009;119:512-523.
17. Voelkel NF, Gomez-Arroyo J. The role of vascular endothelial growth factor in pulmonary arterial hypertension. The angiogenesis paradox. *Am J Respir Cell Mol Biol* 2014;51:474-484.
18. Voelkel NF, Vandivier RW, Tuder RM. Vascular endothelial growth factor in the lung. *Am J Physiol Lung Cell Mol Physiol* 2006;290:L209-L221.
19. Kumpers P, Nickel N, Lukasz A, Golpon H, Westerkamp V, Olsson KM, Jonigk D, Maegel L, Bockmeyer CL, David S, Hoepfer MM. Circulating angiopoietins in idiopathic pulmonary arterial hypertension. *Eur Heart J* 2010;31:2291-2300.
20. Wollin L, Wex E, Pautsch A, Schnapp G, Hostettler KE, Stowasser S, Kolb M. Mode of action of nintedanib in the treatment of idiopathic pulmonary fibrosis. *Eur Respir J* 2015;45:1434-1445.
21. Inomata M, Nishioka Y, Azuma A. Nintedanib: evidence for its therapeutic potential in idiopathic pulmonary fibrosis. *Core Evid* 2015;10:89-98.
22. Wollin L, Maillet I, Quesniaux V, Holweg A, Ryffel B. Antifibrotic and anti-inflammatory activity of the tyrosine kinase inhibitor nintedanib in experimental models of lung fibrosis. *J Pharmacol Exp Ther* 2014;349:209-220.
23. Chaudhary NI, Roth GJ, Hilberg F, Muller-Quernheim J, Prasse A, Zissel G, Schnapp A, Park JE. Inhibition of PDGF, VEGF and FGF signalling attenuates fibrosis. *Eur Respir J* 2007;29:976-985.
24. Richeldi L, Cottin V, du Bois RM, Selman M, Kimura T, Bailes Z, Schlenker-Herzeg R, Stowasser S, Brown KK. Nintedanib in patients with idiopathic pulmonary fibrosis: Combined evidence from the TOMORROW and INPULSIS(R) trials. *Respir Med* 2016;113:74-79.
25. Nicolls MR, Mizuno S, Taraseviciene-Stewart L, Farkas L, Drake JI, Al HA, Gomez-Arroyo JG, Voelkel NF, Bogaard HJ. New models of pulmonary hypertension based on VEGF receptor blockade-induced endothelial cell apoptosis. *Pulm Circ* 2012;2:434-442.
26. Szulcsek R, Happe CM, Rol N, Fontijn RD, Dickhoff C, Hartemink KJ, Grunberg K, Tu L, Timens W, Nossent GD, Paul MA, Leyen TA, Horrevoets AJ, de Man FS, Guignabert C, Yu PB, Vonk-Noordegraaf A, van Nieuw Amerongen GP, Bogaard HJ. Delayed Microvascular Shear-adaptation in Pulmonary Arterial Hypertension: Role of PECAM-1 Cleavage. *Am J Respir Crit Care Med* 2016.
27. Provencher S, Archer SL, Ramirez FD, Hibbert B, Paulin R, Boucherat O, Lacasse Y, Bonnet S. Standards and Methodological Rigor in Pulmonary Arterial Hypertension Preclinical and Translational Research. *Circ Res* 2018;122:1021-1032.
28. van der Heijden M, van Nieuw Amerongen GP, van BJ, Paul MA, Groeneveld AB, van Hinsbergh VW. Opposing effects of the angiopoietins on the thrombin-induced permeability of human pulmonary microvascular endothelial cells. *PLoS One* 2011;6:e23448.
29. de Raaf MA, Schalij I, Gomez-Arroyo J, Rol N, Happe C, de Man FS, Vonk-Noordegraaf A, Westerhof N, Voelkel NF, Bogaard HJ. SuHx rat model: partly reversible pulmonary hypertension and progressive intima obstruction. *Eur Respir J* 2014;44:160-168.
30. Okada K, Tanaka Y, Bernstein M, Zhang W, Patterson GA, Botney MD. Pulmonary hemodynamics modify the rat pulmonary artery response to injury. A neointimal model of pulmonary hypertension. *Am J Pathol* 1997;151:1019-1025.
31. Meadows KN, Bryant P, Vincent PA, Pumiglia KM. Activated Ras induces a proangiogenic phenotype in primary endothelial cells. *Oncogene* 2004;23:192-200.
32. Bogaard HJ, Abe K, Vonk NA, Voelkel NF. The right ventricle under pressure: cellular and molecular mechanisms of right-heart failure in pulmonary hypertension. *Chest* 2009;135:794-804.
33. Rain S, Handoko ML, Trip P, Gan CT, Westerhof N, Stienen GJ, Paulus WJ, Ottenheijm CA, Marcus JT, Dorfmueller P, Guignabert C, Humbert M, Macdonald P, Dos Remedios C, Postmus PE, Saripalli C, Hidalgo CG, Granzier HL, Vonk-Noordegraaf A, van der Velden J, de Man FS. Right ventricular diastolic impairment in patients with pulmonary arterial hypertension. *Circulation* 2013;128:2016-2025, 2011-2010.
34. Awad KS, Elinoff JM, Wang S, Gairhe S, Ferreyra GA, Cai R, Sun J, Solomon MA, Danner RL. Raf/ERK drives the proliferative and invasive phenotype of BMPR2-silenced pulmonary artery endothelial cells. *Am J Physiol Lung Cell Mol Physiol* 2016;310:L187-L201.
35. Abe K, Toba M, Alzoubi A, Koubsky K, Ito M, Ota H, Gairhe S, Gerthoffer WT, Fagan KA, McMurtry IF, Oka M. Tyrosine kinase inhibitors are potent acute pulmonary vasodilators in rats. *Am J Respir Cell Mol Biol* 2011;45:804-808.
36. Pankey EA, Thammasiboon S, Lasker GF, Baber S, Lasky JA, Kadowitz PJ. Imatinib attenuates monocrotaline pulmonary hypertension and has potent vasodilator activity in pulmonary and systemic vascular beds in the rat. *Am J Physiol Heart Circ Physiol* 2013;305:H1288-H1296.
37. Lahm T, Crisostomo PR, Markel TA, Wang M, Lillemoe KD, Meldrum DR. The critical role of vascular endothelial growth factor in pulmonary vascular remodeling after lung injury. *Shock* 2007;28:4-14.
38. Taraseviciene-Stewart L, Kasahara Y, Alger L, Hirth P, Mc MG, Waltenberger J, Voelkel NF, Tuder RM. Inhibition of the VEGF receptor 2 combined with chronic hypoxia causes cell death-dependent pulmonary endothelial cell proliferation and severe pulmonary hypertension. *FASEB J* 2001;15:427-438.
39. Sakao S, Taraseviciene-Stewart L, Lee JD, Wood K, Cool CD, Voelkel NF. Initial apoptosis is followed by increased proliferation of apoptosis-resistant endothelial cells. *FASEB J* 2005;19:1178-1180.
40. Happe CM, de Raaf MA, Rol N, Schalij I, Vonk-Noordegraaf A, Westerhof N, Voelkel NF, de Man FS, Bogaard HJ. Pneumonectomy combined with SU5416 induces severe pulmonary hypertension in rats. *Am J Physiol Lung Cell Mol Physiol* 2016:ajplung.
41. Bogaard HJ, Natarajan R, Henderson SC, Long CS, Kraskauskas D, Smithson L, Ockaili R, McCord JM, Voelkel NF. Chronic pulmonary artery pressure elevation is insufficient to explain right heart failure. *Circulation* 2009;120:1951-1960.
42. Bogaard HJ, Mizuno S, Hussaini AA, Toldo S, Abbate A, Kraskauskas D, Kasper M, Natarajan R, Voelkel NF. Suppression of histone deacetylases worsens right ventricular dysfunction after pulmonary artery banding in rats. *Am J Respir Crit Care Med* 2011;183:1402-1410.

10

Chapter 10

Summary and future perspectives

Pulmonary Arterial Hypertension (PAH) is diagnosed when the mean pulmonary arterial pressure is increased above 25 mmHg and other causes of an increase in pulmonary artery pressure are excluded.(1) Chronic pressure overload leads to dysfunction of the right ventricle and ultimately right ventricular failure and death.(2, 3) The WHO classification of PAH (chapter 1, table 1), based on etiological perceptions, shows the variety of causes contributing to this condition.(1) Experimental animal models support the notion that PAH cannot be narrowed down to one specific cause. Experimentally, multiple hits are required to mimic the characteristic vascular lesions seen in PAH.(4-8) The same is probably true for human PAH, since even the best-known mutation in the heritable form of PAH, located in the Bone Morphogenetic Protein type 2 Receptor (BMPR2), has a low penetrance of 20%.(9-12) Besides genetic mutations, other hits playing a role in the pathophysiology of PAH are altered blood flow, drugs and toxins, growth factors, infections, inflammation, neurohormonal activation, metabolic changes and vasoactive mediators (Figure 1).(2, 13, 14) The end result is the characteristic vasculopathy of PAH with the appearance of plexiform lesions, muscularization of peripheral arteries, medial hypertrophy of the muscular arteries and neointima formation (chapter 1, figure 2).(13-15) Endothelial dysfunction plays a key role in occlusive remodeling and an increased vascular tone, and is targeted with all currently approved PAH therapies.(16, 17) The pathophysiology of initiating hits and cellular dysfunction is studied extensively, but not yet completely understood (Figure 1). Current research is clouded by a mix of factors that could be either functioning as an initiating factor, or as maintenance factor. Because vascular remodeling itself cannot only be induced by altered blood flow, but can also be responsible for further alterations in blood flow, the pathobiology of PAH can well be described as a vicious circle of remodeling and altered blood flow.

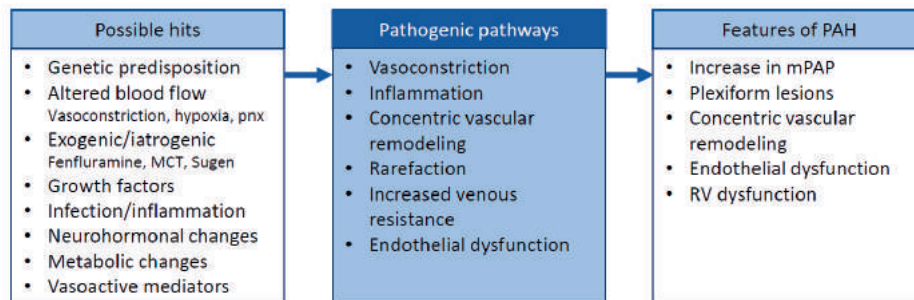


Figure 1 – Pathophysiology of PAH. MCT, monocrotaline rat model; mPAP, mean pulmonary artery pressure; pnx, pneumonectomy; RV, right ventricular.

Effects of altered pulmonary blood flow on vascular remodeling

Endothelial cells (EC) are continuously exposed to the frictional forces that the blood exerts on the vascular wall. The influence of altered blood flow on the pathophysiology of PAH is studied with modeling techniques visualizing these forces and mimicking

this in vitro.(18-20) In **chapter 3** we investigated the effects of altered pulmonary blood flow induced by pneumonectomy in rats. In **chapter 4** we compared findings in pneumonectomized rats with human lung tissue of patients that underwent pneumonectomy because of lung cancer. In both studies, pneumonectomy alone was related to only minor structural alterations. A couple of patients showed thrombotic arteriopathy, a common pathological finding in PAH.(14, 21-23) Although proliferation of EC after pneumonectomy is upregulated, there was no change in intimal wall thickness in rats or patients. The rat model shows that a combination with growth factor inhibition is necessary as a secondary hit to induce both proliferative and pro-apoptotic signaling leading to severe angio-obliterative pulmonary hypertension. This shows that altered blood flow alone is not sufficient to induce structural changes in the pulmonary vasculature, but acts as a hit contributing to the final common pathway.

Contribution of pulmonary vascular remodeling to pulmonary vascular resistance.

Vasoconstriction is the most accepted contributor to increased pulmonary vascular resistance (PVR) in PAH, although vasodilating therapies have limited effect on PAH disease progression. The rat model combining the VEGF inhibitor Sugen with hypoxia (SuHx), shows that hypoxic vasoconstriction is not an obligatory hit for the development of pulmonary hypertension. Concentric remodeling of the pulmonary vasculature is thought to contribute to increased PVR because only a minority of PAH patients exposed to acute vasodilator challenges show substantial pressure decreases. (24) Current information on pulmonary vascular remodeling in PAH is often limited to an assessment of the wall thickness of all small lung vessels taken together. In **chapter 5** we aimed to objectify the remodeling between different vessel orders, to compute the influence of vascular remodeling on resistance. While it is generally assumed that the increase in vascular resistance in PAH is explained by severe structural changes in most, if not all, small pulmonary vessels, our measurements did not support this assumption. First, we found that the majority of vessels (70%) was not affected through a change in inner diameter. Second, the size of the affected vessels and the degree of diameter change varied greatly. Third, our computations showed that remodeling of 30% of the pulmonary vessels could maximally explain a 1.4 fold increase in PVR, resulting in ≈ 140 dynes \cdot cm $^{-5}$ when multiplied by the maximal normal PVR limits of 99 dynes \cdot cm $^{-5}$. This is still far from the PVR of about 857 dynes \cdot cm $^{-5}$ measured in our patient group. We suggest two other factors, besides vasoconstriction and concentric remodeling, contributing to increased vascular resistance. First, vascular rarefaction, a phenomenon that is not only possible in the pulmonary vasculature but is already shown to be involved in RV-dysfunction in PAH(25-28) . Second, there could be a substantial venous involvement in PAH.(29, 30) Different contributors to increased pulmonary vascular resistance is of importance for new therapeutic strategies.

Targeting endothelial dysfunction in PAH

The expanding knowledge on the pathophysiology of PAH might indicate novel treatment strategies.(31) With the main focus on endothelial dysfunction we aimed to explore relevant therapeutic targets. An example of flawed sensitivity in EC can be appreciated from cilia, sensory antennas that integrate signaling and fine-tune EC responses. Cilia dysfunction in different cell types shows the role of cilia in the response to injury, regulating cell sensitivity and cell differentiation. Cilia are known as mechanosensors for fluid shear stress.(32-35) We show in **chapter 6** that the cilia on healthy pulmonary EC are responsive to inflammatory cytokines by elongation, as their length is inhibited by IL-10 and NFkB inhibitors. EC of PAH patients, on the other hand, have elongated cilia unresponsive to pro- and anti-inflammatory treatment. This could be explained by ongoing cytokine production or a contributing mechanism independent of inflammatory signaling, like metabolic changes. Shear stress, of which the importance in PAH is discussed above, even further elongates the cilia that are randomly arranged on the EC surface, indicating defective mechano-responses. Previous studies show that exposure of cilia to shear stress leads to activated TGF-beta signaling, possibly leading to endothelial-to-mesenchymal transition (endo-MT).(35-37) Endo-MT is a process recently recognized to contribute to vascular remodeling seen in PAH.(38-40) The role of changed cilia length in pulmonary EC and their contribution to endothelial dysfunction in the pathogenesis of PAH warrants further research.

Since the discovery of the BMPR2 mutations in 2000 in the context of hereditary PAH, a lot of research has been done on this pathway.(9-12) In different subtypes of PAH increased TGF-beta and decreased BMP-signaling contribute to endothelial dysfunction.(38, 41-46) The complexity of this pathway, described in **chapter 7**, is emphasized by contrasting study results, indicating BMP9 missense mutations as a cause of pulmonary hypertension versus the protective effect of BMP9 knock down in animal models.(45, 47, 48) Not all hits are interchangeable with one another and some hits are more potent than others to induce or worsen PH. In **chapter 8** we studied phenotypic effects and the potential therapeutic role of BMP9 in different types of EC (peripheral blood derived, pulmonary artery and microvascular EC). Microvascular endothelial cells of PAH patients showed the strongest response to BMP9 stimulation, with increased and sustained activation of TGF-beta signaling due to loss of EC suppressor function. This process is also regulated through inflammatory cytokines, shown by prevention of these effects by interleukin-6 (IL-6) inhibition. Caution is warranted in therapeutic use of BMP9 in PAH because of the loss of the antagonistic effects of TGF-beta and BMP signaling and may need to be combined with therapy directed to IL-6.

Disrupted signaling found in PAH EC is also of importance for treatments focused on growth factors, as discussed in **Chapter 9**. Although proliferation of healthy EC is inhibited by nintedanib, a TKI-inhibitor targeting VEGF, PDGF, FGF and TGF-beta

signaling, this effect is not seen in cells from PAH patients. There were no effects on vascular remodeling in lung tissue of SuHx rats, but unexpectedly we found improvement on RV dilatation possibly through inhibition of fibrosis in the heart. This study suggests that nintedanib, approved for idiopathic pulmonary fibrosis (IPF), may be safely used in the context of pulmonary hypertension associated with IPF.(49-52)

Future perspectives

The pulmonary artery pressures are increased in one third of the patients after pneumonectomy.(53-55) As described in chapters 3 and 4, we found only minor alterations in the pulmonary vasculature in our experimental rat model and lung tissue of patients after major lung resection. In combination with other hits, the rat model is of importance to study which component of the pathogenesis can be attributed to altered blood flow. In particular the influence on endo-MT and specific interactions between proliferation and apoptosis of EC would be of interest. To further explore which additional hits are important to shear stress, the lung tissue of patients after pneumonectomy that do develop increased pulmonary artery pressures should be further studied.

In chapter 5 the heterogeneity of the vascular remodeling in PAH became clear. The high pulmonary artery pressures found in PAH cannot be explained by vasoconstriction and concentric remodeling of the pulmonary vasculature alone. Rarefaction is an often debated phenomenon in the field of PAH. There is proof of rarefaction in the heart of PAH patients, but its occurrence in the PAH lung remains controversial.(25-28) An important future study would be to visualize the entire diseased pulmonary circulation all the way down to the capillaries. This approach, to date only attempted with micro-CT in rats, will likely encounter technical difficulties due to tissue properties and limitations in image resolution.(56-58) In addition, it will be important to study the possibility that a profound venous pathology contributes to the increase in PVR in PAH, as it contributes to pulmonary hypertension due to left heart disease. It has been demonstrated that capillary pressures are increased in PAH, suggesting a high venous resistance.(30) Venous resistance is also involved in chronic thromboembolic pulmonary hypertension.(29) We hypothesize that in addition to other forms of pulmonary hypertension venous resistance also has a role in PAH.

The significance of the pro-inflammatory environment of microvascular endothelial cells in PAH is emphasized in chapters 7 and 8. In the context of cilia located on the endothelium, we showed a non-responsiveness of cilia length to inflammatory cytokines or inhibition with IL-10 and NFkB. Also the response of the endothelium to novel therapeutic agents, like BMP9, is altered in PAH by inflammation. EC of PAH patients stimulated with BMP9 showed induction of transcription factors for endo-MT, that could be inhibited with an IL-6 capturing antibody. IL-6, a pro-inflammatory cytokine that is increased in PAH and correlates with prognoses, seems to be a

promising therapeutic target for PAH.(41, 59-62) Recent research shows that BMPR2 mutant rats that develop spontaneous pulmonary hypertension, can be distinguished from the ones that don't by pulmonary IL-6 overexpression.(63) Future studies should explore the precise mechanism via which IL-6 influences the TGF-beta/BMP pathway and the effects of modifying this on the pulmonary vasculature.

Pulmonary arterial hypertension is a complex group of diseases that is caused by a combination of hits leading to a final common pathway that cannot be stabilized or cured by one treatment option alone. Future treatment strategies should focus on targeting multiple pathogenic pathways at once in which combination therapy seems inevitable.

References

1. Simonneau G, Gatzoulis MA, Adatia I, Celermajer D, Denton C, Ghofrani A, et al. Updated clinical classification of pulmonary hypertension. *J Am Coll Cardiol*. 2013;62(25 Suppl):D34-41.
2. Voelkel NF, Gomez-Arroyo J, Abbate A, Bogaard HJ, Nicolls MR. Pathobiology of pulmonary arterial hypertension and right ventricular failure. *Eur Respir J*. 2012;40(6):1555-65.
3. Bogaard HJ, Abe K, Vonk Noordegraaf A, Voelkel NF. The right ventricle under pressure: cellular and molecular mechanisms of right-heart failure in pulmonary hypertension. *Chest*. 2009;135(3):794-804.
4. Yuan JX, Rubin LJ. Pathogenesis of pulmonary arterial hypertension: the need for multiple hits. *Circulation*. 2005;111(5):534-8.
5. Song Y, Jones JE, Beppu H, Keane JF, Jr., Loscalzo J, Zhang YY. Increased susceptibility to pulmonary hypertension in heterozygous BMPR2-mutant mice. *Circulation*. 2005;112(4):553-62.
6. Mizuno S, Farkas L, Al Hussein A, Farkas D, Gomez-Arroyo J, Kraskauskas D, et al. Severe pulmonary arterial hypertension induced by SU5416 and ovalbumin immunization. *Am J Respir Cell Mol Biol*. 2012;47(5):679-87.
7. Nicolls MR, Mizuno S, Taraseviciene-Stewart L, Farkas L, Drake JI, Al Hussein A, et al. New models of pulmonary hypertension based on VEGF receptor blockade-induced endothelial cell apoptosis. *Pulm Circ*. 2012;2(4):434-42.
8. Okada K, Tanaka Y, Bernstein M, Zhang W, Patterson GA, Botney MD. Pulmonary hemodynamics modify the rat pulmonary artery response to injury. A neointimal model of pulmonary hypertension. *Am J Pathol*. 1997;151(4):1019-25.
9. Soubrier F, Chung WK, Machado R, Grunig E, Aldred M, Geraci M, et al. Genetics and genomics of pulmonary arterial hypertension. *J Am Coll Cardiol*. 2013;62(25 Suppl):D13-21.
10. Morrell NW, Aldred MA, Chung WK, Elliott CG, Nichols WC, Soubrier F, et al. Genetics and genomics of pulmonary arterial hypertension. *Eur Respir J*. 2019;53(1).
11. Deng Z, Morse JH, Slager SL, Cuervo N, Moore KJ, Venetos G, et al. Familial primary pulmonary hypertension (gene PPH1) is caused by mutations in the bone morphogenetic protein receptor-II gene. *Am J Hum Genet*. 2000;67(3):737-44.
12. Lane KB, Machado RD, Pauciulo MW, Thomson JR, Phillips JA, 3rd, Loyd JE, et al. Heterozygous germline mutations in BMPR2, encoding a TGF-beta receptor, cause familial primary pulmonary hypertension. *Nat Genet*. 2000;26(1):81-4.
13. Rabinovitch M. Molecular pathogenesis of pulmonary arterial hypertension. *J Clin Invest*. 2012;122(12):4306-13.
14. Humbert M, Guignabert C, Bonnet S, Dorfmueller P, Klinger JR, Nicolls MR, et al. Pathology and pathobiology of pulmonary hypertension: state of the art and research perspectives. *Eur Respir J*. 2019;53(1).
15. K. Grunberg WJM. A practical approach to vascular pathology in pulmonary hypertension. *Diagn Histopath*. 2013;19(8):298-310.
16. Humbert M, Sitbon O, Simonneau G. Treatment of pulmonary arterial hypertension. *N Engl J Med*. 2004;351(14):1425-36.
17. Galie N, Humbert M, Vachiery JL, Gibbs S, Lang I, Torbicki A, et al. 2015 ESC/ERS Guidelines for the diagnosis and treatment of pulmonary hypertension: The Joint Task Force for the Diagnosis and Treatment of Pulmonary Hypertension of the European Society of Cardiology (ESC) and the European Respiratory Society (ERS): Endorsed by: Association for European Paediatric and Congenital Cardiology (AEPC), International Society for Heart and Lung Transplantation (ISHLT). *Eur Respir J*. 2015;46(4):903-75.
18. Szulcek R, Happe CM, Rol N, Fontijn RD, Dickhoff C, Hartemink KJ, et al. Delayed Microvascular Shear Adaptation in Pulmonary Arterial Hypertension. Role of Platelet Endothelial Cell Adhesion Molecule-1 Cleavage. *Am J Respir Crit Care Med*. 2016;193(12):1410-20.
19. Qi YX, Jiang J, Jiang XH, Wang XD, Ji SY, Han Y, et al. PDGF-BB and TGF- β 1 on cross-talk between endothelial and smooth muscle cells in vascular remodeling induced by low shear stress. *Proc Natl Acad Sci U S A*. 2011;108(5):1908-13.
20. Happe CM, Szulcek R, Voelkel NF, Bogaard HJ. Reconciling paradigms of abnormal pulmonary blood flow and quasi-malignant cellular alterations in pulmonary arterial hypertension. *Vascul Pharmacol*. 2016;83:17-25.
21. Nogueira-Ferreira R, Ferreira R, Henriques-Coelho T. Cellular interplay in pulmonary arterial hypertension: implications for new therapies. *Biochim Biophys Acta*. 2014;1843(5):885-93.

22. Pietra GG, Edwards WD, Kay JM, Rich S, Kernis J, Schloo B, et al. Histopathology of primary pulmonary hypertension. A qualitative and quantitative study of pulmonary blood vessels from 58 patients in the National Heart, Lung, and Blood Institute, Primary Pulmonary Hypertension Registry. *Circulation*. 1989;80(5):1198-206.
23. Wagenvoort CA. Lung biopsy specimens in the evaluation of pulmonary vascular disease. *Chest*. 1980;77(5):614-25.
24. Barst RJ, Gibbs JS, Ghofrani HA, Hoeper MM, McLaughlin VV, Rubin LJ, et al. Updated evidence-based treatment algorithm in pulmonary arterial hypertension. *J Am Coll Cardiol*. 2009;54(1 Suppl):S78-84.
25. Bogaard HJ, Natarajan R, Henderson SC, Long CS, Kraskauskas D, Smithson L, et al. Chronic pulmonary artery pressure elevation is insufficient to explain right heart failure. *Circulation*. 2009;120(20):1951-60.
26. Ryan JJ, Huston J, Kutty S, Hatton ND, Bowman L, Tian L, et al. Right ventricular adaptation and failure in pulmonary arterial hypertension. *Can J Cardiol*. 2015;31(4):391-406.
27. Drake JI, Bogaard HJ, Mizuno S, Clifton B, Xie B, Gao Y, et al. Molecular signature of a right heart failure program in chronic severe pulmonary hypertension. *Am J Respir Cell Mol Biol*. 2011;45(6):1239-47.
28. Chaudhary KR, Taha M, Cadete VJ, Godoy RS, Stewart DJ. Proliferative Versus Degenerative Paradigms in Pulmonary Arterial Hypertension: Have We Put the Cart Before the Horse? *Circ Res*. 2017;120(8):1237-9.
29. Dorfmueller P, Gunther S, Ghigna MR, Thomas de Montpreville V, Boulate D, Paul JF, et al. Microvascular disease in chronic thromboembolic pulmonary hypertension: a role for pulmonary veins and systemic vasculature. *Eur Respir J*. 2014;44(5):1275-88.
30. Kafi SA, Melot C, Vachiery JL, Brimiouille S, Naeije R. Partitioning of pulmonary vascular resistance in primary pulmonary hypertension. *J Am Coll Cardiol*. 1998;31(6):1372-6.
31. Sitbon O, Gomberg-Maitland M, Granton J, Lewis MI, Mathai SC, Rainisio M, et al. Clinical trial design and new therapies for pulmonary arterial hypertension. *Eur Respir J*. 2019;53(1).
32. Praetorius HA. The primary cilium as sensor of fluid flow: new building blocks to the model. A review in the theme: cell signaling: proteins, pathways and mechanisms. *Am J Physiol Cell Physiol*. 2015;308(3):C198-208.
33. Hierck BP, Van der Heiden K, Alkemade FE, Van de Pas S, Van Thienen JV, Groenendijk BC, et al. Primary cilia sensitize endothelial cells for fluid shear stress. *Dev Dyn*. 2008;237(3):725-35.
34. Poelmann RE, Van der Heiden K, Gittenberger-de Groot A, Hierck BP. Deciphering the endothelial shear stress sensor. *Circulation*. 2008;117(9):1124-6.
35. Egorova AD, Van der Heiden K, Van de Pas S, Vennemann P, Poelma C, DeRuiter MC, et al. Tgfbeta/Alk5 signaling is required for shear stress induced klf2 expression in embryonic endothelial cells. *Dev Dyn*. 2011;240(7):1670-80.
36. Goumans MJ, van Zonneveld AJ, ten Dijke P. Transforming growth factor beta-induced endothelial-to-mesenchymal transition: a switch to cardiac fibrosis? *Trends Cardiovasc Med*. 2008;18(8):293-8.
37. Andruska A, Spiekerkoetter E. Consequences of BMPR2 Deficiency in the Pulmonary Vasculature and Beyond: Contributions to Pulmonary Arterial Hypertension. *Int J Mol Sci*. 2018;19(9).
38. Ranchoux B, Antigny F, Rucker-Martin C, Hautefort A, Pechoux C, Bogaard HJ, et al. Endothelial-to-mesenchymal transition in pulmonary hypertension. *Circulation*. 2015;131(11):1006-18.
39. Good RB, Gilbane AJ, Trinder SL, Denton CP, Coghlan G, Abraham DJ, et al. Endothelial to Mesenchymal Transition Contributes to Endothelial Dysfunction in Pulmonary Arterial Hypertension. *Am J Pathol*. 2015;185(7):1850-8.
40. Ranchoux B, Harvey LD, Ayon RJ, Babicheva A, Bonnet S, Chan SY, et al. Endothelial dysfunction in pulmonary arterial hypertension: an evolving landscape (2017 Grover Conference Series). *Pulm Circ*. 2018;8(1):2045893217752912.
41. Selimovic N, Bergh CH, Andersson B, Sakiniene E, Carlsten H, Rundqvist B. Growth factors and interleukin-6 across the lung circulation in pulmonary hypertension. *Eur Respir J*. 2009;34(3):662-8.
42. Gore B, Izikki M, Mercier O, Dewachter L, Fadel E, Humbert M, et al. Key role of the endothelial TGF-beta/ALK1/endoGLN signaling pathway in humans and rodents pulmonary hypertension. *PLoS One*. 2014;9(6):e100310.
43. Botney MD, Bahadori L, Gold LI. Vascular remodeling in primary pulmonary hypertension. Potential role for transforming growth factor-beta. *Am J Pathol*. 1994;144(2):286-95.
44. Graham BB, Chabon J, Gebreab L, Poole J, Debella E, Davis L, et al. Transforming growth factor-beta signaling promotes pulmonary hypertension caused by *Schistosoma mansoni*. *Circulation*. 2013;128(12):1354-64.
45. Long L, Ormiston ML, Yang X, Southwood M, Graf S, Machado RD, et al. Selective enhancement of endothelial BMPR-II with BMP9 reverses pulmonary arterial hypertension. *Nat Med*. 2015;21(7):777-85.
46. Yung LM, Nikolic I, Paskin-Flerlage SD, Pearsall RS, Kumar R, Yu PB. A Selective Transforming Growth Factor-beta Ligand Trap Attenuates Pulmonary Hypertension. *Am J Respir Crit Care Med*. 2016;194(9):1140-51.
47. Tu L, Desroches-Castan A, Mallet C, Guyon L, Cumont A, Phan C, et al. Selective BMP-9 Inhibition Partially Protects Against Experimental Pulmonary Hypertension. *Circ Res*. 2019;124(6):846-55.
48. Morrell NW. Finding the needle in the haystack: BMP9 and 10 emerge from the genome in pulmonary arterial hypertension. *Eur Respir J*. 2019;53(3).
49. Wollin L, Wex E, Pautsch A, Schnapp G, Hostettler KE, Stowasser S, et al. Mode of action of nintedanib in the treatment of idiopathic pulmonary fibrosis. *Eur Respir J*. 2015;45(5):1434-45.
50. Wollin L, Maillet I, Quesniaux V, Holweg A, Ryffel B. Antifibrotic and anti-inflammatory activity of the tyrosine kinase inhibitor nintedanib in experimental models of lung fibrosis. *J Pharmacol Exp Ther*. 2014;349(2):209-20.
51. Richeldi L, Costabel U, Selman M, Kim DS, Hansell DM, Nicholson AG, et al. Efficacy of a tyrosine kinase inhibitor in idiopathic pulmonary fibrosis. *N Engl J Med*. 2011;365(12):1079-87.
52. Richeldi L, du Bois RM, Raghu G, Azuma A, Brown KK, Costabel U, et al. Efficacy and safety of nintedanib in idiopathic pulmonary fibrosis. *N Engl J Med*. 2014;370(22):2071-82.
53. Deslauriers J, Ugalde P, Miro S, Ferland S, Bergeron S, Lacasse Y, et al. Adjustments in cardiorespiratory function after pneumonectomy: results of the pneumonectomy project. *J Thorac Cardiovasc Surg*. 2011;141(1):7-15.
54. Foroulis CN, Kotoulas CS, Kakouros S, Evangelatos G, Chassapis C, Konstantinou M, et al. Study on the late effect of pneumonectomy on right heart pressures using Doppler echocardiography. *Eur J Cardiothorac Surg*. 2004;26(3):508-14.
55. Potaris K, Athanasiou A, Konstantinou M, Zaglavira P, Theodoridis D, Syrigos KN. Pulmonary hypertension after pneumonectomy for lung cancer. *Asian Cardiovasc Thorac Ann*. 2014;22(9):1072-9.
56. 56. Ritman EL. Micro-computed tomography of the lungs and pulmonary-vascular system. *Proc Am Thorac Soc*. 2005;2(6):477-80, 501.
57. Shields KJ, Verdellis K, Passineau MJ, Faight EM, Zourelis L, Wu C, et al. Three-dimensional micro computed tomography analysis of the lung vasculature and differential adipose proteomics in the Sugen/hypoxia rat model of pulmonary arterial hypertension. *Pulm Circ*. 2016;6(4):586-96.
58. Faight EM, Verdellis K, Zourelis L, Chong R, Benza RL, Shields KJ. MicroCT analysis of vascular morphometry: a comparison of right lung lobes in the SUGEN/hypoxic rat model of pulmonary arterial hypertension. *Pulm Circ*. 2017;7(2):522-30.
59. Steiner MK, Syrkinia OL, Kolliputi N, Mark EJ, Hales CA, Waxman AB. Interleukin-6 overexpression induces pulmonary hypertension. *Circ Res*. 2009;104(2):236-44, 28p following 44.
60. Humbert M, Monti G, Brenot F, Sitbon O, Portier A, Grangeot-Keros L, et al. Increased interleukin-1 and interleukin-6 serum concentrations in severe primary pulmonary hypertension. *Am J Respir Crit Care Med*. 1995;151(5):1628-31.
61. Soon E, Holmes AM, Treacy CM, Doughty NJ, Southgate L, Machado RD, et al. Elevated levels of inflammatory cytokines predict survival in idiopathic and familial pulmonary arterial hypertension. *Circulation*. 2010;122(9):920-7.
62. Pullamsetti SS, Seeger W, Savai R. Classical IL-6 signaling: a promising therapeutic target for pulmonary arterial hypertension. *J Clin Invest*. 2018;128(5):1720-3.
63. Hautefort A, Mendes-Ferreira P, Sabourin J, Manaud G, Bertero T, Rucker-Martin C, et al. Bmpr2 Mutant Rats Develop Pulmonary and Cardiac Characteristics of Pulmonary Arterial Hypertension. *Circulation*. 2019;139(7):932-48.

11

Chapter 11

Nederlandse samenvatting

List of publications

Curriculum Vitae

Dankwoord

Nederlandse samenvatting

De diagnose Pulmonale Arteriële Hypertensie (PAH) wordt gesteld als de gemiddelde druk in de pulmonale arterie (longslagader) hoger is dan 25 mmHg en andere oorzaken van een verhoogde druk in de pulmonale arterie zijn uitgesloten. De chronisch verhoogde druk zorgt ervoor dat het rechter ventrikel van het hart harder moet pompen. Dit kan uiteindelijk leiden tot dysfunctie van het rechter ventrikel, met hartfalen en overlijden tot gevolg. De WHO classificatie van PAH (hoofdstuk 1, tabel 1), die is gebaseerd op etiologische waarnemingen, laat zien dat een grote verscheidenheid aan oorzaken bijdraagt aan deze aandoening. Voorgaand onderzoek waarin PAH in dieren geïnduceerd wordt, laten zien dat er niet een alleenstaande oorzaak van PAH is, maar dat verschillende 'hits' nodig om de vaatafwijkingen die typisch zijn voor PAH te verkrijgen. Hetzelfde geldt waarschijnlijk voor patiënten met PAH, gezien zelfs de meest bekende en onderzochte mutatie van erfelijke PAH, in het gen Bone Morphogenetic Protein Receptor 2 (BMPR2), maar in 20% van de gevallen leidt tot ziekte. Naast genetische mutaties is bekend dat veranderde bloedstroom, medicatie en toxinen, groeifactoren circulerend in het bloed, inflammatie, neurohormonale activatie, metabole veranderingen en vasoreactieve mediators een rol kunnen spelen in de pathogenese (hoofdstuk 10, figuur 1). Dit resulteert in de voor PAH karakteristieke vasculopathie in de longen gekenmerkt door 'plexiform lesions' (figuur 1D, hoofdstuk 5), muscularisatie van de perifere vaten, mediale hypertrofie en vorming van neointima (hoofdstuk 1, figuur 2). Huidig voorgeschreven medicatie voor PAH werkt allemaal (deels) op endotheliale dysfunctie die een sleutelrol speelt in de occlusieve remodelering en verhoogde tonus van de longvaten (hoofdstuk 2, figuur 2). De pathofysiologie van oorzaken en celdysfunctie is reeds uitgebreid bestudeerd, maar wordt nog niet geheel begrepen (hoofdstuk 10, figuur 1). Het onderzoek hiernaar wordt bemoeilijkt door factoren die zowel als initiërende als onderhoudende factor kunnen fungeren. Zo kan veranderde bloedstroom leiden tot remodelering van de vaten, maar deze remodelering zelf kan ook weer zorgen voor veranderde bloedstroom. De pathofysiologie van PAH zou omschreven kunnen worden als een vicieuze cirkel van remodelering en veranderde bloedstroom.

Effecten van veranderde bloedstroom op remodelering van de vaten

Endotheelcellen, die de binnenkant van bloedvaten bekleden en de intima vormen, worden continu blootgesteld aan wrijvingskrachten (shear stress) die het bloed uitoefent op de vaatwand. De invloed van veranderde bloedstroom op de pathofysiologie van PAH is bestudeerd aan de hand van modeltechnieken die deze krachten visualiseren en het nabootsen in celweek. In **hoofdstuk 3** hebben wij het effect van verhoogde bloedstroom na pneumonectomie in ratten bestudeerd. In

hoofdstuk 4 hebben we die bevindingen vergeleken met humaan longweefsel van patiënten die een pneumonectomie hebben moeten ondergaan wegens longkanker en enkele jaren met één long hebben geleefd. In beide studies was een pneumonectomie gerelateerd aan zeer minimale structurele veranderingen van de vaten. Een aantal patiënten lieten trombotische arteriopathie zien, een gebruikelijke bevinding in PAH. Hoewel er een verhoogde proliferatie van endotheelcellen werd gevonden na pneumonectomie, waren er geen structurele veranderingen in de intima van de longvaten van ratten als patiënten. Het ratmodel toont dat er naast pneumonectomie een tweede 'hit' met remming van groeifactoren nodig is om zowel proliferatieve als pro-apoptotische signalering te verkrijgen die leidt tot ernstige angio-obliteratieve pulmonale hypertensie (PH). Dit bevestigt dat een veranderde bloedstroom kan bijdragen, maar op zichzelf onvoldoende is om structurele veranderingen te veroorzaken in de longvaten.

Bijdragen van vaatremodelering aan pulmonale vaatweerstand

Hoewel vasodilerende medicatie een beperkt effect heeft op de progressie van PAH, wordt vasoconstrictie, het samenknijpen van de longvaten, gezien als de meest geaccepteerde oorzaak van de verhoogde pulmonale vaatweerstand (PVR) in PAH. Het PH ratmodel waarbij waarbij Sugen (een angiogenese remmer) gecombineerd wordt met pneumonectomie in plaats van de gebruikelijke combinatie van Sugen met hypoxie (SuHx), laat zien dat hypoxische vasoconstrictie geen verplichte hit is voor de ontwikkeling van pulmonale hypertensie. Er wordt verondersteld dat concentrische remodelering van de pulmonaalvaten minimaal bijdraagt aan de verhoogde PVR, omdat alleen de minderheid van de patiënten een substantiële drukdaling laten zien na blootstelling aan acute vasodilatoire middelen. De huidig beschikbare informatie omtrent remodelering van de longvasculatuur is vaak beperkt tot gemiddelde wanddikte van alle kleine longvaten. Daarom hebben wij in **hoofdstuk 5** de remodelering van verschillende grootte longvaten gemeten om de invloed van deze verandering op de weerstand te berekenen. Hoewel wordt aangenomen dat verhoogde PVR in PAH wordt verklaard door structurele veranderingen in de meeste, zo niet alle, kleine pulmonaalvaten, lieten onze metingen een ander beeld zien. Allereerst observeerden wij dat de meerderheid van de vaten in longen van PAH patiënten (70%) geen afname van de binnendiameter hadden. Ten tweede varieerden de grootte van de vaten en de afname van de diameter sterk. Ten derde lieten onze berekeningen zien dat het maximale effect dat remodelering van 30% van de vaten een toename van 40% in PVR kunnen verklaren. Dit zou resulteren in een PVR van ongeveer 140 dynes·cm⁻⁵ wanneer men uitgaat van een normaalwaarde onder de 99 dynes·cm⁻⁵. Dit is bij lange na niet de 857 dynes·cm⁻⁵ die gemiddeld gemeten werd in onze patiëntengroep. Mogelijke zijn er andere factoren naast vasoconstrictie en remodelering van de vaten

die bijdragen aan een verhoogde PVR. Zo zou afname van vaten (rarefaction), waarvan aangetoond is dat dit bijdraagt aan rechterventrikeldysfunctie in PH, de PVR in de long kunnen beïnvloeden. Ook zou veneuze betrokkenheid een verklaring kunnen zijn. Als verschillende factoren van invloed zijn op de PVR, zou dit van betekenis kunnen zijn voor nieuwe therapeutische mogelijkheden.

Endotheel dysfunctie als doelwit van therapie in PAH

De toename van kennis over de pathofysiologie van PAH zou kunnen leiden tot nieuwe behandelstrategieën. Met het oog op relevante therapeutische mogelijkheden hebben wij ons voornamelijk gefocust op endotheliale dysfunctie. Een voorbeeld van gebrekkige sensitiviteit van endotheelcellen in PAH kan worden afgeleid uit cilia; zintuiglijke antennes die verantwoordelijk zijn voor signalering en het aanpassen van reacties in endotheelcellen. Voorgaande onderzoeken naar de rol van cilia in verschillende celtypen laten effecten zien in reactie op schade, regulatie van sensitiviteit en differentiatie van cellen. Ook zijn cilia de mechanosensoren van shear stress van het bloed op de vaatwanden. In **hoofdstuk 6** laten we zien dat cilia in gezonde endotheelcellen van de long reageren op inflammatoire cytokinen door te verlengen. Dit kan geremd worden door de toevoeging van IL-10 en NF- κ B remmers. Endotheelcellen van PAH patiënten laten voor stimulatie al verlenging zien, die niet reageert op pro- of anti-inflammatoire behandeling. Dit kan verklaard worden door aanhoudende cytokine productie of een bijdragend mechanisme onafhankelijk van inflammatoire signalering, zoals metabole veranderingen. Shear stress, van belang in PAH zoals hierboven beschreven, zorgt in endotheelcellen van PAH patiënten zelfs voor verdere verlenging van de cilia, wijzend op een defect in de reactie op mechanische verandering. Voorgaande studies lieten zien dat expositie van cilia aan shear stress leidt tot activatie van Transforming Growth Factor (TGF)-beta signalering, mogelijk leidend tot endotheliale naar mesenchymale transitie (Endo-MT). Endo-MT is een proces waarvan recentelijk bekend is geworden dat het bijdraagt aan vaat remodelering in PAH. Toekomstig onderzoek moet uitwijzen wat de rol is van veranderde cilia lengte van pulmonale endotheelcellen en hun bijdrage aan endotheliale dysfunctie in de pathogenese van PAH.

Sinds de ontdekking in 2000 dat BMP2 mutaties erfelijke PAH veroorzaken, is er veel onderzoek gewijd aan het 'TGF-beta/BMP pathway'. In verschillende subtypen van PAH draagt verhoogde signalering van TGF-beta en verlaagde signalering van BMP bij aan endotheliale dysfunctie. De complexiteit van dit pathway, beschreven in **hoofdstuk 7**, wordt benadrukt door contrasterende onderzoeksresultaten. Zo kan enerzijds een BMP9 missense mutatie PAH veroorzaken, maar laat anderzijds een knockdown van BMP9 in diermodellen een beschermend effect tegen PAH zien. Niet alle hits zijn inwisselbaar met elkaar en sommige hits zijn sterker dan andere om PAH te

veroorzaken, dan wel te verergeren. In **hoofdstuk 8** hebben we het effect van BMP9 op het fenotype van verschillende soorten endotheelcellen (uit perifere bloed, pulmonale arterie en pulmonale microvasculatuur) getest en de potentiële therapeutische waarde bestudeerd. Microvasculaire endotheelcellen van PAH patiënten laten de sterkste reactie op BMP9 stimulatie zien, met aanhoudend verhoogde activatie van TGF-beta signalering door verlies van remming in endotheelcellen. Dit proces wordt ook gereguleerd door inflammatoire cytokines, bevestigd door de preventieve werking van interleukine-6 (IL-6) inhibitie. Voorzichtigheid is geboden bij het gebruik van BMP9 als medicatie in PAH vanwege het verlies van antagonistische effecten in de TGF-beta en BMP signalering en het zal mogelijk moeten worden gecombineerd met behandeling gericht op IL-6.

Verstoorde signalering in endotheelcellen van PAH patiënten is ook van belang voor behandelingen gericht op groeifactoren, zoals besproken in **hoofdstuk 9**. Hoewel proliferatie van gezonde endotheelcellen wordt geremd door nintedanib, een tyrosinekinase remmer gericht op VEGF, PDGF, FGF en TGF-beta signalering, wordt dit effect niet gezien in PAH endotheelcellen. Er werd ook geen effect van nintedanib geobserveerd op vaatremodelering in longweefsel van SuHx ratten. Wel vonden wij onverwacht een verbetering op rechterventrikel dilatatie, mogelijk door fibrose remming in het hart. Deze studie suggereert dat nintedanib, een medicament goedgekeurd voor patiënten met idiopathische pulmonale fibrose (IPF), veilig kan worden gebruikt in de context van pulmonale hypertensie geassocieerd met IPF.

Toekomstperspectieven

De resultaten van de gepubliceerde onderzoeken in deze thesis hebben geleid tot nieuwe inzichten die weer nieuwe vraagstukken aankaarten voor toekomstig onderzoek. De druk in de pulmonale arterie is verhoogd in een derde van de patiënten na een pneumonectomie. Zoals beschreven in hoofdstuk 3 en 4, vonden wij minimale veranderingen in de pulmonale vasculatuur in ons ratmodel en longweefsel van patiënten na een pneumonectomie. Welke rol de veranderde bloedstroom exact speelt in de pathogenese van pulmonale hypertensie, kan uitgezocht worden door in ratten een pneumonectomie te combineren met andere hits. Met name de invloed op Endo-MT en specifieke interacties tussen proliferatie en apoptose in endotheelcellen kunnen interessant zijn. Om verder te onderzoeken welke aanvullende hits van belang zijn in combinatie met shear stress, moet het longweefsel van patiënten na pneumonectomie die een verhoogde druk in de pulmonale arterie ontwikkelen verder onderzocht worden.

In hoofdstuk 5 komt de heterogeniteit van de vaat remodelering in PAH sterk naar voren. De hoge drukken in de pulmonale arterie bij PH patiënten kan niet alleen

verklaard worden door vasoconstrictie en concentrische remodelering in de pulmonale vasculatuur. Rarefaction is een vaak bediscussieerd fenomeen in het onderzoeksveld van PAH. Er is bewijs van afname van vaten in hartweefsel van PAH patiënten, maar het voorkomen hiervan in de longen blijft controversieel. Een belangrijke studie die in de toekomst zal moeten plaatsvinden is het visualiseren van de gehele aangedane pulmonale circulatie tot aan de capillairen. Deze benadering, tot op heden alleen geprobeerd middels micro-CT in ratweefsel, zal technische moeilijkheden met zich mee brengen gezien de weefseleigenschappen van de longen en limitaties in afbeeldingsresolutie. Aanvullend, is het van belang de mogelijkheid te bestuderen of veneuze pathologie bijdraagt aan de verhoogde PVR in PAH, gezien dit bijdraagt aan pulmonale hypertensie gerelateerd aan linkerhartfalen. Het is aangetoond dat capillaire drukken verhoogd zijn in PAH, wat een verhoogde veneuze druk suggereert. Veneuze weerstand is ook betrokken bij chronische trombo-embolische pulmonale hypertensie. Wij veronderstellen dat in aanvulling op andere vormen van pulmonale hypertensie veneuze weerstand ook een rol kan spelen in PAH.

De betekenis van een pro-inflammatoire omgeving van microvasculaire endotheelcellen in PAH is besproken in hoofdstuk 7 en 8. In de context van cilia gelokaliseerd op de endotheelcellen, lieten wij een afwezige response op inflammatoire cytokinen en remming met IL-10 en NFκB zien op permanent verlengde cilia in PAH. Ook wordt de reactie van het endotheel op nieuwe therapeutische middelen, zoals BMP9, in PAH negatief beïnvloed door inflammatie. Endotheelcellen van PAH patiënten gestimuleerd met BMP9 laten inductie van transcriptie factoren voor endo-MT zien, wat geremd kan worden met een antilichaam dat IL-6 wegvangt in de circulatie. IL-6, een pro-inflammatoire cytokine die is verhoogd in PAH en correleert met prognose, lijkt een veelbelovende therapeutische doelwit in PAH. Recent onderzoek toont aan dat ratten met een BMPR2 mutatie die spontaan pulmonale hypertensie ontwikkelen, zich onderscheiden van degene die dat niet ontwikkelen door IL-6 overexpressie. Toekomstige studies zouden het precieze mechanisme waarmee IL-6 invloed uitoefent op het TGF-beta/BMP pathway en de effecten van modulatie hiervan op de long vasculatuur moeten uitwijzen.

Pulmonale arteriële hypertensie is een complexe groep aandoeningen die wordt veroorzaakt door een combinatie van hits wat uiteindelijk leidt tot een zogenaamd 'final common pathway' die niet gestabiliseerd of genezen kan worden door één alleenstaand medicijn. Toekomstige behandelstrategieën moeten gericht zijn op meerdere pathogene paden, waarmee een combinatie van verschillende medicatie onvermijdelijk lijkt.

List of publications

- Happé C, Kondababu K, Xiao-Qing Sun, da Silva Goncalves Bos D, **Rol N**, Guignabert C, Tu L, Schlij I, Wiesmeijer KC, Tura-Ceide O, Vonk-Noordegraaf A, de Man FS, Bogaard HJ, Goumans MJ. The BMP receptor 2 in Pulmonary Arterial Hypertension: When and where the animal model matches the patient. *Cells*. 2020 Jun 8;9(6):1422.
- **Rol N**, de Raaf MA, Sun XQ, Kuiper VP, da Silva Goncalves Bos D, Happé C, Kurakula K, Dickhoff C, Thuillet R, Tu L, Guignabert C, Schlij I, Lodder K, Pan X, Herrmann FE, van Nieuw Amerongen GP, Koolwijk P, Vonk-Noordegraaf A, de Man FS, Wollin L, Goumans MJ, Szulcek R, Bogaard HJ. Nintedanib improves cardiac fibrosis but leaves pulmonary vascular remodeling unaltered in experimental pulmonary hypertension. *Cardiovasc Res*. 2019 Feb 1;115(2).
- **Rol N**, Kurakula K, Happé C, Bogaard HJ, Goumans MJ. TGF-beta and BMPR2 signalling in PAH: two black sheep in one family. *Int J Mol Sci*. 2018 Aug 31;19(9).
- **Rol N**, Dummer A, Szulcek R, Kurakula K, Pan X, Visser BI, Bogaard HJ, DeRuiter MC, Goumans MJ, Hierck BP. Endothelial dysfunction in pulmonary arterial hypertension: loss of cilia length regulation upon cytokine stimulation. *Pulm Circ*, 2018 Apr-Jun;8(2).
- da Silva Gonçalves Bós D, Van Der Bruggen CEE, Kurakula K, Sun XQ, Casali KR, Casali AG, **Rol N**, Szulcek R, Dos Remedios C, Guignabert C, Tu L, Dorfmueller P, Humbert M, Wijnker PJM, Kuster DWD, van der Velden J, Goumans MJ, Bogaard HJ, Vonk-Noordegraaf A, de Man FS, Handoko ML. Contribution of impaired parasympathetic activity to right ventricular dysfunction and pulmonary vascular remodeling in pulmonary arterial hypertension. *Circulation*, 2018 Feb 27;137(9)
- **Rol N**, Happé CM, Belien JAM, de Man F, Westerhof N, Vonk Noordegraaf A, Grünberg K, Bogaard HJ. Vascular remodeling in the pulmonary circulation after major lung resection. *ERJ*, 2017 Aug 31;50(2).
- **Rol N**, Timmer EM, Faes TJC, Vonk Noordegraaf A, Grünberg K, Bogaard HJ, Westerhof N. Vascular narrowing in pulmonary arterial hypertension is heterogeneous: rethinking resistance. *Physiological reports*, 2017 Mar;5(6).
- Happé,CM, De Raaf MA, **Rol N**, Schlij I, Vonk Noordegraaf A, Westerhof N, Voelkel N, de Man FS, Bogaard HJ. Pneumonectomy combined with SU5416 induces severe pulmonary hypertension in rats. *AJP Lung Cellular and Molecular Physiology*, 2016 Jun 1;310(11).

- Van der Bruggen CCE, Happe CM, Dorfmueller P, Trip P, Spruit OA, **Rol N**, Hoevenaar FP, Houweling AC, Girerd B, Mercier O, Humbert M, Handoko ML, van de Velden J, Vonk Noordegraaf A, Bogaard HJ, Goumans MJ, de Man FS. Bone Morphogenetic Protein Receptor type 2 mutation in Pulmonary Arterial Hypertension, a view on the right ventricle. *Circulation*, 2016 May 3;133(18).
- Szulcek R, Happe CM, **Rol N**, Fontijn RD, Dickhoff C, Hartemink KJ, Grunberg K, Tu L, Timens W, Nossent GD, Paul MA, Leyen TA, Horrevoets AJ, de Man FS, Guignabert C, Yu PB, Vonk Noordegraaf A, van Nieuw Amerongen GP, Bogaard HJ. Delayed microvascular shear-adaptation in Pulmonary Arterial Hypertension: role of PECAM-1 cleavage. *AJRCCM*, 2016 Jun 15;193(12).
- **Rol N**, Guignabert C, Bogaard HJ. Pathophysiology and treatment of pulmonary arterial hypertension. *Pathophysiology and Pharmacotherapy of Cardiovascular Disease*, 2015: 949-974.
- de Raaf MA, Schalij I, Gomez-Arroyo J, **Rol N**, Happe CM, de Man FS, Vonk Noordegraaf A, Westerhof N, Voelkel NF, Bogaard HJ. SuHx rat model: Partly reversible pulmonary hypertension and progressive intima obstruction. *ERJ*, 2014 Jul;44(1).

Curriculum Vitae

Nina Rol was born in Haarlem, the Netherlands on February 15th 1991. In 2009 she completed secondary school (VWO) at Sancta Maria in Haarlem and started in that same year with medical school at the VU University Medical Center in Amsterdam. In 2011 she got engaged with research through the Honours Programme by doing an internship supervised by Prof. dr. H.J. Bogaard. In 2013 she decided in her fourth year of medical school to postpone her clinical rotations to focus on research in the field of pulmonary hypertension at the pulmonology and physiology departments at the VU University Medical Center under supervision of Prof. dr H.J. Bogaard and later also Prof. dr. M.J.T.H. Goumans. After continuing medical school in 2016, she performed her final internship at the department of pulmonology at the VU University Medical Center. In September 2019, she started to work as a specialist not in training at the department of pulmonology at the AMC. In January 2021 she will start working as a resident at the department of internal medicine at OLVG as part of her specialization in pulmonary medicine at the Amsterdam UMC and OLVG in Amsterdam.

Dankwoord

Na jaren vol studie, experimenten, plezier, twijfels, schrijven, congres bezoeken, 2 kinderen krijgen en co-schappen is het eindelijk klaar: mijn proefschrift. Hoewel het tijdens het schrijven van dit werk af en toe voelde alsof ik Émile Borels gedachte-experiment als een typend aapje probeerde te bewijzen, overheersen alle goede herinneringen, wijze (levens)lessen en de vrienden die ik in deze periode heb ontmoet.

Na wat wisselingen in de wacht heb ik mijn PhD mogen afsluiten met het prof. HJ-MJ team. Mijn PhD is niet alledaags gestart, zo zonder master, zonder enige labervaring een pre-klinisch project aangaan en co-schappen tussendoor. Beste Prof. dr. H.J. Bogaard, Harm-Jan, ik wil je bedanken voor het vertrouwen dat je mij geschonken hebt door mij deze positie te geven en voor je engelengeduld gedurende de afgelopen jaren. Beste Prof. dr. M.J.T.H. Goumans, Marie-José, bedankt voor je aanvullende begeleiding, alle kennis over celkweek die ik in Leiden op heb mogen doen en de gezellige borrels. Beste Geerten, ik wens je al het geluk op de nieuwe weg die je ingeslagen bent.

Tevens wil ik de leescommissie bedanken voor de tijd en aandacht die zij in het lezen van mijn proefschrift gestoken hebben: Peter Hordijk, Bart Boerrigter, Peter ten Dijke en Paula da Costa Martins. Dear Peter Dorfmueller, thank you for always being open to discuss research and participating in the reading committee. Ik kijk ernaar uit mijn proefschrift tegenover zo'n indrukwekkende commissie te verdedigen.

Gedurende mijn promotietraject heb ik verschillende mensen ontmoet die voor mij een grote inspiratiebron zijn en waar ik veel van heb geleerd. Prof. dr. A. Vonk-Noordegraaf, Anton, bij onze eerste ontmoeting mocht ik direct aansluiten bij de onderzoeksbespreking die enkele minuten later zou plaatsvinden. Daarna mocht ik ook meteen meelopen naar de longafdeling, waar je me voorstelde aan één van de eerste PH-patiënte die bij jou onder behandeling was. Hoe druk het ook is, jij blijft altijd vragen stellen, onderwijzen, inspireren.. Hartelijk dank daarvoor. Prof. dr. N. Westerhof, Nico, inspirerend door oneindig veel enthousiasme voor het onderzoek en altijd alles willen begrijpen. Ik heb genoten van onze besprekingen en ben trots op onze publicatie samen. Prof. dr. J. Van der Velden, Jolanda, ik wil je bedanken voor je inspirerende rol als afdelingshoofd van de fysiologie en daarbij ben je ook een ontzettend leuk mens.

Prof. dr. K. Grünberg, Katrien, tijdens mijn eerste ervaringen met onderzoek mocht ik kennismaken met de wereld van de pathologie. Ik ben erg dankbaar voor alle lessen geleerd tijdens het turen door de microscoop. Prof. dr. P.L. Hordijk, Peter, dank dat ik altijd aan kon kloppen met vragen sinds jij de fysiologie afdeling hebt verrijkt.

Ik heb het geluk gehad dat ik gedurende mijn PhD veel heb kunnen leren van de longafdeling, maar ook deel uit mocht maken van het lab van de fysiologie. Uren, dagen,

maanden, jaren heb ik doorgebracht in de labs in de Medische Faculteit en daarna in het O2 gebouw om celkweek onder de knie te krijgen, kennis te maken met dieronderzoek en zwoegend op de beste western blots, immunohistochemische kleuringen en PCRs. Dit had ik natuurlijk nooit voor elkaar gekregen zonder de hulp van velen:

Allereerst mijn paranimfen: Chris en Melissa, wat ben ik trots dat jullie naast mij staan op deze dag. Lieve Chris, het is altijd leuk nieuwe ideeën met je te bespreken en je bent altijd enthousiast te krijgen voor het proberen van nieuwe technieken. Ik ben blij dat we ook buiten het lab goede vrienden zijn geworden en hoop dat we in de toekomst nog veel biertjes doen en festivals pakken. Wat top om deze jaren nu samen af te sluiten en weer samen te gaan werken in de kliniek. Lieve Melissa, wat ben ik blij dat ik bij je op de kamer terecht ben gekomen, waar we naast een hoop bloed, zweet en tranen ook ontzettend hebben kunnen lachen. Ik heb bewondering voor je doorzettingsvermogen in werk, sport en thuis. Misschien durf ik ooit nog eens een loop met je aan. Tot die tijd liever een borrel!

Dear Robert, I am very grateful for the work we accomplished in the lab together through joint forces. I look back with a warm heart on all dinners, after work drinks and parties. How special that Anke could join for a couple of years in the Netherlands as well. I wish you all the happiness and health with your family and good luck with your certainly successful career.

Silvia, ik zal onze trip in Las Vegas nooit vergeten. What happens in Vegas, stays in Vegas. Joana, so much to learn from your skills to organize and plan everything so precisely in the lab. Thanks for numerous hours in the lab at unconventional times. The best of luck to your beautiful family. Barbara, queen of social events, looking forward to all food and drinks parties in the future. Merci beaucoup!

Michiel, collega van het eerste uur. Ik heb genoten van onze labsessies en bediscussieren van onze grootse ideeën. Dank daarvoor. Denielli (and Marcello!), for organizing the best Brazilian barbecues with memorable caipirinhas and getting lost in China town of San Francisco on our way to the Fisherman's Warf. We still plan to visit you in Brazil one day! Max, hoe had ik het moeten redden zonder jouw gezelligheid op het lab en erbuiten! Hoe leuk zou het zijn als we elkaar nu weer tegenkomen aan de andere kant van de Boelelaan? Heel veel succes met je studie verpleegkunde! Babu, always working on hundreds of projects and always writing. Thanks for introducing me in the lab in Leiden! Jurjan, buiten de indrukwekkende hoeveelheden werk die je weet te verzetten in het lab doe je ook nog 'even' het klinische werk en ben je altijd te porren voor een bitterbal. Veel geluk met jouw carrière. Dear Vasco, thanks for the numerous dinners in the always charming restaurant in the hospital and the amazing tour in Portugal, I will never forget. Rick, roomie van het eerste uur, dank voor je eeuwige optimisme. Rob, bedankt voor alle tips 'n tricks bij het Western blotten. Marc,

gracias for bringing Spanish warmth into the lab and a fun tour in Barcelona. Zeineb, de beste mede-paranimf, veel geluk voor je mooie gezin. Aimée, gelukkig kon ik altijd op je rekenen voor de drankinkoop en het optuigen van de feestjes op het lab.

Jan, Pan en Ingrid: wat had ik ontmoeten in het lab zonder jullie? Dank! Ook de rest van de vaatgroep: Erik, Manon, Robert en Joana, bedankt voor het gezelschap tijdens het pipetteren.

Dat er op het lab naast al het harde werk het ook heel gezellig is en er goed geborrelt wordt moge duidelijk zijn. Deze periode was niet hetzelfde geweest zonder: Sun, Dimitar, Ed, Alexander, Michiel, Rob, Pieter, Igor, Andreas, Duncan, Paul, Marian, Dop, Alice, Ilse, Michiel, Kim, Isabelle, Josine, Coen, Aref, Pleuni, Charissa, Chantal, Francisca, Jasmin, Louise, Wies, Emmy, Erik, Willem, Tessa, Sylvia, Ruud, Mark, Rowan, Jeroen, Maïke, Larissa, Aida, Anoeke, Marloes, Martijn, Stefan, Michi en Erik. Dankzij jullie was het lab een fijne tweede thuis.

Manon, Ilse, Barbara: TPO 2015 was duidelijk de beste editie in de geschiedenis van de fysiologie afdeling!

Ook wil ik alle mensen aan de andere kant van de Boelelaan, het klinische deel van de PH-groep bedanken: Frances (dank voor de kritische vragen en adviezen), Cathelijne, Pia, Onno, Josien, Hans, Anna, Joanne, Liza, Bart, Gerrina, Berend, Aida, José. Bedankt voor de interessante labmeetings met leuke discussies, samenwerkingen en uiteraard gezelligheid op congressen. Hopelijk komen we elkaar in de toekomst nog regelmatig tegen. Zonder de longchirurgen hadden we nooit zoveel endotheelcellen kunnen kweken, dankjewel Chris, Rick en Koen. Ook dank aan de dames van het secretariaat: Ella, Anny, Ellen en Irma.

Alle kamergenoten op alle verschillende kamers in het ziekenhuis en de medische faculteit: Jasmijn, Bianca, Rick, Rob, Melissa, Robert, Jan: bedankt voor alle uren gezellig kletsen, verhalen kwijt kunnen en 'second opinions' over nieuwe ideeën.

Thanks to all the great researchers in Paris for fruitful collaborations and inspiring meetings: Prof. Humbert, dr. Guignabert, dr. Tu and Prof. Dorfmüller.

Dank aan alle collega's van de CVON voor de samenwerkingen, het uitwisselen van ideeën en de gezellige jaarlijkse summer schools.

Er is, blijkbaar, ook een leven buiten het lab. Dank aan de vrienden die mij daar zo nu en dan aan herinnerd hebben: Eva, Pheck Hwa, Anouk, Marte. Ook dank aan mijn gezellige co-genoten Eva, Eva, Habibe, Laurien en Anne. Stuk voor stuk parels.

Het is fantastisch om zo'n fijne familie te hebben waar het altijd gezellig is en een vol glas wijn en heerlijk eten klaar staat. Lieve oma, wat een hoop sterke en onafhankelijke keuzes heb je in je leven gemaakt. Trots dat mijn kinderen zo'n fijne omi mogen hebben. Opa en oma Friesland, lieve Jannie, opa zal er in gedachten bij zijn op deze dag. Lieve Tessa, wat een geluk dat ik zo'n leuke, fijne grote zus heb. Heerlijk om het altijd te kunnen hebben over onze grootste interesses: eten, koken, wijn en.. eten. Laten we dat altijd blijven doen. Gelukkig heb ik een ontzettend warme 'koude kant': Beste Joop en Olga, ook bij jullie voelt het als thuis komen. Steef en Eef, wat een mazzel dat ik jullie tot familie kan rekenen. Op naar nog honderden heerlijke borrels en diners.

Lieve pap en mam, dank voor jullie onvoorwaardelijke steun. Als ik zenuwachtig ben voor iets of voor een moeilijke keuze sta, weet ik dat jullie hoe dan ook trots zullen zijn. Het is genieten om jullie als opa en oma te zien. Dank voor alles.

Lieve, lieve Died, het beste dat deze PhD mij heeft gegeven. Jij geeft mij alle ruimte te leren, ontwikkelen en werken, motiveert mij als ik mijn enthousiasme even kwijt ben en geeft mij een warm thuis. Jij bent de liefde van mijn leven en ik kan niet wachten op alle avonturen die we met zijn vieren gaan beleven.

Amsterdam Cardiovascular Sciences

